24 August 2007 | $10

# Science

AAAS

# Engineered for speed

## 2X Faster

**QuikChange® Lightning Saves You Time**

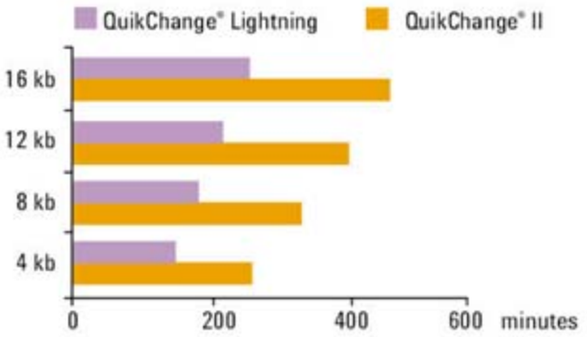


*Time Comparison of QuikChange® Lightning to QuikChange® II*

Our new QuikChange® Lightning Site-Directed Mutagenesis Kit* introduces point mutations, insertions, or deletions two times faster than our previous kits. Using our most advanced high-fidelity enzyme technology, we accelerated the protocols while guaranteeing the highest accuracy for your site-directed mutagenesis.

- Greater than 80% mutagenesis efficiency
- High-fidelity linear amplification minimizes unwanted errors
- Entire procedure performed in under 3 hours

u.s. and canada 1-800-424-5444 x3
europe 00800-7000-7000

www.stratagene.com/QCLightning

Want twice the speed? Go to www.stratagene.com/QCLightning

QuikChange® Lightning Site-Directed Mutagenesis Kit 10 rxn 210518
30 rxn 210519



STRATAGENE
An **Agilent Technologies** Company

# Why Not Speed Up Your Cloning?

## End Subcloning Now

## In-Fusion™ PCR Cloning

- *Construct the clone you need in one step without subcloning*
- *Clone into any vector, even yours*
- *Clone into any location within that vector*

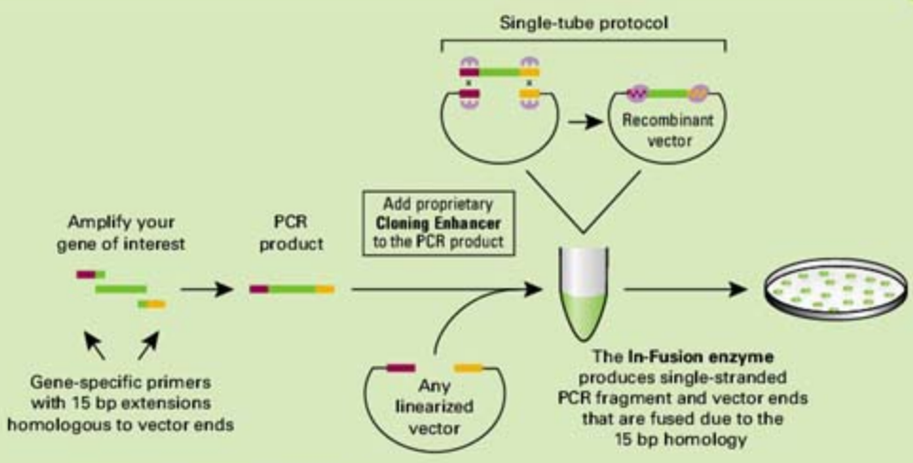


The In-Fusion 2.0 cloning protocol.

**Visit our website today**
**www.clontech.com/ifpcr**
**and plan for tomorrow!**

**Products for your research needs**

Fluorescent & Luminescent Reporters
Gene Expression & Delivery
Gene Expression Profiling
Non-coding RNA Research & RNAi
Nucleic Acid Purification
Oligo Modification
PCR & RT-PCR Products
Protein Arrays
Protein Expression & Purification
Protein-Protein Interaction Systems
RNA

**Clontech Laboratories, Inc.**
**A Takara Bio Company**
**www.clontech.com**
United States/Canada: +1.800.662.2566 • Asia Pacific: +1.650.919.7300 • Europe: +33.(0)1.3904.6880 • Japan: +81.(0)77.543.6116

AD772389

Clontech

GE Healthcare



# Drop. Measure. Done.

# NanoVue, the easy-to-use spectrophotometer.

The new NanoVue™ spectrophotometer, with its special "drop and measure" feature, couldn't be any easier to use in getting accurate results for DNA, RNA, oligos, and proteins.

NanoVue allows sensitive measurements of very small (< 2 µl) samples. Simply pipette onto the sample plate, and in 3 seconds you'll have your results. NanoVue also offers quick and easy cleaning, which reduces the risk of cross-contamination.

Through innovations that save time and make your research easier, we're bringing science to life. We call it **Life Science Re-imagined.**

Be one of the first to experience NanoVue for yourself, register for a trial at:
**www.gelifesciences.com/tryNanoVue**


imagination at work

Volume 317, Issue 5841


## COVER

The rapidly retreating margin of Columbia Glacier, as seen from the air above iceberg-riddled Columbia Bay, Prince William Sound, Alaska. Exposed bedrock on the valley margins shows that the glacier has thinned by more than 400 meters since the early 1980s. See page 1064.

***Photo: R. S. Anderson***

## DEPARTMENTS



## EDITORIAL



## NEWS OF THE WEEK



## NEWS FOCUS




## LETTERS




## BOOKS *ET AL.*



## POLICY FORUM



## PERSPECTIVES



CONTENTS continued >>

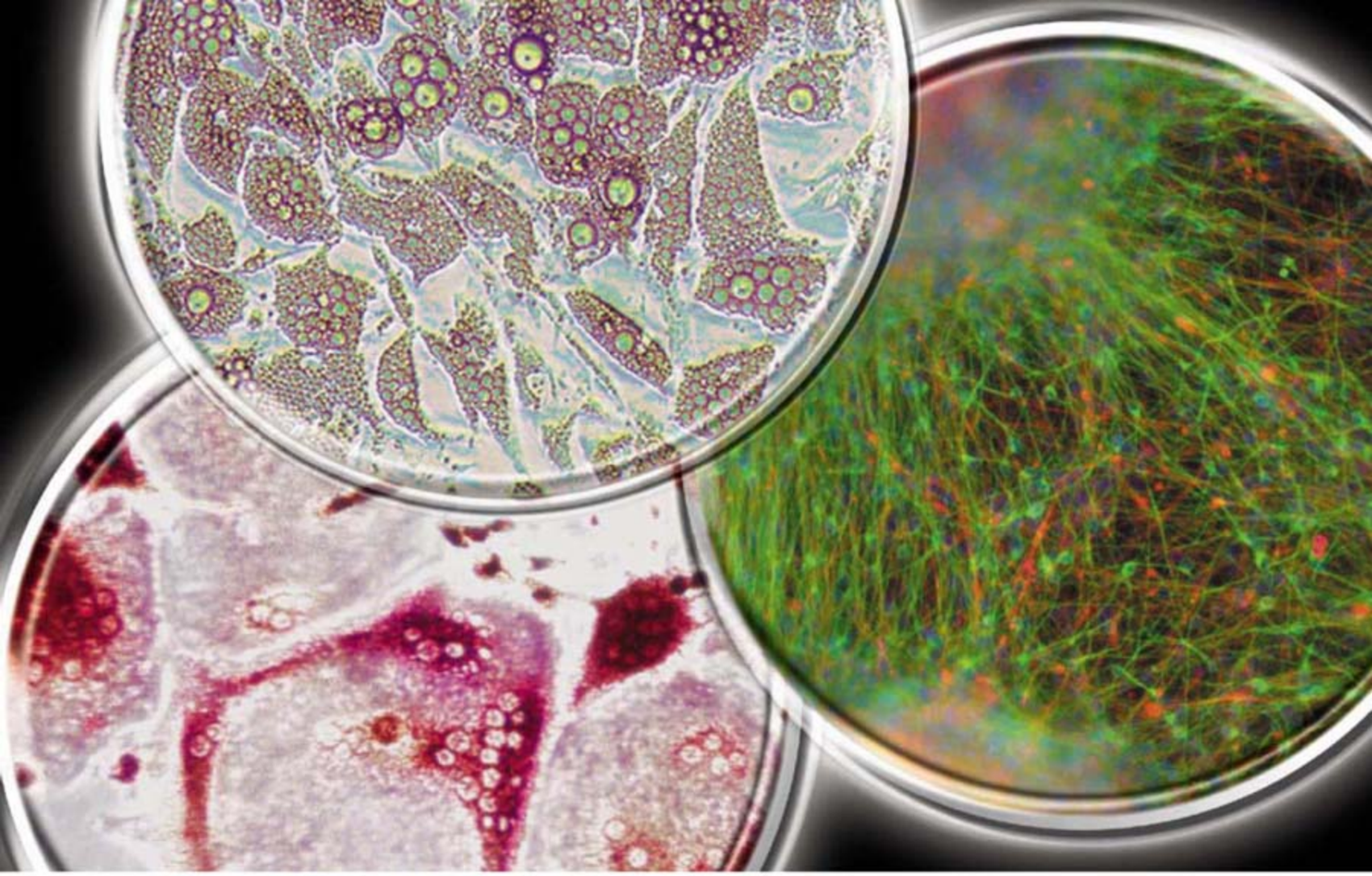

# Poietics® Human Stem Cells & Media

## *In Vivo* Relevance. *In Vitro* Results.

As the leader in primary cell culture, Lonza offers a variety of primary stem cells, including:

**Human Stem Cells**

- New! Poietics® Adipose-Derived Stem Cells purely characterized with relevant stromal and stem markers, and a media kit for growth and expansion
- Multipotent Mesenchymal Stem Cells isolated from bone marrow, and media kits for growth and differentiation of several lineages

**Human Bone, Adipose, and Neural Progenitor Cells and Media Kits**

- Cryopreserved osteoclast precursors, preadipocytes, and neural progenitors with media kits for growth and differentiation

**Human Hematopoietic Progenitor Cells**

- Variety of hematopoietic progenitors including CD34+, CD133+, and mononuclear cells isolated from peripheral blood, bone marrow, and umbilical cord blood

**Visit our website at www.lonzabioscience.com/poietics to receive a FREE Lonza Cell Mug.**

Lonza Walkersville, Inc., 8830 Biggs Ford Road, Walkersville, MD 21793



www.lonza.com

Lonza

Science

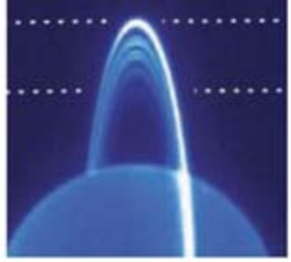



## SCIENCE EXPRESS

www.sciencexpress.org



## TECHNICAL COMMENT ABSTRACTS



## BREVIA



1067

## REPORTS



CONTENTS continued >>

# The power of small x8

## 1µl analysis — increased throughput

## The NanoDrop® ND-8000 8-Sample Spectrophotometer

**1µl samples. No cuvettes. No dilutions.**


Revolutionary technology. **8 readings in under 30 seconds.** The NEW NanoDrop® ND-8000 8-Sample Spectrophotometer is powerful — eight 1µl samples at once.

Full spectrum UV/Vis analysis of 1µl samples for quantitation, purity assessments and more: nucleic acids, microarrays, proteins and general spectrophotometry.

Measurement is quick and easy — pipette up to eight samples and measure. Each sample is read using two path lengths to achieve an extensive dynamic range (e.g., 2-3700 ng/µl dsDNA), virtually eliminating the need for dilutions. Then just a quick wipe clean and you're ready for your next samples. What could be easier — or more powerful?

And for the power of small in single-sample absorbance or fluorescent measurements, check out the NanoDrop® ND-1000 Spectrophotometer or the NanoDrop® ND-3300 Fluorospectrometer (ultra low fluorescent detection limit of sample mass — e.g., 2 pg dsDNA).

Ready to experience the power of small x8? **Test a NanoDrop® ND-8000 8-Sample Spectrophotometer in your own lab.**

**FREE** one-week evaluation **www.nanodrop.com**
**302.479.7707**

NanoDrop

## REPORTS *CONTINUED...*


The Evolution of Selfing in *Arabidopsis thaliana* 1070
*C. Tang* et al.
An analysis of sex genes shows that at several times throughout its history—including about 1 million years ago—*Arabidopsis* has developed the ability to self-fertilize.

BIOCHEMISTRY

Anatomy and Dynamics of a Supramolecular Membrane Protein Cluster 1072

*T. E. Swartz* et al.
A light-activated enzyme with a flavin chromophore is found in several bacterial species, and in one of these it regulates light-stimulated macrophage infection.
>> *Perspective p. 1041*



1043
& 1079

AAAS
ADVANCING SCIENCE, SERVING SOCIETY

**SCIENCE (ISSN 0036-8075) is published weekly on Friday, except the last week in December, by the American Association for the Advancement of Science, 1200 New York Avenue, NW, Washington, DC 20005.** Periodicals Mail postage (publication No. 484460) paid at Washington, DC, and additional mailing offices.  Domestic individual membership and subscription (51 issues): $142 ($74 allocated to subscription). Domestic institutional subscription (51 issues): $710; Foreign postage extra: Mexico, Caribbean (surface mail) $55; other countries (air assist delivery) $85. First class, airmail, student, and emeritus rates on request. Canadian rates with GST available upon request, GST #1254 88122. Publications Mail Agreement Number 1069624. **Printed in the U.S.A.**

**Change of address:** Allow 4 weeks, giving old and new addresses and 8-digit account number. **Postmaster:** Send change of address to AAAS, P.O. Box 96178, Washington, DC 20090–6178. **Single-copy sales:** $10.00 current issue, $15.00 back issue prepaid includes surface postage; bulk rates on request.  The identification code for *Science* is 0036-8075. *Science* is indexed in the *Reader's Guide to Periodical Literature* and in several specialized indexes.

CONTENTS continued >>

**Criterion™ Precast Gel System**

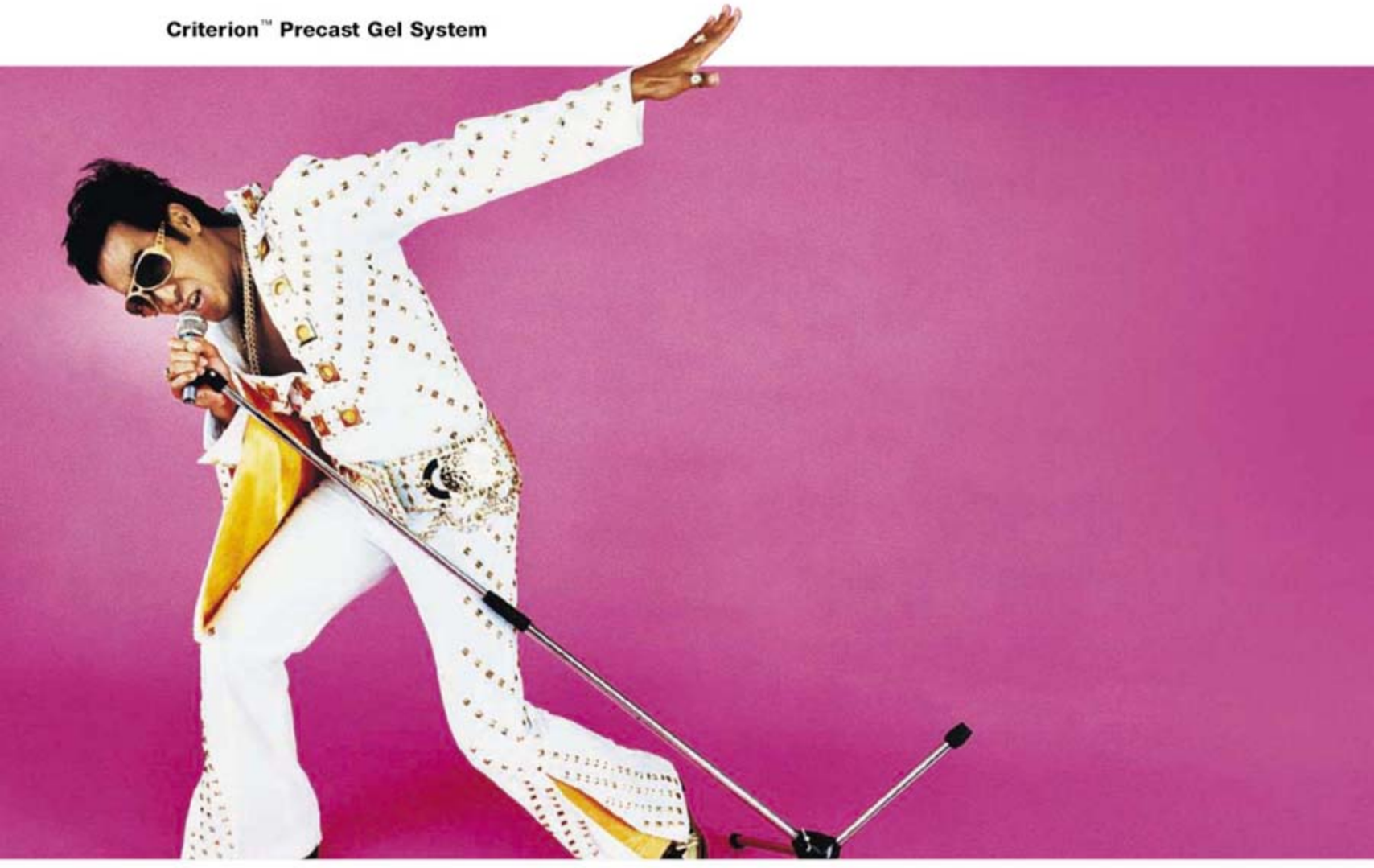

# *Criterion — the real king of protein electrophoresis.*

*Often imitated, never equaled, Bio-Rad's Criterion precast gel system is the right choice for those who demand genuine quality and convenience.*

**Outstanding Performance**
Criterion is famous for straight bands, excellent resolution, and gel-to-gel reproducibility.

**Stellar Composition**
The integrated upper buffer chamber ensures leak-free runs every time. Its patented* design enables quick, safe opening of cassettes without any additional tools.

**Fantastic Footwork**
The patented* J-foot design allows easy removal of the gel from its cassette without ripping or tearing. No tools required!

For a closer look, visit us on the Web at **criterion.bio-rad.com**

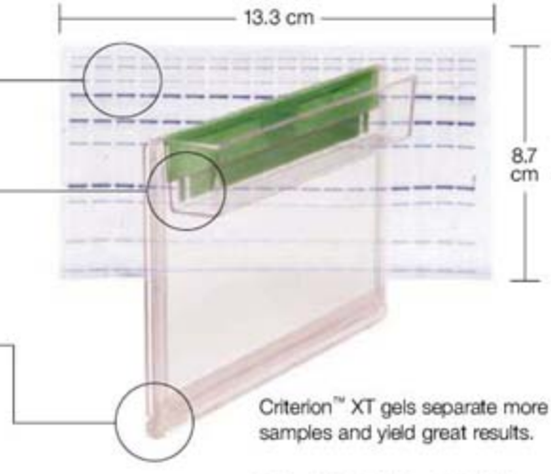


Criterion™ XT gels separate more samples and yield great results.

* U.S. patents 6,093,301 and 5,073,246.

## SCIENCENOW

www.sciencenow.org DAILY NEWS COVERAGE

**Mickey Has Two Mommies**
Researchers take dad out of the mouse procreation equation.

**Making Water Do the Splits**
New catalyst may pave way for greener fuel.

**Think Pink—or at Least a Reddish Blue**
Researchers link gender color preferences to mechanics of vision.

PB1 domains mediate protein interactions.

## SCIENCE'S STKE

www.stke.org SIGNAL TRANSDUCTION KNOWLEDGE ENVIRONMENT

**PERSPECTIVE: The Functions of Plant TIR Domains**
*T. M. Burch-Smith and S. P. Dinesh-Kumar*
Plants have evolved novel uses for the TIR domain in pathogen detection and possibly in controlling transcription factors as well.

**REVIEW: Structure and Function of the PB1 Domain, a Protein-Interaction Module Conserved in Animals, Fungi, Amoebas, and Plants**
*H. Sumimoto, S. Kamakura, T. Ito*
Canonical and noncanonical PB1 interactions contribute to cell organization and function.

Getting through the academia/industry wall.

## SCIENCE CAREERS

www.sciencecareers.org CAREER RESOURCES FOR SCIENTISTS

**US: Tooling Up—The Wall**
*D. Jensen*
Is the wall between academia and industry becoming more or less porous?

**MISCINET: Profile—Susan Estes**
*A. Sasso*
Susan Estes's modest demeanor belies her accomplishments and promise as a genetics researcher and mentor.

**US: Mind Matters—The Complex Biochemistry of Laboratory Friendships**
*I. S. Levine*
Many laboratory relationships that go beyond the lab can have advantages and perils, both personal and professional.

**US: From the Archives—Project Management for Scientists**
*S. Portny and J. Austin*
How can you create a lab environment that allows free exploration yet assures solvency and accountability?

## SCIENCEPODCAST

Download the 24 August *Science* Podcast to hear about a dangerous pathogen in Southeast Asia, the rings of Uranus, how the brain responds to threat, and more.
www.sciencemag.org/about/podcast.dtl

CREDIT: (SCIENCE CAREERS) JACK PARKINSON/CREATIVE COMMONS

***Separate individual or institutional subscriptions to these products may be required for full-text access.***

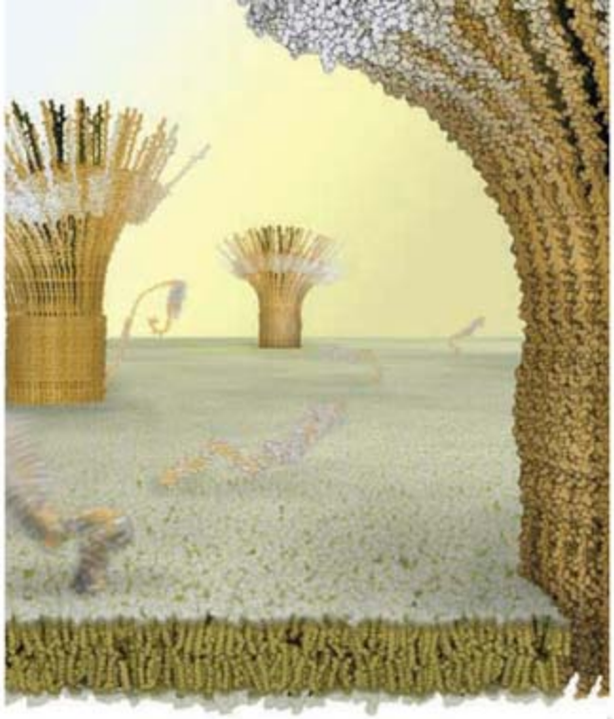

## << Let's Get Together

Proteins in the eukaryotic plasma membrane mediate many different functions and are largely partitioned into clusters. Using the SNARE protein syntaxin 1 as an example **Sieber *et al.*** (p. 1072; see the Perspective by **White**) investigate the mechanism of clustering using high-resolution optical imaging, quantitative biochemistry, and molecular dynamics simulations. Weak protein-protein interactions are balanced by steric repulsion to give densely crowded clusters containing about 75 syntaxins. Proteins within the cluster are immobile, but can exchange with freely diffusing molecules. This conceptual framework likely applies to many other membrane proteins.

## A Clean Break at Tantalum

Bacteria have evolved the remarkably efficient nitrogenase enzyme to metabolize $N_2$ to ammonia, whereas the fertilizer industry has long relied on heterogeneous iron catalysts at high temperature to perform the same reaction. Both systems appear to require the cooperation of multiple metal centers to cut the strong $N_2$ triple bond. **Avenier *et al.*** (p. 1056) have found that tantalum hydride complexes bound to a silica surface can cleave $N_2$ in the presence of $H_2$ at isolated metal centers, yielding Ta-NH and Ta-$NH_2$ products. Infrared spectroscopy reveals that the reaction mechanism is distinct from those in the enzymatic and iron-catalyzed reactions and in homogeneous organometallic systems.

## A Lot from a Little

Sea-level rise from future melting of the Greenland and Antarctic ice sheets has received much attention because these harbor most of Earth's ice, but melting of the other glaciers and ice caps will also contribute, particularly over the next century, as they are melting rapidly. **Meier *et al.*** (p. 1064, published online 19 July; see the cover) survey these glaciers and ice caps and show that they are likely to contribute as much as 10 to 25 centimeters to sea-level rise during the next 100 years, perhaps up to 60% of the estimated total increase.

## Capturing a Surface Crossing

Computer simulations of chemical reaction dynamics tend to rely on the simplifying Born-Oppenheimer approximation, which assumes that electron rearrangement is complete before the nuclei move about. However, experiments have shown that certain triatomic reactions violate the approximation; for example, in the abstraction of one deuterium atom from $D_2$, an electronically excited fluorine atom can form a ground-state DF product. **Che *et al.*** (p. 1061) undertook a more exact theoretical treatment of this reaction, encompassing multiple electronic potential energy surfaces, and also measured product distributions experimentally at different collision energies. They found strong agreement between theory and experiment in capturing the precise quantum-mechanical factors underlying chemical reactivity.

## Fertilizing the Southern Ocean

Experiments have shown that adding iron to surface waters in some parts of the world, can stimulate biological production. By analyzing compiled data and conducting additional experiments, **Cassar *et al.*** (p. 1067) show that gross primary production and net community production in large regions of the Southern Ocean is proportional to the input of soluble iron from aerosols. They conclude that iron addition increases export production and that windblown dust enhances gross primary production across large parts of the Southern Ocean.

## Bacteria Seeing Blue

Phototropins, blue-light receptors in plants, are light-activated serine/threonine kinases with a flavoprotein LOV domain as their light-sensing module. In addition to the phototropins found in eukaryotes, gene-sequence analysis predicts that LOV domains should be present in prokaryotes, and archaea. **Swartz *et al.*** (p. 1090; see the Perspective by **Kennis and Crosson**) show that a subset of genes in prokaryotes encodes for proteins that function as light-activated LOV-histidine kinases. Light activation of the LOV domain leads to the formation of a flavin-cysteinyl adduct, which is the photoreceptor-signaling state that activates the kinase domain. Light-activated LOV-histidine kinases were found in two important plant and animal pathogens and in a marine photosynthetic bacterium and indicate that the LOV-histidine kinases are an important family of bacterial photosensory receptors.

## Disordered but Coherent

When a magnet behaves classically, the spins on adjacent atoms are fixed and ordered and are typically correlated over distances of about 3 nanometers (nm). Confining the spins to a one-dimensional chain allows quantum fluctuations to become important, and the spins become disordered or fluid-like. **Xu *et al.*** (p. 1049, published online 26 July) now present inelastic neutron scattering measurements on the spin chain material $Y_2BaNiO_5$. Their data reveal that coherence between the spins, despite the quantum effects, extends to more than 20 nm, nearly an order of magnitude longer than the classical coherence length.

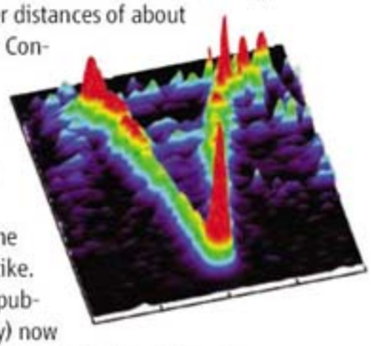

## Threat, Distance, and Dread

Behavioral experiments suggest that the distance from a threat affects the state of fear in

*Continued on page 1007*

CREDITS (TOP TO BOTTOM): IMAGE PROVIDED BY BURKHARD RAMMNER; XU *ET AL.*

www.roche-applied-science.com

## LightCycler® 480
## Real-Time PCR System

# Looking for more versatility in real-time PCR?


**We have what you need to accomplish more… now and in the future.**
Choose the **LightCycler® 480 System** (96- and 384-well format) – and get the power and flexibility to meet changing research needs.

- **Gene Detection:** Benefit from an advanced optical system and enhanced multiplexing capabilities to perform multitarget analysis.
- **Gene Quantification:** Utilize sophisticated software and unique algorithms to generate highly accurate gene quantification data.
- **Genotyping:** Achieve reliable genotyping results based on superior post-PCR melting curve analysis.
- **Gene Scanning:** Employ the innovative high-resolution melting (HRM) method to scan genes for unknown variations.

New

**Be prepared for the evolving demands of real-time PCR.**
Learn more about our cutting-edge technologies that provide versatility without compromise – visit ***www.lightcycler480.com*** today!

**For general laboratory use. Not for use in diagnostic procedures.**



Roche Diagnostics GmbH
Roche Applied Science
68298 Mannheim, Germany

Roche

*Continued from page 1005*

rodents. **Mobbs *et al.*** (p. 1079; see the Perspective by **Maren**) developed a computer program in which human subjects were chased by a virtual predator that could inflict real pain. As the virtual predator closed in, brain activity switched from the prefrontal cortex to the periaqueductal gray part of the midbrain. Higher-cortical systems thus control behavior when the degree of threat is perceived as low, while extreme levels of threat evoke phylogenetically older regions that control fast reflexive behaviors.

## Astrocytes at Single Synapses

Astrocytes respond to synaptic activity and can release different gliotransmitters, which modulate neuronal activity and neurotransmission. **Perea and Araque** (p. 1083) examined the role of astrocytes on synaptic transmission at single hippocampal excitatory synapses. $Ca^{2+}$ elevation in astrocytes led to a transient release of the neurotransmitter glutamate from astrocytes, which was mediated by metabotropic glutamate receptors. Potentiation became long-lasting when glial activation was paired with postsynaptic depolarization.

## Metabolic Enzyme Nailed

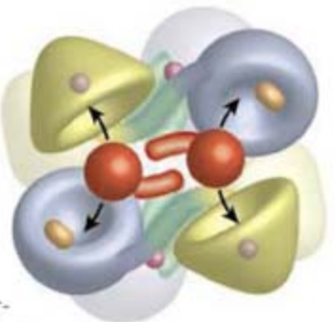

Carboxylases transfer carboxyl groups in a number of essential metabolic reactions. The enzymes have distinct active sites to catalyze different steps of the overall reaction, and the covalently bound biotin cofactor is used to transfer activated carboxyl intermediates between the sites, but how this transfer is achieved has not been clear. Now **St. Maurice *et al.*** (p. 1076) report the complete structure of pyruvate carboxylase. Pyruvate carboxylase is active as a tetramer, and transfer of an activated carboxyl group occurs between active sites on separate polypeptide chains.

## Motoring Chromatin Assembly

Molecular motor proteins, such as the chromodomain-containing factor CHD1, function in remodeling nucleosomes. In vitro analyses suggest that CHD1 acts as an ATP-utilizing chromatin assembly factor. **Konev *et al.*** (p. 1087) now examine the role of CHD1 in vivo in the fruit fly *Drosophila melanogaster*. Elimination of this factor results in infertile females because mutant embryos are unable to incorporate a histone variant into the paternal genome after protamine removal from the sperm. The *Chd1* null eggs cannot decondense sperm chromatin, resulting in the exclusion of paternal chromatin from the zygote and the generation of nonviable haploid embryos.

## From Clone to Species

Because of widespread exchange of genes, bacteria do not fit easily into the conventional paradigm of species. **Retchless and Lawrence** (p. 1093) have devised a method to extract the time of divergence for different genes in different bacterial species. Using these data, they show genes that encode lineage-specific traits became genetically isolated long before recombination ceased at other loci. Thus, as bacterial lineages begin to separate, they can be considered different species at some genes, but the same species at other genes. This is quite different from any speciation process described for eukaryotes. Thus, ecologically distinct species must exist within traditionally named bacterial species, which may impact the use of microbial taxonomy to inform human decisions, such as medical diagnosis, epidemiology, or bioterrorism.

## In Two Places at Once

The sense of being outside of one's physical body (an out-of-body experience) has generally fallen within the realms of neurological dysfunction, either organic or pharmacologically aided, or of paranormal phenomena. The advent of virtual reality has offered a noninvasive and reproducible approach to inducing out-of-body experiences in normal subjects, as shown by **Ehrsson** (p. 1048) and by **Lenggenhager *et al.*** (p. 1096; see the news story by **Miller**). Head-mounted displays were used to demonstrate that subjects would reliably report the sensation of inhabiting a virtual body, from which vantage point they would be looking at themselves. In addition, they reacted autonomically in response to harm directed at their virtual body and displaced their bodily sense of self toward their doppelganger and away from their physical body.

CREDIT: ST. MAURICE *ET AL.*

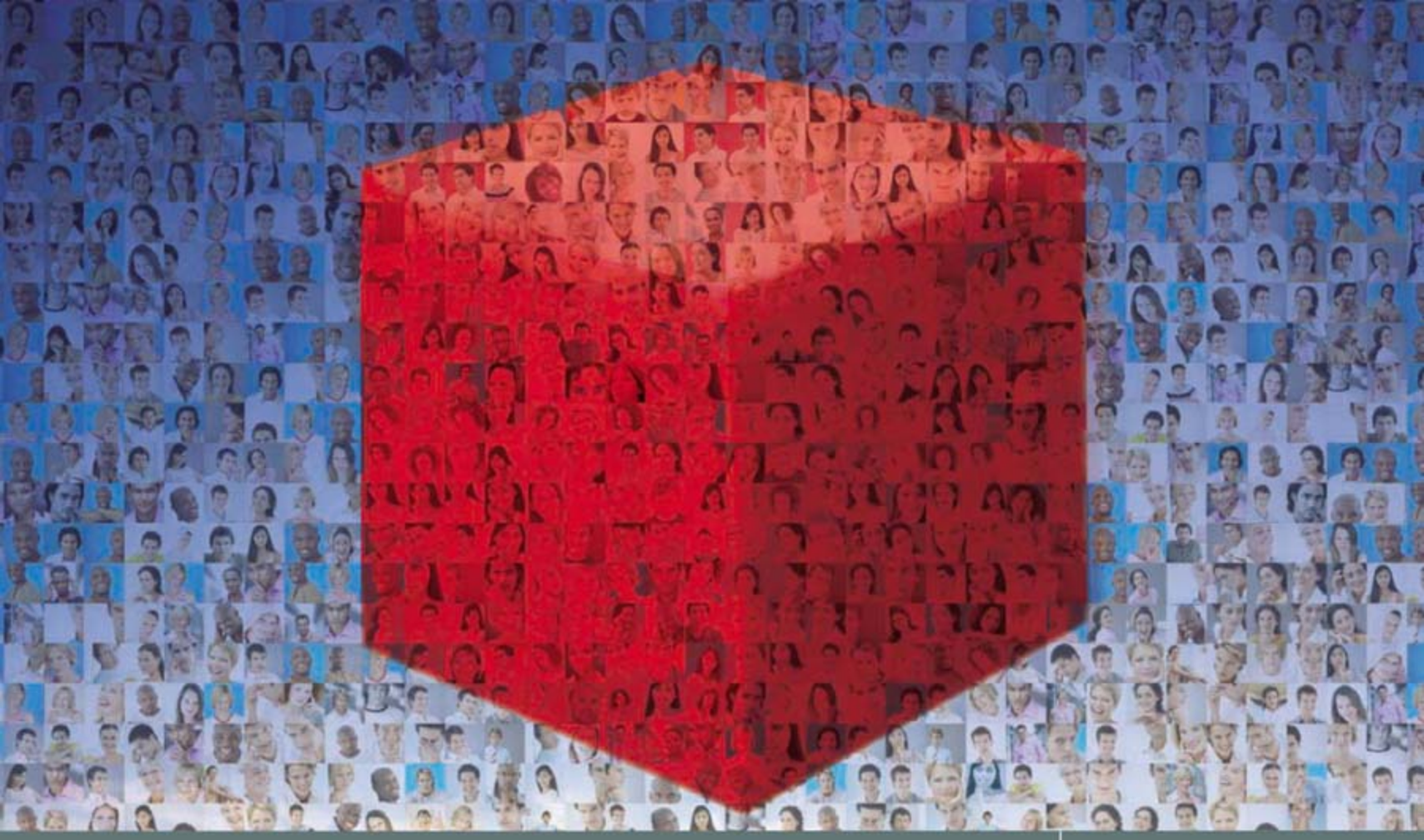

# Unlimited!

INNOVATION @ WORK

## Is your expression visible?

### Sigma enables unlimited gene expression analysis.

Make your gene expression profile visible with the TransPlex® Whole Transcriptome Amplification (WTA) Kit. TransPlex provides rapid amplification of total RNA from various sources such as blood, tissue biopsy, cultured cells, fixed and frozen tissue, plants and microorganisms.

- **Simple** - amplification of total RNA in less than 4 hours with less than 30 minutes of "hands-on" time
- **Sensitive** - only 5 ng of starting material required to produce a highly representative library from total RNA
- **Robust** - effectively amplifies degraded RNA, including formalin-fixed, paraffin-embedded tissues
- **Informative** - amplified DNA suitable for qPCR and microarray profiling

Learn how TransPlex enables unlimited gene expression analysis at: **sigma.com/wta**.

Our Innovation, Your Research

Shaping the Future of Life Science



SIGMA™ Life Science

Donald Kennedy is Editor-in-Chief of *Science*.

# STEM—But No Stem

TWO CONVERGING EVENTS TOOK PLACE ON 9 AUGUST THAT OUGHT TO HAVE THE scientific community scratching its collective head. One of these is an anniversary: On that date in 2001, President George W. Bush signed an Executive Order banning any use of federal funds to support research on stem cells (save, of course, for those 78 preexisting cell lines, only 21 of which are available). That position is reiterated most recently in another Executive Order after Bush's veto of the 2007 Senate bill (S.5) that would have authorized stem cell research.

The convergence is with the presidential signing of the America COMPETES Act (H.R. 2272) precisely on that anniversary. For those who collect fancy congressional titles, the full name of this act is (gasp) America Creating Opportunities to Meaningfully Promote Excellence in Technology, Education, and Science. Its content embodies many of the provisions and the spirit of the president's American Competitiveness Initiative (ACI), and thus both bills are responses to an unusually influential report from the National Academies. Called Rising Above the Gathering Storm and produced by a high-level committee chaired by Norman Augustine, former chairman and CEO of Lockheed Martin, its recommendations included programs for the education of students in science, technology, engineering, and mathematics: STEM, in the acronym of science-ed lingo.

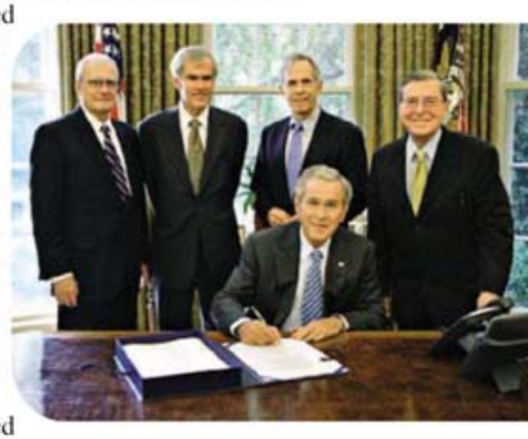

The irony is unmistakable. The prospects of a basic research effort that might have extraordinary clinical applications, one approved by a substantial majority of Americans, are still dim. So, no stem. But STEM is all over the America COMPETES Act, signed on the anniversary of Bush turning the lights out on stem cell research. Surely the president cannot have intended a subliminal message in the convergence. Or could he?

America COMPETES implements a number of initiatives derived from the Augustine report and ACI. It provides substantial increases to three physical science agencies for the period 2008 to 2010: a total of $22 billion for the National Science Foundation (NSF), $17 billion for the Department of Energy's (DOE's) Office of Science, and $2.7 billion for the National Institute of Standards and Technology (NIST). Much smaller annual amounts go to the Department of Education for two new middle-school math programs, advanced courses in high school, and inducements for college science majors to become K-12 teachers.

It is difficult to find fault with these proposals. There is consensus that the physical science agencies were about due for their turn at having research funding doubled. The STEM education programs are a little harder for the White House to swallow: The president's science adviser, John Marburger, has called them an unwarranted expansion of efforts not yet proven effective, and this month Bush declared that he will support only those pieces of the new law that mirror his own ACI. Still, the research direction appears to be right, and scientists supported by NSF or DOE ought to be looking happier than their colleagues in biomedicine. They should be warned, though, that doubling is a blessing only until it ends in a real-dollar dropoff, at which point they'll start to feel dumped on.

So here we are. On the one hand, the scientific community ought to thank the Augustine committee for a report that somehow avoided the usual fate of dying on a government shelf, and be appreciative of a president who says he cares about science. Yet that same chief executive is prepared to apply his own set of "moral values" to prevent some promising research. And we are still grappling with the effects of the 2002 No Child Left Behind Act, Bush's contribution to his legacy in which billions of dollars in unfunded mandates have been left to the 50 states to pay.

America COMPETES, in fact, is an authorization and not an appropriation, full though it is of good intentions. Perhaps the president is attracted to its business-friendly language and welcomes the fact that its focus is on STEM rather than lowercase stem. With that emphasis, it could be the other bookend for his legacy. Maybe "No Grownup Left Behind."

**– Donald Kennedy**

10.1126/science.1149332

CREDIT: AP

EDITED BY GILBERT CHIN AND JAKE YESTON

NEUROSCIENCE

## Replenishing the Power Stations

Mitochondria—the microscopic powerhouses of the cell—contain their own vestigial genome (mtDNA), and each cell needs a collection of healthy organelles to survive. Mitochondria are highly dynamic and undergo both fission and fusion. They produce adenosine 5′-triphosphate by transferring electrons from organic substrates through a series of respiratory enzyme complexes to molecular oxygen. Chen *et al.* examined the function of the mitochondrial fusion protein mitofusin 2; mutations in the gene *Mfn2* have been linked to the peripheral neuropathy Charcot-Marie-Tooth type 2A, in which the very long motor and sensory neurons of the lower leg die. They generated mice that lacked Mfn2 specifically in the cerebellum and found that the mutant mice suffered cerebellar degeneration. Mitochondrial distribution, morphology, and function were all compromised in Mfn2-deficient cells, and many mitochondria appeared to have lost their normal complement of mtDNA. The authors propose that a dynamic fusion capacity is required to maintain the genetic wherewithal for each mitochondrion to synthesize adequate supplies of respiratory enzymes. Furthermore, it seems that the Purkinje cells of the cerebellum are particularly sensitive to changes in the distribution and respiratory activity of their mitochondria, perhaps as a consequence of their extensive ramifications. — SMH

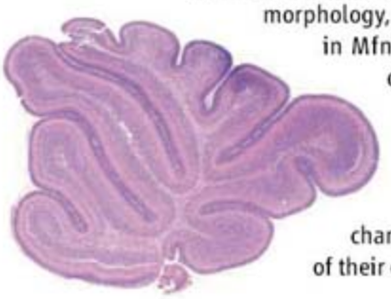

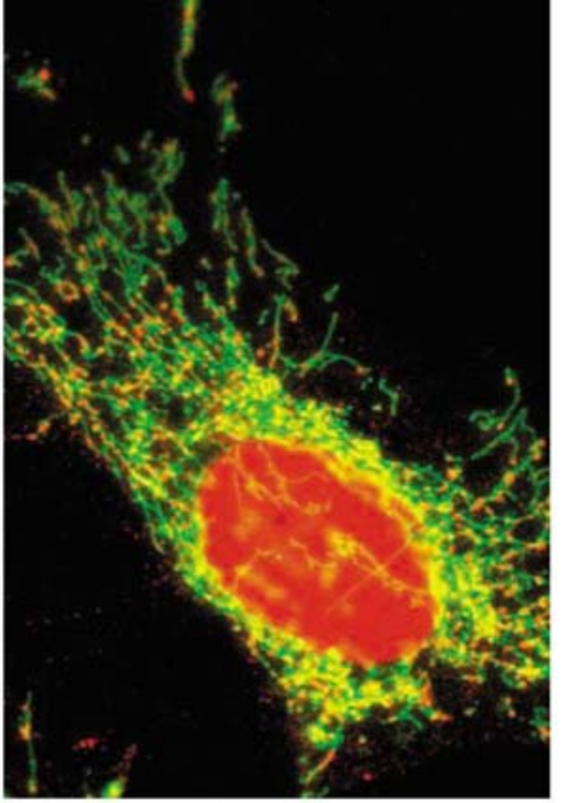

**Cerebellar structure (left) and mitochondrial distribution (right, yellow).**

*Cell* **130**, 548 (2007).

MOLECULAR BIOLOGY

## The Sign of Four

Nucleosomes constitute the principal structural motif of eukaryotic chromosomes and contain octomers of highly conserved histones with the almost invariant stoichiometry of two copies each of H2A, H2B, H3, and H4. Centromeres are specialized regions within chromosomes that play a critical role in the accurate segregation of duplicated chromosomes during cell division. Centromere nucleosomes contain an alternative histone, CenH3, which is thought to define centromere identity and participate in mitotic mechanics.

Dalal *et al.* have explored these issues through a biochemical and biophysical analysis of centromere nucleosomes in *Drosophila*. Cross-linking of bulk chromatin from crude extracts and within purified nuclei revealed that CenH3 appears in a heterotypic tetrameric half-sized nucleosome, with one copy each of CenH3, H2A, H2B, and H4. This composition was confirmed by mass spectrometry, and atomic force microscopy showed tetramers to be half the height of octomers. The tetramers protect less DNA [~120 base pairs (bp)] than the canonical octomers (~150 bp) and do not seem to form as regular higher-order structures as the octomer, yielding longer and more variable DNA linker lengths. This looser chromatin conformation, embedded within heterochromatin, may be critical for tethering the kinetochore to the centromere. — GR

*PLoS Biol.* **5**, e218 (2007).

CHEMISTRY

## Three in a Column

Numerous compounds comprising two bonded metal centers stabilized by bulky organic ligands have been characterized. However, zinc, cadmium, and mercury, which straddle the boundary between d-block and p-block metals, have only very recently been observed in this motif. Zhu *et al.* previously prepared zinc and cadmium dimers bearing bis(diisopropylphenyl)phenyl ligands, and have now synthesized a mercury dimer with the same ligand set to complete a homologous series. The compounds were accessed by reduction of metal halide precursors, and their solid-state structures characterized by x-ray crystallography. As predicted by theoretical calculations, the mercury-mercury bond is longer (and thus likely weaker) than the analogous zinc linkage, but shorter than the cadmium bond. The calculations implicate relativistic effects in this bond shortening, in keeping with a higher proportion of s-orbital character (as well as a measure of $dz^2$ overlap) in the mercury dimer's highest occupied molecular orbital (HOMO). All three compounds have effectively linear C-M-M-C geometries, with the terminal phenyl rings canted at an approximate right angle relative to one another. The authors also prepared zinc and cadmium dimers incorporating bridging hydride ligands for structural comparison; the mercury hydride proved monomeric and was characterized spectroscopically. — JSY

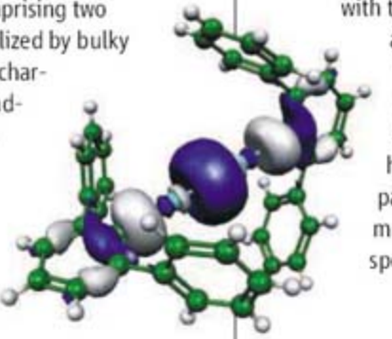

**Calculated HOMO of mercury dimer.**

*J. Am. Chem. Soc.* **129**, 10.1021/ja072682x (2007).

MATERIALS SCIENCE

## An Inside View of Weaving

Fiber-reinforced composites (FRCs) are finding increasing use as structural materials because they offer good performance at low weights. The mechanical properties of any given FRC depend on many variables, including the distribution and

CREDITS (TOP TO BOTTOM): CHEN ET AL., *CELL* **130**, 548 (2007); ZHU ET AL., *J. AM. CHEM. SOC.* **129**, 10.1021/JA072682X (2007)

orientation of the fibers within the matrix material. However, for most composites, nondestructive visualization of the fibers' response to stresses is precluded either by the opacity of the matrix material or by insufficient contrast between the fibers and the matrix.

Davies *et al.* surmount this challenge by probing an FRC through diffraction of a high-flux, microfocused x-ray beam from a synchrotron source. The sample comprised woven poly(*p*-phenylene phthalamide) (PPTA) fiber mats embedded in an epoxy matrix. A hole drilled into the center of the specimens modeled the rivet holes typically used to attach composite panels in aeronautical applications. The diffraction data clearly resolved the interleaved pattern of the woven fibers. Damage to the fibers was localized near the hole, and the tilt angle increased for fibers parallel to the strain direction as the stresses were transferred to neighboring fibers away from the hole. Because PPTA forms oriented fibers, the authors were able to determine changes in orientation of the yarn and could thus observe reorientation of the horizontal fibers caused by stress transfer. — MSL

*Appl. Phys. Lett.* **91**, 044102 (2007).

MATERIALS SCIENCE

## Sublimed Clusters

Inorganic thin films can be formed under vacuum conditions by transferring material from one surface as a vapor and depositing it on a nearby substrate. However, forming the vapor phase often involves harsh conditions—such as heating to very high temperature or bombardment with high-energy ions or photons—to desorb atomic species or a distribution of clusters. As a result, preserving intricate synthetic structures during the transfer is often difficult. Chao *et al.* show that silicon nanocrystals (with mean diameters near 2 nm) capped with undecyl hydrocarbon chains can undergo thermal desorption at relatively low temperature (200°C) and be transferred from one surface to another for a wide variety of substrates. Composition of the transferred particles was confirmed by x-ray photoemission spectroscopy, and morphologies were examined with a range of microscopy techniques. The nanocrystals initially grew as two-dimensional islands but could also form three-dimensional clusters. — PDS

*Nat. Nanotechnol.* **2**, 486 (2007).

ECOLOGY/EVOLUTION

## The Whole Is the Sum of the Parts

The fragmentation of natural ecosystems as a by-product of human activity is generally held to have adverse consequences for biodiversity, because it reduces the area of each habitat as well as the opportunities for dispersal and gene flow. Yaacobi *et al.* tease apart the effects of areal loss from those of degree of fragmentation in a Mediterranean scrub ecosystem in Israel. The total number of species of beetles and plants remained unaffected by the degree of subdivision of the landscape: a patch of area *A* having a similar number of species to *n* smaller patches of total area *A*. Despite this absence of an effect, the authors caution that the absolute number of species is not the only goal of conservation. Fragmentation also affects the abundance of individual species, some of which may be charismatic, and the composition of ecological communities in patches, features that are key determinants of ecosystem health. — AMS

*Proc. R. Soc. London B* **274**, 10.1098/rspb.2007.0674 (2007).

CREDIT: YAACOBI ET AL., PROC. R. SOC. LONDON B 274, 10.1098/RSPB.2007.0674 (2007)

Science stke AAAS

www.stke.org

## << Hyperactive Antimicrobials

Rosacea is a painful acne-like skin disorder, characterized by dilated blood vessels and persistent redness of the face. Yamasaki *et al.* provide evidence that cathelicidin peptides—which are chemotactic, angiogenic, and bactericidal, and are important for innate immune responses in the skin—are involved in the pathogenesis of rosacea. Skin biopsies of patients with rosacea had elevated levels of cathelicidin and cathelicidin mRNA. Processing of the cathelicidin precursor involves cleavage of the proprotein by the kallikrein family protease stratum corneum tryptic enzyme (SCTE); rosacea samples had elevated levels of SCTE and protease activity. The abundant cathelicidin fragment LL-37 stimulated interleukin-8 (IL-8) production in cultured human keratinocytes and caused erythema, vascular dilation, neutrophil infiltration, thrombosis, and hemorrhage when injected subcutaneously into mice; injection of SCTE caused similar symptoms. In mice deficient for the gene *Camp*, which encodes cathelicidin, inflammation was substantially less than normal after application of a contact skin irritant or physical abrasion. — NRG

*Nat. Med.* **13**, 975 (2007).

www.sciencemag.org

# Science

**1200 New York Avenue, NW**
**Washington, DC 20005**
Editorial: 202-326-6550, FAX 202-289-7562
News: 202-326-6581, FAX 202-371-9227

**Bateman House, 82-88 Hills Road**
**Cambridge, UK CB2 1LQ**
+44 (0) 1223 326500, FAX +44 (0) 1223 326501

**SUBSCRIPTION SERVICES** For change of address, missing issues, new orders and renewals, and payment questions: 866-434-AAAS (2227) or 202-326-6417, FAX 202-842-1065. Mailing addresses: AAAS, P.O. Box 96178, Washington, DC 20090-6178 or AAAS Member Services, 1200 New York Avenue, NW, Washington, DC 20005

**INSTITUTIONAL SITE LICENSES** please call 202-326-6755 for any questions or information

**REPRINTS:** Author Inquiries 800-635-7181
Commercial Inquiries 803-359-4578

**PERMISSIONS** 202-326-7074, FAX 202-682-0816

**MEMBER BENEFITS** Bookstore: AAAS/BarnesandNoble.com bookstore www.aaas.org/bn; Car purchase discount: Subaru VIP Program 202-326-6417; Credit Card: MBNA 800-847-7378; Car Rentals: Hertz 800-654-2200 CDP#343457, Dollar 800-800-4000 #AA1115; AAAS Travels: Betchart Expeditions 800-252-4910; Life Insurance: Seabury & Smith 800-424-9883; Other Benefits: AAAS Member Services 202-326-6417 or www.aaasmember.org.

| | |
|---|---|
| science_editors@aaas.org | (for general editorial queries) |
| science_letters@aaas.org | (for queries about letters) |
| science_reviews@aaas.org | (for returning manuscript reviews) |
| science_bookrevs@aaas.org | (for book review queries) |

Published by the American Association for the Advancement of Science (AAAS), *Science* serves its readers as a forum for the presentation and discussion of important issues related to the advancement of science, including the presentation of minority or conflicting points of view, rather than by publishing only material on which a consensus has been reached. Accordingly, all articles published in *Science*—including editorials, news and comment, and book reviews—are signed and reflect the individual views of the authors and not official points of view adopted by the AAAS or the institutions with which the authors are affiliated.

AAAS was founded in 1848 and incorporated in 1874. Its mission is to advance science and innovation throughout the world for the benefit of all people. The goals of the association are to: foster communication among scientists, engineers and the public; enhance international cooperation in science and its applications; promote the responsible conduct and use of science and technology; foster education in science and technology for everyone; enhance the science and technology workforce and infrastructure; increase public understanding and appreciation of science and technology; and strengthen support for the science and technology enterprise.

**INFORMATION FOR AUTHORS**

See pages 120 and 121 of the 5 January 2007 issue or access www.sciencemag.org/feature/contribinfo/home.shtml

EDITOR-IN-CHIEF **Donald Kennedy**
EXECUTIVE EDITOR **Monica M. Bradford**
DEPUTY EDITORS **R. Brooks Hanson, Barbara R. Jasny, Katrina L. Kelner**
NEWS EDITOR **Colin Norman**

**EDITORIAL SUPERVISORY SENIOR EDITOR** Phillip D. Szuromi; **SENIOR EDITOR/PERSPECTIVES** Lisa D. Chong; **SENIOR EDITORS** Gilbert J. Chin, Pamela J. Hines, Paula A. Kiberstis (Boston), Marc S. Lavine (Toronto), Beverly A. Purnell, L. Bryan Ray, Guy Riddihough, H. Jesse Smith, Valda Vinson, David Voss; **ASSOCIATE EDITORS** Jake S. Yeston, Laura M. Zahn; **ONLINE EDITOR** Stewart Wills; **ASSOCIATE ONLINE EDITOR** Tara S. Marathe; **BOOK REVIEW EDITOR** Sherman J. Suter; **ASSOCIATE LETTERS EDITOR** Etta Kavanagh; **EDITORIAL MANAGER** Cara Tate; **SENIOR COPY EDITORS** Jeffrey E. Cook, Cynthia Howe, Harry Jach, Barbara P. Ordway, Jennifer Sills, Trista Wagoner; **COPY EDITORS** Lauren Kmec, Peter Mooreside; **EDITORIAL COORDINATORS** Carolyn Kyle, Beverly Shields; **PUBLICATIONS ASSISTANTS** Ramatoulaye Diop, Chris Filiatreau, Joi S. Granger, Jeffrey Hearn, Lisa Johnson, Scott Miller, Jerry Richardson, Brian White, Anita Wynn; **EDITORIAL ASSISTANTS** Maris M. Bish, Emily Guise, Patricia M. Moore, Jennifer A. Seibert; **EXECUTIVE ASSISTANT** Sylvia S. Kihara; **ADMINISTRATIVE SUPPORT** Maryrose Madrid

**NEWS SENIOR CORRESPONDENT** Jean Marx; **DEPUTY NEWS EDITORS** Robert Coontz, Eliot Marshall, Jeffrey Mervis, Leslie Roberts; **CONTRIBUTING EDITORS** Elizabeth Culotta, Polly Shulman; **NEWS WRITERS** Yudhijit Bhattacharjee, Adrian Cho, Jennifer Couzin, David Grimm, Constance Holden, Jocelyn Kaiser, Richard A. Kerr, Eli Kintisch, Andrew Lawler (New England), Greg Miller, Elizabeth Pennisi, Robert F. Service (Pacific NW), Erik Stokstad; **INTERNS** Benjamin Lester, Marissa Cevallos, Veronica Raymond; **CONTRIBUTING CORRESPONDENTS** Barry A. Cipra, Jon Cohen (San Diego, CA), Daniel Ferber, Ann Gibbons, Robert Irion, Mitch Leslie, Charles C. Mann, Evelyn Strauss, Gary Taubes; **COPY EDITORS** Rachel Curran, Linda B. Felaco, Melvin Gatling; **ADMINISTRATIVE SUPPORT** Scherraine Mack, Fannie Groom; **BUREAUS** New England: 207-549-7755, San Diego, CA: 760-942-3252, FAX 760-942-4979, Pacific Northwest: 503-963-1940

**PRODUCTION DIRECTOR** James Landry; **SENIOR MANAGER** Wendy K. Shank; **ASSISTANT MANAGER** Rebecca Doshi; **SENIOR SPECIALISTS** Jay Covert, Chris Redwood; **SPECIALIST** Steve Forrester; **PREFLIGHT DIRECTOR** David M. Tompkins; **MANAGER** Marcus Spiegler; **SPECIALIST** Jessie Mudjitaba

**ART DIRECTOR** Kelly Buckheit Krause; **ASSOCIATE ART DIRECTOR** Aaron Morales; **ILLUSTRATORS** Chris Bickel, Katharine Sutliff; **SENIOR ART ASSOCIATES** Holly Bishop, Laura Creveling, Preston Huey, Nayomi Kevitiyagala; **ASSOCIATE** Jessica Newfield; **PHOTO EDITOR** Leslie Blizard

***SCIENCE* INTERNATIONAL**

**EUROPE** (science@science-int.co.uk) **EDITORIAL: INTERNATIONAL MANAGING EDITOR** Andrew M. Sugden; **SENIOR EDITOR/PERSPECTIVES** Julia Fahrenkamp-Uppenbrink; **SENIOR EDITORS** Caroline Ash (Geneva: +41 (0) 222 346 3106), Stella M. Hurtley, Ian S. Osborne, Stephen J. Simpson, Peter Stern; **ASSOCIATE EDITOR** Joanne Baker; **EDITORIAL SUPPORT** Deborah Dennison, Rachel Roberts, Alice Whaley; **ADMINISTRATIVE SUPPORT** Janet Clements, Jill White; **NEWS: EUROPE NEWS EDITOR** John Travis; **DEPUTY NEWS EDITOR** Daniel Clery; **CONTRIBUTING CORRESPONDENTS** Michael Balter (Paris), John Bohannon (Vienna), Martin Enserink (Amsterdam and Paris), Gretchen Vogel (Berlin); **INTERN** Krista Zala

**ASIA** Japan Office: Asca Corporation, Eiko Ishioka, Fusako Tamura, 1-8-13, Hirano-cho, Chuo-ku, Osaka-shi, Osaka, 541-0046 Japan; +81 (0) 6 6202 6272, FAX +81 (0) 6 6202 6271; asca@os.gulf.or.jp; **ASIA NEWS EDITOR** Richard Stone +66 2 662 5818 (rstone@aaas.org); **CONTRIBUTING CORRESPONDENTS** Dennis Normile (Japan: +81 (0) 3 3391 0630, FAX 81 (0) 3 5936 3531; dnormile@gol.com); Hao Xin (China: + 86 (0) 10 6307 4439 or 6307 3676, FAX +86 (0) 10 6307 4358; cindyhao@gmail.com); Pallava Bagla (South Asia: +91 (0) 11 2271 2896; pbagla@vsnl.com)

**AFRICA** Robert Koenig (contributing correspondent, rob.koenig@gmail.com)

EXECUTIVE PUBLISHER **Alan I. Leshner**
PUBLISHER **Beth Rosner**

**FULFILLMENT & MEMBERSHIP SERVICES** (membership@aaas.org) **MANAGER** Waylon Butler; **CUSTOMER SERVICE SUPERVISOR** Pat Butler; **SPECIALISTS** Tamara Alfson, Laurie Baker, Latoya Casteel, Lavanda Crawford, Vicki Linton; **DATA ENTRY SUPERVISOR** Cynthia Johnson; **SPECIALISTS** Tomeka Diggs, Tarrika Hill, Erin Layne, Sheila Thomas

**BUSINESS OPERATIONS AND ADMINISTRATION DIRECTOR** Deborah Rivera-Wienhold; **BUSINESS MANAGER** Randy Yi; **SENIOR FINANCIAL ANALYSTS** Michael LoBue, Jessica Tierney; **FINANCIAL ANALYSTS** Nicole Nicholson, Farida Yeasmin; **RIGHTS AND PERMISSIONS: ADMINISTRATOR** Emilie David; **ASSOCIATE** Elizabeth Sandler; **MARKETING DIRECTOR** John Meyers; **MARKETING MANAGERS** Darryl Walter, Allison Pritchard; **MARKETING ASSOCIATES** Julianne Wielga, Mary Ellen Crowley, Alison Chandler, Marcia Leach, Wendy Wise; **INTERNATIONAL MARKETING MANAGER** Wendy Sturley; **MARKETING EXECUTIVE** Jennifer Reeves; **MARKETING/MEMBER SERVICES EXECUTIVE** Linda Rusk; **JAPAN SALES** Jason Hannaford; **SITE LICENSE SALES DIRECTOR** Tom Ryan; **SALES MANAGER** Russ Edra; **SALES AND CUSTOMER SERVICE** Mehan Dossani, Iquo Edim, Kiki Forsythe, Catherine Holland; **ELECTRONIC MEDIA: MANAGER** Lizabeth Harman; **PROJECT MANAGER** Trista Snyder; **ASSISTANT MANAGER** Lisa Stanford; **SENIOR PRODUCTION SPECIALIST** Walter Jones; **PRODUCTION SPECIALISTS** Nichele Johnston, Kimberly Oster

**ADVERTISING DIRECTOR WORLDWIDE AD SALES** Bill Moran

**PRODUCT** (science_advertising@aaas.org); **CONSUMER & SPONSORSHIP SALES MANAGER** Tina Morra: 202-326-6542 **MIDWEST** Rick Bongiovanni: 330-405-7080, FAX 330-405-7081 • **WEST COAST/W. CANADA** Teola Young: 650-964-2266 **EAST COAST/E. CANADA** Christopher Breslin: 443-512-0330, FAX 443-512-0331 • **UK/EUROPE/ASIA** Michelle Field: +44 (0) 1223-326-524, FAX +44 (0) 1223-325-532 **JAPAN** Mashy Yoshikawa: +81 (0) 33235 5961, FAX +81 (0) 33235 5852; **SENIOR TRAFFIC ASSOCIATE** Delandra Simms

**COMMERCIAL EDITOR** Sean Sanders: 202-326-6430

**CLASSIFIED** (advertise@sciencecareers.org); **U.S.: RECRUITMENT SALES MANAGER** Ian King: 202-326-6528, FAX 202-289-6742; **INSIDE SALES MANAGER: MIDWEST/CANADA** Daryl Anderson: 202-326-6543; **NORTHEAST:** Allison Millar: 202-326-6572; **SOUTHEAST:** Tina Burks: 202-326-6577; **WEST:** Nicholas Hintibidze: 202-326-6533; **SALES COORDINATORS** Erika Foard, Rohan Edmonson, Leonard Marshall, Shirley Young; **INTERNATIONAL: SALES MANAGER** Tracy Holmes: +44 (0) 1223 326525, FAX +44 (0) 1223 326532; **SALES** Marium Hudda, Alex Palmer; **SALES ASSISTANT** Louise Moore; **JAPAN:** Jason Hannaford: +81 (0) 52 757 5360, FAX +81 (0) 52 757 5361; **ADVERTISING PRODUCTION OPERATIONS MANAGER** Deborah Tompkins; **SENIOR PRODUCTION SPECIALISTS** Robert Buck, Amy Hardcastle; **SENIOR TRAFFIC ASSOCIATE** Christine Hall; **PUBLICATIONS ASSISTANT** Mary Lagnaoui

**AAAS BOARD OF DIRECTORS RETIRING PRESIDENT, CHAIR** John P. Holdren; **PRESIDENT** David Baltimore; **PRESIDENT-ELECT** James J. McCarthy; **TREASURER** David E. Shaw; **CHIEF EXECUTIVE OFFICER** Alan I. Leshner; **BOARD** John E. Dowling, Lynn W. Enquist, Susan M. Fitzpatrick, Alice Gast, Linda P. B. Katehi, Cherry A. Murray, Thomas D. Pollard, Kathryn D. Sullivan

AAAS
ADVANCING SCIENCE, SERVING SOCIETY

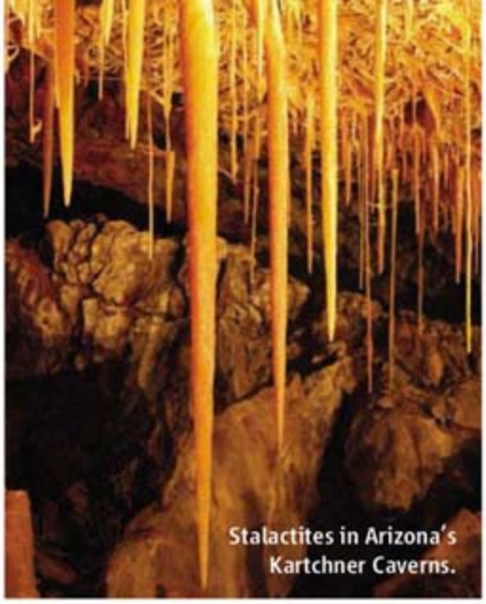

Stalactites in Arizona's Kartchner Caverns.

## Things That Drip

One grows in caves over thousands of years; the other appears in the back of your fridge in a matter of hours. But new research suggests that for all their differences, the mathematics describing stalactites and icicles is the same.

According to work presented last week at a meeting on natural complexity at the British Antarctic Survey in Cambridge, U.K., the rate of growth of either a stalactite or an icicle can be modeled by a simple power law based on the radius and the inclination of the surface at any given point. Raymond Goldstein, a theoretical physicist at the University of Cambridge, U.K., developed the model to describe the growth of stalactites, based on the rate at which calcium carbonate precipitates from water. Icicles grow by an entirely different mechanism: heat transfer from water to the surrounding air, which causes the water to freeze. "Despite the time scales and dimensions of molecules being very different in the two cases, out pops the same mathematical formula," says Goldstein. "It's a big mystery why nature would select the same power law."

"Nobody had a good model for the global shape of either stalactites or icicles before this, so to find a solution for both is impressive," says Stephen Morris, a physicist at the University of Toronto, Canada.

## Polar Ice Watch

A telling sign of climate change is the declining amount of Arctic sea ice that remains at the end of summer. And it's not just an indicator. Arctic ice also influences climate by cooling the planet.

NET WATCH

You can follow changes in sea-ice status at the Web site of the National Snow and Ice Data Center in Boulder, Colorado, which posts regular updates on ice conditions and analyses of trends. By mid-August, this year's melt had already broken the record set in 2005, when only 5.3 million square kilometers of ice were left at the end of the season, 31% below average. The site will provide fresh information until the melting halts, usually in September.
nsidc.org/news/press/2007_seaiceminimum/20070810_index.html

## The Many Facets of Soccer Ball Design

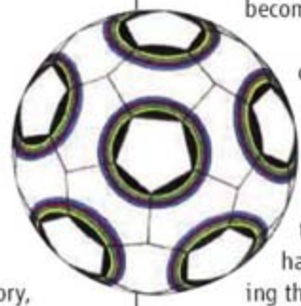

No ball is a perfect sphere, but the closer it is to one, the smoother the trajectory. After goaltenders during the 2006 soccer World Cup in Germany complained that the latest design had an unpredictable trajectory, South African geologist Jos Lurie decided to use his expertise in polyhedra and his 15 years of studying soccer ball designs to come up with a better pattern. Lurie, a professor emeritus who teaches gemology part-time at the University of Johannesburg, South Africa, describes his design as an "equilibrium" combination: 12 panels of a pentagonal dodecahedron and 30 of a rhombic triacontahedron. That makes for 42 panels—10 more than the popular Buckminster design and 28 more than the newer 14-panel Adidas Teamgeist. "The more panels you have, the more spherical the ball becomes," he says.

"A better design would be welcome, considering that the balls used in 2006 moved at times unpredictably, like knuckle balls in baseball," says Ken Bray, a theoretical physicist at the University of Bath, U.K. Lurie has sent his design to Adidas, hoping the company will test the ball for the next World Cup, which will be held in South Africa in 2010. Adidas has so far failed to express interest and has defended its Teamgeist as "a perfectly round ball allowing great accuracy and control."

## Keeping Oz As Is

Northern Australia is gaining fresh attention as one of the less spoiled areas of the world. The region—which extends more than 3000 kilometers from the wet tropics of Cape York Peninsula to Broome on the Indian Ocean—"contains the largest and most intact tropical savanna woodland remaining in the world," says Brendan Mackey of the Australian National University in Canberra. Mackey is a co-author of *The Nature of Northern Australia*, a report released in Darwin last week that aims to supply science-based guidance for conservation and development. Much of the north remains "intact," the authors say. "Great flocks of birds still move over the land. … Rivers still flow naturally. Floods come and go."

But northern Australia is also being threatened by climate change, poor fire management, weeds, and feral animals (including the fast-moving cane toad scourge), according to the Pew Environment Group and The Nature Conservancy. This summer, the two groups launched the Wild Australia Program, a $14 million, 3-year conservation effort.

Open savanna with termite mounds in Queensland.

CREDITS (TOP TO BOTTOM): R. GOLDSTEIN/UNIVERSITY OF CAMBRIDGE; J. LURIE; K. TRAPNELL

# More Microarray Applications

Molecular Devices offers the most broadly applicable microarray scanning and analysis package on the market. With the industry-leading Axon GenePix® system, you can perform virtually any fluorescent microarray application in a standard microscope slide format.

- Gene Expression: Easily scan and analyze 1-color to 4-color arrays from any source, whether home-brewed or commercially manufactured
- Comparative Genomic Hybridization (CGH): Unique AutoPMT function in Axon GenePix Pro ensures optimal scans using all array features
- Protein array: Non-confocal 64 $\mu$m focal depth ensures optimal imaging of membrane-slide protein arrays, and surface scanning allows the use of non-transparent substrates
- ChIP-Chip and Methylation: Visualize results in genomic context with Axon Acuity® software's Chromosome Viewer
- And many others: If it's fluorescent and fits within a standard slide format, we can accommodate it.

**Arcturus® Microgenomics and Axon Microarray Tools**

- **NEW!** Arcturus Turbo Labeling™: RNA/DNA labeling for microarrays
- Axon GenePix 4100A, 4000B, 4200A, and 4200AL microarray scanners for the full spectrum of applications and throughput
- Axon GenePix Pro 6 image analysis and Axon Acuity 4 microarray informatics software

Expect more. We'll do our very best to exceed your expectations.

**Molecular Devices**

*now part of MDS Analytical Technologies*

tel. +1-800-635-5577 | www.moleculardevices.com

## Research Awards for Innovation in Neuroscience (RAIN)

The Society for Neuroscience is pleased to announce the inaugural year of the Research Awards for Innovation in Neuroscience. The prize was established to honor imaginative, innovative research that will advance novel ideas an have the potential to lead to significant breakthroughs in the understanding of the brain and nervous system and related diseases.

**Deadline for receipt of nomination packages: Monday, September 17, 2007.**

**For details please visit www.sfn.org/rain.**

SOCIETY FOR NEUROSCIENCE

## *Smart*Shutter™ Stepper-Motor Driven Shutter

- As fast as 8msec from trigger to open or close
- Choose between fast or "soft" speeds
- Programmable control of exposure time delay
- Free running or timed interval operation
- Variable aperture settings for neutral density
- Life tested to over 100 million cycles
- 25mm, 35mm or 50mm shutters available
- Modular repairable design
- USB or TTL control

SUTTER INSTRUMENT

ONE DIGITAL DRIVE, NOVATO, CA 94949
PHONE: 415.883.0128 | FAX: 415.883.0572
EMAIL: INFO@SUTTER.COM | WWW.SUTTER.COM

EDITED BY YUDHIJIT BHATTACHARJEE

## On Campus

**WAR OVER WORDS.** Pediatrics researcher Frederick Zimmerman (left) is finding out that baby talk can be dangerous. Last week, the Walt Disney Co. attacked a study he published this month in the *Journal of Pediatrics* suggesting that baby videos might do more harm than good to infants' language development. Robert Iger, CEO of Disney, which owns the popular Baby Einstein series of educational videos, said that Zimmerman's work was flawed and that a press release from his institution, the University of Washington (UW), Seattle, misrepresented the study's findings. UW President Mark Emmert has defended the work and rejected Disney's call for a retraction of the release.

The study, based on parental interviews, found that infants who watched a lot of "baby DVDs" understood fewer words than those who viewed fewer videos understood. Disney says Zimmerman and colleagues shouldn't have lumped together all baby videos and that other studies have shown that "the specific nature of content and the way [the video] is consumed are vitally important."

Zimmerman says he would welcome data from Disney on the topic and that his paper "is not the definitive study in the area."

## INSIDE GOVERNMENT

**WHO'S THE BOSS?** Since its creation in 1950, the National Science Foundation (NSF) has provided staff and support to the National Science Board (NSB), the body that oversees the $6 billion agency. The arrangement has grown somewhat contentious in recent years, however, as NSB has sought to assert its independence. This month, the tension reached a new high when Lawrence Rudolph (below), NSF's longtime and influential general counsel, suggested at the board's most recent meeting that the 24-member presidentially appointed panel might want to ask Congress for permission to hire its own general counsel and other key staffers if the board felt its interests and those of NSF were no longer compatible.

Rudolph's blunt words come in the wake of recent congressional unhappiness with the board's behavior (*Science*, 3 August, p. 579). And they appear to have caught NSB chair Steven Beering and NSF Director Arden Bement off-guard. "I can't take seriously the idea that we separate the two bodies," says Beering. "This relationship has worked for 57 years, and I think it should be strengthened, not weakened."

Bement says the board and the agency have endured some rocky times but are now in sync. "The board chairman and I pledged upon his election to do our utmost to improve communications, and as a result they have improved considerably," he notes. Rudolph declined to elaborate on his comments.

## MOVERS

**OFF THE RAILS?** Three research policy leaders within the U.S. Department of Health and Human Services are leaving, and their posts may remain vacant until the next Administration. John Agwunobi, a pediatrician who has been assistant secretary for health since 2005, is joining Wal-Mart as a senior vice president overseeing its health division. Congress doesn't seem to be in any big hurry to approve President George W. Bush's nominee for surgeon general, James Holsinger Jr., especially after the previous incumbent, Richard Carmona, recently denounced his former bosses for stifling science. And next month, career fed Bernard Schwetz steps down as head of the Office for Human Research Protections. Fortunately, says biomedical lobbyist Anthony Mazzaschi, such positions are often held on an acting basis by "pretty competent federal employees … who keep the train on the track."

After 4 years on the job, physicist **Robert Dynes** has announced that he will step down as president of the University of California system in June 2008 and return to full-time research at UC San Diego. Dynes's tenure has been marked by controversy, including what critics said were extravagant salaries and perks awarded to dozens of senior university administrators.

**William Jeffrey**, a physicist by training, is resigning after 2 years as director of the National Institute of Standards and Technology to head the science and technology effort at the Institute for Defense Analysis in Alexandria, Virginia.

## Pioneers >>

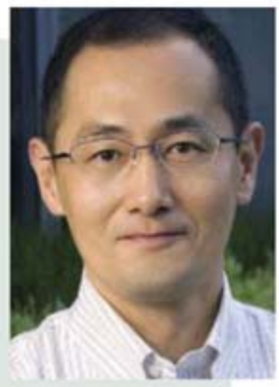

**QUICKENING THE PACE.** One of Japan's hottest stem cell scientists is moving to California, in part because of a more favorable research environment. Shinya Yamanaka, who last year conferred the transformative powers of embryonic stem cells upon skin cells taken from adult mice, will be joining the Gladstone Institute of Cardiovascular Disease in San Francisco, where his work will be partly funded by the state's stem cell initiative. He'll initially split his time between Gladstone and his current institution, Kyoto University, and within a few years leave his Kyoto post and move to San Francisco.

Yamanaka's accomplishment with mouse cells has raised hopes of developing therapies that avoid ethical concerns about using human eggs or embryos (*Science*, 8 June, p. 1404). He is now racing with other researchers to reprogram adult human cells, and he says that work will proceed faster in California than it would in Japan, where lengthy applications and prolonged reviews slow down research. Yamanaka plans first to bring his human cell research to Gladstone, where he did a postdoc in the 1990s, and leave his mice in Japan for now.

CREDITS (TOP TO BOTTOM): SOURCE: FREDERICK ZIMMERMAN; INSET: MISTY BEDWELL/DESIGN PICS/CORBIS; NSF; CHRIS GOODFELLOW/GLADSTONE INSTITUTE

All eyes on the river 1019

Being here and there 1020

PALEOANTHROPOLOGY

# Fossil Teeth From Ethiopia Support Early, African Origin for Apes

Fossils of a new species of large-bodied ape are giving a rare glimpse of the origins of the African apes. This week in *Nature*, a team of Ethiopian and Japanese researchers reports the discovery of nine teeth that resemble those of modern gorillas—but that belonged to an ape that lived about 10 million years ago in the Afar Rift of Ethiopia. The team suggests that the newly discovered ape, called *Chororapithecus abyssinicus*, might have been a primitive gorilla or a close relative. If so, it pushes back the origin of gorillas from about 8 million years ago to more than 10.5 million years ago, says paleoanthropologist Gen Suwa of The University Museum of the University of Tokyo.

Gorilla or not, several experts agree that an ape of this antiquity in Africa strikes a blow at a hypothesis that the common ancestor of African apes arose in Eurasia and migrated to Africa. "These are very important fossils," says Alan Walker, a paleoanthropologist at Pennsylvania State University in State College. "They show that apes have always been in Africa—that they didn't come from Europe and Asia."

Paleoanthropologists have known for decades that apes (Hominoidea) arose in Africa, where researchers have found diverse apes from 22 million to 12 million years ago. But despite many searches, almost no ape fossils have been found in Africa between 12 million and 7 million years ago, with the notable exception of a 9.5-million-year-old upper jaw from Kenya. Some researchers inferred that apes went extinct in Africa while other apes flourishing in Eurasia gave rise to the ancestors of modern African apes.

When the researchers discovered the first canine of *Chororapithecus* on the last day of their field season in February 2006, they realized it came from within the fossil gap. "I knew it was some kind of big ape," says paleoanthropologist Berhane Asfaw of the Rift Valley Research Service in Addis Ababa.

Returning to the site last March, they found eight molars. The teeth, from at least three individuals, were "indistinguishable" in size and proportions from those of gorillas. Micro–computed tomography scans showed more similarities. The team proposed the animal as an early member of the gorilla clade.

**Close match.** Ten-million-year-old fossil teeth (*left*) resemble those of modern gorillas (*right*).

The detailed analysis of the teeth is "one of the best I've seen," says paleoanthropologist Jay Kelley of the University of Illinois, Chicago. Still, he and others say the teeth may have belonged to apes that had independently adapted to a ▶

POSTDOCTORAL TRAINING

# NSF, NIH Emphasize the Importance of Mentoring

Like apprentices in other fields, U.S. postdocs work for peanuts and are discouraged from pursuing their own ideas in return for the chance to learn the profession. But supervisors must also hold up their end of the bargain by being good mentors. That's what two key science agencies have reminded investigators this month in policy directives that emphasize their role in helping postdocs grow into independent researchers.

The message is tucked into the newly enacted America COMPETES Act (*Science*, 10 August, p. 736). It requires researchers to include a mentoring plan in every grant application to the National Science Foundation (NSF). It's also contained in a statement issued by the National Institutes of Health (NIH) clarifying that its grantees may use some of their time to mentor postdocs and students. Both make it clear to universities that "postdocs are not just to be treated like workers," says Alyson Reed, executive director of the National Postdoctoral Association (NPA) in Washington, D.C.

Under the COMPETES Act provision, NSF grant applicants must document proposed mentoring activities, which could include "career counseling, training in preparing grant applications, guidance on ways to improve teaching skills, and training in research ethics." Although many applicants already do this, says James Lightbourne, an adviser in the NSF director's office, making it a requirement should encourage principal investigators (PIs) to take mentoring more seriously. The provision codifies and expands a pilot effort started last year by NSF's geosciences directorate (*Science*, 11 August 2006, p. 748).

The NIH statement (grants1.nih.gov/training/q&a.htm#mentor) says that grantees can count time spent training students and postdocs as grant-related activities provided the training is related to the research being funded. That would enable postdocs to attend workshops and seminars relevant to their project, says Walter Schaffer, senior scientific adviser for extramural research at NIH. But Schaffer says it would not allow PIs to dispatch their postdocs to teach graduate students.

The policy is a small step forward, says Keith Micoli, an NPA board member and a researcher at the University of Alabama, Birmingham. But more steps are needed. "If postdocs can't do work on a project that's not funded by the grant," he asks, "how can they be expected to conduct preliminary experiments to apply for their own grants?"

–YUDHIJIT BHATTACHARJEE

CREDIT: GEN SUWA

The Great Mimicker
1022

Stemming cancer
1029

gorillalike diet. Suwa acknowledges in *Nature* that the dental evidence for a close relationship with gorillas is "inconclusive" but adds that no other living or fossil apes this big have molars as specialized for shredding fibrous vegetation.

If *Chororapithecus* is indeed an early form of gorilla, it would falsify the Eurasian-origins hypothesis, says Walker. It would also push back the origin of gorillas to between 10.5 million and 12 million years ago. That is at least 2 million years earlier than most large nuclear DNA studies predict, says Sudhir Kumar, an evolutionary geneticist at Arizona State University in Tempe. Such a shift would also force researchers to recalibrate when the human and chimp lineages split to between 7 million and 10 million years ago (up from 5 million to 7 million), and when orangutans split from other apes to between 15 million and 23 million years ago (up from 14 million).

But a key author of the Eurasian-origins hypothesis, paleoanthropologist David Begun of the University of Toronto in Canada, says it is too soon to "dismiss the Eurasian evidence," including traits linking Miocene apes in Europe to later African apes—and also too soon to recalibrate the ape family tree.

Regardless of whether *Chororapithecus* is a true protogorilla, it finally provides some hard data with which to test evolutionary models. "It's nice indeed to have at least something hominoid from this time and place," says Harvard University paleoanthropologist David Pilbeam. **–ANN GIBBONS**

VIROLOGY

# China, Vietnam Grapple With 'Rapidly Evolving' Pig Virus

A pig disease ravaging China now appears to have spilled into Vietnam. Scientists fear that a deadlier strain of a longtime foe, porcine reproductive and respiratory syndrome (PRRS), or blue-ear disease, may be on the loose.

"We're fairly confident that there has been an outbreak of PRRS here," says Andrew Speedy, who represents the U.N. Food and Agriculture Organization (FAO) in Vietnam. An FAO mission that completed a weeklong visit to Vietnam on 20 August also uncovered many secondary infections that increase the disease's death toll, Speedy says. The team concluded that PRRS can likely be controlled through vaccination and antibiotic treatment of secondary infections.

PRRS was first identified in the United States in the mid-1980s; the causative arterivirus was isolated in 1991. The virus does not infect humans. In pigs, it attacks macrophages, which ingest and remove invading bacteria. With a crippled immune response, pigs are susceptible to secondary infections. Adults usually recover and develop immunity, but the virus and secondary infections can kill piglets, whose ears often turn blue from the secondary infections.

"The evolution of the virus is really quite startling. It is probably one of the most rapidly evolving viruses that I know of," says Trevor Drew, head of virology at the Veterinary Laboratories Agency in Weybridge, U.K. He explains that, typically, a virus circulating in a new host initially causes severe disease and becomes less pathogenic over time. With PRRS there is evidence that the opposite has occurred: A nonpathogenic strain was circulating among pigs in North America before it evolved and started causing disease.

An even nastier strain seems to be on the rampage in China, killing sows as well as piglets. This strain first appeared in the summer of 2006. China has reported losing 400,000 pigs to the disease through death or culling in 2006 and another 243,000 this year, although some contend that official numbers vastly understate the losses.

In an analysis of viral samples from pigs in China published online in *PLoS ONE* on 13 June, a group led by George Gao, a microbiologist who heads the Institute of Microbiology in Beijing, described a genetic variation that may be responsible for the virus's increased deadliness. Drew, who finds that claim plausible, says that the possibility of a new and deadlier strain "is very worrisome."

Media outlets, including an article last week in *The New York Times*, reported allegations that China has refused to share virus samples and cooperate with international organizations. Drew says that's not so, pointing to Gao's paper and to China's reporting on the outbreak to the Paris-based World Organisation for Animal Health. Guo Fusheng of FAO's Beijing office says that the organization has not yet asked China's Ministry of Agriculture for samples or to allow an outside team to investigate, although it expects to make a formal request shortly.

Vietnam didn't wait to be asked. The disease was first reported there in March. Last month, the government asked FAO for assistance after the outbreaks increased in June and July. Samples have been sent to U.S. labs for analysis. **–DENNIS NORMILE**

CREDIT: REUTERS/CHINA DAILY/LANDOV

**In the pink.** A veterinary worker prepares to vaccinate pigs against PRRS in China's Shandong Province.

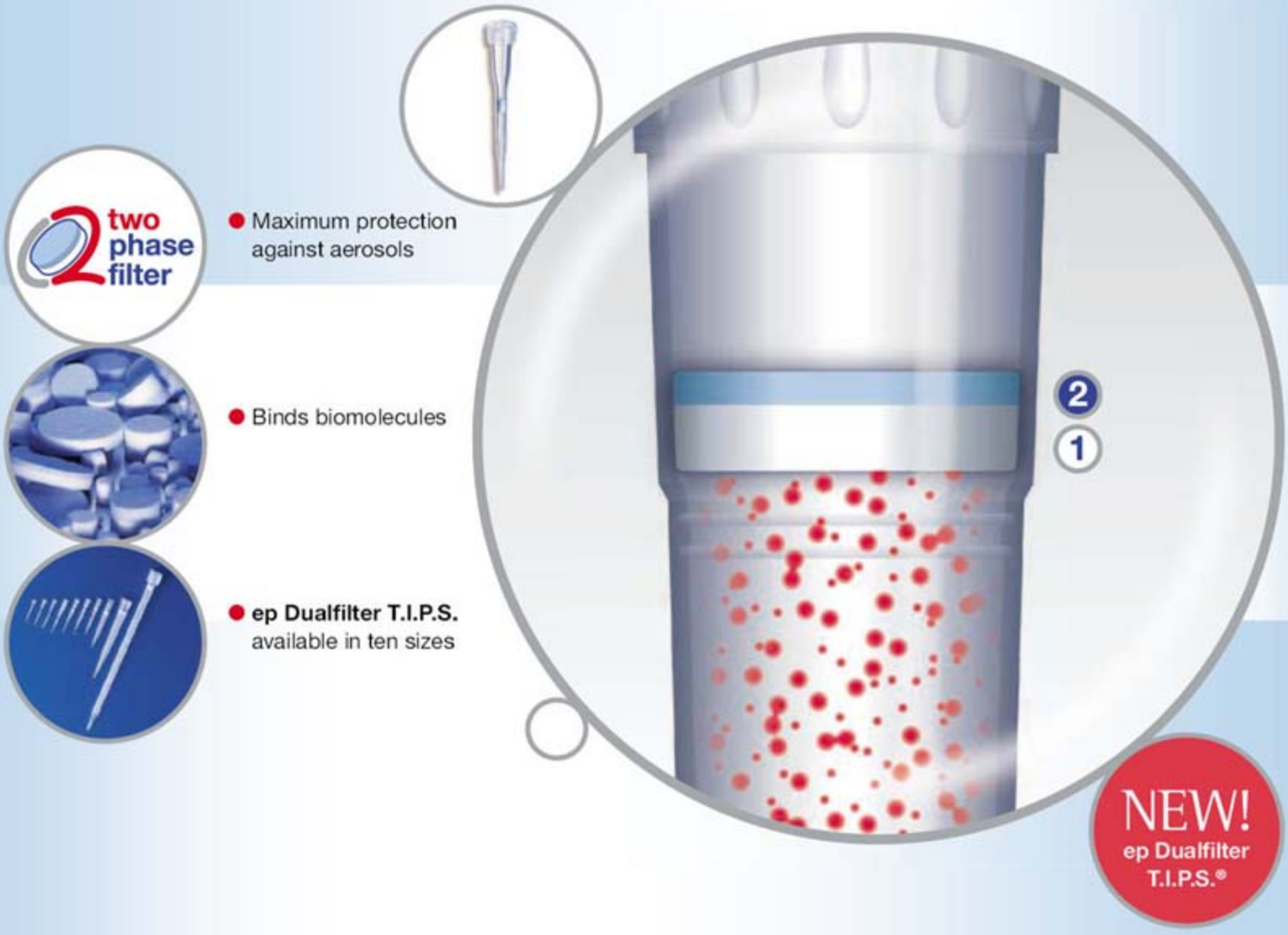




# Stop aerosols!

## Unique two-phase filter protection with ep Dualfilter T.I.P.S.®

**The new Eppendorf ep Dualfilter T.I.P.S., with their unique two-phase filter, provide the perfect shield against contamination.**

The filter consists of two visible phases, each with a different pore size. This two-phase filter protection ensures ultimate absorption of aerosols ❶ and biomolecules ❷, outmatching all conventional filters. Rely on it.

For more information go to
www.eppendorf.com/dualfilter

**Features of the ep Dualfilter T.I.P.S.**
Double protection provided by the two phase filter

- Provides maximum protection for both pipette and sample
- Ultimate absorption of aerosols and biomolecules
- Free from PCR inhibitor additives
- Patent pending two phase filter technology
- Supplied sterile, Eppendorf PCR clean and pyrogen-free
- IvD conformity
- Batch-related certificates available

eppendorf
*In touch with life*

**Your local distributor: www.eppendorf.com/worldwide · Application Support: +49 180-3 66 67 89**
Eppendorf AG · Germany · +49 40 538 01-0 • Eppendorf North America, Inc. 800-645-3050

RIVER MONITORING

# New York Research Institute Hopes to Go With the Flow

An ambitious plan to monitor the entire Hudson River in real time is one step closer to reality, thanks to a new collaboration with IBM announced last week. The ultimate goal is a system that could track the movement of PCB-contaminated sediment, for example, or warn a commercial power plant to shut its intake valve temporarily because of an approaching school of fish. "It will be the first real-time, distributed river network in the world," says John Cronin, director of the nonprofit Beacon Institute for Rivers and Estuaries in New York.

The River and Estuary Observatory Network (REON) is part of a new wave of observing networks, like the even more ambitious Integrated Ocean Observing System, a federally funded program to expand and link regional coastal networks (*Science*, 3 August, p. 591). Meanwhile, another group of scientists is hoping to interest the National Science Foundation in funding a network of eight to 10 research stations around the country that would study threats to water supplies.

Since 2003, the Beacon Institute has been coordinating a prototype, called Riverscope. Researchers from Lamont-Doherty Earth Observatory and Rensselaer Polytechnic Institute have measured temperature, salinity, and other variables in a few spots along the Hudson River. Although REON is still early in the design phase, heavyweights have already signed on. The state of New York has committed $50 million, most of which will support a new research building. Groundbreaking is expected in 2009 at Denning's Point near Beacon, New York, but scientists hope to begin deploying new sensors this spring.

On 16 August, the Beacon Institute announced a major partnership: IBM will pick up the tab for a new computer system designed to analyze streams of data in real time—a contribution worth perhaps tens of millions of dollars. "It is very, very exciting," says ecologist Margaret Palmer of the University of Maryland Center for Environmental Science in Cambridge, Maryland.

The river network will be IBM's first public application of its System S, a new type of computer system called stream computing that can handle many types of data—such as video and sound—simultaneously. With processors distributed near the sensors, the system can filter and classify the data in real time and autonomously decide whether to take more detailed or frequent readings at a particular site, for example, during flooding. "The system will learn," says IBM's Harry Kolar, who says that IBM is getting a chance to test its technology.

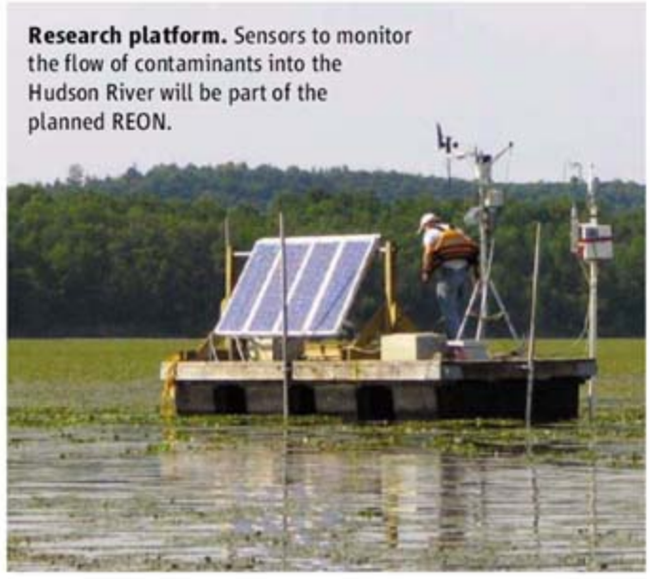

**Research platform.** Sensors to monitor the flow of contaminants into the Hudson River will be part of the planned REON.

CREDIT: WADE MCGILLIS/LAMONT-DOHERTY EARTH OBSERVATORY OF COLUMBIA UNIVERSITY

A second phase, at least 10 years away, would include permanent sensors and perhaps even robotic submersibles that can beam back data. This full system will require another $150 million of fundraising, Cronin estimates. Philip Bodgen, who directs the Gulf of Maine Ocean Observing System, says he thinks the institute has a good chance of finding the money needed for ongoing maintenance and operations because the Hudson River is less challenging logistically than the ocean and the project is more visible to potential donors.

Once running, REON could be used for everything from studying the impact of fertilizers to monitoring the quality of drinking water. "It will be a net savings to the state to get ahead of their environmental problems," predicts Thomas Harmon, an environmental engineer at the University of California, Merced. **–ERIK STOKSTAD**

## Thais Say Aye to GM?

**BANGKOK**—Thailand may lift a 6-year-old ban on field trials of genetically modified (GM) crops. Concerned that the country's agriculture efforts are lagging behind those of China and other neighbors, Thailand's agriculture ministry was expected this week to petition the country's Cabinet, installed after a coup last year, to rescind a moratorium on open-air experiments. Critics of GM crops say the country lacks adequate biosafety laws and are urging the Cabinet to stand firm. The ministry's top priority is a GM papaya strain resistant to a ringspot virus that has decimated orchards in Thailand and elsewhere. **–RICHARD STONE**

## German Physics Facilities Achieve Fusion

**BERLIN**—Materials scientists will have a new one-stop shop in Berlin when BESSY, an accelerator-driven x-ray source, and the Hahn-Meitner Institute (HMI), which boasts a reactor-based neutron source, merge into a single institute in 2009. Both facilities allow scientists to probe the atomic structure of materials, from protein crystals to high-tech ceramics. The merger, announced last week, will produce an institute with 1000 employees and a yearly budget of $136 million, almost entirely from the German federal government. That is a significant funding boost for BESSY, which will no longer have to charge users for beam time. The fusion will produce one of the few places in the world with expertise with both types of probes, says HMI Director Michael Steiner.

**–GRETCHEN VOGEL**

## Mmmm, Beer

Farmers, biofuel enthusiasts, and, yes, brewmasters could soon get a little enlightenment from German plant geneticists. Last week, the German government put up $8 million to more fully map and partially sequence the genome of barley, a key crop used worldwide in animal feed, human food, and beer.

Funding agencies have been slow to tackle crops such as wheat and barley because of the daunting size of their genomes. At 5 billion bases, barley's genome is nearly double the size of the human genome. But it is only one-third wheat's size and lacks that genome's multiple copies, so it should be easier to sequence, says plant geneticist Nils Stein of the Institute of Plant Genetics and Crop Plant Research in Gatersleben, Germany, whose team will create a draft sequence of 10% of the genome. Stein hopes the work, along with a British-led barley sequencing pilot, will set the table for a large-scale sequencing project. **–ELIZABETH PENNISI**

PSYCHOLOGY

# Out-of-Body Experiences Enter the Laboratory

Out-of-body experiences are associated more with tabloid newspapers, New Age Web sites, and large doses of hallucinogenic drugs than serious scientific discussion. Yet they're often reported by reputable people who suffer from migraine headaches, epilepsy, and other neurological conditions. Intrigued by such accounts, some researchers are trying to figure out how the brain creates an aspect of human consciousness so fundamental that we take it for granted: the perception that the "self" conforms to the borders of the physical body.

**Where am I?** Swiss researchers used a video camera to give people wearing display goggles the feeling they inhabited a virtual body (*right*) in front of their real location.

Now, two teams of cognitive neuroscientists independently report on pages 1048 and 1096 methods for inducing elements of an out-of-body experience in healthy volunteers. Both groups used head-mounted video displays to give people a different perspective on their own bodies. Each team also drew upon the sense of touch to enhance the illusion. Although details of the experience differed, the people in both experiments reported feelings of dissociation from their bodies. The researchers say their findings will pave the way to new brain-imaging studies of body perception and could have practical applications, such as helping virtual-reality programmers design environments that make users feel as if they are really *there*.

"It's striking because when you hear about out-of-body experiences, it sounds so deeply weird," says Chris Frith, a cognitive neuroscientist at University College London who did not participate in the new research. "These studies show you can actually manipulate it experimentally." The illusions add to evidence that the brain's representation of the physical body is malleable and can be modified by information from the senses, Frith says.

For one of the studies, a team led by Bigna Lenggenhager and Olaf Blanke, both of the Swiss Federal Institute of Technology in Lausanne, asked people to stand in front of a camera while wearing video-display goggles. In one experiment, subjects saw the camera's view of their own back, computer-enhanced to create a three-dimensional "virtual own body." When the subjects' backs were stroked with a highlighter pen at the same time they saw their virtual back being stroked, they reported that the sensation seemed to be caused by the highlighter on their virtual back, making them feel as if the virtual body was in fact their own body.

Moreover, when the researchers turned ▶

GENETICS

# Epidemiologist Sees Flaws in Papers on Genes and Gender

An epidemiologist who for years has critiqued the veracity of published papers has now tackled a hot area in genomics, sex-based genetic differences. He argues that most reported findings are poorly documented and that about a sixth may actually be wrong.

As researchers move beyond uncovering new disease genes and into the realm of gene-environment interactions, John Ioannidis, a clinical and molecular epidemiologist at the University of Ioannina School of Medicine in Greece, decided to follow them. He wondered especially about genetic associations with diseases that seem to vary by gender—for example, a particular gene variant that confers increased risk in women but not in men, an effect that may be modulated by hormones. Hundreds of such associations have been reported. But when Ioannidis and two colleagues analyzed data from 77 papers covering everything from multiple sclerosis to lung cancer to anger, they found that19 had at least one claim they judged to be "spurious," or apparently incorrect. Only four papers contained neither spurious nor insufficiently documented claims, says Ioannidis.

He and his colleagues searched online for papers whose titles touted gender variation in gene effects, then examined each claim (a total of 432 sex-difference claims in the 77 papers). To determine whether claims were spurious, they considered the groups being compared—for example, older men and older women, which would be appropriate, or older men and younger women, which would not. They looked for evidence in the paper that claims reached statistical significance. Those without were judged not sufficiently documented. The analysis was published in the 22/29 August issue of the *Journal of the American Medical Association*.

Of the gene-gender findings, says Ioannidis, "there is a problem with just accepting them and believing that they're true." Proper documentation was found in only 55 claims, or 13% of the total.

The Ioannidis paper reinforces concerns about the quality of published genetics results, says Neil Risch, a genetic epidemiologist at the University of California, San Francisco. Still, he defends some findings in the field, such as a greater risk for women with an Alzheimer's gene and a greater risk for males who carry a gene variant linked to rheumatoid arthritis. The Ioannidis analysis did not pick up

CREDIT: OLAF BLANKE/LABORATORY OF COGNITIVE NEUROSCIENCE (EPFL)

off the video display, guided the subjects back a few steps, and then asked them to blindly return to their former position, subjects overshot the spot where they'd actually been standing and walked to a point closer to the apparent location of their virtual body.

Adopting a similar strategy to attempt to induce out-of-body experiences, Henrik Ehrsson of the Karolinska Institute in Stockholm, Sweden, asked men and women to sit in a chair and don a video headset connected to two cameras that provided a stereoscopic view of their backs. As a subject viewed his or her own back from behind, Ehrsson used two plastic rods to simultaneously stroke the subject's chest and a location behind the subject's back. Although people felt the rubbing on their chest, in the headset they could only see Ehrsson's arm moving behind their back, reinforcing the sense that they were sitting at a location behind their actual body. The experience often elicited surprised giggles, says Ehrsson, who has tried it out himself. "You really feel that you are sitting in a different place in the room and you're looking at this thing in front of you that looks like yourself and you know it's yourself but it doesn't feel like yourself," he says. "It's almost like you're looking at a dummy." Nearly all subjects reported similar impressions on a questionnaire.

Ehrsson also repeated the illusion with electrodes attached to each person's fingers to measure skin conductance, a physiological measure of emotional arousal. Then he swung a hammer in front of the cameras so that it appeared to hit the region where people perceived themselves to be. The hammer posed no physical danger, but changes in skin conductance indicated that subjects registered a threat (they also reported feeling anxious). By showing that people respond emotionally as if they were located at a position behind their physical body, the findings provide additional evidence that the subjects buy into the illusion, Ehrsson says.

Both experiments show that visual perspective and coordination between the senses of vision and touch are important for the sensation of being within the body, says Peter Brugger, a neuroscientist at University Hospital Zürich in Switzerland. Yet neither study replicated the full-blown out-of-body experiences in which people report "an enormously compelling sensation of separation from the body," he notes. Even so, Brugger says, these illusions may be as close as it is possible to get in the lab.

Previous research has pointed to several brain regions, including the intersection of the temporal and parietal lobes, that may be involved in producing out-of-body experiences in neurological patients, Blanke says. The new illusions can be used to examine which of these brain regions contribute to which aspects of these strange experiences, and that in turn, says Blanke, could lead to a better understanding of how the brain generates a concept of self. **–GREG MILLER**

these papers in its literature search because it netted only those with "polymorphism" and either "sex" or "gender" in the title.

Some scientists whose papers Ioannidis has critiqued agree that it's difficult to know

**"There is a problem with just accepting [the claims]** and believing that they're true."
—John Ioannidis, University of Ioannina

whether a finding will hold until it's been replicated. "Admittedly, the strength of an observation such as ours lies not only with the experimental design, but with the ability of other investigators to reproduce the observation," wrote Judith Miller, a kidney disease specialist at the University of Toronto, Canada, in an e-mail. David Christiani, an epidemiologist at Harvard School of Public Health in Boston, agreed in an e-mail that his 2004 study in *Chest* on acute respiratory distress syndrome had limited statistical power but added that this was noted in the paper.

Ioannidis, however, thinks that researchers need to do a much better job of stating the limits of their findings. "The papers should have been published," he says, noting that "nothing is perfect." But "better transparency" is sorely needed.

"People make claims from their data that just are not there," agrees Kathleen Merikangas of the National Institute of Mental Health in Bethesda, Maryland. Contributing to the problem, she says, is that many studies that fail to replicate a genetic finding are never published because they're "not new and exciting, or the scientists themselves don't find that it's going to advance their career." **–JENNIFER COUZIN**

## Time Out for Institute Leader

A large number of scientists at the National Institute of Environmental Health Sciences (NIEHS) have turned against their embattled director. Of 146 staff scientists who responded to a survey by NIEHS's Assembly of Scientists, 107 said they did not have confidence in David Schwartz's leadership. This week, Schwartz (below) stepped down temporarily as the National Institutes of Health (NIH) launched a sweeping management review of the $642-million-a-year institute in Research Triangle Park, North Carolina. NIH Director Elias Zerhouni said that the review is in response to congressional inquiries, which have included Schwartz's management of his personal lab, his consulting for law firms, and his handling of NIEHS's journal (*Science*, 6 July, p. 26).

CREDIT: NIH

Senator Charles Grassley (R–IA) wrote Zerhouni this week to ask why some NIEHS employees had recently been given a form for logging calls received from congressional investigators. The form could intimidate potential whistleblowers, which would be "not only wrong but also illegal," Grassley says. **–JOCELYN KAISER**

## U.S. Targets Add-On Patents

In an effort to streamline its operations, the U.S. Patent and Trademark office is clamping down on how often applicants can tweak their inventions. Last year, 30% of all patent filings were continuations, in which inventors add details to a pending application. So this week, after 18 months of wrangling with the community, the office decided to limit such filings to two per patent, with petitions required for further continuations.

Biotech companies oppose the new limits, which they believe will deprive the patent office of information that could strengthen applications, including results from ongoing work. But lawyer Peter Zura of Bell, Boyd & Lloyd LLP in Chicago, Illinois, thinks the changes are not an "end-of-the-world thing" because firms that write biotech patent applications, including his own, will devise ways to protect their proposed inventions, such as more rigorously constructing original applications. But "it's definitely going to make life more difficult," he says. **–ELI KINTISCH**

**Once ignored as an obscure disease, melioidosis and the frighteningly versatile bacterium that causes it are drawing attention as a bioterror threat**

# Racing to Defuse a Bacterial Time Bomb

**UBON RATCHATHANI, THAILAND**—A Thai man with lank black hair and grizzled stubble lolls on a cot parked in a hallway outside a crowded ward. The 61-year-old farmer answers tersely as a senior physician, Wipada Chaowagul, quizzes him. When the man was admitted on 9 May with sepsis and an abscess in his chest wall, Wipada fingered an old nemesis: melioidosis. But although nearly nine out of 10 melioidosis patients in Thailand with septic shock die, somehow the farmer beat the odds. After spending 2 months in Sappasithiprasong Hospital here in northeastern Thailand, the taciturn man with watery eyes is almost well enough to go home.

Wipada can't explain how the farmer, who suffers from kidney disease, managed to fend off a bacterium, *Burkholderia pseudomallei*, that in its fiercest incarnation kills most of its victims. Indeed, there is no shortage of scientific puzzles surrounding melioidosis. Over the 2 decades that Wipada has studied the once-obscure malady, more and more experts have become intrigued by the ability of *B. pseudomallei* to alter its form and survive in environments as disparate as soil, distilled water, and the human body.

"There's something incredibly interesting and important going on with *pseudomallei*, and nobody knows what that is," says Colin Manoil, a geneticist at the University of Washington, Seattle.

Melioidosis is largely confined to Southeast Asia and northern Australia and, fortunately for the rest of the world, researchers don't anticipate the shape-shifting bug breaking out of its ecological cage anytime soon. But its characteristics make it an insidious threat as a bioweapon. The bacteria can hide in the body for decades. Once the time bomb detonates, a constellation of symptoms allows melioidosis to masquerade as other ailments. Although many patients are rushed to the hospital with acute disease, others have symptoms more akin to tuberculosis or cancer, says Sharon Peacock of the Mahidol-Oxford Tropical Medicine Research Unit (MORU) in Bangkok. Misdiagnosis can prove fatal: *B. pseudomallei* is impervious to all but a few antibiotics.

"It's not as scary as anthrax or smallpox," says Peacock, who has spent 20 years on the trail of melioidosis. "But it still has a significant terror factor. Once soil is contaminated, *B. pseudomallei* is very hard to get rid of."

Scientists know they are up against a worthy foe. "Viruses are very smart. Bacteria are normally not so smart. *pseudomallei* acts like a virus" in its deviousness, says Surasakdi Wongratanacheewin, director of the Melioidosis Research Center at Thailand's Khon Kaen University. Hoping to strengthen their defenses, researchers launched a drug trial this month at Sappasithiprasong. And a pilot experiment is under way in Ubon Ratchathani to take the battle to *B. pseudomallei*'s home turf: Thailand's ubiquitous rice paddies.

**Certain exposure.** Rice farmers in northeastern Thailand are at high risk of contracting melioidosis.

CREDITS: R. STONE/SCIENCE

## The Great Mimicker

Melioidosis was first described from opium addicts in Burma in 1911, and in 1947, two cases involving POWs held in Siam were reported in the *British Medical Journal*. It wasn't until the Vietnam War, however, when U.S. soldiers came home with the disease, that melioidosis attracted significant attention in the West. The first Thai case was reported in 1955. "No one had ever seen this before," says tropical medicine specialist Sompone Punyagupta, former president of Vichaiyut Hospital in Bangkok. In the 1960s,

**Grim prognosis.** *Burkholderia pseudomallei* colonies in a blood agar dish.

scientists isolated *B. pseudomallei* from soil throughout Thailand and determined that about a third of Thai soldiers sampled had antibodies to it. But with no further confirmed cases among the Thai population, Sompone says, researchers "concluded that it was not a clinically important disease."

That assessment changed in 1973, when Sompone took over a tropical medicine unit at Ramathibodi Hospital in Bangkok and realized that untold numbers of melioidosis cases were being overlooked or misdiagnosed as TB or other ailments. He dubbed the disease "the Great Mimicker." The bacterium eluded detection in part because it grows slowly in culture. Back then, dishes were typically discarded after 3 days, says Sompone, because other pathogens of interest form colonies within hours of inoculation. After giving *B. pseudomallei* colonies more time to form, he says, "we began to see more and more cases."

Since then, scientists have sketched a picture of a malady most perplexing. It's unknown whether *B. pseudomallei* lives freely in soil, in association with rhizomes that stud roots, or in a host like an amoeba. "It infects humans by accident," says Peacock. In northeast Thailand, nearly everyone has been exposed by age 4, although about 30% of the population shows no antibody response, Peacock says. Researchers suspect that *B. pseudomallei* enters the body through cuts or abrasions, or through the lungs. In Ubon Ratchathani province, the incidence fell 3 years ago when boots were handed out to curb leptospirosis, a waterborne disease, says Direk Limmathurotsakul, who runs MORU's Lab Melioid at Sappasithiprasong Hospital. But the farmers didn't like wearing boots, and case numbers shot back up (see graph, p. 1024). "The incidence looks quite bad this year," says Surasakdi.

Once the bacterium enters its human host, illness can set in within hours. "Many patients deteriorate very fast," says geneticist Sirirurg Songsivilai, assistant president of Thailand's National Science and Technology Development Agency. In other people, the bacterium lays low for years. Two years ago, researchers reported the curious case of an 82-year-old U.S. veteran held as a Japanese POW in Indochina during World War II. In 2004, he developed an infected ulcer on his right hand. Lab tests confirmed melioidosis—a whopping 62 years after his presumed exposure to *B. pseudomallei* (*Journal of Clinical Microbiology*, February 2005, p. 970). Although no one knows for sure where the microbe lurks in asymptomatic people, likely hideouts include the lymph nodes, reticular epithelial cells, the spleen, and bone marrow. "We don't understand how the body tolerates it so long," says Peacock. Antibodies don't seem to confer protection.

In more than half the known cases, a chronic illness such as diabetes or kidney disease is the spark that ignites a latent infection or allows infection from a fresh exposure. In Thailand, about 75% of cases occur during the rainy summer, when farmers slog barefoot in paddies, planting rice. Person-to-person transmission is rare, and relapses are common. "Patients need to be followed up for the rest of their lives," says Sirirurg.

Although melioidosis cases pop up sporadically around the world (see map), only northern Australia rivals Thailand in prevalence. The subtropical climate is similar to Thailand's, and in both places the typical patient is someone exposed regularly to soil. But Australian patients, who are treated in intensive-care wards, are much more likely to survive than Thai patients, who are usually treated in ordinary wards.


**Globe-girdling threat.** Although melioidosis is endemic to parts of Southeast Asia and northern Australia, cases have occurred on all continents except Antarctica.

### An emerging threat

MORU microbiologist Vanaporn "Lek" Wuthiekanun knows better than most experts what melioidosis means to victims and to clinicians. "My heart sinks when I open an incubator and see a *pseudomallei* culture. I wonder if the patient is still alive," says Lek, who, with MORU colleagues, has developed immunofluorescence microscopy as an additional tool for rapid diagnosis. The more *B. pseudomallei* colonies that sprout from a single sample, the grimmer the prognosis.

At MORU's main lab at Mahidol University in Bangkok, Lek is running a simple experiment with chilling implications. In 1993, she put some *B. pseudomallei* cells in double-distilled water to see how long the bacterium can survive in sterile conditions without sustenance. Fourteen years later, to the astonishment of Lek and her colleagues, the bacteria are still alive.

Scientists are striving to unravel the genetic machinery that underlies *B. pseudomallei*'s exceptional hardiness and virulence. Its penchant for morphing—a phenomenon called phenotype switching—appears to be central to its versatility. "There is unbelievable variability in how it presents itself. It's like a population of several different organisms," says Manoil. MORU researchers have identified seven morphotypes, each with a distinct gene-expression pattern. Type 1 is most often cultivated from people and soil. "If you cause it to switch to another morphotype by starving it, for example, a whole battery of things switches on or off," Peacock says.

Three years ago, Matthew Holden, a pathogen genome analyst at the Wellcome Trust Sanger Institute in Hinxton, U.K., and 47 colleagues published *B. pseudomallei*'s genome (*Proceedings of the National Academy of Sciences*, 28 September 2004, p. 14240). It weighs in at a hefty 7.25 million base pairs on two chromosomes (most bacteria have one), and its chromosomes are dotted with "genomic islands" harboring genes acquired from other organisms. "Much of the genome is devoted to functions that equip it to survive and thrive in the environment," says Holden. That includes "a well-stocked arsenal of virulence factors," he says.

Like salmonella and shigella, the bacterium appears to use a molecular syringe to invade host cells. Other elements of its repertory remain shadowy. "The virulence mechanisms of this bug are virgin territory," says Manoil, who is working with Sirirurg at Siriraj Hospital in Bangkok to probe the relation between *B. pseudomallei*'s morphotypes and virulence. Genetic differences between strains will shed

SOURCE: ADAPTED FROM *CLINICAL MICROBIOLOGY REVIEWS*

light on variations in virulence and on the bacterium's enigmatic origins, predicts Bart Currie, head of the melioidosis research program at the Menzies School of Health Research in Darwin, Australia. Also intriguing are the mutational hot spots, called short sequence repeats, that are found in two-thirds of its genes. "When I first heard about this, I was stunned," says Manoil. The bottom line, Holden says, is that *B. pseudomallei* is "adept at adapting."

A gnawing fear is that terrorists may exploit this resourceful bug. Unsettlingly, one of the few biowarfare agents ever deployed is a cousin of *B. pseudomallei*'s, *B. mallei*, which causes glanders, a disease that primarily affects horses but can also cause an illness in people that's similar to melioidosis. The bacterium, unleashed on Allied forces in World War I, evolved from *B. pseudomallei*.

Melioidosis is more sinister than glanders. "It's different from most other potential bioweapons in that melioidosis is actually an important human disease," Manoil says. There is no vaccine. And because it takes months on antibiotics to eradicate the bacterium from the body, treating many patients in an emergency "would be extremely expensive, difficult to manage, and pose an enormous burden," says Herbert Schweizer, a microbiologist at Colorado State University in Fort Collins who will speak at a biothreat symposium at the 5th World Melioidosis Congress in November in Khon Kaen.

Preparedness against melioidosis is sorely lacking in countries where the disease is not endemic, Schweizer says. But its ability to taint food or water has led the U.S. Department of Homeland Security and two other agencies to designate "determining the growth and survival characteristics" of *B. pseudomallei* in foods as a research priority.

### At ground zero

Every Tuesday in Ubon Ratchathani, Wipada, vice director of Sappasithiprasong Hospital, runs a melioidosis clinic for survivors. Relapses can occur years after an initial bout. Suwan Baoyai, a 36-year-old diabetic, came in last December with a fever and abscesses in her spleen and right armpit. "I feel strong enough to work in the rice field now," she says. After 7 months of antibiotics, however, the mass in her armpit has not disappeared.

A short walk away, a technician at MORU's Lab Melioid is busy inoculating agar plates under a safety hood. The lab has documented more than 3000 cases since 1986, with northeast Thailand having the highest incidence in the world. Thanks to its location at the disease's epicenter, the laboratory also has been at the forefront of drug testing. In a clinical trial in the late 1980s, researchers found that the antibiotic ceftazidime nearly halved the death rate, bringing overall mortality down from 90% to 50%. (In Thailand, the death rate of septic shock patients remains stubbornly around 90%.)

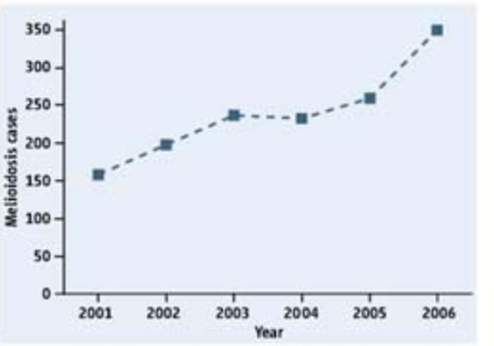


**Unhealthy trend.** Melioidosis cases are rising in the Ubon Ratchathani region.

Earlier this month, Lab Melioid launched a trial pitting ceftazidime against the antibiotic of choice for treating septic melioidosis in Australia, meropenem. Scientists expect to enroll more than 500 patients over 3 years. Another team is testing whether granulocyte colony-stimulating factor, a cytokine that boosts neutrophil counts, can help save patients with sepsis.

One counterintuitive treatment strategy might be to block a Toll-like receptor (TLR), an immune system protein, that recognizes *B. pseudomallei* but appears to interfere with other components of the immune response. A team led by Joost Wiersinga of the Academic Medical Center in Amsterdam, the Netherlands, infected two strains of knockout mice: one deprived of TLR-2, which detects Gram-positive bacteria, the other lacking TLR-4, which detects Gram-negative bacteria. Although *B. pseudomallei* is Gram-negative, it has a sugar on its cell wall that interacts with TLR-2. The TLR-4 knockouts were as likely as normal mice to succumb to melioidosis, whereas TLR-2 knockouts, surprisingly, had a big survival advantage, the researchers reported last month in *PLoS Medicine*. "We've been puzzling over the mechanism," Wiersinga says. The next step, he says, is to test whether compounds that muzzle TLR-2 reduce the severity of melioidosis in mice.

A vaccine, meanwhile, is a distant dream. "This is going to be a tricky one," Peacock says. Because the presence of antibodies does not appear to be protective, she says, a vaccine must also stimulate the cellular immune response. A few groups are scouring *B. pseudomallei*'s virulence factors for vaccine candidates. But "there's still a long way to go," Surasakdi cautions.

A different strategy is to unleash competing microbes that knock down *B. pseudomallei* soil concentrations to levels that cause few or no infections. (A high density is correlated with a high infection rate.) At MORU, Lek added Effective Microorganisms—a commercially available biofertilizer loaded with beneficial bacteria—to soil that had been sterilized and seeded with *B. pseudomallei*. The biofertilizer suppressed *B. pseudomallei*.

Now Lek is trying this out on a rice field on the outskirts of Ubon Ratchathani. A 10-year-old boy, under the watchful eyes of his proud father, is using a motorized plow to prepare a paddy for transplantation while his younger brother, also barefoot, stands idly in the middle of the paddy. The boys are up to their ankles in mud that is almost certainly teeming with *B. pseudomallei*.

Earlier this summer, Lek added Effective Microorganisms to a nearby paddy and left another paddy untouched. Over the coming months, she will compare how *B. pseudomallei* fares in the two plots. "It's too early to say anything," Lek says. But for millions of people at risk of falling prey to the Great Mimicker, even a long shot is one worth taking.

**–RICHARD STONE**


**Pleiades of death.** Type 1 is the most commonly isolated morphotype of *B. pseudomallei*'s seven known incarnations.

SOURCE: MORU; CREDIT: MORU AND JOURNAL OF BACTERIOLOGY, 2007

**Objects at risk.** Poorly curated artifacts, such as those in this mouse-eaten bag, can lose their value.

CREDITS: MARYLAND ARCHAEOLOGICAL CONSERVATION LABORATORY/JEFFERSON PATTERSON PARK AND MUSEUM

ARCHAEOLOGY

# Curation in Crisis

**As the ranks of excavated artifacts grow, museums are running out of space—and money—to care for them all**

In the storage area at the McClung Museum at the University of Tennessee, Knoxville, row upon row of boxes are stuffed with brown paper bags, which are in turn filled with hundreds of thousands of artifacts ranging from 10,000 to 200 years old. The artifacts, including stone tools, pottery, and arrowheads, were excavated during the 1960s and 1970s when the Tennessee Valley Authority (TVA) dammed the Tennessee River and its tributaries, flooding archaeological sites along the banks.

Researchers visit the collections about 10 times a year, but museum curator Lynne Sullivan, like many of her counterparts elsewhere, faces a tough job caring for them. Some of the bags have split, spilling their contents into the boxes. And the artifacts' provenance information—where they came from, which is vital to their research value—is written on the bags. TVA is required by law to care for the artifacts, which belong to the federal government, but the strapped agency doesn't have the money. So the University of Tennessee has stepped up to provide space and staffing, but it can't afford to rehabilitate the collections.

The result: a curatorial crisis. "We don't even know at some level what's going on in those bags," Sullivan says, adding that some of the metal artifacts—axes, knives, gun parts, and hoes—are rusting.

Sullivan isn't alone in her plight. Many collections in other repositories are in "much worse shape," she says. Indeed, says Dean Snow, president of the Society for American Archaeology, "the curation problem is at crisis proportions." The effects are being felt not only by researchers using museum collections but also by archaeologists in the field, who worry about where to store the artifacts they recover—and whether they should recover any at all. "I think it's the end of the days of endless archaeology," says archaeologist Teresita Majewski of Statistical Research Inc., a cultural resource management firm in Tucson, Arizona.

The curatorial problem has been brewing for decades. In 2000, a report on the U.S. Army Corps of Engineers' collections—millions of artifacts occupying nearly 50,000 cubic feet of space that could fill a dozen tractor-trailers—concluded that in about 75% of cases, artifacts had been stored in improper conditions and were quietly disintegrating; about 10% needed immediate attention. "If not properly cared for soon," the report concluded, "many [artifacts] will lose their educational and research value." As archaeologist and former curator Julia King of St. Mary's College of Maryland in St. Mary's City explains, good curation is essential because it is not the objects alone but "the relationships between the artifacts that are the critical contribution of archaeology." Curating the corps' collection, which includes projectile points and stone tools from some of the New World's earliest inhabitants, would cost an estimated $20 million, officials estimate.

In December 2005, Heritage Preservation, a nonprofit organization in Washington, D.C., made the first comprehensive survey of U.S. collections held in the public trust. They found that roughly 20% of archaeological collections need better care and that more than 40% of bulk cataloged archaeological collections have an unknown status, meaning that they hadn't recently been inspected by archaeological staff.

Lack of space is a critical problem. Federal and state laws often require archaeological surveys before construction work, so collections swell wherever development is rapid. A repository at the University of California, Los Angeles' Fowler Museum is almost full, says curator Wendy Giddens Teeter. In Arizona, the fastest growing state in the country, archaeologists are doing more than twice as much work as they did several years ago, says Majewski. The governor recently appointed a commission to study the curation problem, and the resulting report predicted that Arizona's principal repositories will be full in 5 to 10 years; the state's main repository, Arizona State Museum in Tucson, is now storing some items offsite.

As a result, archaeologists are thinking harder about what they collect. "For decades and decades, people were collecting everything and keeping it all," says S. Terry Childs, an archaeologist with the National Park Service in Washington, D.C. Now, archaeologists try to choose a representative sample of artifacts, she says. "They are thinking about 'What do I keep?' " Those decisions must be made in the field, and they aren't always easy, says King. She mentions a dig in Maryland in which one of her colleagues, working pro bono, left the artifacts in the ground instead of cleaning and analyzing them. He identified them—and the house he was trying to date—as 20th century; later, more detailed excavation showed that it was 19th century.

One extreme solution is the use of no-collection surveys, says Childs, in which

researchers simply record artifacts' location on the surface and leave them there. "This is just horrible," she says, adding that anecdotal reports suggest such surveys are on the rise. Omitting actual artifacts risks the discipline's integrity, agrees Christopher Pulliam of the Army Corps of Engineers. "Archaeology professes to be a science," he says. "If one can't replicate research results or reanalyze the materials from a site, then [archaeology] can't proclaim to be a science."

Another solution is to remove redundant items or those with little research value, called deaccessioning. For example, until a few years ago, the San Diego Archaeological Center in California housed 30 boxes of 30-year-old, decomposing soil samples owned by the Department of Defense. Given their minimal research value, center director Cindy Stankowski kept representative samples of various soil types and threw away the rest.

But artifacts uninteresting to some are valuable to others. Back in the 1990s, King co-directed the excavation of the 17th century home of Charles Calvert, governor of Maryland, and found many brick fragments. Bricks were considered expendable and most were discarded, but King says some revealed the earliest evidence of a decorative technique used in the Chesapeake Bay region.

**Ready for a rescue.** Curators took over this collection and now keep it in high-quality storage.

The federal government is drafting new rules to guide deaccessioning some of their hundreds of millions of artifacts; the Department of the Interior alone is responsible for 90 million artifacts. The government tried to implement deaccessioning regulations in 1991 but backed off after ferocious opposition from archaeologists, who said that even artifacts of no research value now might yield important information when examined with future technologies. But Childs, who chairs the working group drafting the guidelines, says the current effort is likely to be more successful. The guidelines are expected to be made available for public comment in the next 6 months or so.

Despite the gloomy outlook, many archaeologists see signs of progress, as institutions such as the National Endowment for the Humanities and Save America's Treasures, both in Washington, D.C., recognize the value of certain archaeological collections and pay to restore them. But there's much to do. "The problem with collections is that they're not considered sexy," says Childs. She and others note that many more Ph.D.s are awarded for field-based than collections-based research, and that few universities offer classes in collections management. She and her collections-minded colleagues hope to change that. The future of archaeology," says Childs, "is in excavating the collections."

**–MICHAEL BAWAYA**

Michael Bawaya is the editor of *American Archaeology*.

EDUCATION

# Who Ranks the University Rankers?

**Everyone would like to score well in an academic beauty contest. But is it really possible to assess an institution's worth?**

Who gets to take credit for Albert Einstein's Nobel Prize? The question seems absurd, but it's important for the reputations of two Berlin universities. The reason: Even Nobels bagged 90 years ago are counted in the "Shanghai ranking," an influential list of the world's 500 best universities. Both Free University (FU), founded in West Berlin in 1948, and Humboldt University (HU), on the other side of the former Wall, claim to be the heirs of the University of Berlin, the erstwhile home of Albert Einstein and many other Nobelists.

The resulting tug of war has had bizarre results. When the team at Shanghai Jiao Tong University produced its first ranking in 2003, it assigned the prewar Nobels to FU, helping it earn a respectable 95th place. Swayed by protests from the other side of town, the team assigned them to HU in 2004, propelling it to 95th rank and dropping FU by more than 100 places. After FU in turn cried foul—and many e-mails between Germany and China later—the team simply took both universities out of the race. Both are still missing in the 2007 edition, published 3 weeks ago.

The controversy is just one among many in the booming business of university rankings. Invented by the magazine *U.S. News & World Report* in 1983 as a way to boost sales, these academic beauty contests—called "league tables" in the U.K.—now exist at the national level in a dozen countries; there are a handful of European and global lists as well. Almost all have come under fire from universities, scientists, and, in some cases, fellow rankers.

This year, for instance, presidents of more than 60 liberal arts colleges refused to participate in a key component of the *U.S. News & World Report* rankings, published last week. The rankings, they wrote, "imply a false precision and authority" and "say nothing or very little about whether students are actually learning at particular colleges or universities." Last year, 26 Canadian universities revolted against a similar exercise by *Maclean*'s magazine.

The critics take aim not only at the rankings' methodology but also at their undue influence. For instance, some U.K. employers use them in hiring decisions, says Ellen Hazelkorn of the Dublin Institute of Technology, adding that funding organizations, philanthropists, and governments are paying increasing attention as well. France's poor showing in the Shanghai rankings—it had only two universities in the first top 100—helped trigger a national debate about higher education that resulted in a new law, passed last month, giving universities more freedom.

### Measuring up

So how do you measure academic excellence? Most rankings start by collecting data about each university that are believed to be indicators of quality. After giving each a different, predetermined "weight," the indicators are added up to a total score that determines a university's rank. But there are vast differences in the number and the nature of the indicators, as well as the way the data are obtained.

National university rankings cater primarily to aspiring students about to choose

CREDIT: MARYLAND ARCHAEOLOGICAL CONSERVATION LABORATORY/JEFFERSON PATTERSON PARK AND MUSEUM

where to study, which is why they focus on education. In the *U.S. News & World Report* ranking of "national universities," for instance (there are separate lists for many other types of institutions and programs), student retention rates count for 20%, the average amount spent on each student for 10%, and alumni donations, believed to reflect student satisfaction, for 5% (see graph). *The University Guide* published by the *Guardian* newspaper in the U.K. has a formula with some of the same indicators, but also a 17% weight on graduates' job prospects.

Most international rankings, meanwhile, put a heavy emphasis on research output. That's in part because they are aimed more at policymakers but also because education systems and cultural contexts are so vastly different from country to country that solid and meaningful data are hard to come by. Average spending per student, for instance, doesn't tell you much if you compare China with Germany. Nonetheless, the *Times Higher Education Supplement* (*THES*) tries to capture education with a few very simple indicators that it believes to be universally valid: the staff/student ratio and the percentages of students and staff from overseas, regarded as a measure of a school's international cachet.

Ranking education poses another problem: Many rankings rely on universities themselves to provide key data, "which is always a deal with the devil," says Alex Usher of the Educational Policy Institute Canada in Toronto, who studies rankings. There are documented cases of universities cheating in the *U.S. News* rankings, for instance, and although *U.S. News* cross-checks the data with other sources, there are always ways to manipulate them. For example, colleges are known to encourage applications just so they can reject more students, thus boosting their score on the "student selectivity" indicator.

Even more controversial are peer-review surveys, in which academic experts judge institutions. *THES*, for instance, assigns a whopping 40% to the opinions of more than 3700 academics from around the globe, whereas the judgment of recruiters at international companies is worth another 10%. But when researchers from the Centre for Science and Technology Studies (CWTS) at Leiden University in the Netherlands compared the reviewers' judgments with their own analysis—based on counting citations, an accepted measure of scientific impact—they found no correlation whatsoever. "The result is sufficient to seriously doubt the value of the *THES* ranking study," CWTS Director Anthony van Raan wrote in a 2005 paper.

The discrepancy might explain why—to the delight of Australian academics and newspapers—six universities from Australia ended up in the *THES* top 50 in 2004, wrote Van Raan, who suspected "strong geographical biases" in the review. Martin Ince, a contributing editor who manages the *THES* ranking, says that the survey has gotten better since 2004 and has a good geographical balance. He believes Australia's strong showing may have been the result of aggressive marketing of its universities in Asia. But he concedes that reputation surveys may favor "big and old universities."

Peer review is also a major bone of contention in the *U.S. News* ranking. "We get a list of several hundred institutions, and we're simply asked to rank them on a scale of 1 to 5. That's preposterous," says Patricia McGuire, president of Trinity University in Washington, D.C., and one of those who boycotted the reputation survey this year. The ranking can't value what her school excels at, she says: providing a degree to mostly minority women from low-income backgrounds.

*U.S. News* editor Brian Kelly dismisses the boycott's significance. The ranking has always had its detractors, he says, but more than half of university officials still fill out the questionnaire. And the magazine could always find other people to review schools.

### Shanghai surprise

The Shanghai ranking avoids all of these problems by eschewing university-provided data and expert reviews. Instead, it uses only publicly available data, such as the number of publications in *Nature* and *Science*, the number of Nobel Prizes and Fields Medals won by alumni and staff, and the number of highly cited researchers. The result is a list based almost exclusively on research. Nian Cai Liu,

## How the Rankings Work

Data provided by universities | Data provided by third party | Expert Reviews

**Shanghai Jiao Tong University**

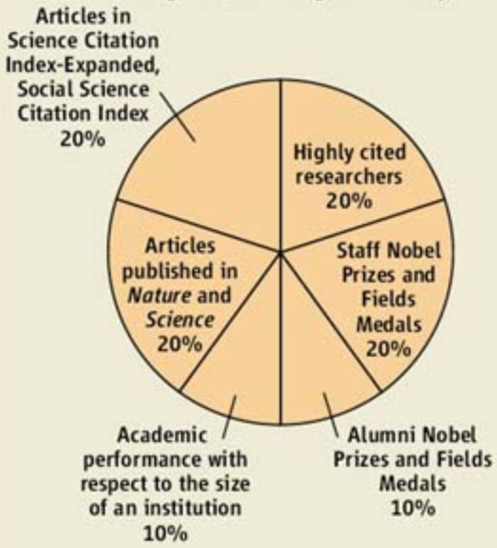


***Times Higher Education Supplement***

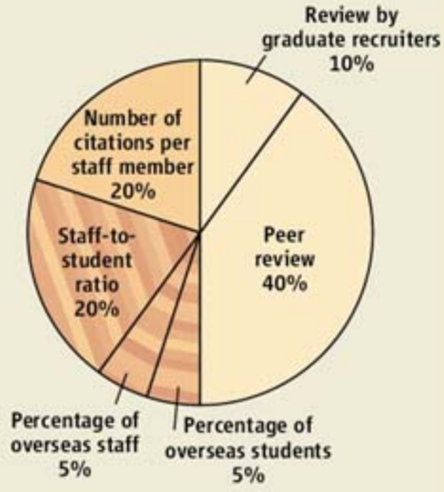


**Leiden University "Green Ranking"**

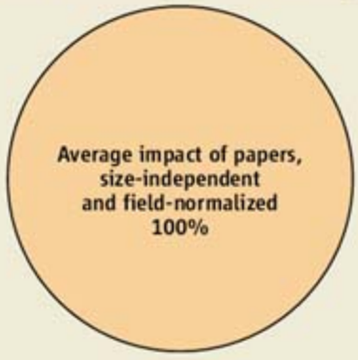


***U.S. News & World Report****

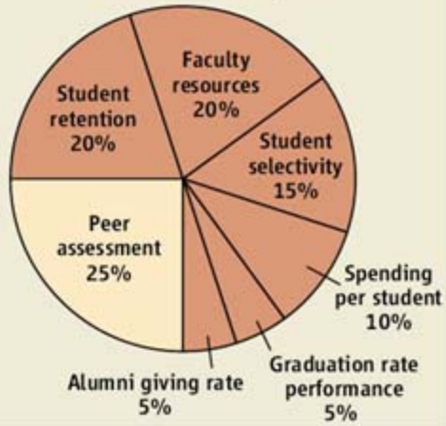


* for national universities

SOURCES: U.S. NEWS & WORLD REPORT, TIMES HIGHER EDUCATION SUPPLEMENT, SHANGHAI JIAO TONG UNIVERSITY, CWTS

who heads the Institute of Higher Education at Shanghai Jiao Tong University, started the ranking 5 years ago because he wanted to know how Chinese universities were placed in the global pecking order. When colleagues started asking for the data, Liu put them on a no-frills Web site, which now gets thousands of visits a day.

But as the Berlin quarrel shows, the ranking has its own problems. For example, Shanghai credits the institution where the Nobelist worked at the time of the award. And that can make a difference. Andrew Fire's 2006 Nobel in physiology or medicine helped his current institution, Stanford University in Palo Alto, California, move up from third to second place, even though Fire did his groundbreaking work on RNA interference while at the Carnegie Institution in Baltimore, Maryland.

Universities that focus on social sciences or humanities also tend to suffer under the Shanghai system. Recognizing that scientists in those disciplines gravitate to different journals, Liu doesn't count *Nature* and *Science* papers and redistributes that 20% share across other indicators. Still, the effect is noticeable: In 2006, the well-respected London School of Economics and Political Science ended up in the 201–300 tier (this far down the list, Liu no longer gives individual ranks), whereas the *THES* awarded the school 17th place.

Well aware of their influence, and the criticisms, the rankers themselves acknowledge that their charts aren't the last word. *U.S. News & World Report*, for instance, advises students to take many factors into account when choosing a college. A pop-up window on Liu's Web site warns that "there are still many methodological and technical problems" and urges "cautions" when using the results.

In response to the critics, some rankers are also continuously tinkering with their formulas. But that opens them up to another criticism, namely, that a university can appear to become significantly better or worse in a single year. Many have accused *U.S. News* of changing its method precisely to shake up the tables and thus boost sales, a charge the magazine rejects.

In part to boost their credibility, the rankers have founded the International Rankings Expert Group (IREG), which in 2006 came up with a set of ranking guidelines. Called the Berlin Principles, they stress factors such as the importance of transparency, picking relevant indicators, and using verified data. Usher, an IREG member, concedes that the principles are quite general in nature because they are the "biggest common denominators" among groups of rankers with very different views. Many rankings aren't fully compliant with the rules yet, says CWTS researcher Henk Moed.

| Country | Shanghai Jiao Tong University | *Times Higher Education Supplement* |
|---|---|---|
| U.S. | UUUUUUUUUUUUUU UUUUUUUUUUUUUU UUUUUUUUUUUUUU UUUUUUUUUUUU | UUUUUUUUUUUUUU UUUUUUUUUUUUUU UUUUUUU |
| U.K. | UUUUUUUUUUU | UUUUUUUUUUUUUUU |
| Netherlands | UU | UUUUUUU |
| Australia | UU | UUUUUUU |
| Japan | UUUUUU | UUU |
| Germany | UUUUU | UUU |
| Switzerland | UUU | UUUUU |
| France | UUUU | UUUUU |
| China* | | UUUUU |
| Canada | UUUU | UUU |
| Sweden | UUUU | |
| Singapore | | UU |
| New Zealand | | UU |
| India | | UU |
| Belgium | | UU |
| Italy | U | |
| Israel | U | |
| Denmark | U | U |
| Norway | U | |
| Finland | U | |
| Russia | U | U |
| Mexico | | U |
| Ireland | | U |
| South Korea | | U |
| Austria | | U |

**U** = one university in the top 100 * includes Hong Kong (3 universities)

**Who's right?** Although both agreed that the U.S. led the list and the U.K. came second, the 2006 Shanghai and *THES* rankings differed markedly on where Earth's 100 best universities were located.

SOURCE: SHANGHAI JIAO TONG UNIVERSITY, *THES*

### DIY ranking

Some believe the way forward lies with more sophisticated ways of presenting the data. The group in Leiden, for instance, produces rankings of European universities based purely on publication and citation data and presents them as not one but four tables. Each uses a different variable; the yellow ranking, for instance, looks at the total number of papers produced, whereas the green ranking (billed as the "crown indicator") is based on papers' impact, adjusted so that it doesn't reward bigger institutions or those working in fields in which scientists cite each other more often. The results aren't as simple as a single list, Moed concedes, but they do provide a more complete picture.

Others are going further. The Centre for Higher Education Development (CHE) in Gütersloh assesses German university departments without trying to aggregate them, and the departments are simply slotted into top, middle, and lower tiers. It also allows the user to sort universities based on their own favorite indicators. Obviously, a ranking such as this one makes for less compelling newspaper or magazine copy—like a Miss Universe contest without a winner. But a spokesperson for *Die Zeit*, the German newspaper that publishes the CHE rankings, says its annual university guide is a bestseller anyway, and the interactive design lures many readers to its Web site.

With all the complaints, it's easy to forget that rankings have benefits as well, says Moed. Competition spurs universities to actually perform better, he says, and the rankings provide students and policymakers with answers—even if they're imperfect—to legitimate questions about quality. Other rankers point out that universities tout the results if they do well, and they don't like being excluded. Perhaps that's why the presidents of the competing Berlin universities announced shortly after the 2007 Shanghai ranking appeared that they would sit down again to discuss the legacy of Einstein and his illustrious colleagues. A compromise might propel both back onto the list in 2008.

Einstein might have appreciated the irony. A sign in his office at Princeton reportedly read: "Not everything that counts can be counted, and not everything that can be counted counts."

**–MARTIN ENSERINK**

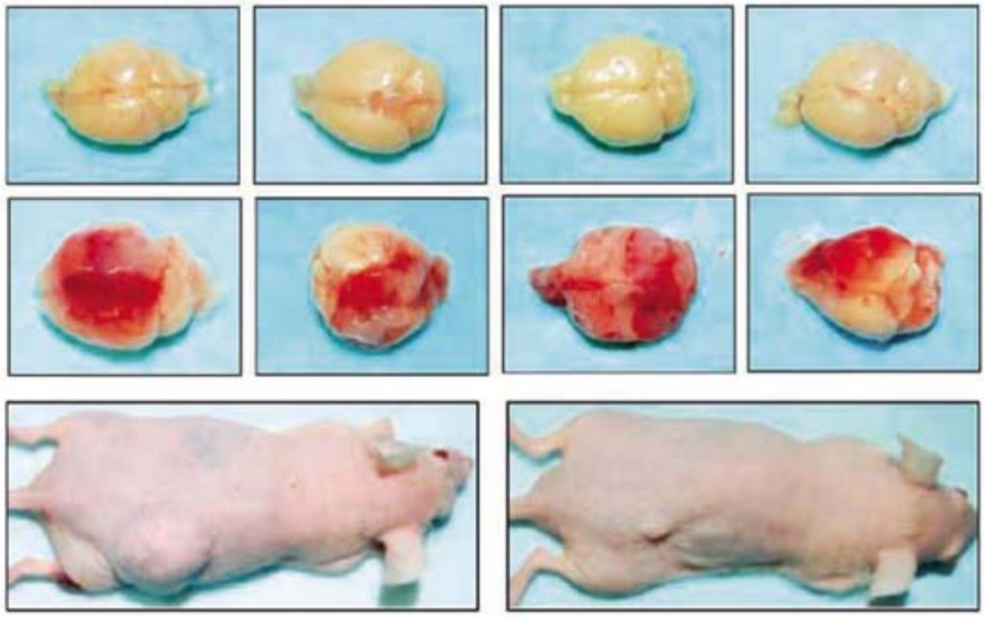

**Blood vessel stimulator.** When transplanted into mouse brains, glioma stem cells form larger and more vascular tumors (*middle row*) than do nonstem cells (*top*). As shown by the mouse at right, an antibody to the angiogenesis-promoting protein VEGF greatly inhibits the growth of glioma stem cell tumors; the mouse at left is an untreated control.

CREDIT: S. BAO ET AL., *CANCER RESEARCH* **66**, 7843 (2006)

MOLECULAR BIOLOGY

# Cancer's Perpetual Source?

**The discovery of tumor cells that behave like stem cells suggests why cancer may be so hard to eradicate—and how new therapies might be targeted**

Beginning about 15 years ago, John Dick's team at the University of Toronto in Canada provided a new clue as to what makes cancer such a formidable foe. They found that only a tiny population of leukemia cells could transmit the cancer from one experimental animal to another. More remarkably, the cells had a property previously seen only in stem cells: the ability to produce an exact copy of themselves each time they divide, thereby maintaining the ability to reproduce in perpetuity. These so-called cancer stem cells, Dick suggested, might be what makes the disease so hard to eradicate with radiation or chemotherapy.

Since then, such cells have been found in many other cancers, including those of the breast, brain, colon, and head and neck. "Cancer stem cells are being identified in virtually every cancer," says Max Wicha of the University of Michigan Comprehensive Cancer Center in Ann Arbor.

Not everyone is convinced that the stem-like cells found in cancers play such a key role in tumor growth and maintenance. But if that idea is correct, "the ramifications could be huge," says Craig Jordan of the University of Rochester School of Medicine and Dentistry in New York state. In that event, therapies that target cancer stem cells may prove more effective than current cancer treatments. Indeed, radiation and many chemotherapeutic drugs wipe out dividing cells, but stem cells may be quiescent most of the time and so may survive these treatments. "You can reduce tumor bulk 90%, and in no time at all, the tumor will take over again," says Levy Kopelovich of the National Cancer Institute in Bethesda, Maryland, which held a workshop in mid-May on stem cells as targets for cancer prevention.

Cancer researchers are beginning to understand what makes cancer stem cells dangerous. Among other things, they foster the formation of new blood vessels needed to feed tumor growth. Recent work is also uncovering the cellular signaling pathways that control cancer stem cell proliferation, raising hopes of new treatments that selectively kill these cancer seeds. Indeed, some existing cancer drugs and others that may soon be tested in people appear to target the cells, new studies indicate. "By gaining a sophisticated understanding of how normal and cancer stem cells differ, we'll be able to design a new class of drugs that is less toxic," predicts Sean Morrison of the University of Michigan Medical School in Ann Arbor.

## Multiple threats

For the first decade after Dick's discovery, the clinical importance of cancer stem cells seemed limited, because leukemias are much rarer than solid cancers. But interest in the cells began to take off in 2003. That year, a team led by Michael Clarke, then at the University of Michigan Medical School, spotted cancer stem cells in breast cancers, and Peter Dirks of the Hospital for Sick Children in Toronto and his colleagues identified them in a variety of brain cancers (*Science*, 5 September 2003, p. 1308).

In the past several months, that early trickle of results has turned into a flood. In the 4 January issue of *Nature*, for example, two independent teams, one led by Dick and the other by Ruggero De Maria of the Istituto Superiore di Sanità in Rome, reported the discovery of cancer stem cells in colon cancer, and others have reported finding them in cancers of the prostate, lung, pancreas, head and neck, and the deadly skin cancer melanoma. "Cancer stem cell research has gone from an interesting sidelight to mainstream in a very short time," Jordan says.

What's more, cancer stem cells display an array of traits that aid in their proposed role of driving and maintaining cancer growth. For example, Jeremy Rich's team at Duke University in Durham, North Carolina, looked at their ability to resist radiation.

In one key set of experiments, these researchers transplanted cells obtained from human glioblastomas, which are highly malignant brain tumors, into mice and then subjected the animals to radiation doses similar to those used to treat human patients. Other than surgery, Rich says, "radiation therapy is the most effective [treatment] for brain tumors, but it is rarely curative."

The transplantation results, which appeared in the 7 December 2006 issue of *Nature*, suggest an explanation. In irradiated tumors, the proportion of cancer stem cells went up from about 2% to about 8%, as indicated by the number bearing the protein CD133, a marker for brain cancer stem cells. This shows that those cells survived the radiation whereas other tumor cells succumbed.

The stem cells overcame the radiation, further analysis suggested, because they repair the DNA damage it induces more effectively than nonstem cancer cells do. "I thought that was a great paper," says Clarke, who's now at Stanford University in Palo Alto, California. "It provided experimental evidence for what we've all been predicting."

A second way that cancer stem cells may pose a threat is by stimulating angiogenesis, the formation of new blood vessels

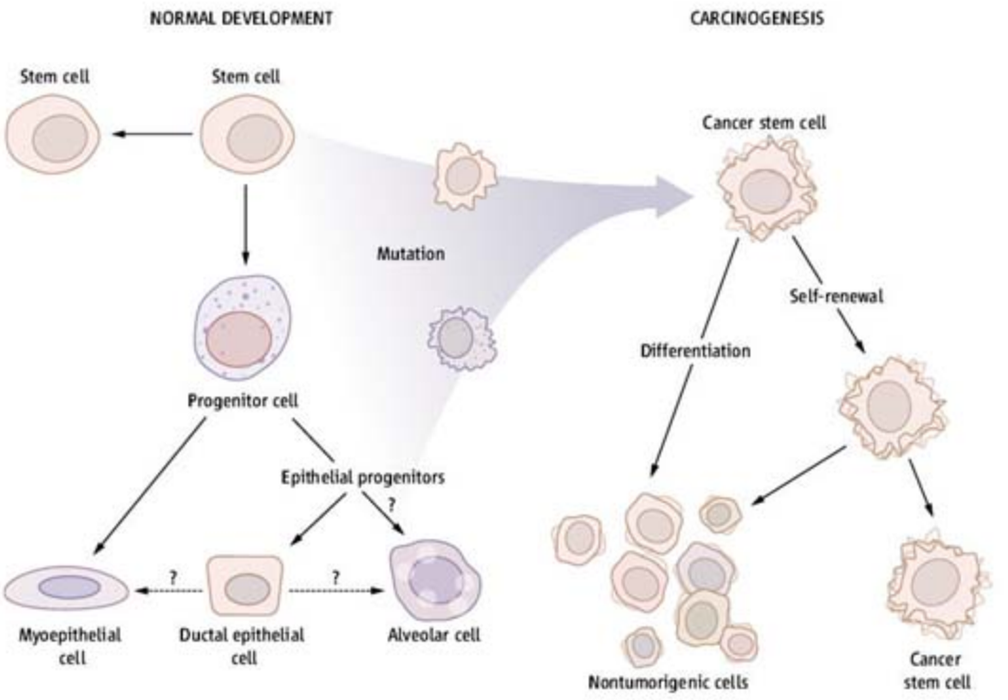


**Dangerous cells.** According to current thinking, oncogenic mutations arising either in normal tissue stem cells or in the more developmentally advanced progenitor cells can produce cancer stem cells. When these cells divide, one daughter is an exact copy of the original and retains the ability to divide—and to initiate additional tumors—whereas the other target differentiates to produce nontumorigenic cells.

that support tumor growth. For example, the Duke team recently found that glioma stem cells in culture produce much more of the angiogenesis-promoting protein VEGF than do other glioma cells.

The VEGF discovery suggests that one current drug may be a prototype of therapies that target cancer stem cells. Bevacizumab (Avastin) is an antibody designed to block VEGF action that is already used for cancer therapy. And when the Duke team transplanted human glioma stem cells into mice and treated the animals with the antibody, "the tumors from cancer stem cells shrank dramatically," Rich says. "It looks like bevacizumab is a kind of anticancer–stem cell therapy."

And cancer stem cells may have yet another dangerous property: the ability to drive metastasis, the spread of tumors in the body. The presence of tumor cells in the bone marrow of breast cancer patients is a bad prognostic sign, indicating that such patients have a high risk of cancer spread. Last fall, Marija Balic, Richard Cote, and their colleagues at the University of Southern California in Los Angeles reported that roughly 70% of the tumor cells in bone marrow carry the surface markers of breast cancer stem cells. Although it hasn't been proven that those cells seed metastatic tumors, such a possibility is in line with the idea that cancer stem cells are the tumor-initiating cells. Other research has shown that genes involved in cell migration and tissue invasion are highly active in breast cancer stem cells.

## Searching for vulnerability

In their search for ways to disrupt cancer stem cell activities, researchers are focusing heavily on the signaling pathways needed for their maintenance and development. And several intriguing connections between genes already linked to cancer development have emerged.

At this year's annual meeting of the American Association for Cancer Research in April, Hasan Korkaya, a member of Wicha's group at Michigan, reported that reducing expression of *PTEN*, a known tumor suppressor gene, in cultured human breast cancer cells increased cancer stem cell populations by as much as fivefold. Boosting expression of the *HER2* oncogene at the same time doubled that increase. In addition, such cells migrate more in culture, an indication that they may seed metastases. This might help explain why women whose breast cancers have both loss of *PTEN* and extra *HER2* copies usually have a poor prognosis.

Other work also points to *PTEN* loss as a trigger for cancer stem cells. Early last year, Owen Witte's team at the David Geffen School of Medicine in Los Angeles found that when *PTEN* is deleted in the prostate cells of mice, the number of cells bearing a stem cell marker called Sca-1 increases, and small premalignant growths form in the prostate. And Linheng Li's team at the Stowers Institute for Medical Research in Kansas City, Missouri, has found that deleting *PTEN* in cells lining the intestines leads to the production of stem cells that form polyps that can develop into full-blown cancers. Finally, Morrison's team has found in mice that *PTEN* deficiency promotes the formation of leukemia stem cells while depleting normal hematopoietic stem cells.

This suggests, he notes, that it may be possible to selectively strike cancer stem cells. Indeed, Morrison and his colleagues have evidence that the drug rapamycin, which can help make up for *PTEN* loss, can prevent leukemia development in their mouse model while at the same time restoring normal hematopoietic stem cell function. This is "exciting," Morrison says, "because it offers the possibility of developing therapies that kill cancer stem cells but are less toxic in normal tissue." Rapamycin is already used clinically as an immunosuppressant and is being studied in cancer therapy, and the group hopes to begin a clinical trial to test it in patients with acute myeloid leukemia (AML).

Researchers seeking to target cancer stem cells are also looking at several more pathways previously implicated in stem cell maintenance. Among these are the Wnt pathway, which is implicated in intestinal and other cancers, and also the Polycomb and sonic hedgehog pathways.

Some surprising aspects of cancer stem cells may also provide unexpected new targets for therapies. In a recent screen of 1267 compounds in a library of pharmacologically active agents, Dirks and his colleagues identified 160 agents that decreased the proliferation of brain cancer stem cells in lab cultures. Many of these drugs affected unexpected neuronal functions, such as neurotransmission, which were supposed to be properties of mature neurons rather than unspecialized stem cells. The mechanisms that control cancer stem cell growth "may be more diverse than what we see right now," Dirks says.

Even a folk remedy is showing some promise against cancer stem cells. Rochester's Jordan, working with Dianna Howard's team at the University of Kentucky Medical Center in Lexington, has evidence from both cells in culture and a mouse model that the drug parthenolide—the active ingredient in a herbal remedy called feverfew—specifically kills AML stem cells.

In addition to simply screening for compounds that kill cancer stem cells, Dick and his colleagues are going after leukemia stem

SOURCE: G. DONTU *ET AL.*, *CELL PROLIFERATION* **36** (SUPPLEMENT 1), 59 (2003)

cells with an antibody that binds to a protein called CD44 that is highly expressed on the surface of AML cells. When the researchers transplanted human AML stem cells into mice and then administered the antibody, the treatment apparently abolished the tumor stem cells driving the leukemia. Closer examination showed that the antibody prevents AML stem cells from migrating to the spleen and bone marrow, where they would otherwise reside. "The [leukemia] stem cells still need to interact with their niche, and if you interfere with their trafficking, they can't maintain themselves," Dick says.

Even if cancer stem cells can't be killed or their spread blocked, they might be restrained in another way: by inducing them to lose their "stemness" and differentiate into nonrenewing cells. Last December, Angelo Vescovi of the University of Milan–Bicocca in Italy and colleagues reported in *Nature* that bone morphogenetic proteins inhibit the tumorigenic properties of human glioblastoma stem cells in this fashion. "It's an interesting paper," says Dirks. "It opens up the field to considering differentiation" as a therapeutic goal.

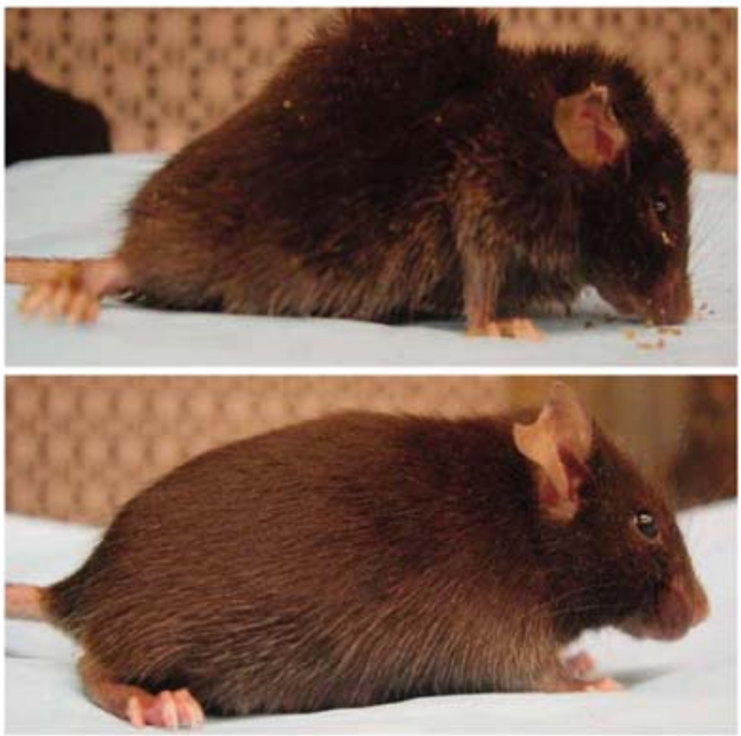

**Staying alive.** The *PTEN* tumor-suppressor gene was deleted from the blood-forming cells of both mice. The mouse at top is near death due to the resulting leukemia. But treatment with the drug rapamycin, which can compensate for *PTEN* loss, kept the mouse at bottom healthy.

CREDIT: O. H. YILMAZ *ET AL.*, *NATURE* **441**, 475 (2006)

### Lingering questions

Despite the outpouring of results in the past few years, fundamental questions remain about cancer stem cells. One big issue concerns the nature of the original cell that gives rise to them. "That's a harder question than people appreciate," Jordan says. "It doesn't have to start with a normal stem cell." In work done a few years ago, Irving Weissman's team at Stanford University examined the genetic mutations in human AML cells and concluded that the original cancer-causing mutations can strike more developmentally advanced, although still immature, progenitor cells.

About a year ago, Scott Armstrong and colleagues at Children's Hospital Boston provided further support for that idea. Many leukemia cells feature gene translocations in which two genes, previously separate from one another, become joined and produce so-called fusion proteins. Human AML cells, for example, make a fusion protein called MLL-AF9. When the Children's Hospital workers genetically engineered granulocyte-macrophage progenitor cells to produce MLL-AF9 and transplanted the cells into mice, they gave rise to a leukemia similar to AML. Subsequent isolation of leukemia stem cells from the mice showed that they resembled the original granulocyte-macrophage progenitors but had activated genes needed for self-renewal.

Indeed, work published by the Clarke team in the 12 June issue of the *Proceedings of the National Academy of Sciences* suggests that stem cells of a given type of cancer may arise from different cells. For these experiments, the researchers looked at colon cancer stem cells obtained from four different patients. There were "subtle differences" in cancer stem cell characteristics from patient to patient, says Clarke. "This suggests that the cell of origin varies from patient to patient."

Despite the huge growth in the cancer stem cell field, skeptics remain. One potential problem is that virtually all the work has involved transplanting human cancer cells into immunodeficient mice. This has raised concerns that the experiments do not accurately reflect what happens during cancer development in humans. Indeed, Andreas Strasser and his colleagues at the Walter and Eliza Hall Institute of Medical Research in Melbourne, Australia, have recently challenged the idea that only rare cancer stem cells can initiate tumor formation.

Instead of using human leukemia cells, these researchers worked with mice genetically engineered to develop leukemia. When they injected leukemic cells from these animals into genetically compatible healthy mice, all the recipients developed leukemia, even those injected with as few as 10 cells, Strasser's team reported in the 20 July issue of *Science* (p. 337). That could not have happened if only a tiny minority of tumor cells had the ability to initiate tumor formation, as the stem cell hypothesis holds, Strasser says. He suggests that the mouse doesn't provide the right environment for the growth of human cancer cells, so that only a few manage to survive and multiply, thus creating a false impression that tumor-initiating cells are rare. "Those data have been massively overinterpreted," Strasser maintains.

Dick disagrees. He notes that the cancer stem cell hypothesis rests on the prospective isolation of distinct populations of tumor-initiating and noninitiating cells rather than just on the rarity of cancer stem cells. Dick points out that his team has re-created human leukemias in mice by injecting the animals with normal human blood-forming cells that had been engineered to carry a fusion gene known to make cells leukemic (*Science*, 27 April, p. 600).

These animals, which are more comparable to Strasser's genetically engineered mice, developed leukemias similar to those seen in humans, and the frequency of tumor-initiating cells was relatively high—one to two in 100—rather than the one in a million seen in the early experiments. Other researchers have reported similar results. Dick suggests that different cancers will vary in cancer stem cell frequency, depending on the particular oncogenic pathways operating in the cells.

Although others share Strasser's skepticism about cancer stem cells and many uncertainties remain, there is one sure bet. Given the possible importance of cancer stem cells as therapeutic targets, the field will continue to grow. And at least one skeptic has already been convinced. Duke University's Rich says that he came into the research hoping to disprove the importance of cancer stem cells. Now, he says, "we are very early in studying cancer stem cells, but understanding them may impact the way we diagnose and treat patients in the near future."

–JEAN MARX

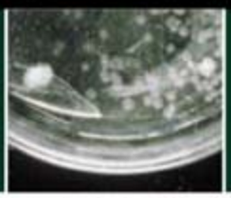





# LETTERS

*edited by Etta Kavanagh*

## Another Threat to Borneo's Rainforests?

I WELCOME THE RECENT INITIATIVE BY THE GOVERNMENTS OF BRUNEI, Indonesia, and Malaysia to commit to conserve the highly diverse forests on the island of Borneo through the "Heart of Borneo" initiative ("Last-gasp effort to save Borneo's tropical rainforests," News Focus, 13 July, p. 192). This is timely and hopefully will lead toward improved conservation efforts and more sustainable land use in this beleaguered biodiversity hotspot.

However, large areas of Borneo are already under threat from a nonsustainable land use—that of open-cast coal mining. The mining giant BHP Billiton plans to develop a number of coal-mining areas directly within the Heart of Borneo (*1*). If these vast surface mines are allowed to proceed, it may lead to a catastrophic destruction of pristine rainforest and associated loss of plant and animal species.

If efforts to allow countries with tropical forests to obtain carbon credits from avoided deforestation come to fruition (*2*), the forests of Borneo will have value in a different currency, that of their forest-carbon stocks rather than the coal buried beneath them.

**FRANCIS Q. BREARLEY**

Department of Environmental and Geographical Sciences, Manchester Metropolitan University, Chester Street, Manchester M1 5GD, UK. E-mail: f.q.brearley@mmu.ac.uk

**References**

1. C. Rewcastle, J. Ungoed-Thomas, "Mining giant to raze apes' forest home," *Sunday Times*, 15 July 2007, p. 20.
2. W. F. Laurance, *Biotropica* **39**, 20 (2007).

## Ocean Acidification and Scleractinian Corals

IN THEIR BREVIA "SCLERACTINIAN CORAL species survive and recover from decalcification" (30 March, p. 1811), M. Fine and D. Tchernov present an exciting experimental approach documenting how coral skeletons dissolve as a physiological response to increased atmospheric $CO_2$, a subject currently at the height of public concern (*1*, *2*). The fact that these authors demonstrated that five species of living scleractinian corals could lose their aragonitic skeletons, in response to elevated $CO_2$, and then continue to exist perfectly well as soft-bodied polyps is a confirmation of the ephemeral or "naked coral" hypothesis (*3*, *4*). This physiological response assists our understanding of the survival potential of corals after mass extinctions such as after the devastating one at the end-Permian (*5*). In addition, it explains the previously unexplained, geologically "sudden" appearance of order Scleractinia in Middle Triassic time, when geochemically perturbed oceans returned to normal. Before this time, corals and reefs disappeared from the fossil record for millions of years but may have continued to exist as "naked corals," thus remaining paleontologically "hidden" from our view.

An important implication of this work is the arbitrary and artificial nature of the current phylogenetic classification of scleractinian corals and some anemones. Why should Order Scleractinia be recognized on the basis of a calcified skeleton when essentially identical soft-bodied, anemone-like forms such as the Corallimorpharia belong to another group?

Fine and Tchernov's decalcification experiments may not be representative of all varieties of corals. I suspect that zooxanthellate reef-building species would have responded very differently to the experiment because of the complex nature of their photosymbiosis (*6*). Readers should not misconstrue this paper as tacit validation that we need not be as concerned about the growing problem of ocean acidification with regard to corals and reefs.

**GEORGE D. STANLEY JR.**

University of Montana Paleontology Center, Department of Geosciences, University of Montana, Missoula, MT 59812, USA.

**References**

1. J. Ruttimann, *Nature* **442**, 978 (2006).
2. E. Kolbert, *The New Yorker*, 20 Nov. 2006, p. 67.
3. G. D. Stanley Jr., D. Fautin, *Science* **291**, 1913 (2001).
4. G. Stanley Jr., *Earth Sci. Rev.* **60**, 195 (2003).
5. D. H. Erwin, *Extinction: How Life on Earth Nearly Ended 250 Million Years Ago* (Princeton Univ. Press, Princeton, NJ, 2006).
6. G. D. Stanley Jr., *Science* **312**, 857 (2006).

### Response

STANLEY HIGHLIGHTS THE DUAL SIGNIFICANCE of our findings: a confirmation of his naked coral hypothesis (*1*) and a plausible explanation for the enigma of discontinuity in the geological record of coral reefs (*2*).

Stanley uses our findings to suggest that scleractinians and noncalcifying species that are typically classified as a different order (such as corallimorpharians) are probably one clade. This is supported also by phylogenetic studies using molecular tools (*3*), demonstrating that a clade of scleractinians is more closely related to noncalcifying corallimorpharia than to another clade of scleractinians.

Stanley criticizes our study for using two Mediterranean coral species that he refers to as "not representative." Indeed, these are not classic reef-building corals; however, we doubt there is a definition of a "typical coral." The evolution and basic physiology of the studied species are indistinguishable from that of tropical reef-building corals (*4*, *5*). Over 98% of the colonies of the studied species are symbiotic, suffering reduced growth, lower competitive abilities, and reduced physiological state when losing their endosymbiotic


The money illusion
1042

Threats, near and far
1043

dinoflagellates (bleach) (*4*). Hence, there is no reason to suspect that they have a different photosymbiosis, as Stanley proposed. We chose the studied species for their relatively slow calcification rate, a preferred condition for our decalcification experiment.

We share Stanley's concern that our findings might be misinterpreted by the reader, as the title suggests "survival." The last sentence in our paper, however, clearly states that while we discovered physiological refugia for corals under acidified conditions, coral reefs and their services will be lost. Corals without carbonate skeleton do not provide protection from predators to both the coral host and the numerous species that are associated with it. So even if corals survive acidification, reefs will not.

**MAOZ FINE[1,3] AND DAN TCHERNOV[2,3]**

[1]Faculty of Life Sciences, Bar-Ilan University, Ramat-Gan 52900, Israel. [2]Department of Evolution, Systematics and Ecology, The Hebrew University of Jerusalem, Givat Ram, Jerusalem 91904, Israel. [3]The Interuniversity Institute for Marine Sciences, Eilat 88103, Israel.

**References**

1. G. D. Stanley Jr., D. G. Fautin, *Science* **291**, 1913 (2001).
2. G. D. Stanley Jr., *Earth Sci. Rev.* **60**, 195 (2003).
3. M. Medina, A. G. Collins, T. L. Takaoka, J. V. Kuehl, J. L. Boore, *Proc. Natl. Acad. Sci. U.S.A.* **103**, 11814 (2006).
4. M. Fine, U. Oren, Y. Loya, *Mar. Ecol. Prog. Ser.* **234**, 119 (2002).
5. M. Fine, H. Zibrowius, Y. Loya, *Mar. Biol.* **138**, 1195 (2001).

## Trait or State?

IN THEIR REPORT "NUCLEUS ACCUMBENS D2/3 receptors predict trait impulsivity and cocaine reinforcement" (2 March, p. 1267), J. W. Dalley *et al.* show that outbred rats displaying high behavioral impulsivity responded more for intravenously administered cocaine than less impulsive rats. What they termed "trait impulsivity" was defined as high levels of anticipatory responding before presentation of a brief light stimulus predictive of food availability during a five-choice serial reaction time task of sustained visual attention.

We offer the caveat that a "trait" as usually defined in biology refers to a heritable, measurable attribute of an individual. Its use here is an unfortunate choice of terminology. This Report and many earlier studies demonstrating a correlation between locomotor activity in a novel environment and subsequent propensity to self-administer psychostimulants (*1*) imply that the impulsivity (or high activity) of this subset of rats can be viewed as an endophenotype (a hereditary characteristic that is normally associated with some condition but is not a direct symptom of that condition) of an inheritable risk for susceptibility to drug abuse. Arguably, however, behavioral differences between outbred high and low responders might be due entirely to effects of environment or past experience, not genotype.

Indeed, exposure to the impulsivity task itself might have caused subsequently observed differences in D2/3 receptor availability or cocaine self-administration. To date, there is little evidence that individual behavioral differences in impulsivity or the activity response in a novel apparatus can be cotransmitted with tendency to self-administer a drug to rat offspring. However, in mouse inbred strains, both activity (*2*) and a similar measure of impulsivity, ability to withold nose poking (*3*), are clearly heritable. Furthermore, response inhibition efficiency shared about 40% of genetic variance with the same strains' consumption of ethanol solutions (*3*). Demonstration of coordinate genetic influence on such traits as impulsivity or activity and drug self-administration would be a simple matter of two to three generations of selective breeding, and would strengthen the relevance of these studies to the human condition considerably.

**JOHN C. CRABBE[1,2] AND CHRISTOPHER L. CUNNINGHAM[1]**

[1]Portland Alcohol Research Center, Department of Behavioral Neuroscience, Oregon Health & Science University, Portland, OR 97239, USA. [2]Research Service, VA Medical Center, Portland, OR 97239, USA.

**References**

1. P. V. Piazza, J. M. Deminière, M. Le Moal, H. Simon, *Science* **245**, 1511 (1989).
2. D. Wahlsten, A. Bachmanov, D. A. Finn, J. C. Crabbe, *Proc. Natl. Acad. Sci. U.S.A.* **103**, 16364 (2006).
3. S. F. Logue, R. J. Swartz, J. M. Wehner, *Alcohol. Clin. Exp. Res.* **22**, 1912 (1998).

## Response

OVERALL, WE WERE SOMEWHAT SURPRISED by the view expressed by Crabbe and Cunningham that impulsivity might be due entirely to the effects of environment or past experience. Impulsivity as operationally defined on the 5-choice serial reaction time task is a highly specific behavioral characteristic, which is actually orthogonal to the high responder (HR) phenotype described by Piazza and colleagues (*1*). It is, in fact, more closely related to the form of inhibitory response control deficit present in attention deficit/hyperactivity disorder (ADHD) and related psychopathology in humans. This is relevant because available evidence suggests that specific endophenotypes linked to response inhibition per se may indeed be heritable in humans (*2*), in line with recent converging evidence from family, twin, and adoption studies indicating a strong genetic component to ADHD (*3*). From these and other twin studies, nonshared environmental components of heritability are generally small, while genetic components are normally much larger. Indeed, it is becoming increasingly clear that some environmental influences exert their effects through gene-environment interactions either directly through a differential functional response of a specific genotype to an environmental stressor or via epigenetic modifications of a DNA sequence motif or polymorphism [e.g., (*4*)]. Nevertheless, we do agree with Crabbe and Cunningham that we cannot dismiss the effects of differential mothering style or other environmental variables without first demonstrating through selective breeding and subsequent cross-fostering experiments an enrichment in impulsivity across successive generations of rat offspring.

Finally, it is disappointing in our view that Crabbe and Cunningham fail to focus on the real significance of our work in demonstrating a potential causal relationship between impulsivity and vulnerability to cocaine-taking based on a common neurobiological substrate, not least a drug receptor target that has

been extensively implicated in analogous brain imaging studies in monkeys and humans (*5*, *6*). Impulsivity and increased cocaine self-administration may actually be related psychological processes, for example, expressed as an inability to bridge delays between future rewarding events. Indeed, this hypothesis is clearly compatible with recent speculations that D2/3 receptors in the ventral striatum function to modulate distal versus proximal rewards (*7*). It is precisely this type of study that lies at the heart of the endophenotype concept and its utility in deconstructing complex neuropsychiatric disorders (*8*).

**JEFFREY W. DALLEY, BARRY J. EVERITT, TREVOR W. ROBBINS**

Behavioral and Clinical Neuroscience Institute, Department of Experimental Psychology, University of Cambridge, Downing Street, Cambridge CB2 3EB, UK.

**References**

1. P. V. Piazza, J. M. Deminière, M. Le Moal, H. Simon, *Science* **245**, 1511 (1989).
2. A. R. Aron, R. A. Poldrack, *Biol. Psychiatry* **57**, 1285 (2005).
3. F. X. Castellanos, R. Tannock, *Nat. Rev. Neurosci.* **3**, 617 (2002).
4. I. C. Weaver *et al.*, *Nat. Neurosci.* **7**, 847 (2004).
5. M. A. Nader *et al.*, *Nat. Neurosci.* **9**, 1050 (2006).
6. N. D. Volkow *et al.*, *Synapse* **14**, 169 (1993).
7. A. J. Smith *et al.*, *Neural Comput.* **17**, 361 (2005).
8. I. I. Gottesman, T. D. Gould, *Am. J. Psychiatry* **160**, 636 (2003).

## Stepping Down from the CIHR

I AM WRITING TO CLARIFY MY REASONS FOR stepping down as president of the Canadian Institutes of Health Research (CIHR) ("Weary," Newsmakers, 13 July, p. 177). I am not "worn out from battling community opposition…" Actually, I have quite enjoyed and appreciated the important discussions that the CIHR vision has prompted. Such discussions are necessary for transformative change. The profound changes taking place in the style and speed of health research and in the societies that fund this research are prompting similar discussions in every country that wishes to be at the leading edge of health research.

I am leaving simply because, after seven and-one-half years as CIHR's first president, I have accomplished what I set out to do: establish a new national funding agency that funds research across all aspects of health and disease, which is strategic, focused on outcomes, and based on peer-reviewed excellence in research. Furthermore, CIHR's unique, cross-Canada Institute structure is now well in place, with 13 highly talented and committed Scientific Directors, 13 Institute Advisory Boards, and a strong senior management. Finally, I have always felt that it's not healthy to be the head of an organization like CIHR for more than seven to eight years: One tends increasingly to look backward, not forward. This is a good time for someone else to take the reins of CIHR.

**ALAN BERNSTEIN**

Canadian Institutes of Health Research, 410 Laurier Avenue West, 9th Floor, Ottawa, ON K1A 0W9, Canada.

## CORRECTIONS AND CLARIFICATIONS

**Table of Contents:** (10 August). The floral image on page 709 was erroneously linked to the News Focus article "The fellowship of the hobbit." It should have been linked to Browsings on page 754.

**Newsmakers:** "Digging for pride" (27 July, p. 435). The credit for the photo accompanying this item was incorrect. It should read "bosnianpyramid.com."

**News of the Week:** "Conservationists and fishers face off over Hawaii's marine riches" by C. Pala (20 July, p. 306). It was suggested incorrectly that a right-to-fish bill was passed in the Hawaii House of Representatives this year in

reaction to a study by marine scientist Alan Friedlander on marine protected areas. In fact, the bill was a reaction to another bill introduced in 2003 that would have set aside a fifth of Hawaii's near-shore waters for conservation.

**Perspectives:** "Reassessing carbon sinks" by D. F. Baker (22 June, p. 1708). In the "Ocean regions" and "Land regions" columns at the bottom of the figure, the column titles should be reversed. "Land regions" should be on the left, and "Ocean regions" should be on the right. In line 4 of the figure caption, "1.5 Pg C" should be "0.15 Pg C." The author's affiliation should be Marine Chemistry and Geochemistry Department, Woods Hole Oceanographic Institution, Woods Hole, MA 02543, USA. E-mail: dfb@ucar.edu.

**Reports:** "Restriction of an extinct retrovirus by the human TRIM5α antiviral protein" by S. M. Kaiser *et al.* (22 June, p. 1756). In the first two full sentences on page 1758, the word "notably" was placed incorrectly. The sentences should read, "However, changing the arginine to the ancestral glutamine abolished the ability of human TRIM5α to efficiently restrict PtERV1 infectivity (Fig. 2B). Notably, the R332Q mutation had the opposite effect on HIV-1, improving the ability of human TRIM5α to restrict this virus (*15*) (Fig. 2B)."

**Reports:** "The vaccine adjuvant monophosphoryl lipid A as a TRIF-biased agonist of TLR4" by V. Mata-Haro *et al.* (15 June, p. 1628). On page 1629, in the 24th line of the first full paragraph in the first column, the callout should have been for figure S4 (not figure S3).

**News Focus:** "Food for thought" by A. Gibbons (15 June, p. 1558). In a hypothetical scene, manioc and potato were suggested as possible tubers roasted and eaten by human ancestors in Africa about 1.5 million years ago. However, manioc and potatoes were domesticated in the New World and did not reach Africa until much later. Yams are a more likely menu item for ancient African *Homo erectus*.

**Reports:** "Replication of genome-wide association signals in UK samples reveals risk loci for type 2 diabetes" by E. Zeggini *et al.* (1 June, p. 1336). In the HTML version of this article, an incorrect, expanded author list was initially included owing to an error at *Science*. The print and PDF versions of the paper had the correct author list. The HTML version has now been corrected to match the print and PDF versions.

## TECHNICAL COMMENT ABSTRACTS

### Comment on Papers by Evans *et al.* and Mekel-Bobrov *et al.* on Evidence for Positive Selection of *MCPH1* and *ASPM*

**Nicholas Timpson, Jon Heron, George Davey Smith, Wolfgang Enard**

Evans *et al.* and Mekel-Bobrov *et al.* (Reports, 9 September 2005, pp. 1717 and 1720, respectively) reported that human genetic variants of *Microcephalin* (*MCPH1*) and *abnormal spindle-like microcephaly associated* (*ASPM*) are under strong positive selection. We genotyped these variants in 9000 children and find no meaningful associations with brain size and various cognitive measures, which indicates that contrary to previous speculation, *ASPM* and *MCPH1* have not been selected for brain-related effects.

Full text at www.sciencemag.org/cgi/content/full/317/5841/1036a

### Response to Comments by Timpson *et al.* and Yu *et al.*

**Nitzan Mekel-Bobrov and Bruce T. Lahn**

The lack of association of the *ASPM* and *MCPH1* genes with brain size or intelligence described by Timpson *et al.* has been reported previously, including by our own group. Moreover, as in most studies of selection, our analyses were entirely independent of phenotypic association. We also respond to the previously published comment by Yu *et al.*, which argued that *ASPM* has not undergone positive selection.

Full text at www.sciencemag.org/cgi/content/full/317/5841/1036b

## Letters to the Editor

Letters (~300 words) discuss material published in *Science* in the previous 3 months or issues of general interest. They can be submitted through the Web (www.submit2science.org) or by regular mail (1200 New York Ave., NW, Washington, DC 20005, USA). Letters are not acknowledged upon receipt, nor are authors generally consulted before publication. Whether published in full or in part, letters are subject to editing for clarity and space.

PHARMACOLOGY

# Tales of the Wonder Drug

**Nicolas Rasmussen**

**Penicillin**
Triumph and Tragedy
***by Robert Bud***
Oxford University Press, Oxford, 2007. 340 pp. $55, £30. ISBN 9780199254064.

German theatergoers in 1919 enjoyed the premiere of *Das Wundermittel* (*The Wonder Drug*), by popular playwright Ludwig Fulda. In it, one of the main characters (a chemist) as a prank announces the discovery of a new medicine, "Mirakulin," that cures all illness. When he attempts to retract his discovery claim and reveal the game, he finds it is too late; his fame and fortune, and society's faith in the drug, cannot be so easily undone. Thus, he tragicomically learns, the hope and expectation of such a miracle drug is eternal. If he had not announced Mirakulin, then someone else would have, and so in every generation. One of the stories with which Robert Bud opens *Penicillin*, this is a fitting place to begin the drama of that drug. For with its terrific efficacy against suitable infections and remarkably low profile of harmful effects at therapeutic doses, penicillin remains the truest example of a wonder drug ever produced by science.

Steeped in mythology, penicillin's history therefore involves much more than a chemical entity less poisonous to humans than to certain bacteria. Penicillin is that chemical, of course, but the drug also has served as an icon of scientific medicine, an emblem of the pharmaceutical industry's beneficence, and a politically charged exemplar of good science. For example, stories making London microbiologist Alexander Fleming the genius of penicillin's discovery—as a contaminant in his old *Staphylococcus* cultures during the late 1920s—have tended to support a tradition of curiosity-driven, individualistic science. Stories contending that the lion's share of the credit for penicillin belongs to the Oxford group of Howard Florey have tended, in contrast, to advocate increased state support for large-scale, high-technology science in Britain. This same perspective has often seen penicillin as a sorry example of how British science and industry have traditionally failed to cooperate, allowing Americans to "steal" their national treasure. Meanwhile in postwar America, where penicillin production by pharmaceutical firms could not have occurred without wartime research by life scientists working at the U.S. Department of Agriculture and universities, the wonder drug served as a key argument for Vannevar Bush and others advocating that government science funding should continue indefinitely. The United States might never have established its present system of grant support for basic science without it, as the atom bomb was a considerably less impressive symbol of social benefit from big science.

To capture the symbolic dimension of penicillin, the stories and rich associations surrounding the miracle drug, Bud (a historian of science at the Science Museum, London) borrows the concept of the brand from marketing. Thus, even though infectious diseases had been in sharp decline through preventative public health measures for a half-century before the war, in the postwar world the penicillin "brand" embodied scientific medicine and captured all credit for the conquest of disease. Hence the dissemination of penicillin production facilities became a key priority of the United Nations and the nascent World Health Organization in the late 1940s, cementing cooperation in the postwar international community with the promise of a better future through science and modern technology.

At one of these UN-funded facilities in Rome in the 1950s, Ernst Chain of the Oxford group and collaborators from Beecham corporation made the key breakthrough that led to methicillin and the range of semisynthetic beta-lactam antibiotics we have today. These semisynthetics are also penicillins, and—stretching the brand concept rather thinly—for Bud so too (symbolically) are streptomycin and the early broad-spectrum antibiotics such as terramycin and chloramphenicol, which the pharmaceutical industry avidly ferreted from the soil, imitating the penicillin discovery even before the original was fully tested. And this same symbolic power of the penicillin brand, standing for salvation through modern medicine, helps explain why penicillin has been so widely overused in outpatient practice, the prescription for sniffles totemically reinforcing doctor-patient relationships in a convenient and time-saving way.

Bud argues that penicillin also ushered in a new morality in medicine and health, freeing both patients and hospital staff from the rigorous self-discipline of traditional hygiene. Most spectacularly, virtually overnight penicillin made syphilis an awkward nuisance rather than a dreaded scourge and heritable taint. Infectious diseases in general lost their associations with moral laxity, becoming mere inconveniences with a pharmacological fix. This ascendance of technology as the vehicle to health brought with it a rise in the status of drug firms and a decline in the status of doctors, whom patients came to regard less as founts of wisdom than as conduits for pills. And the technological fix of penicillin also enabled a massive scale-up in factory farming, making gigantic feedlots and chicken batteries that previously had been foiled by infectious disease not just possible but economical. Penicillin made the modern world, the book basically argues: through it man escaped ancient ecological constraints and reached for total, rationalistic dominance of living nature.

But the magic potion turned out to have its

**Iconic plate.** In 1928, Fleming found that secretions from the fungus *Penicillium notatum* destroyed *Staphylococcus* colonies.

CREDIT: ST. MARY'S HOSPITAL MEDICAL SCHOOL/PHOTO RESEARCHERS, INC.

The reviewer is in the School of History and Philosophy, University of New South Wales, Sydney, NSW 2052, Australia. E-mail: n.rasmussen@unsw.edu.au

limits, in the evolution of resistant bacteria encouraged by overly free antibiotic use. This is the tragedy Bud finds in penicillin's triumphant history. The very success of the hero, the penicillin brand, was its undoing. And there is another element of tragedy, the tragedy of the commons: The probably unnecessary prescription demanded by anxious parents is more likely to benefit than harm their child, but it surely harms the public health in the long run by speeding that antibiotic's obsolescence. However, the penicillin aura is finally changing, Bud believes, thanks in part to public health efforts to rebrand antibiotics from miracle cures to limited resources that require stewardship. In an era that increasingly assumes that science and technology bring costs with every benefit and rejects rationalist fantasies of nature forever dominated by one technological fix after another, the promise that chemistry will always stay ahead of bacterial evolution seems hollow. In any event, prescription demand for antibiotics appears to be declining in developed countries. If our culture's flagging trust in technological institutions like the drug industry means that, after 40 years, we finally heed calls to limit antibiotic use in agriculture and outpatient medicine, then this may be one tragicomedy with a happy ending.

10.1126/science.1144953

ENTOMOLOGY

# Pop Fly

**May Berenbaum**

In September 2004, the U.S. House of Representatives Committee on Resources conducted a field hearing in San Bernardino County, California, to evaluate public support for maintaining the endangered species status of the Delhi Sands flower-loving fly, *Rhaphiomidas terminatus abdominalis*, the only fly officially recognized on the U.S. endangered species list. Proponents of de-listing the species, who claimed that its federal protection compromised major development projects in the area, attended the hearings carrying large flyswatters to emphasize their point (*1*). Their use of that prop graphically illustrates the general public perception problems faced by the insects collectively known as flies. Although most people equate "fly" with *Musca domestica*—the house fly commonly associated with dung, decomposition, dirt, and disease—the word technically applies to over 120,000 species that meet the entomological definition: members of the order Diptera, a tremendously diverse collection of species united by virtue of possessing two, instead of the typical four, wings in their adult stage. Thus, the order Diptera comprises not just the pestiferous house fly and its dung-infesting relatives in the family Muscidae but also members of 28 other families, which include robber flies, fruit flies, crane flies, and others even less familiar to the general public.

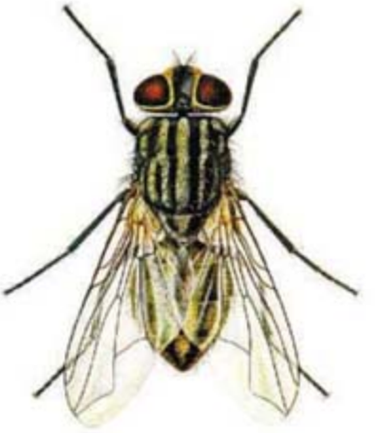

**Disease carrier.** The house fly, *Musca domestica*.

**Fly**
***by Steven Connor***
Reaktion, London, 2006. 222 pp. Paper, $19.95, £12.95. ISBN 9781861892942. Animal.

In *Fly*, Steven Connor undertakes the monumental task of acquainting a prejudiced public with the spectacular diversity of Diptera. The book is a tour de force (or, for the pun-inclined, a tour de *Forcipomyia*) of all manner of flies through both scientific and cultural lenses. On the scientific side, flies in the broad sense have played a key role in many of the most important intellectual advances of the past half-millennium, including the debunking of spontaneous generation, the identification of insects as vectors of human diseases, and the elucidation of the mechanics of mutation and development. On the cultural side, while familiarity in the case of the house fly has certainly bred contempt, it has also, across the centuries, produced a grudging respect and affection. Flies have been imbued with a spectacular array of metaphorical meanings, ranging from ephemerality to metamorphosis and resurrection to sexual lubricity, in virtually every form of human expression.

Connor, a professor of modern literature and theory at Birkbeck College, London, not surprisingly devotes a majority of pages to cultural aspects of flies. The book is organized around metaphorical themes, with science interwoven among historical references spanning 3000 years and cultural references involving almost every continent. The illustrations are an unremitting delight—the author has done a fantastic job of hunting down images of all manner of flies in all manner of media. Turning the page might reveal a fly as portrayed in an ancient artifact, a 17th-century still life, a close-up photograph, or a poster of a 1950s science-fiction film.

Although the science is present, the book may have benefited from more rigorous scientific review. At times, the author plays a bit loose with the definition of "fly" such that in places the flies under discussion, although perhaps considered to be flies prior to 18th-century classification schemes, today are classified in entirely different orders (e.g., mayflies, in the order Ephemeroptera, and agents of "phthiriasis, or lousy disease," in the order Phthiraptera). As seems inevitable in popular books about insects, some scientific names are misspelled. For example, John Curtis's illustration was of *Tabanus alpinus*, not *Tabinus alpinus*, although today it is known as *Atylotus fulvus* (*2*). A 1740 illustration by August Johann Roesel von Rosenhof is presented to show that "some flies have a fondness for the sweet nectar of flowers," despite the fact that the flower depicted is a stapeliad, a group best known for attracting flies with a nauseating stench resembling the odor of rotting flesh. As well, the author interprets a late 19th century advertising image "showing a baby frolicking among flies" as suggesting that "flies acquired their fearsome reputation relatively recently." The fact that the "flies" in the image clearly have four wings (including two colorful elytra) indicates that the baby is likely frolicking with ladybeetles, which have long enjoyed popular approbation.

These criticisms are minor (mere flyspecks, as it were). *Fly* is a joy to read, and it will particularly appeal to entomologists who have a stake in correcting misperceptions about one of the largest orders of animals. The "timeline of the fly" at the end of the book dramatically illustrates the abiding impact these insects have had on human affairs. For the record, the Delhi Sands flower-loving fly remains on the federal endangered species list; Richard Pombo, among the architects of the congressional field hearing to undermine its protected status, was voted out of office on 7 November 2006.

The reviewer is at the Department of Entomology, 320 Morrill, University of Illinois, 505 South Goodwin, Urbana, IL 61801–3795, USA. E-mail: maybe@uiuc.edu

**References**

1. E. Pennisi, *Science* **304**, 27 (2004).
2. http://delta-intkey.com/britin/tri/www/curtisid.htm.
3. L. O. Howard, *The House-Fly, Disease Carrier: An Account of Its Dangerous Activities and of the Means of Destroying It* (Stokes, New York, 1911).

10.1126/science.1140074

CREDIT: FROM *FLY*; ORIGINALLY (*3*)

SOCIAL SCIENCE

# Sacred Barriers to Conflict Resolution

Resolution of quarrels arising from conflicting sacred values, as in the Middle East, may require concessions that acknowledge the opposition's core concerns.

Scott Atran,[1] Robert Axelrod,[2] Richard Davis[3]

Efforts to resolve political conflicts or to counter political violence often assume that adversaries make rational choices (*1*). Ever since the end of the Second World War, "rational actor" models have dominated strategic thinking at all levels of government policy (*2*) and military planning (*3*). In the confrontations between nation states, and especially during the Cold War, these models were arguably useful in anticipating an array of challenges and in stabilizing world peace enough to prevent nuclear war. Now, however, we are witnessing "devoted actors" such as suicide terrorists (*4*), who are willing to make extreme sacrifices that are independent of, or all out of proportion to, likely prospects of success. Nowhere is this issue more pressing than in the Israeli-Palestinian dispute (*5*). The reality of extreme behaviors and intractability of political conflicts there and discord elsewhere—in the Balkans, Kashmir, Sri Lanka, and beyond—warrant research into the nature and depth of commitment to sacred values.

The Spirit of Mahatma Gandhi, for whom "values become your destiny," on the wall at the Kalandiya checkpoint separating the West Bank from Israel.

CREDIT: PHOTOGRAPH BY S. ATRAN

## Sacred Values

Sacred values differ from material or instrumental ones by incorporating moral beliefs that drive action in ways dissociated from prospects for success. Across the world, people believe that devotion to core values (such as the welfare of their family and country or their commitment to religion, honor, and justice) is, or ought to be, absolute and inviolable. Such values outweigh other values, particularly economic ones (*6*).

To say that sacred values are protected from trade-offs with economic values does not mean that they are immune from all material considerations. Devotion to some core values, such as children's well-being (*7*) or the good of the community (*8*), or even to a sense of fairness (*9*), may represent universal responses to long-term evolutionary strategies that go beyond short-term individual calculations of self-interest, yet advance individual interests in the aggregate and long run. Other such values are clearly specific to particular societies and historical contingencies, such as the sacred status of cows in Hindu culture or the sacred status of Jerusalem in Judaism, Christianity, and Islam. Sometimes, as with cows (*10*) or forests (*11*), the sacred may represent accumulated material wisdom of generations in resisting individual urges to gain an immediate advantage of meat or firewood for the long-term benefits of renewable sources of energy and sustenance. Political leaders often appeal to sacred values as a way of reducing "transaction costs" (*12*) in mobilizing their constituents to action and as a least-cost method of enforcing their policy goals (*13*).

Matters of principle or "sacred honor," when enforced to a degree far out of proportion to any individual or immediate material payoff, are often seen as defining "who we are." After the end of the Vietnam War, successive U.S. administrations resisted Hanoi's efforts at reconciliation until Hanoi accounted for the fate of U.S. soldiers missing in action (*14*). Granted, the issue was initially entwined with rational considerations of balance of power at the policy-making level: The United States did not want to get too close to Hanoi and so annoy Beijing (a more powerful strategic ally against the Soviet Union). But popular support for the administration's position, especially among veterans, was a heartfelt concern for "our boys," regardless of numbers or economic consequences.

The "who we are" aspect is often hard for members of different cultures to understand; however, understanding and acknowledging others' values may help to avoid or to resolve the hardest of conflicts. For example, at the peaceful implementation of the occupation of Japan in 1945, the American government realized that preserving, and even signaling respect for, the emperor might lessen the likelihood that Japanese would fight to the death to save him (*15*).

## Symbolic Concessions

Our research team has measured emotional outrage and propensity for violence in response to peace deals involving compromises over issues integral to the Israeli-Palestinian conflict with Israeli settlers, Palestinian refugees, and Hamas versus non-Hamas students. Our proposed compromises were exchanging land for peace, sovereignty over Jerusalem, the right of Palestinian refugees to return to their former lands and homes inside Israel, and recognition of the validity of the adversary's own sacred values (*1*). We found that the use of material incen-

[1]CNRS—Institut Jean Nicod, 29 rue d'Ulm, 75005 Paris, France; University of Michigan, Ann Arbor, MI; and John Jay College of Criminal Justice, New York, NY, USA; e-mail: satran@umich.edu. [2]University of Michigan, Ann Arbor, MI 48109, USA; e-mail: axe@umich.edu. [3]RTI International, 3040 Cornwallis Road, Research Triangle Park, NC 27709, and ARTIS Research and Risk Modeling, Washington, DC, USA; e-mail: richdavis@rti.org.

tives to promote the peaceful resolution of political and cultural conflicts may backfire when adversaries treat contested issues as sacred values. Symbolic concessions of no apparent material benefit may be key in helping to solve seemingly intractable conflicts.

These results correspond to the historical sense of experts. One senior member of the National Security Council responded recently (*16*), "This seems right. On the settlers [who were to be removed from Gaza], Sharon realized too late that he shouldn't have berated them about wasting Israel's money and endangering soldiers' lives. Sharon told me that he realized now that he should have made a symbolic concession and called them Zionist heroes making yet another sacrifice."

As further illustration that sacred values can be at the heart of deep-seated political disputes, Isaac Ben Israel, a former Israeli Air Force general who currently heads his country's space agency, told us: "Israel recognizes that the [Hamas-led] Palestinian government is still completely focused on what it considers to be its essential principles. … For Hamas, a refusal to utter the simple words 'We recognize Israel's right to exist' is clearly an essential part of their core values. Why else would they suffer the international boycott … and let their own government workers go without pay, their people go hungry, and their leaders risk assassination?" Ghazi Hamad, a Hamas leader and then-spokesman for the Palestinian government, told us: "In principle, we have no problem with a Palestinian state encompassing all of our lands within the 1967 borders. But let Israel apologize for our tragedy in 1948, and then we can talk about negotiating over our right of return to historic Palestine." In rational-choice models of decision-making, something as intangible as an apology could not stand in the way of peace.

Apologies may not be so much deal-makers in themselves as facilitators for political compromise that may also involve material transactions. At its founding in 1948, Israel was in dire economic straits (*17*). But Israel and the World Jewish Congress refused to demand compensation directly from Germany for the property of murdered European Jews. Israel insisted that before any money could be considered, Germany must publicly declare contrition for the murder and suffering of Jews at German hands.

An Iranian scholar and former top diplomat remarked recently that "symbolic statements are important if sincere, [and] without reservation. In 2000, [then-Secretary of State Madeleine] Albright seemed to apologize to Iran for past offenses but then said [in a memorandum] 'despite the trend towards democracy, control over the military, judiciary, courts and police remain in unelected hands.' Our leadership interpreted this as a call for a coup" (*18*).

### Recent Discussions

We went to the Middle East in February 2007 to directly probe issues of material trade-offs and symbolic concessions with leaders of the major parties to the Israel-Palestine dispute. We asked 14 interviewees in Syria, Palestine, and Israel to verify statements for citation. No off-the-record statements contradicted these.

Responses were consistent with our previous findings (*1*), with one important difference. Previously, people with sacred values had responded "No" to the proposed trade-off; "No" accompanied by emotional outrage and increased support for violence to the trade-off coupled with a substantial and credible material incentive; and "Yes, perhaps" to trade-offs that also involve symbolic concessions (of no material benefit) from the other side. Leaders responded in the same way, except that the symbolic concession was not enough in itself, but only a necessary condition to opening serious negotiations involving material issues as well. For example, Musa Abu Marzouk (former chairman, and current deputy chairman, of Hamas) said "No" to a trade-off for peace without granting a right of return; a more emphatic "No, we do not sell ourselves for any amount," when given a trade-off with a substantial material incentive (credible offering of substantial U.S. aid for the rebuilding of Palestinian infrastructure); but "Yes, an apology is important, but only as a beginning. It's not enough, because our houses and land were taken away from us and something has to be done about that."

Similarly, Binyamin Netanyahu (former Israeli prime minister and current opposition leader in parliament) responded to our question, "Would you seriously consider accepting a two-state solution following the 1967 borders if all major Palestinian factions, including Hamas, were to recognize the right of the Jewish people to an independent state in the region?" with the answer: "Yes, but the Palestinians would have to show that they sincerely mean it, change their textbooks and anti-Semitic characterizations and then allow some border adjustments so that Ben Gurion [Airport] would be out of range of shoulder-fired missiles."

For Israel's former chief hostage negotiator, Ariel Merari, "Trusting the adversary's intentions is critical to negotiations, which have no chance unless both sides believe the other's willingness to recognize its existential concerns." Indeed, recognition of some "existential values" may change other values into material concerns, e.g., "since the PLO's [Palestine Liberation Organization's] recognition of Israel, most Israelis no longer see rule over the West Bank as existential" (*19*).

We urgently need more scientific research to inform better policy choices. Our findings about sacred values suggest that there may be fewer differences than are publicly acknowledged in the material trade-offs that "moderate" and "radical" leaders in Palestine, Israel, and elsewhere may be willing to make. Overcoming moral barriers to symbolic concessions and their emotional underpinnings may pose more of a challenge but also offer greater opportunities for breakthroughs to peace than hitherto realized.

### References and Notes


1. J. Ginges, S. Atran, D. Medin, K. Shikaki, *Proc. Natl. Acad. Sci. U.S.A.* **104**, 7357 (2007).
2. J. Gaddis, *Strategies of Containment: A Critical Appraisal of Postwar National Security* (Oxford Univ. Press, New York, 1995).
3. G. Allison, *Essence of Decision: Explaining the Cuban Missile Crisis* (Longman, New York, 1999).
4. S. Atran, *Science* **299**, 1534 (2003).
5. "America's image slips, but allies share U.S. concerns over Iran, Hamas" (Survey Report, Pew Research Center, 13 June 2006); http://pewglobal.org/reports/display.php?ReportID=252.
6. P. E. Tetlock, *Trends Cogn. Sci.* **7**, 320 (2003).
7. W. D. Hamilton, *J. Theor. Biol.* **7**, 1 (1964).
8. E. Durkheim, *The Elementary Forms of Religious Life* (1912) [translated by K. E. Fields] (Free Press, New York, 1995).
9. M. Hauser, *Moral Minds: How Nature Designed Our Universal Sense of Right and Wrong* (Ecco, New York, 2000).
10. M. Harris, *Curr. Anthropol.* **7**, 51 (1966).
11. S. Atran, D. Medin, N. Ross, *Psychol. Rev.* **112**, 744 (2005).
12. A. Varshney, *Perspect. Polit.* **1**, 85 (2003).
13. R. Goodin, *Policy Sci.* **12**, 131 (1980).
14. O. Babson, "Diplomacy of isolation: United States unilateral sanctions policy and 1975–1995" (WWS case study 4/02, Woodrow Wilson School, Princeton Univ., Princeton, NJ, 2002); www.wws.princeton.edu/cases/papers/sanctions.html.
15. J. Dower, *Embracing Defeat: Japan in the Wake of World War II* (Norton, New York, 1999).
16. The response was given to the final point mentioned in S. Atran, R. Axelrod, R. Davis, Synopsis of briefing to National Security Council staff, The White House, 28 March 2007; www.sitemaker.umich.edu/satran/files/synopsis_atran-sageman_nsc_brief_28_march_2007.pdf.
17. I. Lustick, *J. Int. Aff.* **60**, 51 (2006).
18. Remarks made at the Fifth Meeting, Permanent Monitoring Panel on Terrorism, World Federation of Scientists, Erice, Italy, 18 May 2007.
19. In May 2007, we broached ideas of mutual symbolic concession. Hamas would renounce Article 32 of its 1988 Covenant, which highlights "Zionist scheming … laid out in *The Protocols of the Elders of Zion*," a notorious anti-Semitic tract forged by Russian Czarist police. Israel would renounce the slogan, "A land without people for a people without land," coined by Israel Zangwill a century ago to describe Zionist aspirations. Leaders on both sides acknowledge they would be renouncing a falsehood and grant that such statements by the other side could represent a psychological breakthrough. But discussion was halted because of civil strife in Gaza.


20. Supported by the NSF, U.S. Air Force Office of Scientific Research, and Centre National de la Recherche Scientifique. Thanks to D. E. Axelrod, J. Ginges, and D. Medin for suggestions.

10.1126/science.1144241

MICROBIOLOGY

# A Bacterial Pathogen Sees the Light

An unusual photosensitive kinase is discovered in bacteria, where it increases virulence in response to light.

John T. M. Kennis and Sean Crosson

Light, a nearly ubiquitous environmental signal, regulates myriad developmental and behavioral responses in plant, fungal, bacterial, and animal cells. Photosensitive proteins abound in the bacterial kingdom, but their cellular functions often remain a mystery. On page 1090 in this issue, Swartz *et al.* (*1*) identify a functional role for a new type of light sensor in bacteria—light, oxygen, or voltage (LOV) histidine kinase. In the notorious pathogen *Brucella abortus*, light increases the enzymatic activity of this kinase, which, remarkably, increases virulence of the bacterium. Related LOV histidine kinases are conserved across a range of bacterial taxa, suggesting that this virulence pathway could be one of many new photosensory pathways regulating bacterial physiology.

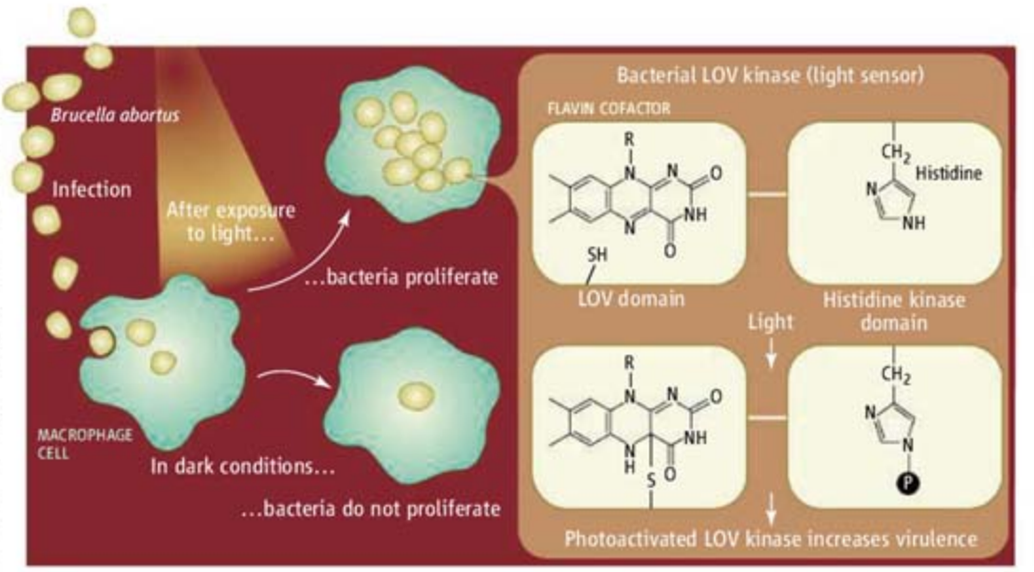


**Infectious light.** Infection of cells by the pathogenic bacterium *B. abortus* is accentuated by visible light. Absorption of light by a photosensory histidine kinase causes a change of its chemical and physical properties that increases virulence.

LOV domains belong to the PAS (Per-Arnt-Sim) protein domain superfamily (*2*), and were initially described as the light-absorbing region in plant serine-threonine kinases known as phototropins (*3*). A compact protein module of ~110 amino acids, the LOV domain is rendered sensitive to blue light through a noncovalently bound flavin cofactor. Upon absorbing a blue photon, the flavin cofactor forms a covalent bond with a conserved cysteine residue in the LOV domain (*4*–*8*). This event triggers a conformational change within the LOV domain that communicates photon detection to regions outside the domain's core (*9*, *10*). This unique signaling mechanism underlies several well-known photomorphogenic and circadian responses in plants and fungi (*3*, *11*).

Flavin-binding LOV domains are broadly distributed across the plant, fungal, and bacterial kingdoms (*12*, *13*), and thus, serve as evolutionarily conserved sensory modules. Because they are fused to a range of "output" domains including bacterial diguanylate cyclases and phosphodiesterases, zinc-finger transcription factors, and histidine kinases, this flavin-binding protein fold provides a means for the light environment to control a wide range of cellular phenomena.

Surprisingly, many bacterial species that encode LOV domains in their genomes are nonpigmented heterotrophs (*12*, *13*) with no known or anticipated response to visible light. What, then, is the function of this widely distributed light-sensing domain in these species [LOV domains are encoded in 16% of sequenced bacterial genomes (*13*)]? A particularly intriguing family of bacterial LOV proteins is the LOV histidine kinases. Histidine kinases, along with a response regulator family of proteins, form the two-component signaling systems that constitute the predominant mode of signal transduction in bacteria (*14*).

Swartz *et al.* show that light increases the enzymatic (autophosphorylation) activity of a *Brucella* LOV histidine kinase (see the figure). Strikingly, they demonstrate that visible light increases the virulence of *B. abortus* in a macrophage infection model: Wild-type *Brucella* is 10 times more virulent after exposure to visible light than bacteria that were never exposed to light. Deletion of the gene encoding LOV kinase from *Brucella* abolished this light-mediated virulence response, reducing bacterial proliferation in light-exposed macrophage cells to the level observed in the dark. These results provide a clear link between *B. abortus* LOV histidine kinase and the light-induced increase in virulence. Moreover, mutagenesis of the conserved cysteine in the LOV domain abolished the light response, demonstrating that cysteinyl-flavin bond formation in the LOV domain is necessary for light-mediated virulence. The result of Swartz and colleagues suggests that upon ejection from an infected animal host, sunlight acts as an environmental signal that increases the virulence of *B. abortus*. Thus, exposure to visible radiation in natural reservoirs outside the host could increase the likelihood of infecting another host.

In addition, Swartz *et al.* demonstrate that light regulates histidine kinase activity across multiple bacterial taxa. By cloning, expressing, and purifying LOV histidine kinases from *Brucella* as well as from the plant pathogen *Pseudomonas syringae* and the marine bacterium *Erythrobacter litoralis*, the authors show that each species of LOV histidine kinase exhibits canonical LOV domain photochemistry as well as light-driven autophosphorylation activity.

The study raises many important questions in what promises to become an important new field of bacterial photobiology. For instance, what are the functions of LOV histidine kinases in other species? What are the downstream signaling partners of these photosensors? How does activation of *B. abortus* LOV

J. T. M. Kennis is in the Biophysics Department, Faculty of Sciences, Vrije Universiteit, 1081HV Amsterdam, Netherlands. S. Crosson is in the Department of Biochemistry and Molecular Biology, The University of Chicago, Chicago, IL 60637, USA. E-mail: j.kennis@few.vu.nl, scrosson@uchicago.edu

histidine kinase increase virulence? And mechanistically, how does absorption of photons by the LOV sensory domain trigger enzymatic activity?

Although high-resolution structures are available for a number of histidine kinase domains, it is not known how signal information is communicated from the sensor domain to the kinase domain, and how autophosphorylation is initiated. Because of the photochromic properties of LOV domains (*15*), LOV histidine kinase activity can be switched between active and inactive states by a simple pulse of light, permitting one to monitor the transition between the ground state and the signaling state. In this way, the light-driven structural changes initiated in the LOV domain that finally result in kinase phosphorylation can be assessed in real time. Moreover, by combining microscopy with microfocused laser excitation, intracellular signaling processes involving a LOV histidine kinase and its signaling partners can be followed in a single bacterial cell. Certainly, LOV histidine kinases are poised to enable a deep understanding of key processes in signal transduction at both the molecular and cellular levels.


**References**

1. T. E. Swartz *et al.*, *Science* **317**, 1090 (2007).
2. B. L. Taylor, I. B. Zhulin, *Microbiol. Mol. Biol. Rev.* **63**, 479 (1999).
3. J. M. Christie, W. R. Briggs, in *Handbook of Photosensory Receptors*, W. R. Briggs, J. L. Spudich, Eds. (Wiley-VCH, Weinheim, Germany, 2005), pp. 277–304.
4. M. Salomon *et al.*, *Proc. Natl. Acad. Sci. U.S.A.* **98**, 12357 (2001).
5. S. Crosson, K. Moffat, *Plant Cell* **14**, 1067 (2002).
6. T. E. Swartz, R. A. Bogomolni, in *Handbook of Photosensory Receptors*, W. R. Briggs, J. L. Spudich, Eds. (Wiley-VCH, Weinheim, Germany, 2005), pp. 305–323.
7. J. T. M. Kennis *et al.*, *Biochemistry* **42**, 3385 (2003).
8. E. Schleicher *et al.*, *J. Am. Chem. Soc.* **126**, 11067 (2004).
9. S. M. Harper, L. C. Neil, K. H. Gardner, *Science* **301**, 1541 (2003).
10. D. Nozaki *et al.*, *Biochemistry* **43**, 8373 (2004).
11. J. C. Dunlap, J. J. Loros, *Curr. Opin. Microbiol.* **9**, 579 (2006).
12. S. Crosson, S. Rajagopal, K. Moffat, *Biochemistry* **42**, 2 (2003).
13. A. Losi, in *Flavins: Photochemistry and Photobiology*, E. Silva, A. M. Edwards, Eds. (Royal Society of Chemistry, Cambridge, 2006), vol. 6, pp. 217–269.
14. A. M. Stock, V. L. Robinson, P. N. Goudreau, *Annu. Rev. Biochem.* **69**, 183 (2000).
15. J. T. M. Kennis *et al.*, *J. Am. Chem. Soc.* **126**, 4512 (2004).


10.1126/science 1147609

ECONOMICS

# Money Illusion and the Market

Individuals often pay more attention to price tags than to real value. Evidence shows that this may also have important effects on markets.

**Jean-Robert Tyran**

Imagine a consumer who discovers to his surprise that the money in his bank account and his salary have doubled overnight. Now suppose that all prices have also doubled overnight. Will this consumer be happy about being awash with money? Will he feel richer today and buy more or different goods than he did yesterday? Not according to standard economic theory. After all, he has to work the same number of minutes to buy, say, a loaf of bread, and can therefore afford to buy exactly the same set of goods as he did yesterday. In short, the boost in purely "nominal" terms (which inflates all monetary values by the same factor) should not affect behavior because nothing has changed in "real" terms (i.e. when taking this inflation properly into account).


CREDIT: JOE SUTLIFF

This is the textbook example that economists use to explain the standard assumption that economic agents are free from money illusion, i.e., that they think about economic transactions exclusively in real terms. But now imagine a situation in which all prices increase by 3.1% and nominal wages increase by, for example, 2.3% over 1 year. Do people behave the same way in this situation as in the effectively equivalent case when their nominal wages fall by about 0.8% at constant prices? Or do some people perceive these two situations differently because of different nominal representations?

Despite increasing evidence that thinking in nominal terms is common and that purely nominal changes can affect individual choices (*1*, *2*), economists have only started to understand when and how money illusion affects market outcomes. Economists often claim that learning and market forces eliminate distortions from money illusion at the market level if irrational agents are swiftly selected out of the market (e.g., because they go bankrupt) or if rational agents can effectively take advantage of irrational behavior. Yet, recent evidence, from both the experimental laboratory and the field, suggests that money illusion can affect market outcomes.

An intriguing example comes from the housing market. Housing prices have reached unprecedented heights in recent years in several countries. Sharp run-ups followed by busts are a common feature of housing prices. Recently, Brunnermeier and Julliard proposed that a particular type of money illusion, which results from confusing nominal and real interest rates, could explain such "housing frenzies" (*3*). They found that falling nominal interest rates and inflation increased housing prices, and vice versa, even when controlling for other factors that affect real housing prices such as construction costs, housing quality, property taxes, demographics, and general economic conditions.

The reasoning for this result is as follows. When inflation is low, monthly nominal interest payments on mortgages are low compared to the rent on a similar house. Because houses seem cheap, illusion-prone investors entering the market tend to buy rather than rent and cause an upward pressure on housing prices when inflation declines. However, decreasing inflation not only reduces entrants' current payments on the mortgage but also increases the real cost of future mort-

The author is in the Department of Economics, University of Copenhagen, Studiestræde 6, DK-1455 Copenhagen, Denmark. E-mail: jean-robert.tyran@econ.ku.dk

gage payments. Investors who base their decisions on the salient low nominal mortgage payments, but ignore the less-visible effect of inflation on the future real mortgage cost, are prone to an illusion. In a sense, these investors act like a person who thinks that a car is cheaper if the down-payment is spread over 4 years rather than 2 years because the monthly payments are lower. Some researchers have suggested that a similar relationship between inflation and real asset prices exists in the stock market, and have proposed money illusion as a cause (*4*, *5*).

Experimental studies by Fehr and I on markets with competition among a small number of price-setting firms show that money illusion can have pronounced effects on market prices (*6*, *7*). Decision-makers are presented with either real or nominal information on profits under otherwise identical conditions to test whether money illusion is induced by a framing effect (i.e., by inflating all nominal values) (*1*, *8*). Money illusion has strong effects on market prices when rational agents have incentives to "follow the crowd," but only minor effects if rational agents have incentives to "go against the tide" (*9*).

One of our studies finds that money illusion can cause a sluggish reduction of nominal prices in response to a monetary contraction (i.e., deflation of all nominal values) (*6*). These sluggish downward nominal prices may be the result of what economists call "nominal loss aversion" if firms are reluctant to cut prices to avoid lower nominal profits associated with lower price levels. This stems from an interaction of money illusion and "loss aversion," which is a tendency for losses to loom larger in people's minds than corresponding gains. Several field studies have shown that real wage cuts are more common when inflation is positive rather than zero [see (*10*) for a review]. This finding is consistent with nominal loss aversion because employers can cut real wages despite increasing nominal wages in an inflationary environment, but nominal wages must fall to cut real wages with zero inflation. Earlier work showed that nominal loss aversion also affects portfolio choices in laboratory experiments (*11*) and seems to be an important factor in housing markets. Residential home owners seem to be more reluctant to sell a house at a real loss if this is associated with a nominal loss rather than masked by a nominal gain (*12*).

There are complications, however. Researchers cannot directly observe money illusion but can only indirectly infer its effects. Evidence consistent with money illusion may also be consistent with alternative accounts, involving fully rational agents. Laboratory work can convincingly rule out such alternative accounts, but laboratory economies tend to be simple. Conversely, field data are rich, but the relevance of alternative accounts is often open to debate.

Given that both modes of research have their advantages and limitations, they ought to inspire each other. For example, experimental evidence on the effects of money illusion in competitive asset markets (e.g., stock markets) would strengthen the interpretation of field evidence. Conversely, field studies on the relevance of incentives to "follow the crowd" identified in the laboratory would be a step forward in understanding when money illusion matters in markets.

**References**


1. E. Shafir, P. A. Diamond, A. Tversky, *Q. J. Econ.* **112**, 341 (1997).
2. P. Kooreman, R. P. Faber, H. M. Hofmans, *J. Money Cred. Bank.* **36**, 1121 (2004).
3. M. K. Brunnermeier, C. Julliard, *Rev. Fin. Stud.*, in press.
4. F. Modigliani, R. Cohn, *Fin. Analysts J.* **35**, 24 (1979).
5. R. B. Cohen, C. Polk, T. Vuolteenaho, *Q. J. Econ.* **120**, 639 (2005).
6. E. Fehr, J.-R. Tyran, *Am. Econ. Rev.* **91**, 1239 (2001).
7. E. Fehr, J.-R. Tyran, *Games Econ. Behav.* **58**, 246 (2007).
8. A. Tversky, D. Kahneman, *Science* **211**, 453 (1981).
9. E. Fehr, J.-R. Tyran, *J. Econ. Perspect.* **19**, 43 (2005).
10. J. L. Yellen, G. A. Akerlof, *Econ. Inq.* **44**, 1 (2006).
11. R. H. Thaler, A. Tversky, D. Kahneman, A. Schwartz, *Q. J. Econ.* **112**, 647 (1997).
12. D. Genesove, C. Mayer, *Q. J. Econ.* **116**, 1233 (2001).


10.1126/science.1143917

NEUROSCIENCE

# The Threatened Brain

The human brain's distinct reactions to distant dangers and nearby threats may be deregulated in anxiety disorders.

**Stephen Maren**

The world is a dangerous place. Every day we face a variety of threats, from careening automobiles to stock market downturns. Arguably, one of the most important functions of the brain and nervous system is to evaluate threats in the environment and then coordinate appropriate behavioral responses to avoid or mitigate harm.

Imminent threats and remote threats produce different behavioral responses, and many animal studies suggest that the brain systems that organize defensive behaviors differ accordingly (*1*). On page 1079 of this issue, Mobbs and colleagues make an important advance by showing that different neural circuits in the human brain are engaged by distal and proximal threats, and that activation of these brain areas correlates with the subjective experience of fear elicited by the threat (*2*). By pinpointing these specific brain circuits, we may gain a better understanding of the neural mechanisms underlying pathological fear, such as chronic anxiety and panic disorders.

To assess responses to threat in humans, Mobbs and colleagues developed a computerized virtual maze in which subjects are chased and potentially captured by an "intelligent" predator. During the task, which was conducted during high-resolution functional magnetic resonance imaging (fMRI) of cerebral blood flow (which reflects neuronal activity), subjects manipulated a keyboard in an attempt to evade the predator. Although the virtual predator appeared quite innocuous (it was a small red circle), it could cause pain (low- or high-intensity electric shock to the hand) if escape was unsuccessful. Brain activation in response to the predatory threat was assessed relative to yoked trials in which subjects mimicked the trajectories of former chases, but without a predator or the threat of an electric shock. Before each trial, subjects were warned of the contingency (low, high, or no shock). Hence, neural responses evoked by the anticipation of pain could be assessed at various levels of threat imminence not only before the chase, but also during the chase when the predator was either distant from or close to the subject.

How does brain activity vary as a function of the proximity of a virtual predator and the severity of pain it inflicts? When subjects were warned that the chase was set to commence, blood oxygenation level–dependent (BOLD) responses (as determined by fMRI) increased in frontal cortical regions, including the anterior cingulate cortex, orbitofrontal cortex, and ventromedial prefrontal cortex. This may reflect threat detection and subsequent action planning to navigate the forthcoming chase.

The author is in the Department of Psychology and Neuroscience Program, University of Michigan, Ann Arbor, MI 48109, USA. E-mail: maren@umich.edu

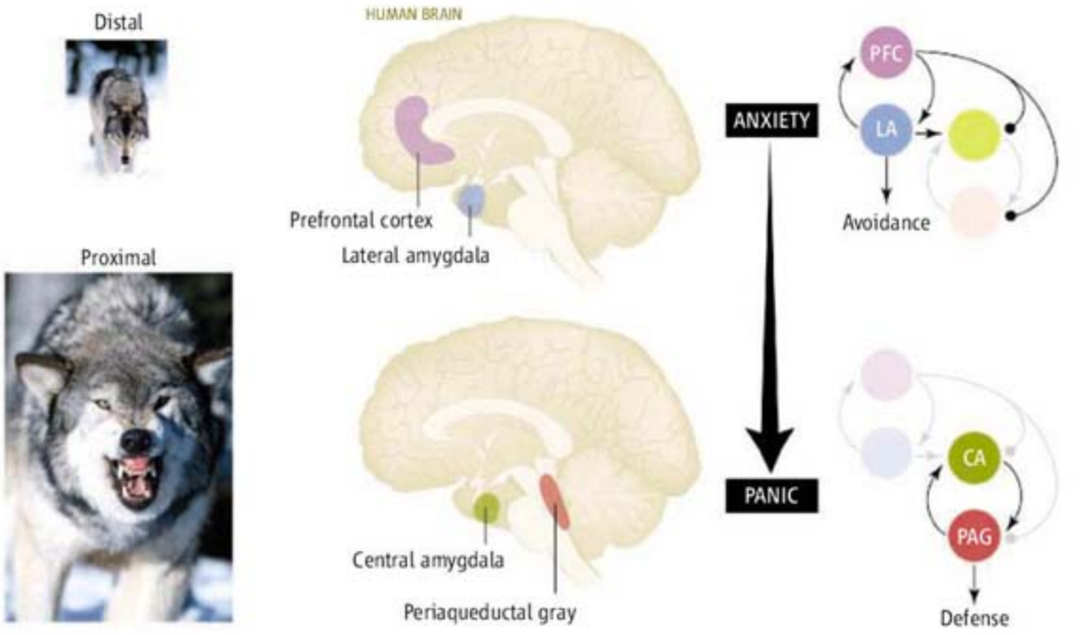


**Topography of fear.** As a predatory threat approaches, neural activity in the human brain shifts from the forebrain to the midbrain.

Once the chase commenced (independent of high- or low-shock trials), BOLD signals increased in the cerebellum and periaqueductal gray. Activation of the latter region is notable, as it is implicated in organizing defensive responses in animals to natural and artificial predators (*3*, *4*). Surprisingly, this phase of the session was associated with decreased activity in the amygdala and ventromedial prefrontal cortex. The decrease in amygdala activity is not expected, insofar as cues that predict threat and unpredictable threats activate the amygdala (*5*, *6*).

However, activity in these brain regions varied considerably according to the proximity of the virtual predator and the shock magnitude associated with the predator on a given trial (see the figure). When the predator was remote, blood flow increased in the ventromedial prefrontal cortex and lateral amygdala. This effect was more robust when the predator predicted a mild shock. In contrast, close proximity of a predator shifted the BOLD signal from these areas to the central amygdala and periaqueductal gray, and this was most pronounced when the predator predicted an intense shock. Hence, the prefrontal cortex and lateral amygdala were strongly activated when the level of threat was low, and this activation shifted to the central amygdala and periaqueductal gray when the threat level was high.

The shift in neural activity from the forebrain to the midbrain may reflect increases in fear as the predator approaches. In support of this view, Mobbs *et al.* also showed that BOLD signals in the periaqueductal gray and the nearby dorsal raphe nucleus were highly correlated with the degree to which subjects feared the predator and how confident they were that they could escape. In animals, similar variations in fear define the topography of behavior along a "predatory imminence continuum" (*7*). According to this view, the prefrontal cortex and lateral amygdala may coordinate behavior (such as avoidance) in the face of a distal threat, whereas the central amygdala and periaqueductal gray may coordinate defensive responses (such as freezing) when threat is imminent (*8*). Forebrain systems engaged by a remote predator may even inhibit midbrain defense systems to promote escape behavior. Indeed, when escape fails and capture becomes inevitable (when control is lost), prefrontal inhibition of amygdala activity (*9*) and midbrain defense circuits may be released to shift behavior into a defensive mode (*10*). Although Mobbs *et al.* show that subjects were motivated to escape the virtual predator, it would be of interest to know whether the brain activation patterns they observed predicted fear responses (such as sweating or tachycardia) during the task.

The majority of fMRI studies investigating the neural substrates of aversive emotions—including fear—have used tasks in which the imminence of the threat does not vary, or varies in a way that would elude detection in a neuroimaging study (*11*). For example, many studies have used Pavlovian fear conditioning procedures, in which a conditioned stimulus is paired with an aversive event (shock, loud noise, or a fear-evoking image). In this situation, the imminence of the aversive outcome does not vary, at least in a spatial domain, when the conditioned stimulus is presented. Although imminence might vary during the conditioned stimulus as the unconditioned stimulus approaches in time, modern fMRI techniques cannot resolve brain activity during the short conditioned stimuli (2 to 4 s) typically used in these experiments. Nonetheless, these approaches have identified brain responses to stimuli that predict aversive outcomes, and activation of the amygdala also figures prominently in this response (*12*–*15*).

What do the findings tell us about human anxiety and panic? As the imminence of a threat increases, the successive activation of neural circuits in the forebrain and midbrain may yield qualitative changes in the subjective experience of fear: Activation of the prefrontal cortex by distal, unpredictable threats might foster anxiety, whereas activation of the periaqueductal gray by proximal threats that predict pain may fuel panic. Dysfunction in these circuits is therefore likely to yield a variety of chronic anxiety disorders (*16*–*18*). Indeed, decoupling of the midbrain periaqueductal gray from cortical-amygdaloid regulation may contribute to panic disorder, which is characterized by intense somatic and autonomic fear responses to stimuli or situations that pose no immediate threat. Mobbs and colleagues have now set the stage for future efforts to explore this intriguing possibility in patients with anxiety disorders.

**References**

1. M. S. Fanselow, *Psychon. Bull. Rev.* **1**, 429 (1994).
2. D. Mobbs *et al.*, *Science* **317**, 1079 (2007).
3. B. M. De Oca, J. P. DeCola, S. Maren, M. S. Fanselow, *J. Neurosci.* **18**, 3426 (1998).
4. R. Bandler, M. T. Shipley, *Trends Neurosci.* **17**, 379 (1994).
5. G. Hasler *et al.*, *J. Neurosci.* **27**, 6313 (2007).
6. S. Maren, G. J. Quirk, *Nat. Rev. Neurosci.* **5**, 844 (2004).
7. M. S. Fanselow, L. S. Lester, in *Evolution and Learning*, R. C. Bolles, M. D. Beecher, Eds. (Erlbaum, Hillsdale, NJ, 1988), pp. 185–211.
8. P. Amorapanth, J. E. LeDoux, K. Nader, *Nat. Neurosci.* **3**, 74 (2000).
9. G. J. Quirk, E. Likhtik, J. G. Pelletier, D. Paré, *J. Neurosci.* **23**, 8800 (2003).
10. J. Amat *et al.*, *Nat. Neurosci.* **8**, 365 (2005).
11. C. Buchel, R. J. Dolan, *Curr. Opin. Neurobiol.* **10**, 219 (2000).
12. K. S. LaBar, J. C. Gatenby, J. C. Gore, J. E. LeDoux, E. A. Phelps, *Neuron* **20**, 937 (1998).
13. D. C. Knight, D. T. Cheng, C. N. Smith, E. A. Stein, F. J. Helmstetter, *J. Neurosci.* **24**, 218 (2004).
14. J. S. Morris, A. Ohman, R. J. Dolan, *Nature* **393**, 467 (1998).
15. E. A. Phelps *et al.*, *Nat. Neurosci.* **4**, 437 (2001).
16. C. Grillon, S. M. Southwick, D. S. Charney, *Mol. Psychiatry* **1**, 278 (1996).
17. I. Liberzon, B. Martis, *Ann. N.Y. Acad. Sci.* **1071**, 87 (2006).
18. M. R. Milad, S. L. Rauch, R. K. Pitman, G. J. Quirk, *Biol. Psychology* **73**, 61 (2006).

10.1126/science.1147797

BIOCHEMISTRY

# Crowds of Syntaxins

Diffusion of the membrane-fusion protein syntaxin in cell membranes can be explained by a simple model of attraction and repulsion.

**Stephen H. White**

In the 1970s, Frye and Edidin (*1*) demonstrated two-dimensional diffusion of fluorescently labeled surface antigens in the plasma membranes of fused mouse and human cells. This observation led to the idea that membranes are a mosaic composed of a fluid lipid bilayer with embedded membrane proteins, which diffuse freely in the plane of the bilayer (*2*–*4*). This concept received early support from measurements of the diffusion of rhodopsin molecules in the rod outer segment photoreceptors of the eye (*5*). But questions soon arose about restriction of protein mobility as a result of protein-protein interactions or attachment of membrane proteins to other cell components (*6*). The questions have not abated, as evidenced by the debates about partitioning of selected proteins into lipid rafts (*7*, *8*) and restriction of membrane protein mobility by submicrometer compartments in the cell membrane (*9*, *10*).

On page 1072 of this issue, Sieber, Lang, and co-workers (*11*) refreshingly turn our attention back to the problem of simple diffusion and clustering of proteins in fluid membranes. They show that the clustering of syntaxin 1 in the plasma membrane of neuroendocrine PC12 cells (*12*) can be described by a simple physical model. The work is particularly notable because of the importance of syntaxin 1 in the docking and fusion of secretory vesicles to allow external release of their contents (exocytosis).

Syntaxins are members of the SNARE (*13*) family of proteins that mediate membrane fusion events associated with intracellular membrane trafficking (*14*). All SNARE proteins contain highly conserved heptad-repeat amino acid sequences that readily form coiled-coil structures that link secretory vesicles to target membranes during fusion. The active link structure, required for exocytosis, is a four-helix coiled-coil structure known as the SNARE core complex. This complex is formed from SNARE proteins on the secretory vesicles (vesicle-associated membrane protein or VAMP) and a soluble SNARE protein (synaptosome-associated protein or SNAP). Syntaxins and VAMPs are anchored to their membranes by single carboxyl-terminal transmembrane helices. The two proteins are distinguished from one another by the subdomain structures of their amino-terminal domains, but in both cases the SNARE heptad-repeat sequences are immediately adjacent to the transmembrane helix anchors.

Lang *et al.* (*15*) have shown that effective exocytosis of PC12 secretory vesicles requires syntaxin 1 to form clusters. Harkening back to an earlier time when changes in lipid bilayer properties—especially lipid composition—were believed to be primarily responsible for the aggregation of membrane proteins (*16*), these clusters disperse when the normally high concentration of cholesterol in the cell membrane is reduced. Cluster dispersal through membrane cholesterol depletion strongly reduced the vesicle secretion rate. But even though cholesterol affects clustering, it is not directly responsible for it. Lang and co-workers recently showed that the syntaxin 1 SNARE motif drives clustering through self-association (*17*).

This observation set the stage for the experiments presented by Lang and co-workers in this issue. In a technical tour de force, they have quantitatively characterized cluster formation with a combination of stimulated emission depletion fluorescence microscopy, fluorescence recovery after photobleaching, and computer simulations. The results show that freely diffusing syntaxins exchange dynamically with syntaxin clusters containing ~75 densely crowded syntaxins, with a cluster diameter of 50 to 60 nm (see the figure).

The technically demanding procedure is simple in concept. First, measure the size and number of clusters per $\mu m^2$. This is where stimulated emission depletion fluorescence microscopy (*18*) is invaluable, because it allows features with diameters below the diffraction limit to be resolved. Second, determine the total number of clusters from measurements of the average cell surface area using confocal microscopy. Third, establish the total number of syntaxin 1 copies per cell with quantitative immunoblotting. Combined, these measurements yield the cluster diameter and syntaxin:cluster ratio.

Measurements of fluorescence recovery after photobleaching of living PC12 cells showed that the mobility of native syntaxin 1 was highly restricted. In contrast, mutant syntaxins that lacked most of the amino-terminal cytoplasmic domain were highly mobile. Restricted mobility was recovered when only the SNARE domain was added back to the transmembrane domain. Further observations of small numbers of clusters suggested that fluorescence recovery occurred via exchange of syntaxin molecules between the clusters,

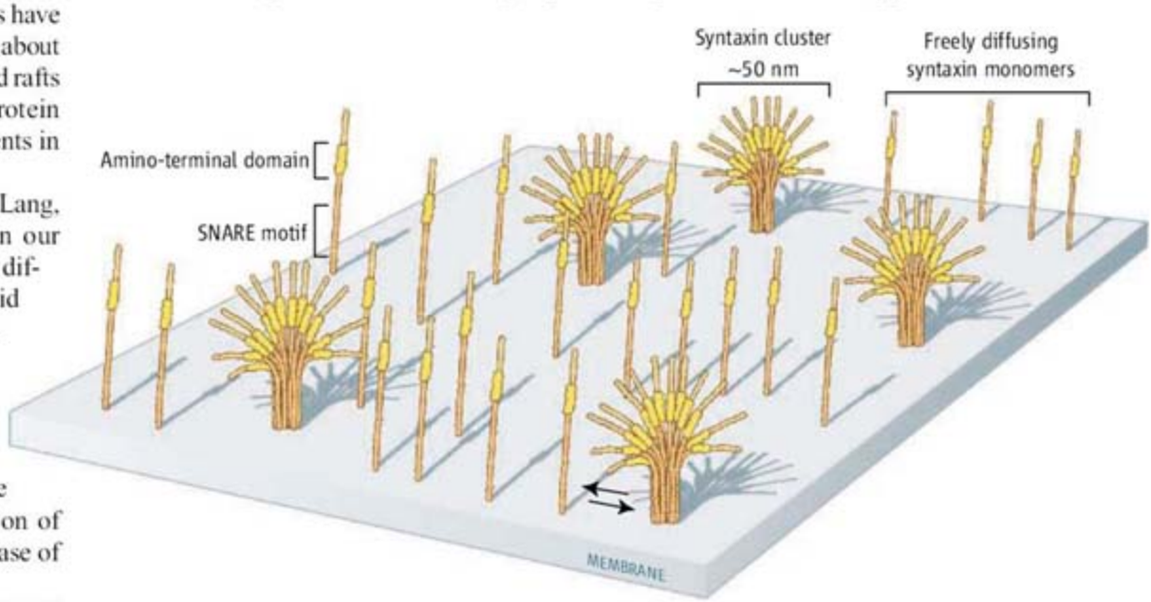


**How syntaxin clusters form.** Syntaxins freely diffuse in the plasma membrane to form clusters of ~75 molecules (*11*). Clustering appears to obey a simple physical principle: mutual attraction due to SNARE domains balanced by repulsion due to crowding. The clusters likely play an important role in vesicle secretion processes.

CREDIT: P. HUEY/SCIENCE

The author is in the Department of Physiology and Biophysics, University of California at Irvine, Irvine, CA 92697, USA. E-mail: stephen.white@uci.edu

implying a dynamic equilibrium between monomers and clusters.

The coup de grace was delivered by Brownian dynamics simulations with a simple interaction potential between individual syntaxins. The photobleaching observations were reproduced perfectly by a simple model of weak homophilic attraction between monomers balanced by a repulsive potential due to steric repulsion. One can readily imagine the arms of the resulting anemone-like structures (see the figure) snaring passing vesicles in preparation for exocytosis.

The image of syntaxin clusters that emerges from this study is far more complex than textbook images, which generally show only two copies of the SNARE core complex bringing the vesicle and target membranes together for fusion. One must wonder how the components of the core complex can locate one another in the protein tangle presented by the syntaxin cluster. How many SNARE core complexes are necessary for docking and fusion? Do the interactions proceed in the coordinated, structurally attractive manner of textbook cartoons? The impressions gained from the report by Lang and co-workers will be influential in designing experiments to answer these questions.

### References and Notes


1. L. D. Frye, M. Edidin, *J. Cell Sci.* **7**, 319 (1970).
2. J. Lenard, S. J. Singer, *Proc. Natl. Acad. Sci. U.S.A.* **56**, 1828 (1966).
3. M. Glaser, H. Simpkins, S. J. Singer, M. Sheetz, S. I. Chan, *Proc. Natl. Acad. Sci. U.S.A.* **65**, 721 (1970).
4. S. J. Singer, G. L. Nicolson, *Science* **175**, 720 (1972).
5. M.-M. Poo, R. A. Cone, *Nature* **247**, 438 (1974).
6. R. J. Cherry, *FEBS Lett.* **55**, 1 (1975).
7. K. Simons, E. Ikonen, *Nature* **387**, 569 (1997).
8. K. Simons, D. Toomre, *Nat. Rev. Mol. Cell Biol.* **1**, 31 (2000).
9. A. Kusumi, Y. Sako, *Curr. Opin. Cell Biol.* **8**, 566 (1996).
10. A. Kusumi *et al.*, *Annu. Rev. Biophys. Biomol. Struct.* **34**, 351 (2005).
11. J. J. Sieber *et al.*, *Science* **317**, 1072 (2007).
12. Neuroendocrine cells respond to nervous stimulation by releasing hormones.
13. SNARE, soluble *N*-ethylmaleimide–sensitive factor attachment protein receptor.
14. Y. A. Chen, R. H. Scheller, *Nat. Rev. Mol. Cell Biol.* **2**, 98 (2001).
15. T. Lang *et al.*, *EMBO J.* **20**, 2202 (2001).
16. J. C. Owicki, H. M. McConnell, *Proc. Natl. Acad. Sci. U.S.A.* **76**, 4750 (1979).
17. J. J. Sieber, K. I. Willig, R. Heintzmann, S. W. Hell, T. Lang, *Biophys. J.* **90**, 2843 (2006).
18. K. I. Willig, S. O. Rizzoli, V. Westphal, R. Jahn, S. W. Hell, *Nature* **440**, 935 (2006).


19. This work was supported in part by grant GM74637 from the National Institute of General Medical Sciences.

10.1126/.science.1148010


GEOCHEMISTRY

# The Oldest Fossil or Just Another Rock?

Recent evidence strengthens the case for signs of ancient life in rocks from Akilia, Greenland, but important questions remain.


**John M. Eiler**


The history of the past 542 million years of life on Earth can be read from shells, bones, teeth, and leaf casts preserved in the geological record. For the preceding 4 billion years, more subtle clues, such as remnants of microbial cells, biomolecules, and the impressions left by soft-bodied organisms, may be preserved in sedimentary rocks. But in sediments deposited in the first billion years of Earth history, these traces have been destroyed by metamorphism (recrystallization without melting, often accompanied by reaction and chemical exchange). Here, the only widely recognized evidence for life comes from measurements of carbon isotopes in kerogen and graphite (*1*). Because metabolic carbon fixation discriminates against $^{13}C$, the $^{13}C/^{12}C$ ratio in biogenic carbon is ~3% lower than in inorganic carbon. This signature can be preserved through metamorphic processes that destroy microfossils and biomolecules.

In 1996, Mojzsis *et al.* reported the oldest indications of life on Earth to date (*2*) in a rock collected from a patch of intensely folded and metamorphosed quartz-rich rocks on Akilia, a tiny, barren island off the southwest coast of Greenland. The authors suggested that these quartz-rich rocks are banded iron formations (a type of iron-rich marine sediment) deposited more than 3860 million years ago, and that at least one of them contains $^{13}C$-poor graphite derived from organic matter. Rocks nearly this old from elsewhere also contain $^{13}C$-depleted carbon (*1*).

The graphitic, quartz-rich rocks on Akilia have been widely discussed and intensely scrutinized. Much of this scrutiny has been critical and has eroded confidence in the original finding (*3*–*11*). But this year, the authors of the original study have punched back in a pair of papers (*12*, *13*) that address the critics' most serious charges.

The ages of old, metamorphosed sediments can be constrained through isotope dating of igneous rocks that cut through, or contain inclusions of, those sediments. The originally reported age of the Akilia quartz-rich rocks [(*2*) and references therein] was based on the isotopic age of the mineral zircon in such a cross-cutting granitoid (an igneous rock rich in quartz and feldspar). But these zircons could be minerals from an unknown older rock that were entrained in the igneous rock while it was still liquid (*3*). It has also been suggested that the intense deformation undergone by nearly all Akilia island rocks prevents confident identification of places where granitoids cross-cut older volcanic or sedimentary rocks (*4*).

Manning *et al.* (*12*) refute the first criticism by showing that the trace-element contents of the suspect zircons (redated at 3820 to 3840 million years ago) are consistent with them having crystallized from their host rocks; thus, at least some granitoids on Akilia very likely are as old as originally claimed. The authors also strive to address the second critique, but against long odds: No cross-cutting relations between granitoids and the quartz-rich rocks have been observed. In some places, granitoids to cross-cut volcanic strata that are part of the same original set of strata as the quartz-rich rocks, providing a minimum age for the whole stratigraphic section. However, even these cross-cutting relations are partially obscured or otherwise ambiguous. Barring discovery of further cross-cutting relations, it is difficult to foresee how this part of the debate can be more definitively resolved.

Even if the Akilia rocks are as old as originally suggested, it is not obvious that any of them are sediments that could contain primary deposits of organic matter. Akilia island is largely composed of metamorphosed volcanic rocks and the granitoids that appear to intrude them; the thin layer of quartz-rich rocks is an anomaly (*12*). Moreover, the one sample of quartz-rich rock in which $^{13}C$-poor


The author is in the Division of Geological and Planetary Sciences, California Institute of Technology, Pasadena, CA 91125, USA. E-mail: eiler@gps.caltech.edu

graphite has been found (*2*) differs in mineralogy and trace element composition from subsequently collected quartz-rich Akilia rocks (*5*, *12*). The original sample resembles banded iron formations elsewhere in Greenland, but the rest of the quartz-rich unit does not (*5*, *12*). Fedo and Whitehouse have suggested that the compositions of most quartz-rich Akilia rocks are more consistent with volcanic rocks that underwent metasomatism (chemical modification during metamorphism) (*11*). If this is correct, then the carbon was added to the rocks after they formed, is younger than originally claimed, and may not be biological in origin.

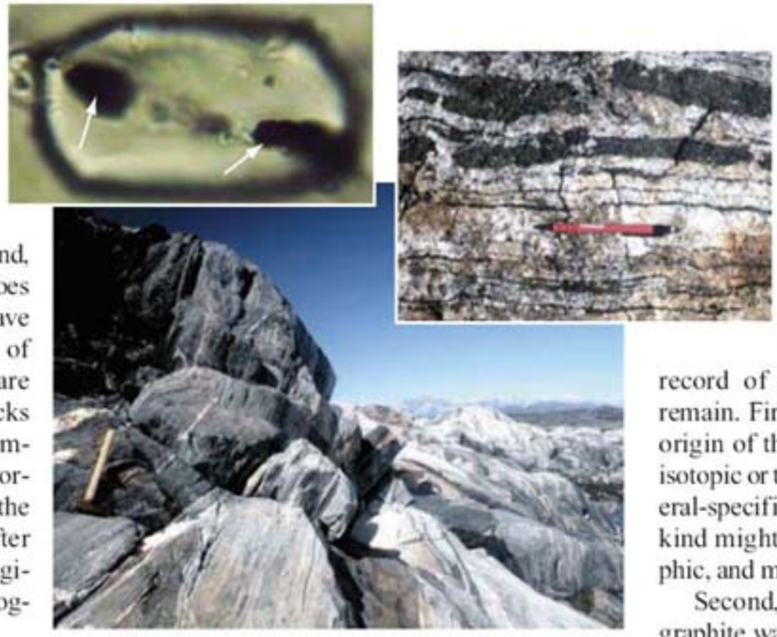

**Signs of early life?** In this photograph from Akilia island, the light gray, finely banded rocks are a quartz-rich unit that some interpret as a marine sediment (*2*, *12*, *14*, *15*). The dark gray bands are metamorphosed volcanic rocks. The field of view is ~5 m across. **(Upper right inset)** Hand specimen of the quartz-rich unit. The field of view is ~10 cm across. **(Upper left inset)** Photomicrograph of an apatite crystal from sample G92-197b of the quartz-rich unit. The field of view is ~30 μm across. The white arrows indicate inclusions identified as graphite (*13*).

Attempts to determine the origin of quartz-rich rocks on Akilia through isotopic "fingerprints" that only occur in sedimentary rocks have given mixed results. Sulfides in these rocks contain anomalous deficits in $^{33}S$, implying photochemical processing in the atmosphere and thus formation of the host rock at or near the Earth surface (*14*). However, it is unclear how or when this sulfur was incorporated in the rocks. Also, one of the attempts to replicate this result found no $^{33}S$ anomaly (*6*). The iron isotope composition of Akilia quartz-rich rocks is unlike that of fresh igneous rocks and resembles that of real banded iron formations (*15*). However, metamorphic and metasomatic processes could have modified the iron isotope compositions of the Akilia rocks, so this result does not prove a sedimentary origin. The silicon isotope compositions of the Akilia rocks are similar to common igneous and metamorphic rocks and lack the $^{30}Si$ depletions of banded iron formations (*7*). The Akilia rocks are enriched in $^{18}O$ relative to common igneous rocks, consistent with sedimentary origins (*12*), but far less so than in other Archean quartz-rich sediments (*16*); these data also permit metasomatic origins.

Manning *et al.* (*12*) show that the quartz-rich rocks on Akilia have the same deformation history as adjacent metamorphosed volcanic rocks and were not formed by addition of $SiO_2$ to igneous rocks. Furthermore, if the quartz-rich unit was a "pipe" through which $SiO_2$-rich fluid flowed, then the walls of that pipe should contain specific metamorphic minerals; the latter are not observed. These arguments weigh against a metasomatic origin but do not prove a sedimentary origin. The only clearly demonstrated point is that the Akilia quartz-rich rocks are peculiar: They do not closely resemble common sediments (they are clearly not normal banded iron formations), nor do they fit the expected properties of metasomatic veins. Manning *et al.*'s suggestion that they are metamorphosed marine sediments (*12*) is the most reasonable and detailed hypothesis to date.

The $^{13}C$-poor graphite found in Akilia rocks was originally described as inclusions in apatite, a calcium phosphate mineral (*2*). However, this association was not clearly documented. Two independent searches for graphitic inclusions in apatites from Akilia rocks (*8*, *9*) failed to find a single crystal of graphite in hundreds of investigated apatite crystals, including dozens from the same rock reported on by Mojzsis *et al.* (*2*). These studies refute Mojzsis *et al.*'s assertion that carbon inclusions are not only present but ubiquitous (*2*, *10*) and raise the possibility that the original discovery was an artifact.

McKeegan *et al.* have used Raman confocal spectroscopy to make three-dimensional images of carbonaceous inclusions in Akilia apatites and to establish that the inclusions are graphitic (*13*). This method is less prone to false negative results than the previous approach of polishing into each grain until a graphitic inclusion is exposed at the sample surface. Ion microprobe measurements of the newly found graphitic inclusions demonstrate that they are poor in $^{13}C$ (*13*), as originally claimed. This new report appears definitive, although it remains difficult to understand why the two independent searches did not find any inclusions (*8*, *9*). Perhaps apatite-hosted graphite exists in at least one Akilia quartz-rich rock but is less common than originally suggested.

These newest papers (*12*, *13*) revive hope that Akilia rocks could contain the first known record of life on Earth, but ambiguities remain. First, most efforts to understand the origin of the quartz-rich rocks by means of isotopic or trace-element signatures omit mineral-specific or in situ data. More data of this kind might untangle the primary, metamorphic, and metasomatic influences.

Second, the sample in which low-$^{13}C$ graphite was discovered is unlike other rocks recovered from the quartz-rich unit on Akilia. Fedo and Whitehouse have suggested that this sample was collected "out of place" (*11*)—pejorative geologist slang for rocks that are not attached to their outcrops. Confidence in the discovery would be improved if more rocks closely resembling this sample were newly collected from outcrop.

Finally, the quartz-rich rocks on Akilia underwent several periods of metamorphism long after they were originally deposited. The apatite in these rocks (and the flakes of graphite they contain) may have recrystallized, reacted, and/or undergone chemical exchange during these events (*9*, *10*). Thus, the carbon in these rocks—whatever its origin—may have been introduced at some unknown time after deposition. This may be the greatest hurdle to upgrading Akilia graphites from the oldest suggestion of life on Earth to the oldest evidence.




**References**

1. M. A. Schidlowski, *Nature* **333**, 313 (1988).
2. S. J. Mojzsis *et al.*, *Nature* **384**, 55 (1996).
3. M. J. Whitehouse, B. S. Kamber, S. Moorbath, *Chem. Geol.* **160**, 201 (1999).
4. M. J. Whitehouse, C. M. Fedo, *Precambrian Res.* **126**, 259 (2003).
5. C. M. Fedo, M. J. Whitehouse, *Science* **296**, 1448 (2002).
6. M. J. Whitehouse, *Chem. Geol.* **222**, 112 (2005).
7. L. Andre *et al.*, *Earth Planet. Sci. Lett.* **245**, 162 (2006).
8. A. Lepland *et al.*, *Geology* **33**, 77 (2005).
9. A. P. Nutman, C. R. L. Friend, *Precambrian Res.* **147**, 100 (2006).
10. Y. Sano *et al.* (comment), S. J. Mojzsis *et al.* (reply), *Nature* **400**, 127 (1999).
11. C. S. J. Mojzsis *et al.*, *Science* **298**, 917a (2002) (www.sciencemag.org/cgi/content/full/298/5595/917a).
12. C. E. Manning *et al.*, *Am. J. Sci.* **306**, 303 (2006).
13. K. D. McKeegan, A. B. Kudryavtsev, J. W. Schopf, *Geology* **35**, 591 (2007).
14. S. J. Mojzsis *et al.*, *Geochim. Cosmochim. Acta* **67**, 1635 (2003).
15. N. Dauphas *et al.*, *Science* **306**, 2077 (2004).
16. F. Robert, M. Chaussidon, *Nature* **443**, 969 (2006).


10.1126/science.1146923

# The Experimental Induction of Out-of-Body Experiences

H. Henrik Ehrsson

An out-of-body experience (OBE) has been defined as the experience in which a person who is awake sees his or her body from a location outside the physical body (*1*, *2*). OBEs have been reported in clinical conditions that disturb normal brain functioning, such as strokes, partial epileptic seizures, and drug abuse (*1*–*4*). Here, I report that this illusory experience can be induced in healthy participants. I report a perceptual illusion in which individuals experience that their center of awareness, or "self," is located outside their physical bodies and that they look at their bodies from the perspective of another person. This illusion demonstrates that the sense of being localized within the physical body can be fully determined by perceptual processes, that is, by the visual perspective in conjunction with multisensory stimulation on the body.

In the first experiment, participants sat on a chair, wearing a pair of head-mounted displays that were connected to two video cameras placed side by side 2 m behind the participant's back (Fig. 1A). The images from the left video camera were presented on the left eye display and the images from the right camera on the right display. Thus, the person would see his or her back with the perspective of a person sitting behind him or her with stereoscopic vision. The experimenter stood just beside the participant (in their view) and used two plastic rods to touch simultaneously the person's actual chest, which was out of view, and the chest of the "illusory body," by moving one rod toward a location just below the cameras in view (*5*).

After 2 min of stimulation, the participants were asked to complete a questionnaire on which they had to affirm or deny 10 possible perceptual effects with a seven-point visual analog scale. Three statements were designed to capture the experience of the illusion, and the other seven served as controls for suggestibility and task compliance (SOM text). The participants affirmed illusion statements and denied the controls, and the difference in ratings was significant [$P < 0.0001$, $F(1, 170) = 189.92$, $P < 0.00001$ (fig. S1 and SOM text)]. Thus, the participants reported the experience of sitting behind their physical bodies and looking at them from this location.

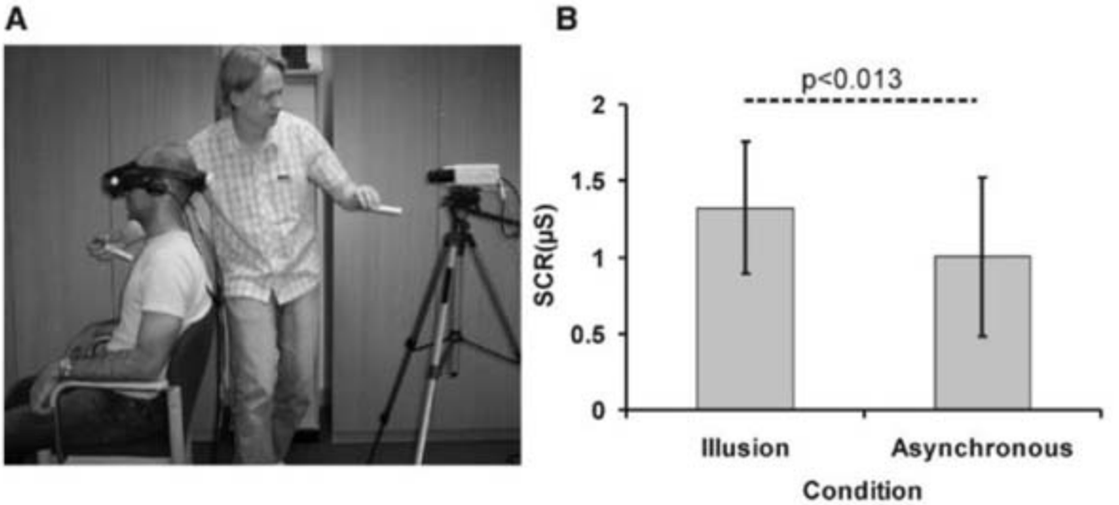


**Fig. 1.** (**A**) The setup used to induce the out-of-body illusion. (**B**) The SCRs from the 12 participants when the illusory body was "hurt." Mean values and standard deviations (error bars) are presented.

I hypothesized that the illusion is caused by the first-person visual perspective in combination with the correlated visual and tactile information from the body. To test this and to provide objective evidence for the illusion, I registered the skin-conductance response (SCR) as a measure of the emotional response when the illusory body was "hurt" by hitting it with hammer after a period of stimulation (SOM text). I compared the illusion condition (with synchronous touches) to an asynchronous condition in which the person's real and illusory chests were touched alternatingly. I observed significantly greater threat-evoked SCRs after the illusion condition ($P < 0.013$; paired $t$ test) (Fig. 1B and SOM text) and stronger ratings of the illusion ($P < 0.05$; paired $t$ test) (SOM text). A control experiment was conducted to rule out that the SCR difference was due to a conditioned response after a period of synchronously presented stimuli (SOM text, experiment 3). The observed SCR difference provides objective evidence that the participants were emotionally responding as if they were located behind their physical bodies.

The present illusion is fundamentally important because it informs us about the perceptual processes that underlie the sense of being located inside the body. There are two key components to this process. First, visual information from the first-person perspective provides indirect information about the location of one's own body in the environment (*6*). The first-person visual information also updates the proprioceptive representations and defines the origo of the body-centered reference frames that are used to represent near-personal space (*7*, *8*). The second key factor is the detection of correlated tactile and visual events on the (illusory) body. Multisensory correlations are known to be important for self-attribution of single body parts in near-personal space (*9*, *10*). Thus, these correlations, in conjunction with the first-person visual perspective, are sufficient to determine the perceived location of one's own whole body. This finding represents a fundamental advance because the natural "in-body experience" forms the foundation for self-consciousness.

## References and Notes

1. O. Blanke, T. Landis, L. Spinelli, M. Seeck, *Brain* **127**, 243 (2004).
2. P. Brugger, M. Regard, T. Landis, *Cognit. Neuropsychiatry* **2**, 19 (1997).
3. P. Brugger, *Cognit. Neuropsychiatry* **7**, 179 (2002).
4. O. J. Grüsser, T. Landis, in *Visual Agnosias and Other Disturbances of Visual Perception and Cognition*, J. Cronley-Dillon, Ed. (MacMillan, Amsterdam, 1991), pp. 297–303.
5. Materials and methods are available on *Science* Online.
6. N. Burgess, *Trends Cognit. Sci.* **10**, 551 (2006).
7. M. S. Graziano, G. S. Yap, C. G. Gross, *Science* **266**, 1054 (1994).
8. L. Fogassi *et al.*, *Exp. Brain Res.* **89**, 686 (1992).
9. M. Botvinick, J. Cohen, *Nature* **391**, 756 (1998).
10. D. M. Lloyd, *Brain Cognit.* **64**, 104 (2007).
11. I thank R. Passingham, C. Frith, and H. Lau for valuable comments and for serving as pre-reviewers. I also thank P. Aston and O. Josephs for technical support. The study was supported by the Wellcome Trust and the PRESENCCIA (Presence: Research Encompassing Sensory Enhancement, Neuroscience, Cerebral-Computer Interfaces, and Applications) project, a European Union–funded project under the Information Society Technologies program. H.H.E. was supported by the Human Frontier Science Program, the Swedish Medical Research Council, and the Swedish Foundation for Strategic Research.

## Supporting Online Material

www.sciencemag.org/cgi/content/full/317/5841/1048/DC1
Materials and Methods
SOM Text
Figs. S1 and S2
References

6 March 2007; accepted 28 June 2007
10.1126/science.1142175

Wellcome Trust Centre for Neuroimaging, Institute of Neurology, 12 Queen Square, London WC1N 3BG, UK. Department of Clinical Neuroscience, Karolinska Institutet, 171 76 Stockholm, Sweden. E-mail: Henrik.Ehrsson@ki.se

# Mesoscopic Phase Coherence in a Quantum Spin Fluid

Guangyong Xu,[1,2]* C. Broholm,[1,3] Yeong-Ah Soh,[4] G. Aeppli,[5] J. F. DiTusa,[6] Ying Chen,[1,3] M. Kenzelmann,[1,3] C. D. Frost,[7] T. Ito,[8] K. Oka,[8] H. Takagi[8,9]

Mesoscopic quantum phase coherence is important because it improves the prospects for handling quantum degrees of freedom in technology. Here we show that the development of such coherence can be monitored using magnetic neutron scattering from a one-dimensional spin chain of an oxide of nickel ($Y_2BaNiO_5$), a quantum spin fluid in which no classical static magnetic order is present. In the cleanest samples, the quantum coherence length is 20 nanometers, which is almost an order of magnitude larger than the classical antiferromagnetic correlation length of 3 nanometers. We also demonstrate that the coherence length can be modified by static and thermally activated defects in a quantitatively predictable manner.

A wave is deemed coherent when it is perfectly periodic in space and time. Quantum-mechanical phase coherence means that the corresponding wave function is actually a coherent wave. Typically, though, classical disorder limits quantum phase coherence. The occasions where this is not the case and the quantum phase coherence length far exceeds that given by classical considerations remain a major theme of physics. The longstanding examples are superconductivity and superfluidity, in which macroscopic quantum phase coherence (*1*) has been revealed by persistent current and Josephson junction experiments (*2*, *3*). The effects of phase coherence have also been seen recently in the incompressible quantum fluid phase of two-dimensional (2D) electron gas (*4*) and in a laser-cooled Bose-Einstein condensate (*5*). Curiously, although magnetism itself is a quantum mechanical phenomenon, originating from the shell model of the atom, mesoscopic (in the sense of extending over distances in excess of 10 nm) quantum coherence in the absence of classical static order has not been explicitly demonstrated for a magnet. We show that the development of such coherence can be readily monitored with the use of magnetic neutron scattering from a 1D spin chain, in the form of an oxide of nickel, and that it is limited by static and thermally activated defects.

One of the best-known magnets that remains disordered because of quantum fluctuations is a chain of integer spins coupled antiferromagnetically (that is, favoring antiparallel alignment) to their neighbors (*6*, *7*). The two-spin correlation function $\langle \mathbf{S}_j \cdot \mathbf{S}_{j'} \rangle$, where $j$ and $j'$ are site indices of the spins, decays exponentially with large distances $|j - j'|$ between spins $S_j$ and $S_{j'}$ in the chain as in a 1D liquid; whereas in a classical magnet, static correlations persist over macroscopic length scales when the system orders. Even so, theoretical work has shown that the ground state is coherent in the sense that the more complex "string" correlation function (*8*), $O(j-j') = \langle S^z_j \exp[i\pi \sum_{j<k<j'} S^z_k] S^z_{j'} \rangle$, tends to a constant (*9*) for $j - j' \to \infty$. A simple way to understand the string order is to look at the spin chain in terms of the spin-projection quantum numbers $S^z = -1$, 0, and +1 at individual sites. Correspondingly, for S = 1, the basis states are $|\pm 1\rangle$, which has clear classical analogs and can be used to build a perfect Néel state $|\ldots,-1,+1,-1,+1,-1,+1\ldots\rangle$ for the chain, and $|0\rangle$, which does not. String order is carried by states where sites with $S^z = 0$ are inserted into the perfect Néel state (Fig. 1B). A good approximation to the ground-state wave function for the Heisenberg S = 1 chain is a coherent superposition of all such states with a weighting factor that decreases exponentially with the number of $|0\rangle$ sites (*10*). In general, long-range quantum coherence is believed to exist in all 1D systems with spectral gaps (*11*).

For the spin-1 chain, the lowest excited state above the ground state entails inserting a defect into the string order. The defect can propagate throughout the lattice (Fig. 1C) until it encounters another defect, and so will have a mean free path limited by either static defects, such as

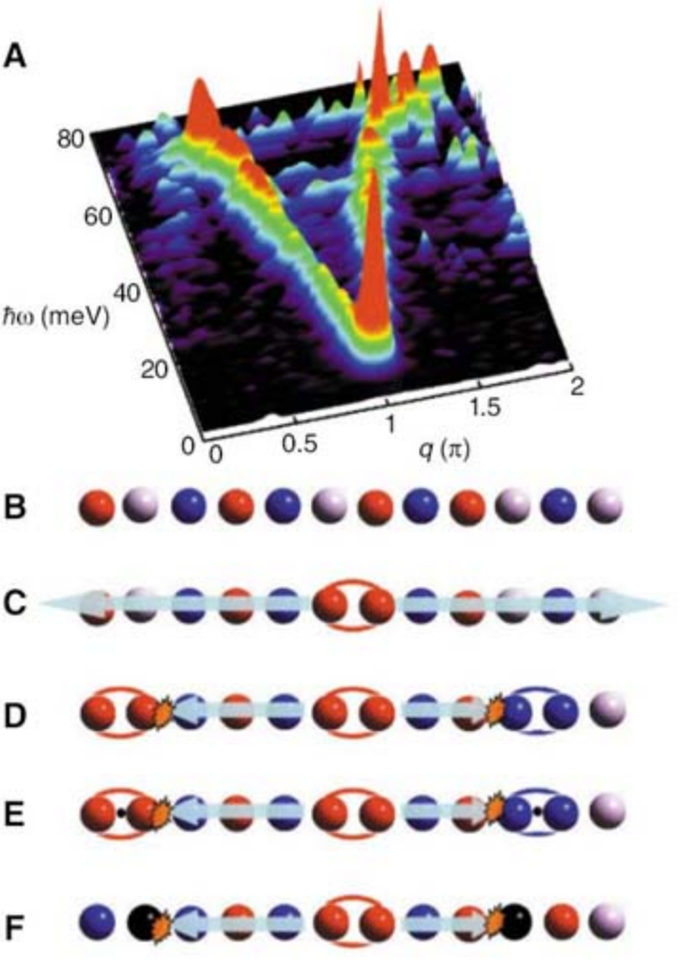


**Fig. 1.** (**A**) Map of the dynamic spin-correlation function multiplied by energy for the 1D spin-1 chain $Y_2BaNiO_5$ at low temperature ($T$ = 10 K). (**B** to **F**) Diagrams of the string order in the spin-1 chain. The red, blue, and gray spheres represent sites with $S^z$ of 1, −1, and 0, respectively. Chemical impurities are represented by large black spheres (Mg). (B) S = 1 chain at $T$ = 0 and no chemical impurity. (C) One triplet wave packet propagating on the chain. (D) At $T > 0$, triplet wave packets act as thermal defects and confine each other into boxes. (E) Box confinement by Ca impurities, which introduce holes (indicated by small black spheres) into the chain and cause neighboring spins to form ferromagnetic pairs. (F) Box confinement by Mg impurities, which remove Ni spins from the chain.

[1]Department of Physics and Astronomy, The Johns Hopkins University, Baltimore, MD 21218, USA. [2]Condensed Matter Physics and Materials Sciences Department, Brookhaven National Laboratory, Upton, NY 11973, USA. [3]NIST Center for Neutron Research, National Institute of Standards and Technology (NIST), Gaithersburg, MD 20899, USA. [4]Department of Physics and Astronomy, Dartmouth College, Hanover, NH 03755, USA. [5]London Centre for Nanotechnology and Department of Physics and Astronomy, University College London, 17–19 Gordon Street, London, WC1H OAH UK. [6]Department of Physics and Astronomy, Louisiana State University, Baton Rouge, LA 70803, USA. [7]ISIS Facility, Rutherford Appleton Laboratory, Chilton, Didcot OX11 0QX, UK. [8]National Institute of Advanced Industrial Science and Technology, Tsukuba, Ibaraki 305–8562, Japan. [9]Department of Advanced Materials Science, Graduate School of Frontier Sciences, University of Tokyo, Kashiwa, Chiba 277–8561, Japan.

*To whom correspondence should be addressed. E-mail: gxu@bnl.gov

chain terminations (*12*, *13*) (Fig. 1, E and F), or other moving, thermally excited defects of the same type (Fig. 1D). Thus, the coherence of the ground state should be manifested in the mean free path of its triplet excitations. By imaging these excitations and their mean free path using inelastic neutron scattering, we can establish the perfection, or quantum coherence, of the ground state.

Neutron scattering measures the Fourier transform $S(q,\omega)$ in space and time of the magnetic correlation function $\langle \mathbf{S}_j(0) \cdot \mathbf{S}_j(t) \rangle$. The experiments were conducted on single crystals of $Y_2BaNiO_5$, which contain an ensemble of spin-1 chains formed by the O-Ni-O backbone of corner-linked $NiO_6$ octahedra (*14*, *15*). The system behaves as a quantum spin liquid because of the 1D nature of the magnetic interactions. That this liquid is not a conventional classical liquid, however, is clear from Fig. 1A, which shows the full dynamical structure factor $S(q,\omega)$, multiplied by energy transfer $\hbar\omega$, for $Y_2BaNiO_5$. Instead of broad overdamped excitations, which soften toward zero energy as the ordering vector ($q = \pi$ in this case) for the corresponding classical solid is approached, a gapped band of well-defined modes dominates the data. The lowest-energy mode appears at $q = \pi$, and its energy is termed the Haldane gap (*6*, *7*). Although $S(q,\omega)$ from chemically doped $Y_2BaNiO_5$ is qualitatively similar, there are important differences (fig. S1). Our paper focuses on characterizing the mean free path and energetics of the lowest-energy Haldane gap mode.

The temperature ($T$)–dependent equal-time spin correlation length $\xi_0$ is shown as open circles in Fig. 2. $\xi_0$ is inversely proportional to the peak width of the equal-time spin correlation function $S(q) = \sum_{jj'} \langle \mathbf{S}_j \cdot \mathbf{S}_{j'} \rangle \exp(iq(j-j'))$, which in the $T \rightarrow 0$ limit directly displays the magnetic correlations built into the ground state. $S(q)$ is the magnetic analog of the structure factor measured by x-rays for ordinary liquids. Represented by the open circles in the insets of Fig. 2, A and B, $\mathbf{S}(q)$ has a maximum at $q = \pi$, indicating that the underlying classical solid is antiferromagnetic (AFM) where each spin points in a direction opposite to that of its two nearest neighbors. The peak width, however, does not vanish even as $T \rightarrow 0$, and the correlations between spins remain liquidlike for $T \rightarrow 0$, as anticipated by Haldane (*6*, *7*) and seen experimentally in several S = 1 chain compounds (*14*, *16*–*18*). The dash-dotted line in Fig. 2 is the prediction of the quantum nonlinear σ model (*19*), which is valid only for $T < \Delta/k_B$, where $\Delta$ is the Haldane gap.

The solid circles in the inset of Fig. 2 are the magnetic structure factor measured as a function of $q$ with the energy transfer fixed, at the Haldane gap energy for insets A and B and at 36 meV for inset C. The peak approaches a resolution-limited delta function at low temperature (inset A). Because we have tuned to the gap energy, the process probed is the creation of a triplet wave packet at rest. The intrinsic width [half width at half maximum ($\delta q$)] of this peak is therefore inversely proportional to the distance over which the triplet retains quantum phase coherence. The data show that $\delta q \approx 0.007\pi$, implying phase coherence over approximately 50 lattice units $a$, which is much longer than the measured correlation length for AFM order $\xi_0$. The experiment thus provides direct evidence for mesoscopic coherence in the spin-1 chain. The peak broadens significantly when the sample is warmed (inset B) or doped by chemical impurities (inset C), indicating that quantum coherence in this system requires low temperatures and perfect crystallinity. The two length scales obtained from the two types of $q$ scans vary differently with $T$. At high $T$, the lengths converge to nearly the same value. In contrast, as $T \rightarrow 0$, the mean free path for the Haldane gap excitation $\xi$ nearly diverges even while the AFM length $\xi_0$ approaches a finite value. The AFM length is the distance between defects in the AFM order, which at $T = 0$ is simply the typical distance between sites with $S^z = 0$. Such defects do not disrupt string order. On warming, excitations in the form of ferromagnetic neighbor pairs with $S^z$ both equal to +1 or −1 will also appear, and these disrupt not only antiferromagnetism but the underlying string order as well. Classical (gapless) AFM chains (*20*–*22*), such as the $Mn^{2+}$ (S = 5/2) chain compound TMMC (*20*), behave very differently from $Y_2BaNiO_5$ in the sense that a single distance, namely the equal-time correlation length $\xi_0$, sets the scale for both the static and dynamic correlations.

Detailed analysis of thermal conductivity provides estimates of the magnetic mean free path in various spin chains and ladders (*23*). The results (*24*) for $Y_2BaNiO_5$ differ considerably from our direct measurements in the sense that they pass through a strong peak of $15a$ at 100 K and rapidly decrease below that, with a value of $7a$ at 70 K, the lowest temperature at which there was confidence in the measurements. The discrepancy with our results is not surprising given the indirect nature of the thermal conductivity measurements as well as the fact that the lower-temperature magnetothermal properties of S = 1 chains are dominated by the effective spins of chain ends rather than the triplet excitations of the entire chain segments.

To quantify the effects of chemical impurities on quantum phase coherence, consider an excited triplet wave packet on the chain. At low temperatures, the population of such wave packets is relatively low and they can travel almost freely before encountering a physical impurity, such as a chain end caused by a chemical defect. Correspondingly, the mean free path is on average half of the spin chain length. To obtain an independent measure of the latter, we recalled specific-heat work (*25*) on $Y_2BaNiO_5$, which showed the residual S = 1 degrees of freedom expected for chains containing odd numbers of Ni atoms (*10*, *13*, *26*). The outcome was a Curie-like dc magnetic susceptibility $C/T$, which we measured for the nominally pure material using superconducting quantum interference device magnetometry. The resulting Curie constant $C$ gives an average impurity concentration of ~1.5%, or a mean distance $\ell$ of ~70 lattice spacings between chain breaks, which is, within error, consistent with twice the zero-$T$ coherence length measured in our inelastic neutron-scattering experiments. The same is true for our deliberately

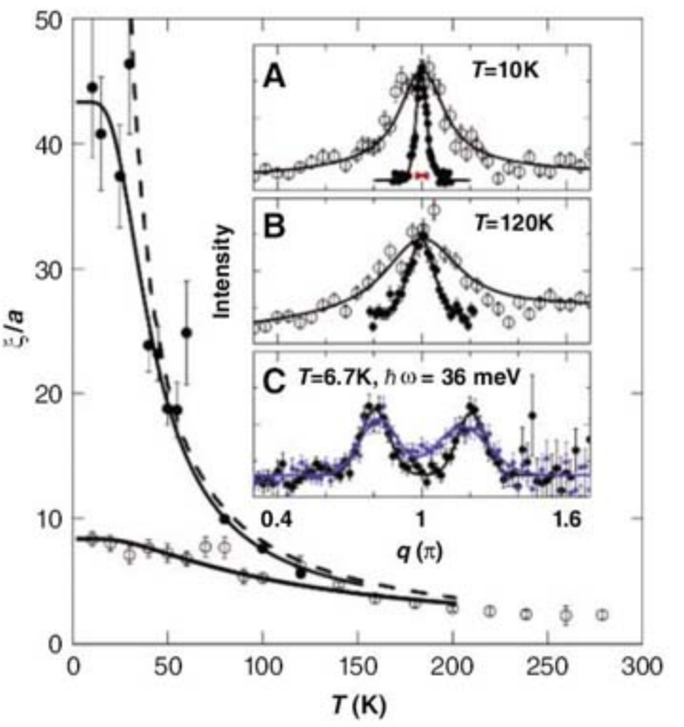


**Fig. 2.** Equal-time correlation length $\xi_0$ (open symbols) and magnetic phase coherence length $\xi$ (solid symbols) for the 1D spin-1 chain $Y_2BaNiO_5$, as measured with inelastic magnetic neutron scattering (inset). Lines are theoretical results described in the text. (**A**) Low-temperature structure factor data obtained for the equal-time spin correlations ($\hbar\omega > 8$ meV) (open circles), and the bottom of the Haldane continuum at $\hbar\omega = 7.5$ meV (solid circles, where instrument resolution is shown as the red horizontal bar) in a nominally pure sample. Fits to such data produced the main frame data points as described in the supporting online material. (**B**) Higher-temperature data in which the coherence length approaches the equal-time correlation length. (**C**) Data acquired at a fixed energy transfer (36 meV) for the nominally pure (black symbols) and Ca-doped ($Y_{2-x}Ca_xBaNiO_5$, x = 0.1) samples (blue symbols).

doped (with Ca and Mg) samples. The coherence lengths extracted from samples with nominal Ca doping of 4% and 10% ($Y_{2-x}Ca_xBaNiO_5$) and Mg doping of 4% ($Y_2BaNi_{1-x}Mg_xO_5$) were 9(1), 5(1), and 10(1) Ni-Ni spacings $a$, respectively, which is consistent with the scenario suggested above, for which $2\xi/a = 1/x$.

With increasing temperature and therefore triplet population, the mean free path will be limited by both thermally created defects and chain ends. In keeping with the physical picture developed above, the coherence length should approximately match half the inverse density of all (chemical and thermal) defects $\xi/a = [x + \rho(T)]^{-1}/2$. Here $\rho(T) = 3\sqrt{\frac{k_B T \Delta}{2\pi v^2}}\exp\left(-\Delta/k_B T\right)$ is the thermal triplet density (*27*) and $v = 70$ meV is the triplet velocity (*14*). The corresponding solid line in Fig. 2 shows that this model provides an excellent description of the $T$-dependent quantum coherence length.

Another consequence of the above picture should be a finite temperature blue shift as triplets confine each other into boxes. In other words, quantum mechanics acts not only to produce the singlet Haldane ground state and the associated gap to triplet excited states, but also gives quantum particlelike properties to the excited states, including a kinetic quantum confinement contribution. Instead of being created with energy $\Delta$, the triplet is created with an additional kinetic energy given by the curvature of the dispersing mode shown in Fig. 1A, associated with a quasiparticle of nonzero momentum $q \sim 1/\xi$. Such a quantum contribution is found on warming as well as doping, where the quantum confinement is due to fixed boundaries. Experimentally, others have also noticed the thermally induced blue shift for $Y_2BaNiO_5$ (*28*) as well other Haldane systems (*17*, *29*, *30*).

Figure 3, A and B, show the temperature dependence of the mean triplet energy ($\Delta$) and the half-width at half-maximum HWHM ($\hbar\Gamma$) of the triplet, assuming Gaussian or Lorentzian spectral functions, respectively. The measured Haldane gap (see also fig. S2) moves to higher energies on warming, which is exactly the thermal blue shift anticipated. The energy width of the triplet excitation in the $T \rightarrow 0$ limit is resolution-limited, imposing an upper bound of $\hbar\Gamma = 0.1$ meV on the excited-state relaxation rate. This means that the lifetime of the triplet is $>10^{-10}$ s, implying a quality factor for the triplet oscillations $Q = \Delta/\hbar\Gamma > 100$. This represents the largest (by an order of magnitude) bound on $Q$ reported to date for an S = 1 chain. When we introduce excited states through warming, the HWHM increases, thus providing evidence for an increasing triplet relaxation rate, which goes hand in hand with the reductions in mean free path discussed above.

Although the quantum nonlinear σ model (*19*) provides a reasonable prediction for the spin correlation lengths, it severely overestimates the thermal blue shift (the dash-dotted line in Fig. 3A). A more successful approach exploits Monte Carlo calculations (*31*), which provide the $T = 0$ gap energy due to finite chain confinement. By using twice the coherence length $\xi$ obtained in Fig. 2 as the size of the confinement "box" (top scale in Fig. 3A), the gap energies can be calculated and plotted as the blue solid line in Fig. 3. The agreement between experimental data and the parameter-free calculation is truly remarkable. It is also worthwhile to note that introducing chemical impurities is another approach to creating the same quantum confinement effect. Average gap energies for 4 and 10% Ca-doped and 4% Mg-doped $Y_2BaNiO_5$ are extracted from measurements done at base temperature and plotted as diamonds in Fig. 3A, which agree very well with the calculated gap energies based on $2\xi/a = 1/x$.

Although we have described all of our $T$-dependent data in terms of a very simple model whose underlying driver is thermal activation across a gap to triplet formation, it is important to realize that this model is largely phenomenological. Fortunately, there is a rigorous formulation, with similar conclusions, due to Damle and Sachdev (*27*), whose finite temperature theory is based on a semiclassical treatment of scattering between triplet excited states with a temperature-independent quadratic dispersion relation. Although this parameter-free theory does not account for the thermal blue shift, it determines the triplet lifetime and leads to the phenomenological expression for $\xi$ in the clean limit ($x = 0$), in impressive agreement (dashed lines in Figs. 2 and 3B) with the data.

Our experiments have shown that although quantum spin chains with a gap have a finite equal-time spin correlation length, the coherence of excited states at low temperature is limited only by quenched disorder. At finite temperatures, the coherence length decreases and the excited states acquire a finite mean free path due to collisions with other excitations. Both effects are quantitatively accounted for by a semiclassical theory of triplet wave packets scattering from each other and from defects in the sample. This demonstration of mesoscopic phase coherence in a magnet adds a fifth example—the other four are superconductors, superfluids, fractional quantum Hall states, and optically confined Bose-Einstein condensates—to the list of systems in which quantum phase coherence has been demonstrated in the absence of classical order.

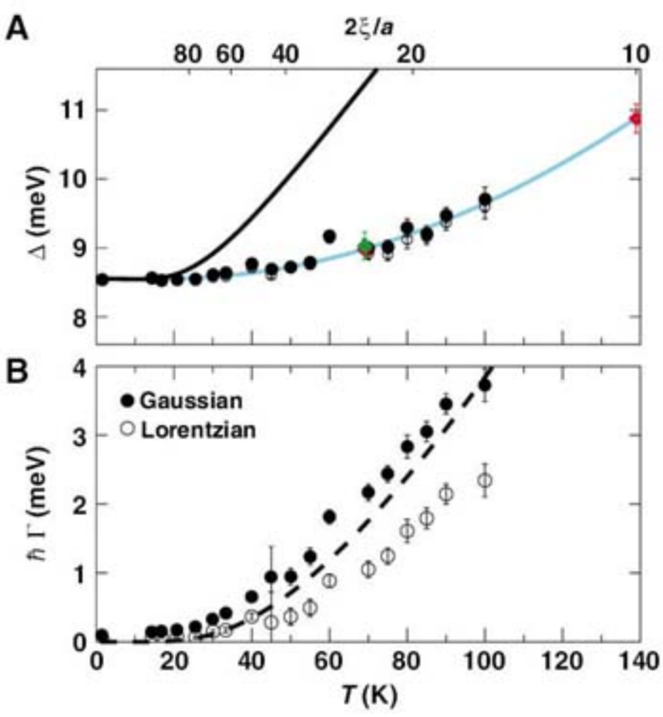


**Fig. 3.** (**A**) Haldane gap energy, and (**B**) half width of the excited triplet mode measured at different temperatures for $Y_2BaNiO_5$. The open and solid circles are results from assuming Lorentzian and Gaussian spectral functions, respectively, which the data do not distinguish. The lines in (A) are model calculations described in the text. The dashed line in (B) is a parameter-free theoretical result (*27*). The diamonds are gap energies derived from measurements at base temperature on Ca (red)– and Mg (green)–doped samples (concentration $x$) and placed according to $2\xi/a = 1/x$ of the top scale in (A), which indicates the effective thermal chain lengths for a pure sample (twice the coherence length from the dashed line in Fig. 2), resulting from thermal defects.


**References and Notes**

1. In superconductors and superfluids, phase coherence is macroscopic, whereas the microscopic coherence lengths associated with the single or paired particles participating in the condensate are finite and remain so down to zero temperature. The equal-time correlation length $\xi_0$ in the experiments reported here is analogous to the latter quantity.
2. B. D. Josephson, *Phys. Lett.* **1**, 2511 (1962).
3. L. B. Ioffe *et al.*, *Nature* **415**, 503 (2002).
4. M. Kellogg, J. P. Eisenstein, L. N. Pfeiffer, K. W. West, *Phys. Rev. Lett.* **93**, 036801 (2004).
5. M. R. Andrews *et al.*, *Science* **275**, 637 (1997).
6. F. D. M. Haldane, *Phys. Lett. A* **93**, 464 (1983).
7. F. D. M. Haldane, *Phys. Rev. Lett.* **50**, 1153 (1983).
8. M. den Nijs, K. Rommelse, *Phys. Rev. B* **40**, 4709 (1989).
9. U. Schollwock, Th. Jolicoeur, T. Garel, *Phys. Rev. B* **53**, 3304 (1996).
10. I. Affleck, T. Kennedy, E. H. Lieb, H. Tasaki, *Phys. Rev. Lett.* **59**, 799 (1987).
11. B. L. Altshuler, R. M. Konik, A. M. Tsvelik, *Nucl. Phys. B* **739**, 311 (2006).
12. G. Xu *et al.*, *Science* **289**, 419 (2000).
13. M. Kenzelmann *et al.*, *Phys. Rev. Lett.* **90**, 087202 (2003).
14. G. Xu *et al.*, *Phys. Rev. B* **54**, R6827 (1996).
15. Materials and methods are available as supporting material on *Science* Online.
16. W. J. L. Buyers *et al.*, *Phys. Rev. Lett.* **56**, 371 (1986).
17. J. P. Renard, M. Verdaguer, L. P. Regnault, W. A. C. Erkelens, J. Rossat-Mignod, *J. Appl. Phys.* **63**, 3538 (1988).

18. L. P. Regnault, I. A. Zaliznyak, J. P. Renard, C. Vettier, *Phys. Rev. B* **50**, 9174 (1994).
19. Th. Jolicur, O. Golinelli, *Phys. Rev. B* **50**, 9265 (1994).
20. M. T. Hutchings, G. Shirane, R. J. Birgeneau, S. L. Holt, *Phys. Rev. B* **5**, 1999 (1972).
21. J. Skalyo Jr., G. Shirane, R. J. Birgeneau, H. J. Guggenheim, *Phys. Rev. B* **2**, 4632 (1970).
22. S. Itoh, Y. Endo, K. Kakurai, H. Tanaka, *Phys. Rev. Lett.* **74**, 2375 (1995).
23. A. V. Sologubenko, T. Lorenz, H. R. Ott, A. Freimuth, *J. Low Temp. Phys.* **147**, 387 (2007).
24. K. Kordonis, A. V. Sologubenko, T. Lorenz, S.-W. Cheong, A. Freimuth, *Phys. Rev. Lett.* **97**, 115901 (2006).
25. A. P. Ramirez, S.-W. Cheong, K. L. Kaplan, *Phys. Rev. Lett.* **72**, 3108 (1994).
26. M. Yoshida *et al.*, *Phys. Rev. Lett.* **95**, 117202 (2005).
27. K. Damle, S. Sachdev, *Phys. Rev. B* **57**, 8307 (1998).
28. T. Sakaguchi, K. Kakurai, T. Yokoo, J. Akimitsu, *J. Phys. Soc. Jpn.* **65**, 3025 (1996).
29. A. Zheludev *et al.*, *Phys. Rev. B* **53**, 15004 (1996).
30. M. Kenzelmann, R. A. Cowley, W. J. L. Buyers, D. F. McMorrow, *Phys. Rev. B* **63**, 134417 (2001).
31. M. P. Nightingale, H. W. J. Blöte, *Phys. Rev. B* **33**, 659 (1986).
32. We thank K. Damle, B. Keimer, S. Sachdev, S. Shapiro, and J. M. Tranquada for helpful discussions. Work in London was supported by a Wolfson–Royal Society Research Merit Award and the Basic Technologies program of Research Councils UK. Work at Johns Hopkins University, NIST, and Louisiana State University was supported by NSF and that at Brookhaven National Laboratory was supported by the Office of Science of the U.S. Department of Energy.

**Supporting Online Material**
www.sciencemag.org/cgi/content/full/1143831/DC1
Materials and Methods
Figs. S1 and S2
References

16 April 2007; accepted 12 July 2007
Published online 26 July 2007;
10.1126/science.1143831
Include this information when citing this paper.

# Electron-Induced Oxygen Desorption from the $TiO_2$(011)-2×1 Surface Leads to Self-Organized Vacancies

**Olga Dulub,[1] Matthias Batzill,[2] Sergey Solovev,[3] Elena Loginova,[3] Alim Alchagirov,[1] Theodore E. Madey,[3] Ulrike Diebold[1]***

When low-energy electrons strike a titanium dioxide surface, they may cause the desorption of surface oxygen. Oxygen vacancies that result from irradiating a $TiO_2$(011)-2×1 surface with electrons with an energy of 300 electron volts were analyzed by scanning tunneling microscopy. The cross section for desorbing oxygen from the pristine surface was found to be 9 (±6) × $10^{-17}$ square centimeters, which means that the initial electronic excitation was converted into atomic motion with a probability near unity. Once an O vacancy had formed, the desorption cross sections for its nearest and next-nearest oxygen neighbors were reduced by factors of 100 and 10, respectively. This site-specific desorption probability resulted in one-dimensional arrays of oxygen vacancies.

Desorption of atoms or molecules can occur when sufficient energy is available to overcome the potential barrier that forms the surface bond. Often this process occurs through thermal routes and the barrier is overcome through vibrational energy, but electronic transitions induced by photons or particles (typically electrons or ions) can lead to rapid desorption when the atom or molecule is excited to a higher-energy configuration that is repulsive in nature. This desorption induced by electronic transitions (DIET) has important fundamental and technological applications (*1*, *2*). DIET-related phenomena must be taken into account in areas as diverse as the modification of semiconductors (*3*), the radiation damage of optical materials (*4*, *5*), nuclear waste storage, and planetary science (*6*, *7*). By using the tip of a scanning tunneling microscope (STM) as an electron source, such processes can be used for the electronic control of single-molecule dynamics (*8*–*10*).

[1]Department of Physics, Tulane University, New Orleans, LA 70118, USA. [2]Department of Physics, University of South Florida, Tampa, FL 33620, USA. [3]Department of Physics and Astronomy and Laboratory for Surface Modification, Rutgers University, Piscataway, NJ 08855, USA.

*To whom correspondence should be addressed. E-mail: diebold@tulane.edu

Central to DIET phenomena is the efficient conversion of an initial electronic excitation into the motion of an atom. One of the earliest proposed mechanisms (*11*, *12*) invokes a Frank-Condon excitation of an adsorbate to a repulsive potential energy curve; under strong excitation conditions, such excitations can also be achieved by multiple electronic transitions (DIMET) (*13*). Desorption will occur only if the electronic excitation is long-lived and the nucleus starts to move before the excitation is quenched. Understanding the basic physics that quenches such excitations is important for technical applications, for example, in processes that convert solar energy into chemical reactions or electrical energy (*14*) or in contamination of optical elements in extreme ultraviolet lithography applications (*15*).

DIET processes differ from thermal desorption in several important ways. Surface species undergoing thermal desorption are close to equilibrium in that the vibrational energy can redistribute rapidly relative to the time scale of breaking surface bonds. Thermal desorption usually involves neutral species, but the much higher energies available in DIET processes allow charged species to leave the surface and overcome attractive forces, and cascading electron transfer processes can lead to desorption of anions, cations, metastables, and ground-state neutrals. Because thermal desorption processes are near to equilibrium, the effect of a desorption event on the remaining surface neighbors is a small perturbation; rapid diffusion will delocalize and randomize vacancies created by desorption. In DIET processes that occur far from equilibrium at low temperature, a vacancy created by desorption remains localized and cannot diffuse. One might expect that such immobile DIET-produced vacancies would be randomly arrayed on the surface.

We have investigated one of the canonical materials for studying DIET processes, $TiO_2$, and we find highly unusual and unexpected behavior for vacancy distributions on the (2×1) termination of $TiO_2$(011): Electron bombardment leads to formation of vacancy clusters, one-dimensional arrays of O vacancies. Why? Although the initial probability for $O^+$ desorption and the formation of an O vacancy is nearly unity, the creation of a vacancy markedly decreases the desorption probability of its nearest-neighbor and next-nearest-neighbor O atoms. The surface charge that accompanies defect formation must be the factor causing desorption probabilities to change so greatly.

Self-organization can be achieved where an initial process controls subsequent events. A string of such interrelated events can then lead to pattern formation. The unexpectedly high alteration of the desorption probability upon formation of an O vacancy is an example of this phenomenon; the initial desorption event is responsible for the self-organization of subsequent defects. This process should apply generally to DIET processes. Consequently, the formation of well-defined O-vacancy patterns must be taken into consideration in the radiation damage of insulating surfaces and can be used to enhance the chemical reactivity of DIET-modified surfaces.

We have investigated the effects of electron irradiation on $TiO_2$ not only because it has been a model system for DIET processes, but because it is a very promising material for solar energy conversion; it is also the prototypical material for fundamental studies of metal oxide surface reactivity (*16*, *17*). Its chemical, electronic, and optical properties depend strongly on the presence of steps, vacancies, and other surface defects

(*18*). It was recognized early on that electron-induced DIET processes remove oxygen from a $TiO_2$ surface (*19*). This allows control of the formation of O vacancies and modification of the surface reactivity on $TiO_2$ (*20*, *21*).

Knotek and Feibelman (K-F) proposed a mechanism for $O^+$ desorption from $TiO_2$ and other maximal-valence oxides (such as $V_2O_5$, $WO_3$, and NiO) (*19*). Their model is based on the interesting observation that the threshold energy for the electron-stimulated desorption (ESD) of $O^+$ from $TiO_2$ corresponds to the excitation energy of the Ti 3p core hole. To rationalize the formation of an $O^+$ ion from a (formally) $O^{2-}$ species in the oxide lattice, it was proposed that the Ti core hole is filled with electrons from O 2p orbitals via an interatomic Auger process from a neighboring O atom. (It was argued that an intra-atomic Auger process, which is usually much faster, is not possible when the Ti 3d band is empty.) If three electrons escape from the oxygen, for example, in a double Auger decay, the $O^{2-}$ ion becomes $O^+$. This $O^+$ ion can be ejected from the surface by Coulomb repulsion from the surrounding $Ti^{4+}$ lattice ions.

The invoked double Auger decay is not a very likely process, however, and the K-F model ignores the high degree of covalency in $TiO_2$ (*22*) and many other transition metal oxides. Indeed, recent photo (Auger)–electron/ion coincidence spectroscopy measurements on $TiO_2$ (110) indicate that the K-F mechanism needs to be refined (*23*), because a Ti atom's initial and final states—before and after the core-hole excitation, respectively—contain mixtures of electron configurations that have one or more holes in a neighboring O atom. To date, there exists little information about the distribution of the O vacancies that result from electron irradiation (*20*), and no information that suggests self-organization.

We used STM to evaluate the effect of electron beam irradiation on a $TiO_2$(011)-2×1 surface. The (2×1) reconstruction of $TiO_2$(011) is produced by sputtering and thermal annealing to 1000 K. This surface is stable and stoichiometric, and its structure has been investigated extensively both experimentally and theoretically (*24*, *25*). The model of Fig. 1 is characterized by singly coordinated O atoms. Although details of bonding in the lowest-energy (2×1) structure are currently undergoing study (*26*), both STM (Fig. 2A) and all theoretical models to date confirm that O atoms are arranged in double rows with zigzag configuration. Whereas we display this structure in Fig. 1A because it appears to be consistent with experiment, other models with multiply coordinated O atoms are under evaluation (*26*). The desorbing species ($O^+$ and some $H^+$) have been monitored with a time-of-flight technique [electron-stimulated desorption ion angular distribution (ESDIAD) optics] and a quadrupole mass spectrometer. In the ESD process, ions are ejected at discrete angles determined by the orientation of the ruptured bonds (*2*). Figure 1B shows the angular distribution of $O^+$ ions desorbed from the surface. The ESDIAD pattern exhibits two off-normal emission lobes symmetric about the $[0\bar{1}1]$ direction.

Heating $TiO_2$ surfaces in vacuum produces O vacancies (*17*); the concentration of O vacancies typically amounts to 5 to 9% of surface O sites for the $TiO_2$(011) sample used. Such thermally induced defects appear as missing bright spots on $TiO_2$(011)-2×1 and do not show any apparent ordering (*25*). The $TiO_2$(011)-2×1 surface can sustain a large number of O vacancies without restructuring, which allows monitoring of O desorption over a large range of defect densities. This is different from the extensively investigated $TiO_2$(110) surface (*27*), which reconstructs after a maximum defect concentration of 10 to 12% is reached (*20*, *28*). Using the $TiO_2$(011)-2×1 surface instead of $TiO_2$(110) also has another practical advantage: Surface hydroxyl groups, which form readily when water dissociates at O vacancies, appear as brighter atoms in STM (*29*) and can be clearly distinguished from the black O vacancies on the $TiO_2$ (011)-2×1 surface. [The similarity of surface OH and O vacancies in STM images of $TiO_2$(110) can lead to ambiguities (*28*).]

After exposure to 300-eV electrons, ~55% of the surface O atoms had been desorbed (Fig. 2B). This desorption did not occur in a random fashion: Most of the remaining oxygen atoms were lined up along one side of the original zigzag row (yellow lines in Fig. 2B). These single-atom strands were up to 12 atoms long, whereas patches where the original zigzag configuration was preserved were much smaller. The defective surface was quite reactive; the very bright spots in Fig. 2B were caused by unknown impurities from the residual gas of the chamber that reacted with the defective surface.

The effect of electron irradiation is shown in more detail in Fig. 3, B to D. The vacancy concentration increased with increasing electron dose, up to a defect density of 70% of a monolayer (ML). (One monolayer of surface O

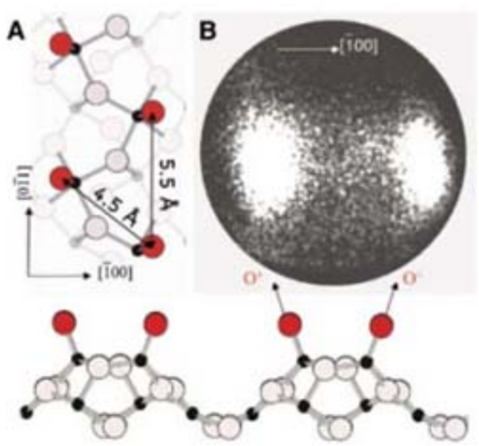


**Fig. 1.** (**A**) Model of the $TiO_2$(011)-2×1 surface. Titanium and oxygen atoms are represented as black and gray spheres, respectively; the red spheres represent one-fold coordinated surface oxygen atoms. The arrows in the side view illustrate the direction of $O^+$ ions when desorbed by an electron beam. (**B**) Experimental pattern of the angular $O^+$ ion distribution during electron-stimulated desorption from the $TiO_2$(011)-2×1 surface.

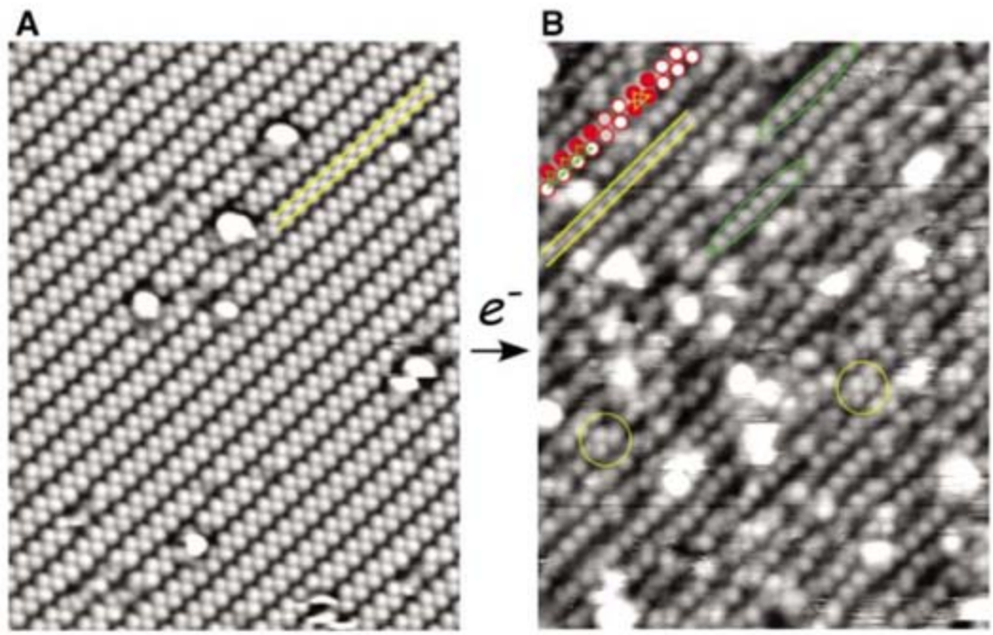


**Fig. 2.** (**A**) Scanning tunneling microscopy images (170 Å by 220 Å) of a clean $TiO_2$(011)-2×1 surface. Surface O atoms are arranged in double rows with a zigzag configuration; O vacancies appear as black spots. (**B**) The same surface after irradiation with 300-eV electrons, which causes the desorption of oxygen. Remaining O atoms are mainly arranged in one-dimensional strands along one side of the original double-row structure, as indicated by green ovals and yellow lines. Small areas that have maintained the original zigzag configuration are marked with yellow circles.

atoms corresponds to $N_0 = 4 \times 10^{14}$ atoms cm$^{-2}$.) Single-atom strands were observed for a wide range of doses (see Fig. 3 and the sketch of empty and filled O sites in Fig. 3G). Above a dose of $2.8 \times 10^{17}$ electrons cm$^{-2}$, however, the surface became disordered in low-energy electron diffraction. Such surface vacancy arrays could not be created through thermal desorption; indeed, heating the electron-bombarded surface to 300°C in vacuo yielded the original, nearly stoichiometric surface.

In stimulated desorption a first-order process is often assumed, that is, a random removal of oxygen with a desorption cross section σ that does not change throughout the irradiation time. Figure 3F shows a Monte Carlo simulation of a typical distribution of 55% O vacancies that would result from a constant desorption cross section. (From the STM snapshot and the electron dose in Fig. 3C, a first-order desorption yield of one O per 420 incoming electrons was assumed.) The simulated arrangement of the remaining surface O atoms is very different from the one observed in the experiment (compare Fig. 3, C and G, with Fig. 3F). The characteristic, single-strand O rows that remain on one side of the original zigzags can only be attributed to a change in the desorption probability as vacancies are being formed. Moreover, for high densities of thermally induced point defects, such long single-atom strands were not observed, indicating that these do not represent a low-energy configuration. Hence, electron-stimulated diffusion (*30*) can be ruled out as a cause for the formation of the nonuniform distribution of O vacancies.

A site-dependent desorption process was modeled with a Monte Carlo simulation (Fig. 3H) with three adjustable parameters. The first parameter describes the probability for desorbing the first O atom from the pristine surface. Once a DIET-induced O vacancy has been produced, the probability for desorbing an O neighbor on the other side of the zigzag was reduced by a factor that was treated as the second parameter. One-dimensional strands could also be formed if the desorption probability for an oxygen neighbor on the same side of the zigzag row were increased; for some systems, an increased probability was indeed observed next to defects (*5*). Thus, the desorption probability for an O neighbor right next to a vacancy was treated as the third parameter in the simulations. As shown in Fig. 3G, a good qualitative agreement can be achieved with a desorption yield of 1:20 for the pristine surface, which is decreased by one and two orders of magnitude for oxygen neighbors adjacent to and opposite an existing O vacancy, respectively. In contrast, an increase in the desorption cross section for an O atom adjacent to an O vacancy does not result in the correct dose-dependent behavior.

To put these simulations on a more quantitative footing, we analyzed different vacancy configurations for a large number of images (total area $5 \times 10^5$ Å$^2$) obtained after various electron doses. Atoms in high-resolution STM images were binned in triangles, and three configurations were considered: (α) triangles with one atom filled and two sites empty (these are part of the single-atom strands); (β) triangles with three atoms filled (such configurations are part of zigzag patches); and (γ) triangles with two atoms filled and one empty; such atoms would reside at the edge of a zigzag patch, or at a location where single-atom strands cross over from one side of a double row to the other side. The results of a simulation with values of $\frac{1}{20}:\frac{1}{200}:\frac{1}{2000}$ for the probability of removing the first atom, the adjacent atom, and the opposite atom, respectively, show excellent agreement for the density of the configurations α and β (Fig. 4A),

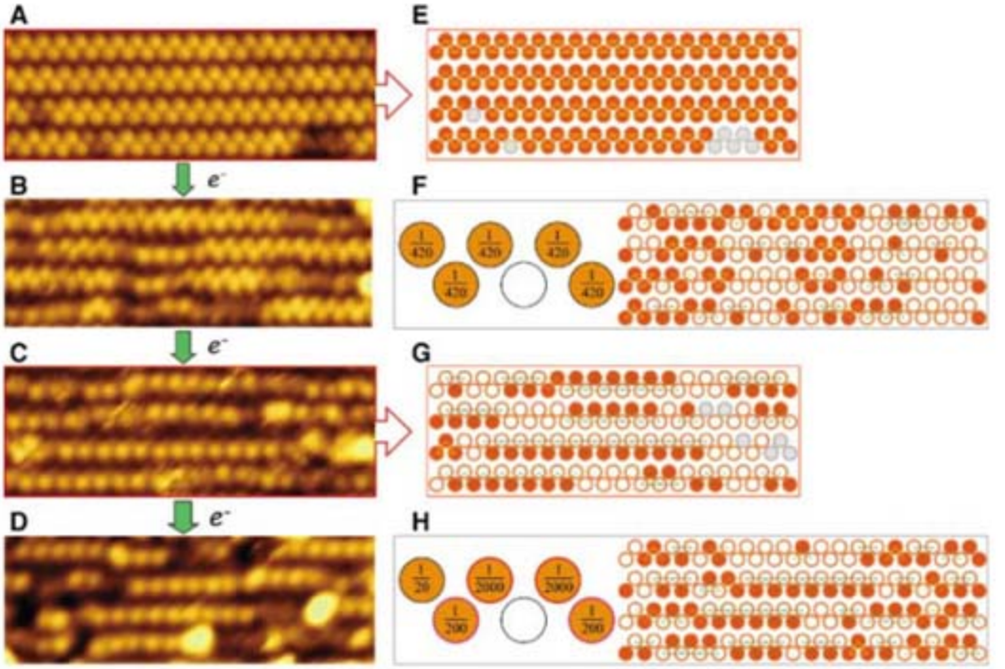


**Fig. 3.** (**A** to **D**) STM images before (A) and after [(B) to (D)] irradiation with 300-eV electrons. Electron doses and the resulting vacancy concentrations (given as percentages of a monolayer) are (B) $2.3 \times 10^{16}$ electrons cm$^{-2}$, 35%; (C) $9.2 \times 10^{16}$ electrons cm$^{-2}$, 55%; and (D) $1.8 \times 10^{17}$ electrons cm$^{-2}$, 70%. (**E** and **G**) Sketches of the remaining O atoms (orange) and O vacancies (white circles). (**F** and **H**) Monte Carlo simulations of O-vacancy configurations corresponding to (F) a random, first-order desorption process (with an assumed constant yield of one desorbing O atom per 420 incoming electrons), and (H) desorption yields of $\frac{1}{20}:\frac{1}{200}:\frac{1}{2000}$ for the first O atom, an O atom adjacent to an O vacancy, and an O atom opposite an O vacancy, respectively.

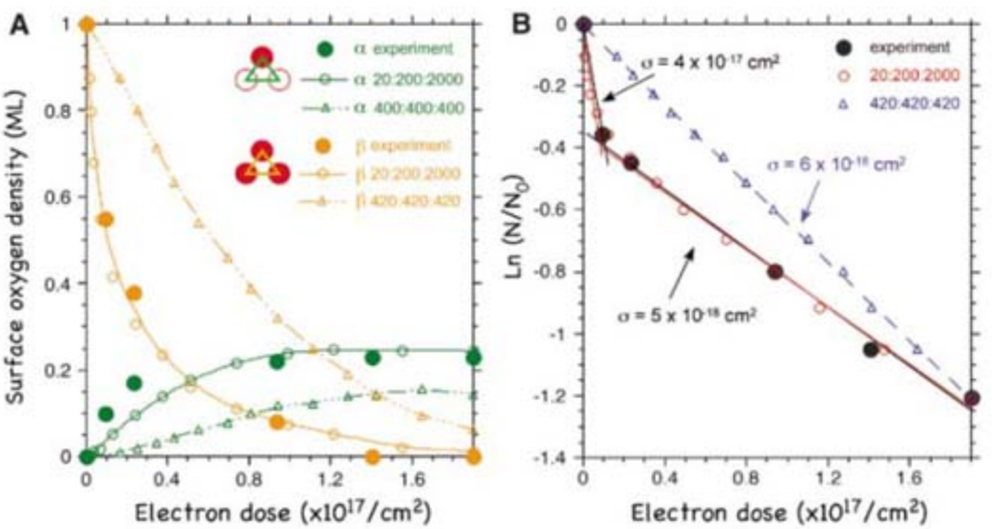


**Fig. 4.** (**A**) Number of configurations of O atoms with two O vacancies (α) and two oxygen atoms (β) as nearest neighbors, as a function of irradiation with 300-eV electrons. (**B**) Total number of O atoms on the surface versus electron dose. Experimental values are compared with the results of Monte Carlo simulations with the same desorption probabilities as in Fig. 3, F and H. A linear fit in the semilogarithmic plot in (B) allows for an evaluation of the average cross section for electron-stimulated desorption.

the size distribution of the resulting single-atom strands and zigzag patches, and the decrease of the total number of surface O atoms as a function of electron dose (Fig. 4B).

In principle, for a first-order desorption process, a semilogarithmic plot of the number of remaining atoms versus the electron dose would follow a straight line; the slope of the line gives the cross section (triangular points and associated line in Fig. 4B). The experimental data in Fig. 4B deviate from such a behavior. The much more rapid decrease for low electron doses, where atoms are mainly desorbed from pristine areas without O vacancy sites, is well described by our Monte Carlo results (circles in Fig. 4B). Our statistical analysis allows the determination of the site-specific desorption probability on an atom-by-atom basis. In contrast, a signal that is proportional to the total surface O concentration (such as in Fig. 4B), or to the desorbing species, can only be used to determine an average cross section that lumps together the probabilities for all individual desorption events.

The few average cross sections reported for ESD of $TiO_2$ (*31*, *32*) are of magnitudes similar to that of the average cross section indicated in Fig. 4B. The probability for electron-stimulated desorption from the pristine surface is very high, however. A value of 1 in 20 electrons provides the best fit to all experimental observables; taking into account the parameter values that lie within our confidence value, we determine the initial cross section to be ~9 (±6) × $10^{-17}$ $cm^2$ (*33*).

Why is the desorption from the pristine surface so efficient, and why does the proximity to a defect site decrease the probability so effectively? Previous measurements have firmly established that core-hole excitations are connected to O desorption (*19*, *23*); we also find that irradiation with ~25-eV electrons, an energy smaller than the core-level binding energies in $TiO_2$, does not produce any observable defects on $TiO_2$(011)-2×1. The cross section for stimulated desorption can be described by $\sigma = I \times P$, where $I$ denotes the cross section for a core-hole ionization, and $P$ is the probability that this excitation results in a desorption event (i.e., an excited state that is both repulsive and long-lived enough to induce nuclear motion). Measured cross sections for Ti 3p ionization of Ti ions in the gas phase vary between 1 × $10^{-17}$ $cm^2$ and 9 × $10^{-17}$ $cm^2$, depending on the ionization state (*34*, *35*).

Electron backscattering can increase the ionization probability in a solid by up to a factor of 2 relative to the same species in the gas phase; this could be the reason why the measured cross section for O desorption from pristine $TiO_2$ lies at the upper range of the values for isolated Ti. However, this value implies that the desorption cross section is comparable in magnitude to the cross section for ionization ($\sigma \sim I$) and that the probability for desorption after core-hole excitation, $P$, must be near unity.

In the K-F model (*19*), the decay of the initial excitation results in the conversion of $O^{2-}$ to $O^+$. This $O^+$ ion then finds itself surrounded by positively charged lattice Ti and will be repelled by the reversed Madelung potential. (The $O^+$ ions can also capture an electron on their way out of the surface and desorb as neutral atoms, as long as the neutralization does not occur too close to the original position, which would quench the emission process.) Classical trajectory calculations of the ion emission process show that ejection from the surface will only occur for highly undercoordinated surface O atoms (*36*); apparently, this is the case on $TiO_2$(011)-2×1.

What is the probability, then, for a core-hole excitation resulting in a three-hole final state in a surface O atom? Recent electron-ion coincidence spectroscopy measurements (*23*) have helped refine the K-F picture, which relied on a (relatively unlikely) interatomic Auger decay, accompanied by the [also not highly probable (*37*)] emission of two Auger electrons from an O ligand. Calculations of core-hole excitations (*38*), based on a cluster model in the framework of the Anderson impurity model, show that a multihole final state of the ligand is in fact quite probable for early transition metal oxides, even without accounting for a consecutive Auger de-excitation process. The high degree of covalency in ground-state configurations of $TiO_2$ is expressed as $|c\underline{d}^{0+q}L^q\rangle$, where $q$ denotes the number of electrons that have been transferred from the ligand orbital, $L$, to the (formally empty) d electron shell on the metal atom. In a simple physical picture, the creation of a core hole, $c$, pulls the 3d band down in energy, and electrons flow from the oxygen ligand to the Ti. For $TiO_2$ the core-hole final state, $|c\underline{d}^{0+q}L^q\rangle$, exhibits configurations with $q$ up to 5, with a fractional parentage for $q \geq 3$ of 25% (*38*). Similar values have been reported for other transition metal oxides with a high degree of hybridization (*38*); thus, an excited state that could lead to O desorption is in fact quite probable. It remains to be tested whether the unexpectedly high cross section observed for pristine $TiO_2$(011)-2×1 is specific to this surface, or if it will occur on other $TiO_2$ surfaces, or other oxides, as well.

It is well established that an O vacancy on $TiO_2$ surfaces results in a filled-gap state located ~0.8 eV below the conduction band minimum (*17*). The drastic decrease in the desorption probability for O atoms next to an O vacancy is likely caused by these extra electrons at defect sites "screening" the repulsive excited state. The absence of mobile conduction electrons is the reason why, in general, DIET processes are much more efficient on semiconductors than on metals. The strong site dependence of the screening that results in the distinct one-dimensional rows needs some explanation, however, given that the separations between opposite O neighbors across and parallel to the zigzag rows are not too different (measured values of 4.5 Å and 5.5 Å, respectively). Yet we estimate that the desorption probabilities are reduced by one and two orders of magnitude for an O adjacent and opposite to an O vacancy, respectively. An explanation based on the recent observation of anisotropic conductivity in rutile does not appear to be adequate (*39*).

One possible explanation is quenching of the electronic excitation by defect-induced electronic states. Lattice distortions that occur during the desorption process may enhance this effect. Recent density functional theory calculations give strong evidence that the degree of charge localization of vacancy electrons is sensitively dependent on small distortions within the lattice (*40*). During a desorption event, the lattice starts to distort dynamically (*9*); this could cause electrons in the defect state to flow toward the location of the O atom as it starts to leave the surface. This scenario gives a plausible explanation for the differences in the reduced desorption probability along and across the row of the O vacancy. Nearest O neighbors are much more directly linked, whereas weaker coupling to next-nearest O neighbors makes a sharing of charges, or a charge redistribution during the lattice distortion, less efficient. Thus, the strong anisotropy in the bonding geometry at this particular surface is fundamental for the anisotropic quenching of electronically excited states in the vicinity of O vacancies.

In general, atomic vacancies on dielectric surfaces result in a modification of the local electronic structure. We have shown that this altered electronic configuration causes a strong variation of DIET processes in the vicinity of O vacancies, as excess electrons from the defects slosh toward a neighboring atom that has been put into a repulsive state via a core-hole excitation. Thus, defects have a self-limiting effect in the modification of surfaces, and the resulting self-organization of defect structures can be used to pattern surfaces at the atomic scale. In the case of the anisotropic $TiO_2$(011) surface, the formation of one-dimensional defect structures is favored; because O vacancies react strongly with molecular and metal adsorbates (*41*, *42*), such structures could be used to template interesting overlayers (e.g., one-dimensional rows of catalytically active Au atoms). Quenching of excitations is expected to be observable not only in the presence of O vacancies; other intrinsic or extrinsic electron donors will have similar effects. This has implications for materials design issues such as increasing the radiation resistance of coatings or optimizing responses of photoactive materials.

### References and Notes


1. J. T. Yates Jr. *et al.*, *Science* **255**, 1397 (1992).
2. T. E. Madey, *Science* **234**, 316 (1986).
3. K. Nakayama, J. H. Weaver, *Phys. Rev. Lett.* **82**, 980 (1999).
4. T. E. Madey, D. E. Ramaker, R. Stockbauer, *Annu. Rev. Phys. Chem.* **35**, 215 (1984).
5. B. Such *et al.*, *Phys. Rev. Lett.* **85**, 2621 (2000).

6. J. Herring, A. Aleksandrov, T. M. Orlando, *Phys. Rev. Lett.* **92**, 187602/1 (2004).
7. B. V. Yakshinskiy, T. E. Madey, *Nature* **400**, 642 (1999).
8. M. Lastapis *et al.*, *Science* **308**, 1000 (2005).
9. R. E. Walkup, P. Avouris, *Phys. Rev. Lett.* **56**, 524 (1986).
10. J. R. Hahn, W. Ho, *J. Chem. Phys.* **123**, 214702 (2005).
11. D. Menzel, R. Gomer, *J. Chem. Phys.* **41**, 3311 (1964).
12. P. A. Redhead, *Can. J. Phys.* **42**, 886 (1964).
13. J. A. Misewich, T. F. Heinz, D. M. Newns, *Phys. Rev. Lett.* **68**, 3737 (1992).
14. K. Hashimoto, H. Irie, A. Fujishima, *Jpn. J. Appl. Phys.* **44**, 8269 (2005).
15. T. E. Madey, N. S. Faradzhev, B. V. Yakshinsksiy, N. V. Edwards, *Appl. Surf. Sci.* **253**, 1691 (2006).
16. A. L. Linsebigler, G. Lu, J. T. Yates Jr., *Chem. Rev.* **95**, 735 (1995).
17. U. Diebold, *Surf. Sci. Rep.* **48**, 53 (2003).
18. X.-Q. Gong, A. Selloni, M. Batzill, U. Diebold, *Nat. Mater.* **5**, 665 (2006).
19. M. L. Knotek, P. J. Feibelman, *Phys. Rev. Lett.* **40**, 964 (1978).
20. C. L. Pang *et al.*, *Nanotechnology* **17**, 5397 (2006).
21. Q. Wang, J. Biener, X.-C. Guo, E. Farfan-Arribas, R. J. Madix, *J. Phys. Chem. B* **107**, 11709 (2003).
22. C. Noguera, *Physics and Chemistry of Oxide Surfaces* (Cambridge Univ. Press, Cambridge, 1996).
23. S.-i. Tanaka, K. Mase, S.-i. Nagaoka, *Surf. Sci.* **572**, 43 (2004).
24. T. J. Beck *et al.*, *Phys. Rev. Lett.* **93**, 036104/1 (2004).
25. O. Dulub, C. Di Valentin, A. Selloni, U. Diebold, *Surf. Sci.* **600**, 4407 (2006).
26. X.-Q. Gong, A. Selloni, personal communication.
27. The rutile structure is tetragonal, and the $TiO_2$(011)/(101) surface is inequivalent to the often-investigated $TiO_2$(110) surface.
28. S. Wendt *et al.*, *Surf. Sci.* **598**, 226 (2005).
29. C. Di Valentin *et al.*, *J. Am. Chem. Soc.* **127**, 9895 (2005).
30. A. G. Fedorus, E. V. Klimenko, A. G. Naumovets, E. M. Zasimovich, I. N. Zasimovich, *Nucl. Instrum. Methods Phys. Res. B* **101**, 207 (1995).
31. S. A. Joyce, M. Bertino, K. Kim, G. Flynn, *Chemical Structure and Dynamics 1999 Annual Report* (Environmental Molecular Sciences Laboratory, U.S. Department of Energy, 1999) (www.emsl.pnl.gov/docs/annual_reports/csd/annual_report1999/1578b_3f.html).
32. L.-Q. Wang, D. R. Baer, M. H. Engelhard, *Surf. Sci.* **320**, 295 (1994).
33. See supporting material on *Science* Online.
34. P. L. Bartlett, A. T. Stelbovics, *Atomic Data Nuclear Data Tables* **86**, 235 (2004).
35. U. Hartenfeller *et al.*, *J. Phys. B* **31**, 2999 (1998).
36. R. E. Walkup, R. L. Kurtz, *Desorption Induced by Electronic Transitions Diet III* (Springer-Verlag, New York, 1988), pp. 160–166.
37. M. Y. Amus'ya, I. S. Lee, V. A. Kilin, *Phys. Rev. A* **45**, 4576 (1992).
38. R. Zimmermann *et al.*, *J. Phys. Condens. Matter* **11**, 1657 (1999).
39. O. Byl, J. T. Yates Jr., *J. Phys. Chem. B* **110**, 22966 (2006).
40. C. Di Valentin, G. Pacchioni, A. Selloni, *Phys. Rev. Lett.* **97**, 166803/1 (2006).
41. E. Wahlstrom *et al.*, *Phys. Rev. Lett.* **90**, 026101 (2003).
42. T. V. Choudhary, D. W. Goodman, *Appl. Catal. Gen.* **291**, 32 (2005).



43. The Tulane group acknowledges the hospitality of Rutgers University while displaced by Hurricane Katrina, during which time this study was initiated. We thank A. Selloni for useful discussions. Supported by U.S. Department of Energy grants DE-TG02-05ER15702 and DE-FG02-93ER14331, NSF grants CHE-0315209 and CHE-010908, and the Intel Corporation.


**Supporting Online Material**

www.sciencemag.org/cgi/content/full/317/5841/1052/DC1
Materials and Methods
Figs. S1 and S2
References


8 May 2007; accepted 11 July 2007
10.1126/science.1144787


# Dinitrogen Dissociation on an Isolated Surface Tantalum Atom


P. Avenier,[1] M. Taoufik,[1]* A. Lesage,[2] X. Solans-Monfort,[3] A. Baudouin,[1] A. de Mallmann,[1] L. Veyre, J.-M. Basset,[1]* O. Eisenstein,[4] L. Emsley,[2] E. A. Quadrelli[1]*



Both industrial and biochemical ammonia syntheses are thought to rely on the cooperation of multiple metals in breaking the strong triple bond of dinitrogen. Such multimetallic cooperation for dinitrogen cleavage is also the general rule for dinitrogen reductive cleavage with molecular systems and surfaces. We have observed cleavage of dinitrogen at 250°C and atmospheric pressure by dihydrogen on isolated silica surface–supported tantalum(III) and tantalum(V) hydride centers $[(\equiv Si\text{-}O)_2Ta^{III}\text{-}H]$ and $[(\equiv Si\text{-}O)_2Ta^{V}H_3]$, leading to the $Ta^{V}$ amido imido product $[(\equiv SiO)_2Ta(=NH)(NH_2)]$: We assigned the product structure based on extensive characterization by infrared and solid-state nuclear magnetic resonance spectroscopy, isotopic labeling studies, and supporting data from x-ray absorption and theoretical simulations. Reaction intermediates revealed by in situ monitoring of the reaction with infrared spectroscopy support a mechanism highly distinct from those previously observed in enzymatic, organometallic, and heterogeneous $N_2$ activating systems.


Ammonia is the almost exclusive nitrogen source for living organisms, fertilizers and other artificial chemicals, hence making the Haber-Bosch process for ammonia synthesis from dinitrogen among the most relevant heterogeneous catalytic reactions (*1*), with approximately $10^8$ tons of ammonia produced yearly (*2*, *3*). The catalysts for nitrogen fixation in biological systems are nitrogenase enzymes, which produce yearly about the same amount of ammonia (*2*, *3*). These two major catalytic processes, as well as the only well-defined, homogeneous catalyst reported so far (*4*), are structurally and chemically very different. The first is essentially based on a surface of Fe or Ru atoms (*1*), the second on high molecular weight proteins with typically FeMo sulfur clusters (*5*–*7*) and the third on a molecular monometallic molybdenum complex (*4*). Additionally, these systems use different sources of hydrogen (gas phase molecular dihydrogen, NADH, and inorganic acids in solution) and different surrounding "cofactors" [such as inorganic promoters (*1*), coenzymes (*5*), or an organometallic redox system (*4*)] to catalyze the stepwise transformation of dinitrogen to ammonia.

Whether heterogeneous, enzymatic, or homogeneous, all these catalytic processes must entail a succession of elementary steps—involving reactant bond cleavage of the very robust N≡N triple bond and N-H bond formation in the product—possibly mediated by one or more metal atoms. Current understanding of the distinct elementary steps in heterogeneous (*8*, *9*), biochemical (*5*, *6*, *10*), and organometallic (*4*) systems is summarized in Fig. 1. We report herein the observed cleavage of dinitrogen by a silica-supported isolated tantalum atom (*11*, *12*), linked to silica by two (≡Si-O)-Ta bonds and obtained by surface organometallic chemistry (*13*). This $N_2$ dissociation pathway is unexpectedly different from all the three catalytic systems described above and, more generally, from previously observed surface and solution reactivity patterns.

The dinitrogen activation reported here is based on the use of highly electrophilic electron-deficient Ta hydrides: $[(\equiv Si\text{-}O)_2Ta^{III}\text{-}H]$ (**1a**) and $[(\equiv Si\text{-}O)_2Ta^{V}H_3]$ (**1b**) (*11*, *12*). These hydrides have already proven very active in the catalytic transformation of alkanes (e.g., alkane metathesis) by C-H and C-C bond cleavage (*14*, *15*) and more recently in ammonia activation by N-H bond cleavage (*16*). In this latter case, the characterized product was the $Ta^{V}$ amido imido complex $[(\equiv SiO)_2Ta(=NH)(NH_2)]$ (**2**), along with its ammonia adduct **2**·$NH_3$.

The starting tantalum hydrides **1** are obtained in two steps, which have already been


[1]Université de Lyon, C2P2, Laboratoire de Chimie Organométallique de Surface UMR5265 CNRS-CPE-UCBL1 43, Boulevard du 11 Novembre 1918, BP 2077 F-69616, Villeurbanne Cedex, France. [2]Université de Lyon, Laboratoire de Chimie, UMR-5182 CNRS-ENS, Lyon, Ecole Normale Supérieure de Lyon, F-69364 Lyon Cedex, France. [3]Departament de Química, Universitat Autònoma de Barcelona, 08193 Bellaterra, Spain. [4]Institut Charles Gerhardt, UMR 5253 CNRS, UM 2- ENSCM, UM1, Chimie Théorique, Méthodologies, Modélisations, Université Montpellier 2, F-34095 Montpellier Cedex 05, France.

*To whom correspondence should be addressed. E-mail: quadrelli@cpe.fr (E.A.Q.); taoufik@cpe.fr (M.T.); basset@cpe.fr (J.-M.B.)

described (*12*): reaction of the organometallic molecular precursor $[Ta(CH_2\text{-}CMe_3)_3(=CH\text{-}CMe_3)]$ with isolated silanols of a MCM-41 silica surface, followed by treatment with dihydrogen at 150°C. This method of preparation yields a mixture of **1a** and **1b**, which interconvert depending on the dihydrogen partial pressure, presumably through the intermediacy of an $\eta^{-2}$ dihydrogen ligand. The spacing of Ta centers precludes substantial Ta···Ta interactions (average Ta···Ta distance of ~8 Å). The formation of **1** also results in [≡Si-O-Si≡] bridges and a [≡Si-H] moiety in the vicinity of each Ta hydride (Fig. 2A) (*12*). At higher temperatures, the number of surface silanes [≡Si-H] increases with concomitant decrease in the number of surface tantalum hydrides as a result of hydrogen transfer from the Ta atom to an adjacent siloxy bridge to yield $[(\equiv SiO)_3Ta^{III}]$ and [≡SiH] (Fig. 2B) (*17*).

We found that at 250°C, exposure of the tantalum hydrides **1a** and **1b** to a 1:1 $N_2/H_2$ mixture at subatmospheric pressure ($P_{TOT}$ = 0.5 bar upon gas introduction in a closed vessel at room temperature; $P_{TOT}$ = 0.9 bar at 250°C) results in cleavage of the N≡N triple bond to yield the surface $Ta^V$ amido imido complex $[(\equiv SiO)_2Ta(=NH)(NH_2)]$ (**2**) (Fig. 2C), the same product previously observed from reaction of **1** with ammonia (*16*).

The reaction reaches >95% conversion in 3 days. Under these conditions, partial surface-embedding of **1a** and **1b** to $[(\equiv SiO)_3Ta]$ also

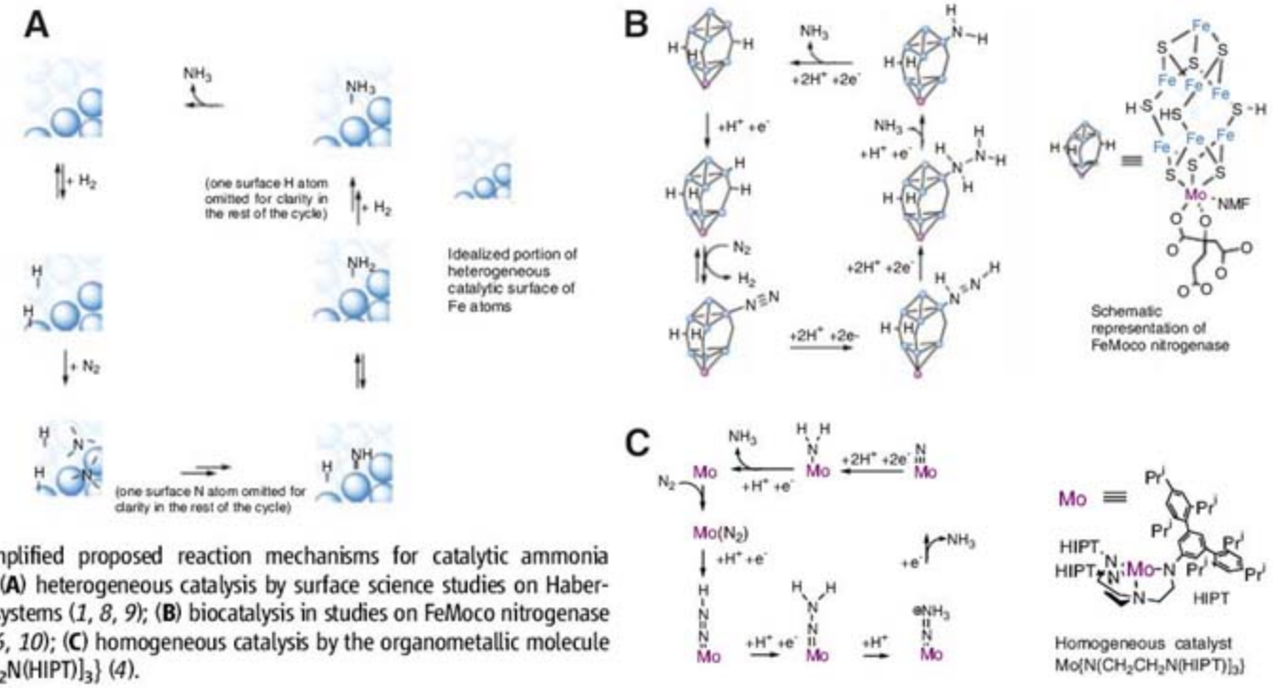


**Fig. 1.** Simplified proposed reaction mechanisms for catalytic ammonia synthesis in: (**A**) heterogeneous catalysis by surface science studies on Haber-Bosh model systems (*1*, *8*, *9*); (**B**) biocatalysis in studies on FeMoco nitrogenase enzymes (*5*, *6*, *10*); (**C**) homogeneous catalysis by the organometallic molecule $Mo\{N(CH_2CH_2N(HIPT)]_3\}$ (*4*).

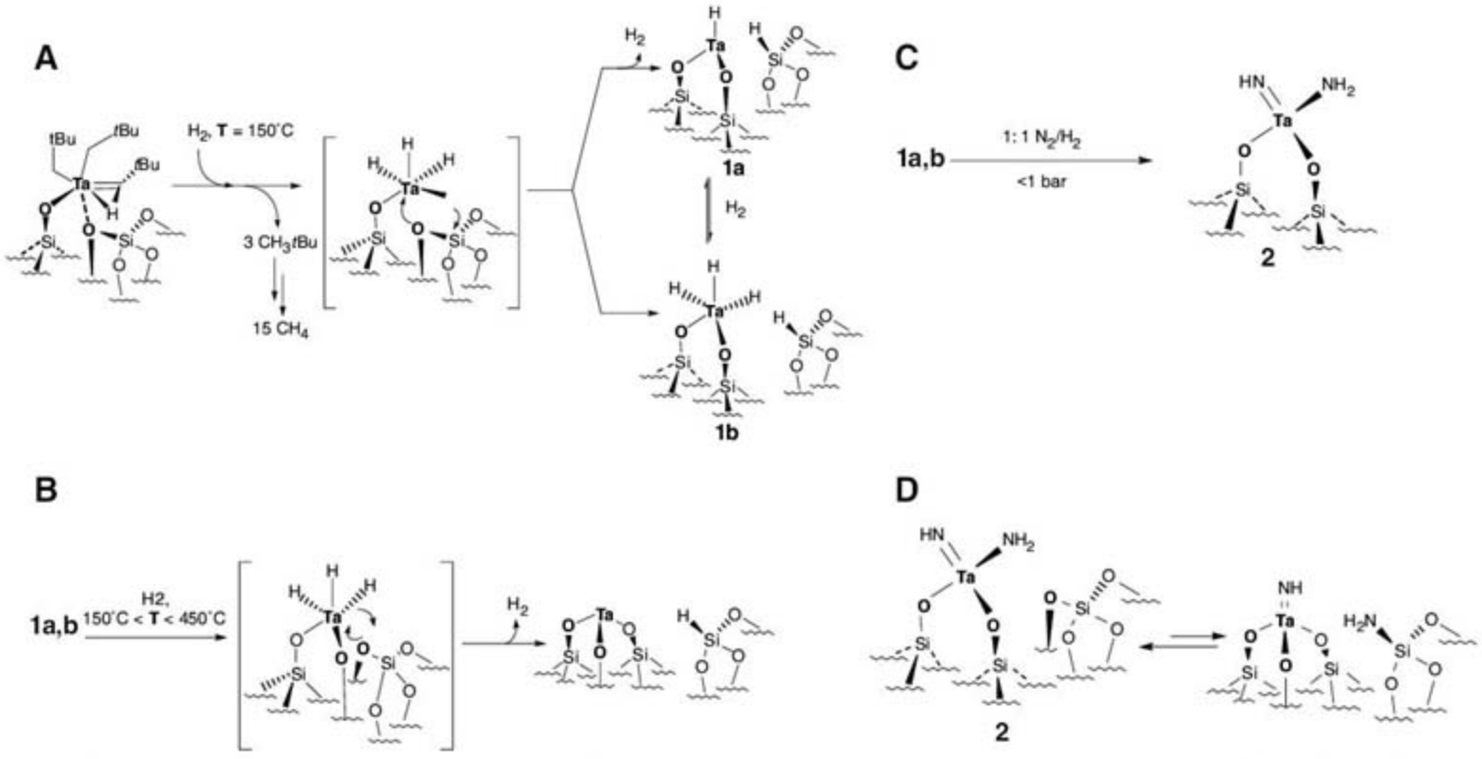


**Fig. 2.** (**A**) Reaction equation for synthesis of **1a** and **1b**. (**B**) Reaction equation for the thermal reaction of **1a** and **1b** to yield $[(\equiv SiO)_3Ta]$. (**C**) Reaction equation for synthesis of $[(\equiv SiO)_2Ta(=NH)(NH_2)]$, **2**. (**D**) Reaction equation of $NH_2$ transfer from **2** to adjacent siloxy bridge.

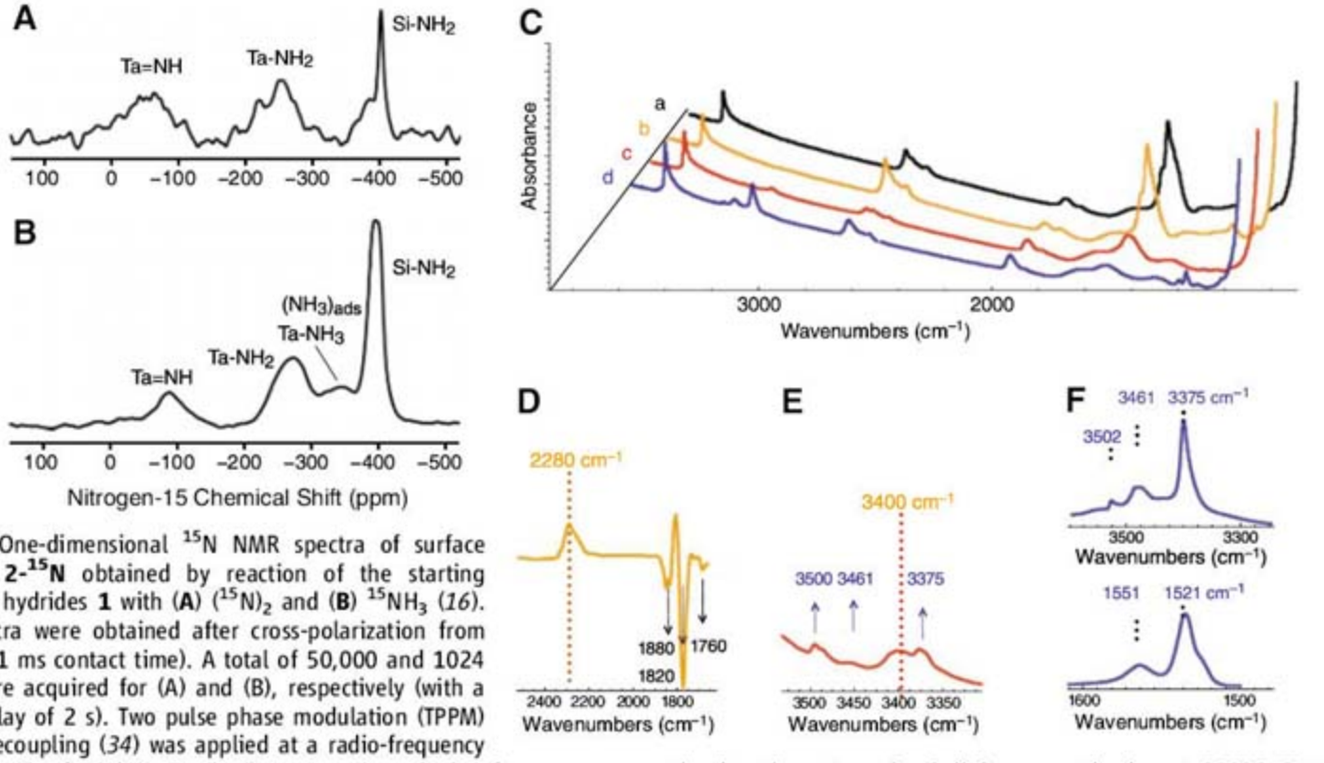


**Fig. 3.** One-dimensional $^{15}N$ NMR spectra of surface complex **2-$^{15}$N** obtained by reaction of the starting tantalum hydrides **1** with (**A**) $(^{15}N)_2$ and (**B**) $^{15}NH_3$ (*16*). The spectra were obtained after cross-polarization from protons (1 ms contact time). A total of 50,000 and 1024 scans were acquired for (A) and (B), respectively (with a recyle delay of 2 s). Two pulse phase modulation (TPPM) proton decoupling (*34*) was applied at a radio-frequency field strength of 80 kHz. For both spectra, the spinning frequency was 12.5 kHz (*20*). Chemical shifts are given with respect to $CH_3NO_2$ at 0 ppm using $NH_4Cl$ as external reference. (**C**) IR spectra of: (a) starting hydrides [(≡SiO)$_2$TaH] and [(≡SiO)TaH$_3$] (**1**) (20mg, T = 15 wt %); (b) after addition of excess $N_2$ at room temperature; (c) After heating at 250°C for 1h; (d) After addition of $H_2$ (300 torr) and heating at 250°C (36 hours). (**D**) Enlarged portion difference spectrum [(*b*) − (*a*)] (2550 cm$^{-1}$ − 1700 cm$^{-1}$ region) showing the net result of dinitrogen addition at room temperature. Dotted line, ν(TaN$_2$) of intermediate species at 2280 cm$^{-1}$; dotted arrows, decreasing ν(TaH$_x$) of starting complexes **1**. (**E**) Enlarged portion of the difference spectrum [(c) − (a)] (3600 cm$^{-1}$ − 3300 cm$^{-1}$ region) showing the net result of dinitrogen activation at 250°C. Dotted line, ν(TaN$_2$H$_x$) of intermediate species at 3400 cm$^{-1}$; dotted arrows, increasing ν(TaNH$_x$) of final product **2** observed in spectrum (d) (*20*). (**F**) Zoom in to the ν(NH$_x$) (above) and δ(NH$_x$) (below) spectral regions of spectrum (*d*) (3650 to 3250 and 1600 to 1500 cm$^{-1}$, respectively). Resulting assignments, after isotopic labeling studies (fig. S6) cm$^{-1}$: ν(NH): 3502, 3461, 3375 [ν($^{15}$NH): 3494, 3448, 3370; ν(ND): 2581, 2525, 2473]; δ(SiNH$_2$): 1551 [δ(Si$^{15}$NH$_2$): 1546]; δ(TaNH$_2$): 1521 [δ(Ta$^{15}$NH$_2$): 1516]. The deformation bands δ(SiND$_2$) and δ(TaND$_2$) (not observed) are expected to be obscured by silica absorption region (calculated deformation at 1131 and 1110 cm$^{-1}$) (*20*).

occurs (Fig. 2B). The final nitrogen content of the sample is 1.34 weight percent (wt %), N/Ta = 1.1 ± 0.8, as measured by elemental analysis, indicating the coexistence of [(≡SiO)$_3$Ta$^{III}$] and [(≡SiO)$_2$Ta(=NH)(NH$_2$)], **2**, in about a 1:1 ratio (*18*). In analogy with the hydrido transfer from Ta to Si (Fig. 2B), the imido amido species [(≡SiO)$_2$Ta(=NH)(NH$_2$)] (**2**) can transfer an amido ligand to neighboring siloxy bridges [≡Si-O-Si≡] to yield a surface silylamido moiety [≡Si-NH$_2$] and [(≡SiO)$_3$Ta(NH)] (Fig. 2D). Accordingly, under the condition of Fig. 2C, surface silylamido species [≡Si-NH$_2$] are also formed {0.25 (≡Si-NH$_2$) equivalents form for each [(≡SiO)$_2$Ta(=NH)(NH$_2$)], as determined by infrared spectral analysis}.

The structure of the surface complex **2** and [≡Si-NH$_2$] coproduct have been fully determined by solid-state nuclear magnetic resonance (NMR) spectroscopy, extended x-ray absorption fine structure (EXAFS) analyses, and infrared (IR) spectroscopy coupled with extensive isotopic labeling studies. Despite the low content of active sites on the surface, solid-state NMR spectroscopy under magic angle spinning (MAS) proved to be particularly powerful to characterize complex **2**. Specifically, we applied one-dimensional (1D) proton and nitrogen-15 NMR, 2D $^1$H-$^{15}$N heteronuclear correlated (HETCOR), and 2D proton double quantum (DQ) MAS NMR techniques to a fully labeled $^{15}$N sample, **2-$^{15}$N**, obtained by reaction of $^{15}N_2$ with tantalum hydrides **1**. Through the HETCOR data (which yield correlations between spatially close $^1$H and $^{15}$N spins), the DQ data [which yield correlations between pairs of dipolar coupled (i.e., spatially close) protons, thus discriminating between amido and imido resonances (*16*)], and the comparison of these data with the corresponding data recorded on the product obtained directly by reaction of $^{15}$N-

**Table 1.** $^1$H and $^{15}$N NMR chemical shifts of [(≡SiO)$_2$Ta(=NH)(NH$_2$)], **2** and **2·NH$_3$**. All $^{15}$N chemical shifts are referenced with respect to $CH_3NO_2$ at 0 ppm (*20*). In the "Assignments" columns, the atom to which the resonance is assigned is in bold and italics.

| Complex | $^{15}$N NMR, δ (ppm) | | $^1$H NMR, δ (ppm) | |
|---|---|---|---|---|
| | Resonances | Assignments | Resonances | Assignments |
| [(≡SiO)$_2$Ta(=$^{15}$NH)($^{15}$NH$_2$)], **2-$^{15}$N*** | −70‡ | Ta=***N***H | 11.0–9.0 | Ta=N***H*** |
| | −260–230‡ | Ta–***N***H$_2$ | 4.5 | Ta–N***H$_2$*** |
| | −400 ‡ | Si–***N***H$_2$ | 0.0 | Si–N***H$_2$*** |
| [(≡SiO)$_2$Ta(=$^{15}$NH)($^{15}$NH$_2$)($^{15}$NH$_3$)], **(2-$^{15}$N)•$^{15}$NH$_3$†** | −70‡ | Ta=***N***H | 9.0–8.6 | Ta=N***H*** |
| | −260‡ | Ta–***N***H$_2$ | 4.0 | Ta–N***H$_2$*** |
| | −340 | Ta(***N***H$_3$) | 2.4 | Ta(N***H$_3$***) |
| | −400 | Si–***N***H$_2$ | 0.1 | Si–N***H$_2$*** |
| | −385§ | physisorbed ***N***H$_3$ | 2.4 | physisorbed N***H$_3$*** |

*Obtained from reaction of **1** with $^{15}N_2$. band that disappears on vacuum treatment. †Obtained from reaction of **1** with $^{15}NH_3$ (*16*). ‡Broad signal. §Only

ammonia (*16*), we have been able to observe and unequivocally assign the imido, amido, and silylamido resonances (Fig. 3, figs. S1 to S3, and Table 1) (*19*, *20*). Our assignments are in good agreement with available solution $^{1}$H- and $^{15}$N-NMR data reported for analogous imido and amido molecular species (*16*).

An EXAFS study of surface species $[(\equiv SiO)_2Ta(=NH)(NH_2)]$ (**2**) yielded spectra in good agreement with the proposed structure (fig. S4) (*20*). Namely, the best-fit structure was obtained with a model in which isolated tantalum atoms bond to one nitrogen atom at a distance of 1.81(2) Å, two oxygen atoms at 1.93(1) Å, and one nitrogen atom at 2.04(1) Å [Debye-Waller factors $\sigma^2$ = 0.0025(10), 0.0007(5), and 0.0007 (constrained) Å$^2$, respectively; fit residue: $\rho$ = 5.5%; k1 weighting has minimal impact on the results of the fit], yielding measured distances in good agreement with literature data for similar Ta(V) imido and amido molecular species (*21*). No improvements in the fit were obtained by taking into account the coexistence of **2** with $[(\equiv SiO)_3Ta^{III}]$. Second-shell data, which were tentatively added to improve the fit, are compatible with vicinal $SiNH_2$, but extra parameters decreased the quality factor. Given the known capacity of bimetallic systems (*22*–*25*), including ditantalum hydrides (*24*, *25*), to activate dinitrogen, we explored possible Ta···Ta contacts in the EXAFS study. No significant Ta-Ta path contribution to the EXAFS could be found.

The reaction of **1** with dinitrogen was also studied by in situ infrared absorption spectroscopy (Fig. 3). As expected, reaction of the tantalum hydrides mixture $[(\equiv SiO)_2Ta\text{-}H]$ and $[(\equiv SiO)_2TaH_3]$ (**1**) with $N_2/H_2$ under the conditions described above led to the disappearance of the starting hydride stretching bands [$\nu(TaH_x)$ centered at 1830 cm$^{-1}$] and to the appearance of new vibration and deformation bands of $NH_x$ groups in $[(\equiv SiO)_2Ta(=NH)(NH_2)]$ (**2**) (*16*). Upon reaction of **1** with $^{15}N_2$ and $H_2$, as well as $^{14}N_2$ and $D_2$, all expected isotopic frequency shifts ($^{14}N/^{15}N$ and H/D) for **2-$^{15}$N** and **2-d** were observed (fig. S6) (*16*). Surface silylamido moieties, $[\equiv Si\text{-}NH_2]$, are also formed, with diagnostic $\delta(SiNH_2)$ bands observed at 1550 cm$^{-1}$ (*16*). No evidence for either coordinated or physisorbed ammonia was observed in IR and NMR spectra.

Density functional theory (DFT) periodic calculations using Vienna ab initio simulation package (VASP) (*26*, *27*) were performed to add additional support to our structural assignments of $[(\equiv SiO)_2Ta(NH)(NH_2)]$ and its posited stability. The structure of model $[(\equiv SiO)_2Ta(NH)(NH_2)]$, supported on cristobalite (100) surface, $\mathbf{2_q}$, was optimized (fig. S5), and selected IR frequencies and NMR chemical shifts calculated [yielding noncorrected calculated IR frequencies of 3602 cm$^{-1}$ ($\nu_{NH}$), 3546 and 3418 ($\nu_{NH2}$), and 1502 cm$^{-1}$ ($\delta_{NH2}$), and calculated $^{15}$N-NMR chemical shifts of –71 parts per million (ppm) and –268 ppm for NH and $NH_2$, respectively (*20*), in close agreement with the experimental values]. The coordination geometry of Ta in $\mathbf{2_q}$ is calculated to be pseudotetrahedral, with L-M-L angles ranging from 101.1° to 112.2° and M-L bond lengths in good agreement with the EXAFS spectrum (*20*), and similar distances reported for molecular Ta-O(Si), Ta-N(R), and Ta-N($R_2$) species (*21*). Notably, the imido (NH) and amido ($NH_2$) ligands in $\mathbf{2_q}$ are coplanar, facilitating maximal orbital overlap between the metal *d* orbitals and the ligands, as already discussed for the isolobal silica-supported $d^0$ metal species $Re(\equiv C^tBu)(=CH^tBu)(CH_2{}^tBu)(OSi\equiv)$ and $Mo/W(=NR)(=CH^tBu)(CH_2{}^tBu)(OSi\equiv)$ (R = Me, Ph) (*28*).

Thermodynamically, formation of $\mathbf{2_q}$ from reaction of $N_2$ with either the tantalum monohydride $[(\equiv SiO)_2TaH]$ (**1a**) or tantalum trihydride $[(\equiv SiO)_2TaH_3]$ (**1b**) supported on the same cristobalite (100) surface is highly exothermic (–125.4 and –80.9 kcal mol$^{-1}$, respectively) (fig. S5B). This result substantiates the mechanistic feasibility of the reaction in Fig. 2C proceeding through irreversible cleavage of the N≡N triple bond on isolated Ta atoms.

The capacity of isolated Ta atoms in **1** to fully cleave the N≡N bond is original in the context of surface science: The dissociative chemisorption of dinitrogen on metallic surfaces, which is the rate-determining step in ammonia synthesis (*8*, *9*), is assumed to occur on a two-site (or higher) ensemble of surface atoms, with the surface acting as an electron reservoir. In contrast, the alternative associative pathway—a single-site metallic activation to induce full N-N cleavage through reduction to an amido imido species (*1*)—was not considered efficient based on IR and microkinetic data.

The reactivity of **1** toward dinitrogen is also distinct from previous observations in homogeneous molecular systems. The dinuclear Zr molecule $[(\eta^5\text{-}C_5Me_4H)_2Zr]_2(\mu_2, \eta^2, \eta^2\text{-}N_2)$ relies on two metal centers for dinitrogen cleavage with dihydrogen (*23*). The two-molecule system *cis*-$[W(N_2)_2(PMe_2Ph)_4]$ / $[RuCl(\eta^2\text{-}H_2)(dppp)_2]PF_6$ (dppp = 1,3-bis(diphenylphosphino)propane) is the only other organometallic system capable of reducing coordinated dinitrogen with dihydrogen, presumably by Ru-mediated heterolytic H-H cleavage (*29*). More generally, when reduction systems other than dihydrogen are also taken into consideration, multimetallic cooperation remains the general rule for $N_2$ activation by inorganic (*30*) or organometallic complexes (*22*–*25*).

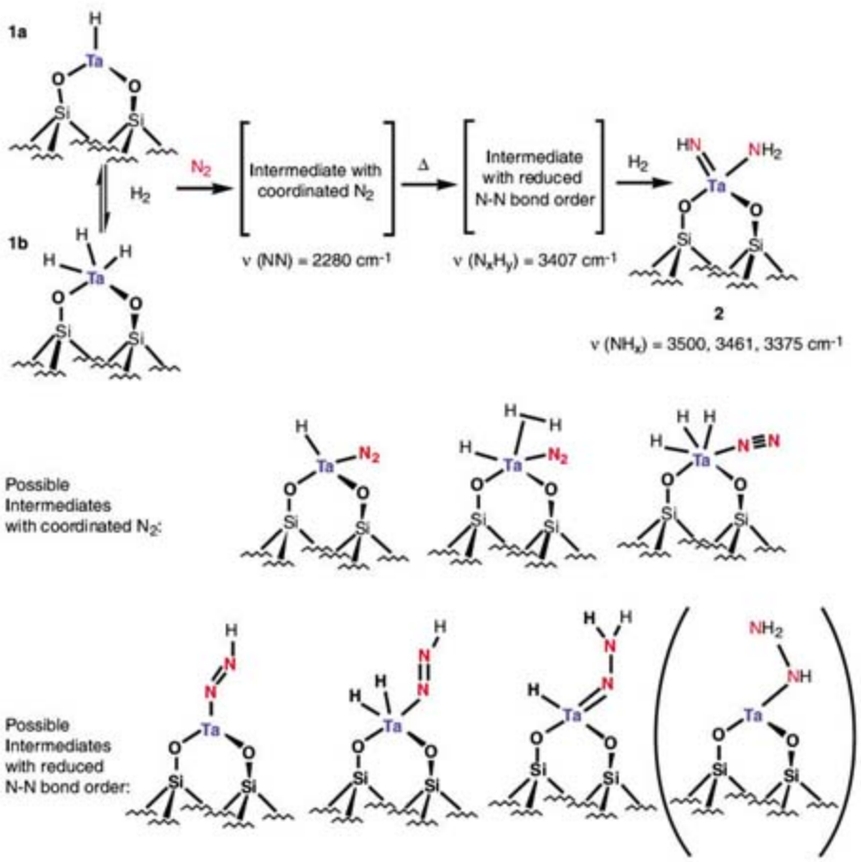


**Fig. 4.** Final product, **2**, and IR evidence for reaction intermediates observed by in situ IR monitoring of the dinitrogen activation on isolated tantalum hydrides on silica surface **1a** and **1b** (pertinent stretching frequencies reported below) and proposed possible structures for intermediates. Not all the dinitrogen adducts are expected to be IR-active. The hydrazido intermediate is in bracket because independent experiments have shown that it can be involved in the formation of **2** but cannot be observed under our reaction condition (*32*).

Likewise, biochemical systems are believed to require as many as 20 metals—the number of unique metals in FeMo cofactor, P cluster, and Fe protein of nitrogenases—to achieve dinitrogen reduction to ammonia (*4*).

The only exception to multimetallic cooperation for dinitrogen cleavage is the aforementioned Mo(III) organometallic complex (*4*). The single-molybdenum center prevents dimerization side reactions, presumably through the strong steric protection afforded by the hexaisopropylmetaterphenyl triamidoamine ligand around the $Mo^{III}$ atom (Fig. 1). Likewise, our surface organometallic approach yields isolated $Ta^{III/V}$ centers protected against bimetallic decomposition by the strong and inert siloxy bonds to the rigid silica surface. Furthermore, the characteristic chemistry displayed by **1a** and **1b** toward dinitrogen is likely due to the capacity of surface organometallic chemistry to synthesize highly uncoordinated, electronically unsaturated, highly thermally stable, isolated metal atoms. No solution or surface molecular system has so far achieved all these properties simultaneously (i.e., well-defined isolated $Ta^{III/V}$ atoms, three or five coordinate, stable up to 250°C), which probably contributes to the capacity reported here of cleaving the N≡N bond on an isolated metal atom with dihydrogen [rather than with the judicious alternate additions of protons and electron sources in solution applied in the Schrock system (*4*)].

This unusual reactivity raises challenging mechanistic questions. To gain further insight into the possible elementary steps involved in the synthesis of **2** (Fig. 2C), we attempted in situ monitoring of the reaction by IR spectroscopy: A fraction of the tantalum hydrides appeared very reactive, enabling observation of several intermediate species when starting the reaction at room temperature (Fig. 3D).

When exposed to a hydrogen-free $N_2$ atmosphere at room temperature, a fraction of the tantalum sites coordinated dinitrogen reversibly with concomitant elimination of dihydrogen (0.3 $H_2$/Ta) and appearance of a $Ta(N_2)$ stretching band in the IR spectrum at $\nu(TaN_2)$ = 2280 $cm^{-1}$ (Fig. 3D). The high wave number supports an end-on coordination motif of $N_2$ on tantalum (*31*). The band disappears on vacuum treatment. When $^{15}N_2$ is used, the band shifts to $\nu(Ta^{15}N_2)$ = 2197 $cm^{-1}$, in agreement with expectations using the harmonic oscillator approximation (fig. S6).

On heating the sample to 250°C the $\nu[Ta(\eta^1\text{-}N_2)]$ band disappears, accompanied by further decrease of the ν(TaH), and a new band appears in the ν(NH) region [$\nu(TaN_xH_y)$ = 3400 $cm^{-1}$], along with traces of final product **2** (Fig. 3E). No further evolution is observed unless dihydrogen is added to the reaction vessel. Addition of dihydrogen led to the complete formation of final product **2** (Fig. 3F); no further intermediary reduction products could be observed (*32*).

This IR spectral evidence is consistent with the formation of dinitrogen, diazenido and/or hydrazido metal complexes (Fig. 4) (*32*), which are the expected intermediates of dinitrogen activation by organometallic compounds, as described by the Chatt (*33*) and Schrock (*4*) cycles (Fig. 1C), with the notable peculiarity that the reaction does not require the alternate addition of protons and electrons to a dinitrogen adduct. In our case, we have the direct involvement of dihydrogen. It is presently unclear whether the reaction proceeds by, for example, Ta-promoted heterolytic H-H cleavage on a Ta dinitrogen adduct in some analogy with literature precedents (*29*), or by unprecedented $N_2$ insertion in a Ta-H bond. The Chatt cycle relies on a distal $N_2$ reduction mechanism (also known as the d-mechanism) in which the reduction of the nitrogen atoms occurs sequentially, involving first only the β-nitrogen of $M(N_2)$, and thereby leading to dianionic hydrazido intermediates, $M(=N\text{-}NH_2)$ (*4*, *33*). In contrast, the reactivity of the isolated surface tantalum hydrides **1** with $N_2/H_2$ is consistent with an alternating $N_2$ reduction mechanism, involving both nitrogen atoms of $M(N_2)$ and proceeding through a monoanionic hydrazido intermediates, $M(\text{-}NH\text{-}NH_2)$. Recent evidence has implicated such an alternating, rather than distal, $N_2$ reduction mechanism for nitrogenase (*6*, *10*).

## References and Notes


1. A. Nielsen, Ed. *Ammonia: Catalysis and Manufacture* (Springer Verlag, Berlin, 1995).
2. Nitrogen Fixation Special Issue, *Proc. Natl. Acad. Sci. U.S.A.* **103** (2006).
3. R. R. Schrock, *Proc. Natl. Acad. Sci. U.S.A.* **103**, 17087 (2006).
4. D. V. Yandulov, R. R. Schrock, *Science* **301**, 76 (2003).
5. J. B. Howard, D. C. Rees, *Proc. Natl. Acad. Sci. U.S.A.* **103**, 17088 (2006).
6. B. Hinnemann, J. K. Nørskov, *Top. Catal.* **37**, 55 (2006).
7. O. Einsle *et al.*, *Science* **297**, 1696 (2002).
8. K. Honkala *et al.*, *Science* **307**, 555 (2005).
9. R. Imbihl, R. J. Behm, G. Ertl, W. Moritz, *Surf. Sci.* **123**, 129 (1982).
10. B. M. Barney *et al.*, *Proc. Natl. Acad. Sci. U.S.A.* **103**, 17113 (2006).
11. V. Dufaud, G. P. Niccolai, J. Thivolle-Cazat, J.-M. Basset, *J. Am. Chem. Soc.* **117**, 4288 (1995).
12. S. Soignier *et al.*, *Organometallics* **25**, 1569 (2006).
13. C. Copéret, M. Chabanas, R. Petroff Saint-Arroman, J.-M. Basset, *Angew. Chem. Int. Ed.* **42**, 156 (2003).
14. D. Soulivong *et al.*, *Angew. Chem. Int. Ed.* **43**, 5366 (2004).
15. V. Vidal, A. Théolier, J. Thivolle-Cazat, J.-M. Basset, *Science* **276**, 99 (1997).
16. P. F. Avenier *et al.*, *J. Am. Chem. Soc.* **129**, 176 (2007).
17. G. Saggio *et al.*, *Organometallics* **21**, 5167 (2002).
18. Diagnostic features such as [ν(SiH) versus $\nu(NH_2)$] in IR spectra and [δ(SiH) versus $\delta(NH_2)$] in $^1$H-NMR spectra of the final solid allow extrapolation of the relative $[(\equiv SiO)_2Ta(=NH)(NH_2)]$: $[(\equiv SiO)_3Ta^{III}]$ ratio and agree with this estimate. Furthermore, control experiments performed on $[(\equiv SiO)_2TaH]$ and $[(\equiv SiO)_2TaH_3]$ under the same conditions as Fig. 2C, but with dinitrogen replaced by helium, showed the conversion of ~50% of the surface tantalum hydrides to $[(\equiv SiO)_3Ta^{III}]$, in agreement with the estimate. Independent experiments have shown that $[(\equiv SiO)_3Ta^{III}]$ does not react with dinitrogen under the conditions of Fig. 2C.
19. Spin-diffusion experiments supported attribution of the peak broadening observed for **2**-$^{35}$**N** to surface heterogeneity and not to Ta-anisotropy effects, consistent with the already established surface heterogeneity of the starting hydrides $[(\equiv SiO)_2TaH]$ and $[(\equiv SiO)_2TaH_3]$ (**1**) (*12*) and of **2**-$^{15}$**N** formed by reaction of **1** with $^{15}NH_3$ (*16*). Furthermore, the reaction in Fig. 3D accounts for the further increase of surface heterogeneity.
20. Materials and methods and additional data are available as supporting material on *Science* Online.
21. The Cambridge Structural Database, F. H. Allen, *Acta Crystallogr.* **B58**, 380 (2002).
22. S. Gambarotta, J. Scott, *Angew. Chem. Int. Ed.* **43**, 5298 (2004).
23. J. A. Pool, E. Lobkovsky, P. J. Chirik, *Nature* **427**, 527 (2004).
24. M. D. Fryzuk *et al.*, *J. Am. Chem. Soc.* **123**, 3960 (2001).
25. M. D. Fryzuk, B. A. MacKay, B. O. Patrick, *J. Am. Chem. Soc.* **125**, 3234 (2003).
26. G. Kresse, J. Furthmüller, *Phys. Rev. B* **54**, 11169 (1996).
27. G. Kresse, J. Furthmüller, *Comput. Mater. Sci.* **6**, 15 (1996).
28. X. Solans-Monfort, E. Clot, C. Copéret, O. Eisenstein, *Organometallics* **24**, 1586 (2005).
29. Y. Nishibayashi, S. Iwari, M. Hidai, *Science* **279**, 540 (1998).
30. T. A. Bazhenova, A. E. Shilov, *Coord. Chem. Rev.* **144**, 69 (1995).
31. Other $N_2$ coordination motifs to the tantalum center of **1a** and **1b** are possible, some of which are expected to show no IR absorption or have such absorption obscured by the opaque region of the silica support under study (*32*).
32. We have independently assessed that (i) the hydrazido complex $[(\equiv SiO)_2TaH_x(NH\text{-}NH_2)]$ can be an intermediate in the synthesis of **2** and (ii) if formed, it cannot be detected under our experimental conditions because it leads directly to the final product **2**. We have exposed starting hydrides **1** directly to hydrazine, $N_2H_4$ (10 torr, five-fold excess with respect to tantalum, 80°C) and observed the direct formation of **2** (*20*). Under the assumption that the primary reaction product between hydrazine and **1** is due to N-H activation by tantalum-hydrides, thus leading to the transient hydrazido complex, this result shows that a single-metal hydrazido complex of type $[(\equiv SiO)_2Ta(N_2H_3)H_x]$ leads directly to **2**. The IR spectroscopic evidence presented in the text for the formation of intermediates with reduced N-N bond order upon heating the dinitrogen adducts is thus most compatible with the formation of a diazenido complex, $[(\equiv SiO)_2TaH_x(N_2H)]$ and/or a dianionic dihydrazido complex, $[(\equiv SiO)_2TaH_x(NNH_2)]$.
33. J. Chatt, J. R. Dilworth, R. L. Richards, *Chem. Rev.* **78**, 589 (1978).
34. A. E. Bennett, C. M. Rienstra, M. Auger, K. V. Lakshmi, R. G. Griffin, *J. Chem. Phys.* **103**, 6951 (1995).


35. Some of the solid-state NMR spectra were recorded at the Rhone-Alpes European Large Scale Facility for NMR. Centre Informatique National de l'Enseignement Supérieur (CINES) and Institut du Développement et des Ressources en Informatique Scientifique (IDRIS) French national computing centers are thanked for generous donation of computing time. We are grateful to S. Fiddy of Council for the Central Laboratory of the Research Councils (CCLRC) Daresbury Laboratory for help in the EXAFS studies. The Centre National pour la Recherche Scientifique (CNRS) and Ecole Supérieure de Chimie Physique Electronique de Lyon (ESCPE-Lyon) are gratefully acknowledged for funding, the French Ministère délegué à la recherche for a Ph.D. fellowship to P.A., and CNRS for an associate research position to X.S.M.


## Supporting Online Material

www.sciencemag.org/cgi/content/full/317/5841/1056/DC1

Materials and Methods
Figs. S1 to S6
References

27 March 2007; accepted 13 July 2007
10.1126/science.1143078

# Breakdown of the Born-Oppenheimer Approximation in the F + *o*-$D_2$ → DF + D Reaction

Li Che,[1*] Zefeng Ren,[1*] Xingan Wang,[1] Wenrui Dong,[1] Dongxu Dai,[1] Xiuyan Wang,[1] Dong H. Zhang,[1] Xueming Yang,[1†] Liusi Sheng,[2] Guoliang Li,[3] Hans-Joachim Werner,[3†] François Lique,[4] Millard H. Alexander[4†]

The reaction of F with $H_2$ and its isotopomers is the paradigm for an exothermic triatomic abstraction reaction. In a crossed-beam scattering experiment, we determined relative integral and differential cross sections for reaction of the ground F($^2P_{3/2}$) and excited F*($^2P_{1/2}$) spin-orbit states with $D_2$ for collision energies of 0.25 to 1.2 kilocalorie/mole. At the lowest collision energy, F* is ~1.6 times more reactive than F, although reaction of F* is forbidden within the Born-Oppenheimer (BO) approximation. As the collision energy increases, the BO-allowed reaction rapidly dominates. We found excellent agreement between multistate, quantum reactive scattering calculations and both the measured energy dependence of the F*/F reactivity ratio and the differential cross sections. This agreement confirms the fundamental understanding of the factors controlling electronic nonadiabaticity in abstraction reactions.

The Born-Oppenheimer (BO) approximation is invaluable in the application of quantum mechanics to molecular spectroscopy and molecular reaction dynamics. This approximation (*1*) postulates that electrons adapt adiabatically to the motion of the much heaver nuclei, so that the forces on the nuclei are generated by the variation with geometry of the electronic energy of a single electronic state. The BO approximation allows us to model molecular dynamics as the motion of multiple nuclei on a single electronic potential energy surface (PES).

Despite its great success, the BO approximation breaks down whenever two (or more) electronic states become degenerate (or nearly so). This breakdown is responsible for fundamental molecular phenomena such as predissociation or internal conversion in an isolated molecule (*2*, 3) and is ultimately crucial in more complex chemical processes.

In most bimolecular reactions involving an open-shell reactant, two (or more) electronic states are degenerate at large separations. As the reaction proceeds, the degeneracy is lifted. Often, not all the PESs correlate with the lowest electronic state of the products (*4*, *5*). In the F or F* (F/F*) + $H_2$ reaction under investigation, the BO approximation prohibits the reaction of the excited F-atom spin-orbit state (*6*, *7*) (Fig. 1). The extent to which reaction flux can move from one PES to another during the reaction is largely unknown.

Interest in the reactivity of spin-orbit excited F atom with $H_2$, induced by the breakdown of the BO approximation, dates back 30 years (*8*). Earlier experimental studies of the F + $H_2$ (*9*) and F + $D_2$ (*10*, *11*) reactions showed no concrete evidence of F* reactivity. Nesbitt and co-workers (*12*, *13*) did find such evidence by looking at the production of HF ($v = 3$) in rotational levels that are energetically inaccessible by reaction of ground spin-orbit state F atoms. Concurrently, in a crossed-beams study of the F/F* + HD reaction, Liu and co-workers also found experimental evidence of the HF ($v = 3$) product from the F* reaction at threshold collision energies (*14*). The great experimental difficulty in evaluating the relative F* reactivity is the separation of HF products produced by the reaction of F*.

Despite the importance of F* reactivity, the majority of prior theoretical work on the F + $H_2$ (HD, $D_2$) reaction has been limited to calculations on the lowest, electronically adiabatic PES. Building on earlier work (*15*–*17*), Alexander, Manolopoulos, and Werner (*7*) presented an exact framework for the fully quantum-mechanical study of this reaction with inclusion of all three PESs shown in Fig. 1, as well as spin-orbit and Coriolis coupling. Alexander and co-workers have shown that, as the collision energy decreases, the BO-allowed reaction of F becomes suppressed by the small reaction barrier (Fig. 1) more rapidly than the reaction of F*. Thus, at low energy the BO-forbidden reaction becomes increasingly important because of the additional internal energy available in the spin-orbit excited state (1.2 kcal/mol) (*7*, *18*).

In an effort to determine the extent of the breakdown of the BO approximation in this benchmark system and to test fully our ability to measure, and predict, the degree of reactivity of the spin-orbit excited F atoms, we report here a high-resolution crossed molecular beam study on the F/F* + *ortho*-$D_2$ reaction using the D-atom Rydberg tagging method (*19*). We concentrated on very low collision energies ($0.2 \leq E_c \leq 1.2$ kcal/mol), where nonadiabatic effects are expected to be most pronounced. The choice of $D_2$, rather than $H_2$ or HD, was made for several reasons: The absence of D atom background allows a higher detection signal-to-noise ratio, and the smaller rotational constant of DF (compared with HF) allows a cleaner separation of the DF ($v'$) products from the reaction of F compared with F*. In addition, because of the absence of a transition state resonance (*20*) in the F + $D_2$ reaction at low collision energy, the investigation and the comparison with theory can focus solely on the relative reactivity of the two F atom spin-orbit states, without any additional complexity introduced by the resonance.

In the experiments (*21*–*24*), the F atom beam was generated by expanding a mixture of 50% $NF_3$/2.5% $F_2$/47.5% He through a two-

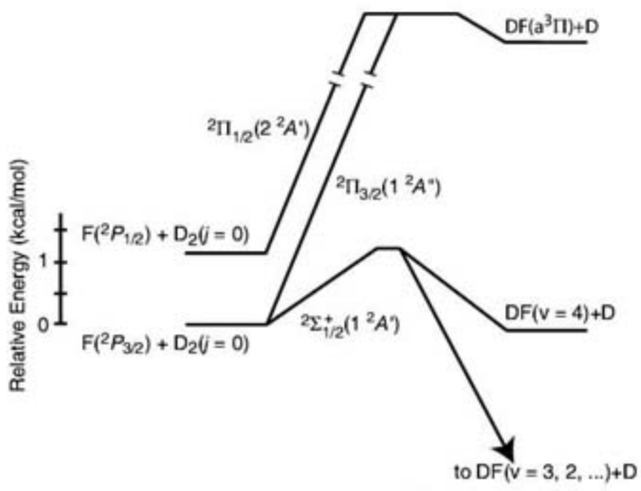


**Fig. 1.** Relative energies (to scale) for the F/F* + $D_2$ reaction, after inclusion of the spin-orbit splitting, with a schematic representation of the three $FH_2$ electronically adiabatic PESs, labeled for both collinear and coplanar geometry. The vibrational zero-point energy (for reactants and products and at the barrier) has been included. Although the F($^2P_{3/2}$) + $D_2$ → DF ($v = 0$) + D reaction exothermicity is 31.80 kcal/mol, the DF ($v = 4$) + D channel is exoergic by only 0.088 kcal/mol. The potential energy surfaces for the two $\Pi$ states correlate, in the product arrangement, with DF($a^3\Pi$) + D, which lies at least 38 kcal/mol above the F($^2P_{3/2}$) + $D_2$ asymptote. Consequently, the position of this asymptote is not drawn to scale.

[1]State Key Laboratory of Molecular Reaction Dynamics, Dalian Institute of Chemical Physics, Chinese Academy of Sciences, Dalian, Liaoning 116023, People's Republic of (P. R.) China. [2]National Synchrotron Radiation Laboratory, University of Science and Technology of China, Hefei, Anhui 230029, P. R. China. [3]Institüt für Theoretische Chemie, Pfaffenwaldring 55, Universität Stuttgart, D-75069 Stuttgart, Germany. [4]Department of Chemistry and Biochemistry and Institute for Physical Sciences and Technology, University of Maryland, College Park, MD 20742–2021, USA.

*These authors contributed equally to this work.
†To whom correspondence should be addressed. E-mail: xmyang@dicp.ac.cn (X.Y.); werner@theochem.uni-stuttgart.de (H.-J.W.); mha@umd.edu (M.H.A.)

stage discharge. Single photon vacuum ultraviolet (VUV) absorption to two autoionizing states of the F atom (*25*) showed that the F:F* ratio in the discharge was 4.8 (fig. S1). Measurement of this ratio made it possible for us to extract the relative cross sections for the F and F* reactions with $D_2$.

The $o$-$D_2$ was made by passing $n$-$D_2$ gas through a column filled with an $o$-$p$ conversion catalyst cooled down to about 20 K. A neat $o$-$D_2$ sample was expanded through a pulsed nozzle cooled down to liquid nitrogen temperature, at which point >93% was cooled down to the lowest ($j = 0$) rotational state (*19*). By varying the crossing angle of the F and $o$-$D_2$ beams, we can vary the collision energy.

Time-of-flight (TOF) spectra of the D atom products from the F/F* + $o$-$D_2$ reaction (with an initial F:F* ratio of 4.8) were measured over a range of laboratory (LAB) angles varied in ~10° intervals. Fig. 2 shows two typical TOF spectra of the D atom product at $E_c$ values of 0.55 and 1.12 kcal/mol. The most pronounced structures in the TOF spectra can be clearly assigned to DF product rotational (ro)-vibrational states from the F + $D_2$ ($j = 0$) reaction. In addition, we also see features that can be assigned to reaction of F*. It is evident that the relative F* reactivity is more pronounced at the lower collision energy.

The spectra, which are proportional to the DF product intensity at various LAB scattering angles, were then converted to relative differential cross sections (DCSs) in the center-of-mass (CM) frame by means of a standard Jacobian transformation to obtain the product kinetic energy (KE) distributions. During the conversion, detection efficiencies of the D atom product at different LAB angles and different velocities were simulated and included. The KE distributions obtained experimentally in the LAB frame were simulated by adjusting the relative populations of the ro-vibrational states of the DF product. From these simulations, relative population distributions of the DF product at each ro-vibrational state were determined at all LAB angles measured.

Because the D + DF ($v = 4, j = 0$) products are nearly isoergic with F + $D_2$ ($v = 0, j = 0$) (see the caption to Fig. 1), complete separation is seen in the TOF spectra for reactions of F and F* that produce DF in $v = 4$, which is the highest energetically allowed product vibrational level. For DF products in lower vibrational levels, any overlap between the signals arising from the F and F* reactions will cause some uncertainty in the simulations. Fortunately, in most of the cases here, the rotational excitation of the DF product from both the F and F* reactions is limited mainly to the lowest few rotational states, and so the dominant peaks from the F and F* reactions are well separated. Therefore, we can obtain a decent fit by assuming that DF product rotational excitation from the excited state F* reaction is similar to or slightly hotter than that from the ground state F reaction.

We expect that the F* reaction should produce DF with slightly hotter rotational distributions (figs. S2 and S3) because, for a given collision energy, the total energy available to the DF products will be larger (*26*). We estimated that the error caused by assuming similar degrees of rotational excitation should be about 10% both in the relative integral cross sections (ICSs) for the F* reaction and in the ratio of the ICSs for reaction of F and F*. This estimate is comparable to our measurement error.

At all collision energies, quantum-state-resolved DCSs of the DF product in the CM frame ($\theta_{cm} = 0°$ to 180°) were then determined by fitting the above experimental results. Fig. 3 displays the topology of these DCSs at a $E_c$ = 0.48 kcal/mol and compares these with the results of the theoretical calculations, which are summarized in the following two paragraphs. Except for some small forward scattering in the theoretical simulations, which lies below the detection limit in our experiments, the overall agreement in the DCSs between experiment and theory is excellent, in terms of both scattering angle and DF product state and for reactions of both F and F*.

The theoretical simulations entailed time-independent, fully quantum, reactive scattering calculations based on the formalism we presented earlier (*7*, *27*). These calculations include explicitly all three PESs shown schematically in Fig. 1. The PESs used were fits to a new set of highly accurate ab initio calculations (*24*). To correct for residual errors, we scaled the correlation energy so that the calculated F + $H_2$ → HF + H exoergicity agreed with the currently accepted experimental value (*12*) to within the uncertainty in the latter. This overcomes the drawback (*18*) in the earlier set of PESs of Werner and co-workers (*6*, *7*), namely, the underprediction by ~0.7 kcal/mol of the F + $H_2$ reaction exoergicity. Although this error is much smaller than the typical accuracy of ab initio calculations of PESs, it is a large fraction of the F + $H_2$ ($D_2$) collision energy in the regime of low energies where one might expect to see the most noticeable evidence of nonadiabatic reaction dynamics.

The overall topology of the DCSs displayed in Fig. 3 is very similar for F and F* reactions. The F* reaction can occur only by means of a non-BO (nonadiabatic) transfer of incoming collision flux from the PES of the nonreactive excited state of $A'$ reflection symmetry (labeled $2A'$ in Fig. 1) to the PES of the ground (reactive) $1A'$ state. Flux transfer will occur most readily at geometries for which the F-atom spin-orbit splitting is equal to the energetic splitting between the PESs of the two states of $A'$ reflection symmetry (*7*, *28*, *29*).

This seam of geometries occurs well out in the F + $D_2$ reactant valley [see figure 2 of (*7*)]. After undergoing the nonadiabatic $2A' \rightarrow 1A'$ transfer, the initially nonreactive flux will be subject to the same forces that affect the ground state reactants, in particular over the barrier and out into the HF + H product arrangement. Because the product distributions are a manifesta-

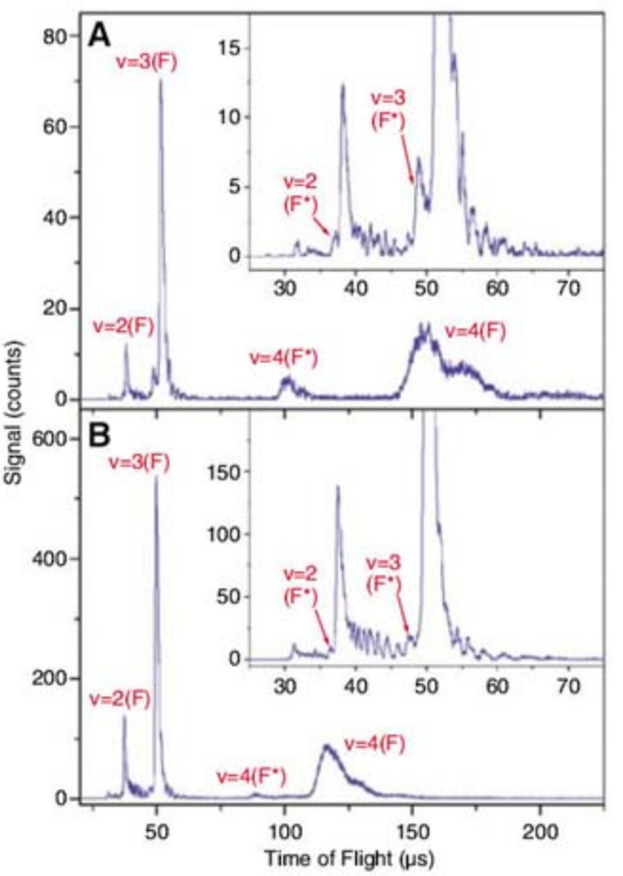


**Fig. 2.** TOF spectra of the D atom product from the F($^2P_{3/2}$)/F*($^2P_{1/2}$) + $D_2$ ($j = 0$) reaction at collision energies of (**A**) 0.55 kcal/mol at a laboratory angle of 110° and (**B**) 1.12 kcal/mol at a laboratory angle of 125°. These laboratory angles correspond roughly to D products scattered in the backward direction in the center-of-mass frame (relative to the incoming $D_2$ beam).

tion of these forces, we would anticipate the DF + D DCSs arising from reaction of F and F* to be quite similar, as observed here.

The largest F* versus F difference can be seen in the DF ($v$ = 4) products (Fig. 3). Because of the relative energetics (Fig. 1), for $E_c$ = 0.48 kcal/mol only the $j$ = 0 and $j$ = 1 DF rotational levels in $v$ = 4 are energetically accessible in the F + $D_2$ reaction. The $j$ = 0 products will emerge with a translational energy of only 0.004 kcal/mol. However, at the same collision energy, the first seven rotational levels in $v$ = 4 are energetically accessible for the F* reaction, and the $j$ = 0 products will emerge with a translational energy of 0.054 kcal/mol, substantially larger than that from the F reaction. It is for this reason that the DF ($v$ = 4) DCSs from F and F* show the largest dissimilarity.

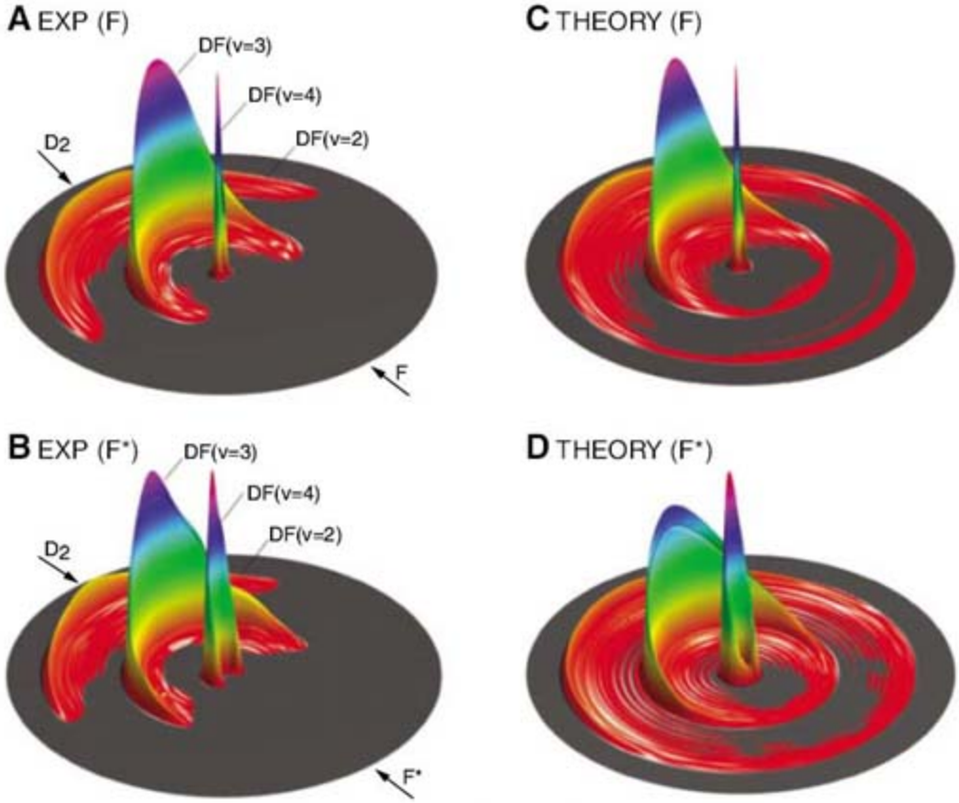


**Fig. 3.** Experimental (**A** and **B**) and theoretical (**C** and **D**) three-dimensional D-atom product flux surface plots for the F/F* + $D_2$ ($j$ = 0) reaction at $E_c$ = 0.48 kcal/mol. The concentric circles correspond to different HF product ro-vibrational states. The direction of the F atom beam defines the forward scattering direction.

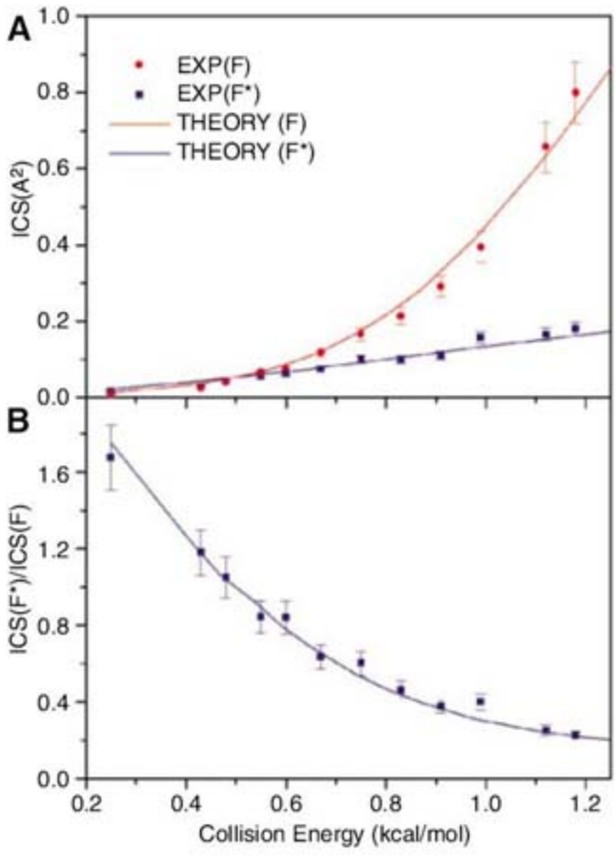


**Fig. 4.** (**A**) Collision energy dependence of the overall integral reactive cross sections, summed over product vibrational and rotational levels, for the F/F*+$D_2$($j$ =0) reactions for $0.25 \leq E_c \leq 1.2$ kcal/mol. (**B**) The ratio of the cross sections shown in (A). The solid curves are the results of our theoretical calculations, whereas the points indicate the experimental results. The error bars indicate the range of measurement errors in the experiment.

To assess the relative reactivity of the F and F* reactions, we determined the dependence on collision energy of the ICSs. These are the integrals of the corresponding DCSs over all scattering angles and so are a measure of the total reactivity at a particular $E_c$. To carry out this integration over scattering angle, we have chosen a set of laboratory angles that corresponds to the backward scattering direction for DF ($v$ = 3) product at a particular collision energy. We then measured TOF spectra at these lab angles and corresponding collision energies back and forward more than 10 times to put the ICS measurements at different collision energies on the same scale, such that the relative ICS could be determined experimentally by just integrating over all scattered products. Fig. 4A shows the experimentally determined ICSs for the F and F* reactions in the collision energy range between 0.25 and 1.2 kcal/mol. Over the entire set of collision energies, the experimental ICSs are scaled to the theoretical values by means of a single scaling factor for both the F and F* reactions.

The barrier on the lowest PES (Fig. 1), corrected for zero-point energy, is ~1.2 kcal/mol. Thus, we see that, over almost the entire range of collision energies investigated here, the F + $D_2$ reaction proceeds solely by quantum mechanical tunneling of the D atom.

In Fig. 4A, the reactive cross section for the BO-allowed F atom reaction increases much more rapidly with increasing $E_c$ than that for the BO forbidden reaction of F*, which was the qualitative prediction of our earlier calculations (*7*, *18*). The energy dependence of the ratio of the ICSs for the F and F* reactions is shown in Fig. 4B. The agreement with the predictions of the present scattering calculations based on the new PESs is remarkable. At the lowest $E_c$ studied here, ~0.25 kcal/mol, both experiment and theoretical calculations show that F* is ~1.6 times more reactive than F.

The excellent overall agreement between experiment and the results of quantum reactive scattering calculations on a new set of ab initio PESs (*24*) indicates that the theoretical formulation and simulations correctly include the essential physics governing the nonadiabatic processes of importance in the F + $H_2$ reaction and its isotopomers. Of particular interest would be the use of our new set of PESs to investigate the F + HD reaction, for which the HF + D

channel displays a pronounced transition-state resonance at $E_c = \sim 0.6$ kcal/mol (*20*, *23*). Liu and co-workers (*14*, *30*) have investigated the F/F* + HD reaction in some detail but primarily at energies considerably above the resonance. Studies on an earlier set of PESs show that the resonance is absent in the F* + HD channel (*18*), so that the influence of the resonance should be seen in the energy dependence of the F*/F ratio.

Ultimately, we hope that one will reach a similarly good degree of agreement between experiment and theory in the investigation of nonadiabaticity in abstraction reactions of F with polyatomic targets, such as $H_2O$ (*31*) or $CD_4$ (*32*).

Our conclusion that at low collision energy the F* reactivity becomes increasingly more efficient, relative to the BO-allowed F reaction of the ground spin-orbit state, agrees well with theoretical simulations of similar sophistication for the homologous Cl/Cl* + $H_2$ reaction (*33*, *34*) but contrasts with prior experimental work (*35*, *36*). Future theoretical and experimental study of the Cl + $H_2$ reaction is necessary to reach a level of agreement similar to what we have reported here for the F + $D_2$ reaction.

### References and Notes


1. M. Born, J. R. Oppenheimer, *Ann. Phys.* **84**, 457 (1927).
2. M. S. Child, *Molecular Collision Theory* (Academic, New York, ed. 2, 1974).
3. L. J. Butler, *Annu. Rev. Phys. Chem.* **49**, 125 (1998).
4. K. E. Shuler, *J. Chem. Phys.* **21**, 624 (1953).
5. R. J. Donovan, D. Husain, *Chem. Rev.* **70**, 489 (1970).
6. K. Stark, H.-J. Werner, *J. Chem. Phys.* **104**, 6515 (1996).
7. M. H. Alexander, D. E. Manolopoulos, H. J. Werner, *J. Chem. Phys.* **113**, 11084 (2000).
8. J. C. Tully, *J. Chem. Phys.* **60**, 3042 (1974).
9. D. M. Neumark, A. M. Wodtke, G. N. Robinson, C. C. Hayden, Y. T. Lee, *J. Chem. Phys.* **82**, 3045 (1985).
10. D. M. Neumark *et al.*, *J. Chem. Phys.* **82**, 3067 (1985).
11. M. Faubel, B. Martinez-Haya, L. Y. Rusin, U. Tappe, J. P. Toennies, *J. Phys. Chem. A* **101**, 6415 (1997).
12. S. A. Nizkorodov, W. W. Harper, D. J. Nesbitt, *Faraday Disc. Chem. Soc.* **113**, 107 (1999).
13. W. W. Harper, S. A. Nizkorodov, D. J. Nesbitt, *J. Chem. Phys.* **116**, 5622 (2002).
14. F. Dong, S.-H. Lee, K. Liu, *J. Chem. Phys.* **113**, 3633 (2000).
15. F. Rebentrost, W. A. Lester Jr., *J. Chem. Phys.* **63**, 3737 (1975).
16. F. Rebentrost, W. A. Lester Jr., *J. Chem. Phys.* **64**, 3879 (1976).
17. G. C. Schatz, *J. Phys. Chem.* **99**, 7522 (1995).
18. Y. R. Tzeng, M. H. Alexander, *J. Chem. Phys.* **121**, 5812 (2004).
19. L. Schnieder, K. Seekamp-Rahn, E. Wrede, K. H. Welge, *J. Chem. Phys.* **107**, 6175 (1997).
20. K. Liu, R. T. Skodje, D. E. Manolopoulos, *PhysChemComm* **4**, 27 (2002).
21. S. A. Harich *et al.*, *Nature* **419**, 281 (2002).
22. D. Dai *et al.*, *Science* **300**, 1730 (2003).
23. M. Qiu *et al.*, *Science* **311**, 1440 (2006).
24. Methods are detailed on *Science* Online. See fig. S1 for the VUV autoionization sprectrum and figs. S2 and S3 for the predicted rotational distributions in DF ($v = 2$) and DF ($v = 3$), respectively.
25. B. Ruscic, J. P. Greene, J. Berkowitz, *J. Phys. B* **17**, L79 (1984).
26. R. D. Levine, R. B. Bernstein, *Molecular Reaction Dynamics and Chemical Reactivity* (Oxford Univ. Press, New York, 1987).
27. M. H. Alexander, Y.-R. Tzeng, D. Skouteris, in *Chemical Reaction Dynamics*, G. Lendvay, A. Laganá, Eds. (Kluwer Academic, Amsterdam, 2004), pp. 45–65.
28. E. E. Nikitin, *Theory of Elementary Atomic and Molecular Processes in Gases* (Clarendon, Oxford, 1974).
29. V. Aquilanti, G. Grossi, *J. Chem. Phys.* **73**, 1165 (1980).
30. S.-H. Lee, F. Dong, K. Liu, *Faraday Disc. Chem. Soc.* **127**, 49 (2004).
31. M. Ziemkiewicz, M. Wojcik, D. J. Nesbitt, *J. Chem. Phys.* **123**, 224307 (2005).
32. J. Zhou, W. Shiu, J. J. Lin, K. Liu, *J. Chem. Phys.* **124**, 104309 (2006).
33. M. H. Alexander, G. Capecchi, H.-J. Werner, *Science* **296**, 715 (2002).
34. M. H. Alexander, G. Capecchi, H.-J. Werner, *Faraday Disc. Chem. Soc.* **127**, 59 (2004).
35. S.-H. Lee, L.-H. Lai, K. Liu, H. Chang, *J. Chem. Phys.* **110**, 8229 (1999).
36. F. Dong, S.-H. Lee, K. Liu, *J. Chem. Phys.* **115**, 1197 (2001).


37. X.Y. and D.H.Z. were supported by the Chinese Academy of Sciences, the National Natural Science Foundation of China and the Ministry of Science and Technology of China. H.J.W. was supported by the Deutsche Forschungsgemeinschaft and the Fonds der Chemischen Industrie. M.H.A. is grateful to the U.S. NSF for support under grant CHE-0413743.


### Supporting Online Material

www.sciencemag.org/cgi/content/full/317/5841/1061/DC1
Materials and Methods
Figs. S1 and S2
References


11 May 2007; accepted 2 July 2007
10.1126/science.1144984


# Glaciers Dominate Eustatic Sea-Level Rise in the 21st Century


Mark F. Meier,[1]* Mark B. Dyurgerov,[1,2] Ursula K. Rick,[1,3] Shad O'Neel,[1,4,5] W. Tad Pfeffer,[1,6] Robert S. Anderson,[1,5] Suzanne P. Anderson,[1,7] Andrey F. Glazovsky[8]



**Ice loss to the sea currently accounts for virtually all of the sea-level rise that is not attributable to ocean warming, and about 60% of the ice loss is from glaciers and ice caps rather than from the two ice sheets. The contribution of these smaller glaciers has accelerated over the past decade, in part due to marked thinning and retreat of marine-terminating glaciers associated with a dynamic instability that is generally not considered in mass-balance and climate modeling. This acceleration of glacier melt may cause 0.1 to 0.25 meter of additional sea-level rise by 2100.**


Disintegrating glacier ice constitutes a substantial and accelerating cause of global sea-level rise. We synthesized results from a variety of recent ice mass change studies in an effort to present a more accurate picture of changes and trends in ice volume and associated sea-level rise. This synthesis includes current results that update the Intergovernmental Panel on Climate Change (IPCC) Fourth Assessment Report (*1*), stresses the importance of dynamic processes in transporting terrestrial ice to the sea, compares the contributions of glaciers and ice caps with those from the ice sheets, and presents new projections of ice mass change to the end of the 21st century.

We included all glaciers and ice caps (GIC). We excluded the Greenland and Antarctic ice sheets, but included the GIC that surround and are peripheral to the great ice sheets. We focused on present-day behavior (from about 1996 to 2006) because of its critical importance to society now and its relevance for runoff and sea-level projections to the year 2100.

A primary driver of recent ice loss is the rapid retreat and thinning of marine-terminating glaciers, which are susceptible to a nonlinear dynamic instability when their beds are below sea level. The increased role of this phenomenon in delivering ice to the ocean during recent warming has been demonstrated for ice sheet outlets (*2*–*4*) but is also important for many GIC. This instability can markedly raise the sensitivity of glaciers to climate change. It is conventionally assumed that under near–steady state conditions, the climatically controlled surface balance (inputs by snow and loss through melt) controls the geometry of an ice mass, and geometric transitions (changes in thickness) are forced by changes in surface mass balance. In contrast, under dynamically forced conditions, changes in ice velocity are forced instead by changes in subglacial mechanics, and geometric transitions are governed by changes in flux divergence rather than surface balance.


[1]Institute of Arctic and Alpine Research, UCB 450, University of Colorado at Boulder, Boulder, CO 80309–0450, USA. [2]Department of Physical Geography and Quaternary Geology, Stockholm University, SE-1061, Stockholm, Sweden. [3]Department of Atmospheric and Oceanic Sciences, UCB 311, University of Colorado at Boulder, Boulder, CO 80309–0311, USA. [4]Geophysical Institute, University of Alaska-Fairbanks, Fairbanks, AK 99775–7320, USA. [5]Department of Geological Sciences, UBC 399, University of Colorado at Boulder, Boulder, CO 80309–0399, USA. [6]Department of Civil, Environmental, and Architectural Engineering, UCB 428, University of Colorado at Boulder, Boulder, CO 80309–0428, USA. [7]Department of Geography, UCB 260 University of Colorado at Boulder, Boulder, CO 80309–0260, USA. [8]Institute of Geography, Russian Academy of Sciences, Staromonetny 29, 119107, Moscow, Russia.

*To whom correspondence should be addressed. E-mail: mark.meier@colorado.edu

The whole-glacier continuity equation for the rate of change of glacier ice mass, $M$, is

$$\dot{M} = \dot{M}_b + \dot{M}_h + \dot{M}_L = \int_A \rho_i \dot{b} dA + \int_A (-\nabla q)\rho_i dA + \rho_i W_T H_T (u_T - u_c)$$

where dots denote differentiation with respect to time, $\dot{M}_b$ is the glacier-wide net meteorological mass balance (the local surface mass balance, $\dot{b}$, integrated over the glacier area, $A$); $\dot{M}_h$ represents average thickening or thinning associated with the local divergence of ice discharge, $q$, integrated over the glacier area; and $\dot{M}_L$ represents net mass change due to extension or retraction of the terminus governed by the balance between calving at a rate $u_c$ and terminus ice speed, $u_T$, at a terminus of width $W_T$ and ice thickness $H_T$. $\rho_i$ is the density of ice. The contribution of mass to the sea from a retreating tidewater glacier ($-\dot{M}$) is therefore the sum of ice losses driven by meteorology ($\dot{M}_b$), by drawdown of the ice reservoir due to ice dynamics ($\dot{M}_h$), and by terminus dynamics ($\dot{M}_L$). We report these as mass fluxes in gigatons (Gt) per year (1 Gt = mass of 1 km$^3$ water = 1/362-mm sea-level change).

For many marine-terminating outlet and tidewater glaciers, thinning and hence ice loss associated with dynamic instability can be appreciably greater than thinning caused by the local surface mass balance. Alaska's Columbia Glacier provides a useful example. Before the onset of rapid retreat around 1980, this glacier maintained a nearly steady-state elevation profile (a robust proxy for a steady-state thickness profile), for which the positive surface mass balance, estimated at $\dot{M}_b$= 0.37 Gt/year, was closely balanced by dynamic surface lowering. During the late 1970s, however, net thinning began to occur ($\dot{M}_b + \dot{M}_h$ = –0.88 Gt/year), portending dynamic retreat (*5*, *6*); about 15 km of terminus retreat ensued. Columbia Glacier's discharge has since increased. In 2000 to 2001, the ice flux through the terminus reached 6.6 Gt/year even though the surface mass balance was probably decreasing (*7*). Arendt *et al.* (*8*) have pointed out the critical role of these effects in the wastage of other calving glaciers in the western Chugach Mountains, Alaska. This switch from balance-controlled to dynamically forced modes must be understood in comparing global ice-wastage observations and in predicting future delivery of glacier ice to the oceans. The time scale for extracting large volumes of ice from tidewater glaciers as well as from the margins of the major ice sheets can be notably shorter than one would predict from surface mass-balance estimates or climate-balance modeling.

Other calculations of losses due to changes in ice dynamics are rare. Studies in the Russian Arctic (Franz Josef Land, Novaya Zemlya, and Severnaya Zemlya) over the period from 1952 to 2001 estimate $\dot{M}_L$ = –1.3 Gt/year and $\dot{M}_b$+ $\dot{M}_h$ = –3.2 Gt/year (*9*). Recent studies on the Devon Island Ice Cap (*10*) indicate that iceberg calving caused up to 30% of the mass loss between 1960 and 1999. These results suggest that, in areas where tidewater and calving glaciers occur, the errors in estimating ice loss of GIC from classic surface observations are likely to be higher than stated because of the paucity of data on ice dynamic contributions to volume losses.

Rates of ice mass change ($\dot{M}$) from 1995 to 2005 (Table 1, Fig. 1, and table S1) show accelerating rates of mass loss ($\ddot{M} > 0$) from almost all glacier inventories. The rates are indexed to the common year 2006, and the current accelerations of loss in ice mass ($\ddot{M}$) are obtained by linear regressions of published values of rate of mass loss versus time, beginning in 2000 or slightly before (figs. S1 to S3). These rates of ice loss include dynamically forced losses where known; because these are not known in many areas, the values reported must be considered underestimates. For comparison, we also present recent results from the Greenland and Antarctic ice sheets in Table 1 and Fig. 2. The rate of GIC ice loss (±SD) of 402 ± 95 Gt/year dominates the contributions to sea-level rise from the various ice masses in 2006 (Table 1), and the GIC around the Gulf of Alaska contribute substantially (>100 Gt/year; Fig. 1).

The recent rate of worldwide sea-level rise is about 3.1 ± 0.7 mm/year; of this, ocean warming (the steric effect) accounts for about 1.6 ± 0.5 mm/year (*1*). The results given in Table 1 suggest that glacier and ice sheet wastage currently generates 1.8 mm/year of sea-level rise, accounting for slightly more than the remainder of the nonsteric sea-level change. Our results, consistent with those in the IPCC Fourth Assessment (*1*), suggest that GIC contribute about 60% of the eustatic, new-water component of sea-level rise (Table 1 and Fig. 2). Our GIC wastage numbers are slightly greater than those reported in a recent consensus statement (*11*) prepared for the IPCC because the Fourth Assessment reports on an earlier period (1993 to 2003) and the acceleration of ice loss is very large (Fig. 1).

We explored the future effect of ice wastage for two scenarios in Table 1: (i) The present acceleration of mass loss remains constant ($\ddot{M}$= present value; figs. S1 to S3), and (ii) the present rate of mass loss remains constant ($\dot{M}$= present value; $\ddot{M}$ = 0). The surface mass-balance contribution to estimates of mass loss would presumably be more accurate if linked to atmospheric models incorporating changes in $CO_2$ emissions, but our emphasis is on dynamic changes to the glacier mass budget. We included only observed and documented dynamic changes in our assessment, and made no attempt to include changes that may be initiated by ice-ocean interaction in the near future. We note that dynamic adjustments can be rapid and may turn on and off asynchronously, as demonstrated in Alaska (*12*) and Greenland (*3*); one should also assume that with further warming these dynamic changes will likely accelerate. These extrapolations suggest that the GIC contribution will exceed or equal that of either ice sheet throughout at least the first half of this century, and perhaps all of this century, and will deplete at most 35% of the available GIC volume, taken here as 250 × 10$^3$ km$^3$ water equivalent (*13*, *14*), by 2100.

**Table 1.** Present-day rate of ice mass loss ($\dot{M}$), its projected rate of change ($\ddot{M}$) and rates of sea-level rise (SLR). The $\dot{M}$ includes surface mass balance, as well as dynamic effects where known. For Greenland and Antarctica, we used published results, as in (*4*), but we subtracted GIC mass balances [–26 to –50 Gt/year (*13*), depending on gravity signal leakage pattern] from the Greenland gravity results to avoid double counting the GIC ice losses. We did not make this adjustment for the Antarctic because the known major changes in the Antarctic Peninsula are not necessarily reflected in the gravity results.

| | $\dot{M}$ in 2006 Gt/year | $\ddot{M}$ in 2006 Gt/year$^2$ | SLR rate in 2006 mm/year | Total SLR to 2050 mm | Total SLR to 2100 mm |
|---|---|---|---|---|---|
| Glaciers and ice caps | | | | | |
| Assuming current acceleration | –402 ± 95 | –11.9 ± 5.6 | 1.1 ± .24 | 81 ± 43 | 240 ± 128 |
| Assuming no acceleration | –402 ± 95 | 0.0 | 1.1 ± .24 | 49 ± 12 | 104 ± 25 |
| Greenland Ice Sheet | | | | | |
| Assuming current acceleration | –182 ± 34 | –16.2 ± 6.3 | 0.5 ± 0.1 | 65 ± 28 | 245 ± 106 |
| Assuming no acceleration | –182 ± 34 | 0 | 0.5 ± 0.1 | 22 ± 4 | 47 ± 8 |
| West Antarctic Ice Sheet | | | | | |
| Assuming current acceleration | –117 ± 15 | –7.3 ± 3? | 0.32 ± 0.04 | 34 ± 15? | 120 ± 50? |
| Assuming no acceleration | –117 ± 15 | 0 | 0.32 ± 0.04 | 14 ± 2 | 30 ± 4 |
| East Antarctic Ice Sheet | | | | | |
| Assuming current acceleration | 56 ± 26 | 3.4 ± 2? | –0.15 ± 0.07 | –16 ± 12? | –56 ± 40? |
| Assuming no acceleration | 56 ± 26 | 0 | –0.15 ± 0.07 | –7 ± 3 | 15 ± 7 |
| Global total | | | | | |
| Assuming current acceleration | –645 ± 170 | –32 ± 10? | 1.8 ± 0.5 | 160 ± 65? | 560 ± 230? |
| Assuming no acceleration | –645 ± 170 | 0 | 1.8 ± 0.5 | 78 ± 21 | 167 ± 44 |

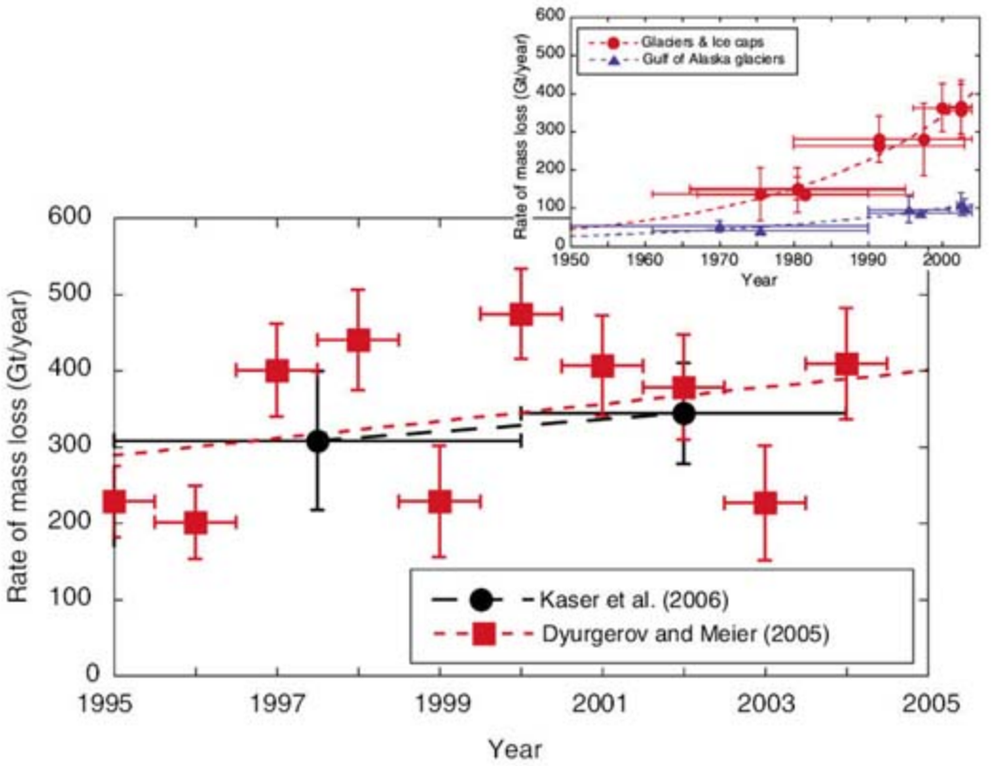


**Fig. 1.** Rate of ice mass loss from all GIC since 1995 (*11*, *13*). Vertical error bars indicate the published uncertainty; horizontal bars show the years over which the mass balance has been averaged. (Inset) Rate of mass loss from all GIC for the period from 1950 to 2005. The red dashed curve exponential indicates the best fit through the total mass loss; the blue dashed curve applies only to the glaciers in the Gulf of Alaska. Data, method, and authorships are given in table S1.

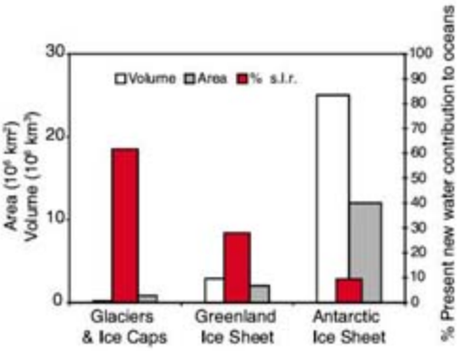


**Fig. 2.** Contributions of GIC, Greenland, and Antarctic Ice Sheets to present-day rate of sea-level rise (s.l.r.), along with their respective volumes and areas.

These projections appear to be larger than those suggested by the IPCC (*1*), much larger than suggested by some authors [e.g., (*15*)], but in close agreement with other recent work (*16*). At the very least, our projections indicate that future sea-level rise may be larger than anticipated and that the component due to GIC will continue to be substantial.

The values suggested for the GIC contribution to rising sea-level in future years might be questioned because they do not consider the loss of glacier area. Most previous models of GIC discharge begin with a fixed "reservoir" of GIC ice that decreases in area and volume as global warming progresses. Indeed, many of the smallest glaciers are likely to vanish during the 21st century. However, (i) most of the GIC area on Earth is accounted for by a relatively few large glaciers (such as subpolar ice caps) that will not shrink appreciably in area during the 21st century; and (ii) cold glaciers in the polar regions, which do not now produce runoff to the ocean, will warm to the point where appreciable runoff to the sea can be expected.

Using a global size distribution of glaciers combined with volume, area, and thickness scaling (*17*, *18*), we found that more than half of the ice volume in GIC is contained in ice masses that are individually >4000 km$^2$, with mean thicknesses of ≈300 m (*19*). The current average global thinning rate of all GIC is about 0.55 m (ice equivalent)/year and is increasing at about 0.0164 m/year$^2$ (Table 1). Total projected thinning by the year 2100 is only 50 and 120 m for steady and accelerating wastage scenarios, respectively. Although this is heartening, the median area of 34 "benchmark glaciers," which have time series of glacier mass balance since the 1960s, is only 4.18 km$^2$, corresponding to a mean thickness of a few tens of meters (~60 m). Thus many of these will likely disappear along with their valuable long-term records.

Our estimates include many possible errors, including measurement errors and area uncertainties, which are difficult to quantify but are likely only a few percent of the global totals. Our neglect of warming of polar firn and subsequent runoff, and of both mass balance–altitude feedback and ill-understood dynamic instabilities, leads to underestimation of sea-level rise. Neglecting area losses and ignoring the density change correction for ice removed from below sea-level produce small overestimates. Total errors (Table 1) do not significantly affect our conclusions.

To improve our understanding of the ice melt contribution to sea level, we must recognize that the GIC, not the big ice sheets, are most important today, and will continue to be important throughout this century. Complex processes driving the behavior of glaciers need better characterization. With the growing emergence of dynamically forced thinning and retreat as a dominant mass-loss process on both calving glaciers and ice sheet outlets, rates of volume change have become very nonsteady. Studies of retreating tidewater glaciers, completed and under way, are very helpful in understanding the analogous phenomenon at ice sheet outlet streams. The GIC around the edges of the big ice sheets, with total area estimated to be more than 200 × 10$^3$ km$^2$, require detailed examination. Spatial extrapolation to obtain regional averages from representative samples, as well as temporal extrapolation to predict future behavior, requires better knowledge of statistical distributions of glacier area and volume. Glacier volume scales nonlinearly with area, thus global grids (e.g., 1° by 1°) must be applied with great care to avoid dividing glacier areas into pieces that do not scale correctly for thickness (*20*).

Ice wastage contributions to sea-level rise will likely continue to increase in the future as warming of cold polar and subpolar glaciers continues and dynamically forced responses continue to occur. Our results suggest a sea-level rise of about 0.1 to 0.25 m in this century due to GIC wastage alone. This range can be compared with the IPCC projection total sea-level rise (all sources) of about 0.2 to 0.5 m depending on the emission scenario (the full effects of changes in ice sheet flow are not included). Although large ice masses may surpass the glacier contribution to sea-level rise in the distant future, the GIC contribution is important now and will be for the remainder of this century.

### References and Notes


1. IPCC, *Climate Change 2007: The Physical Basis: Summary for Policymakers* (IPCC Secretariat, c/o World Meteorological Organization, Geneva, 2007).
2. E. Rignot, P. Kanagaratnam, *Science* **311**, 986 (2006).
3. I. M. Howat, I. R. Joughin, T. A. Scambos, *Science* **315**, 1559 (2007).
4. A. Shepherd, D. Wingham, *Science* **315**, 1529 (2007).
5. M. F. Meier *et al.*, *U.S. Geol. Surv. Open-File Rep. 80–582* (1980), pp. 1–47.
6. *U.S. Geol. Surv. Prof. Pap. 1258A* to *U.S. Geol. Surv. Prof. Pap. 1258H* (1982 to 1989).
7. S. O'Neel, W. T. Pfeffer, R. Krimmel, M. Meier, *J. Geophys. Res.* **110**, F03012 (2005).
8. A. Arendt *et al.*, *J. Geophys. Res.* **111**, F03019 (2006).
9. A. F. Glazovsky, Yu. Ya. Macheret, in *Glaciation of North and Central Eurasia at Present Time*, V. M. Kotlyakov, Ed. (Institute of Geography of the Russian Academy of Science, Nauka, Moscow, 2006).

10. D. O. Burgess, M. J. Sharp, D. W. F. Mair, J. A. Dowdeswell, T. J. Benham, *J. Glaciol.* **51**, 219 (2005).
11. G. Kaser, J. G. Cogley, M. B. Dyurgerov, M. F. Meier, A. Ohmura, *Geophys. Res. Lett.* **33**, L19501 (2006).
12. M. F. Meier, A. Post, *J. Geophys. Res.* **92**, 9051 (1987).
13. M. B. Dyurgerov, M. F. Meier, *Occasional Paper No. 58*, (Institute of Arctic and Alpine Research, Univ. of Colorado, Boulder, CO, 2005).
14. We have revised the total area of GIC from $785 \times 10^3$ km$^2$ to $763 \times 10^3$ km$^2$ because of an overestimate of the glaciers peripheral to Greenland Ice Sheet. This adjustment has been applied throughout.
15. S. C. B. Raper, R. J. Braithwaite, *Nature* **439**, 311 (2006).
16. S. Rahmstorf, *Science* **315**, 368 (2007).
17. D. B. Bahr, M. F. Meier, *Water Resour. Res.* **36**, 495 (2000).
18. D. B. Bahr, *Water Resour. Res.* **33**, 1669 (1997).
19. Because there are many areas without complete inventories of GIC sizes, we used two estimation processes to fill gaps. First, we used an estimate of the probability of the number of glaciers greater than a certain area versus that area, based on percolation theory and on known size distribution relations. The error in this process for a global total was estimated at about 13% (*13*). Next, we estimated the thickness of GIC based on power-law scaling with glacier area. Without sufficient independent data, it is difficult to estimate the error in the method. We estimated that the error in calculating thicknesses and thus volumes from area values is on the order of 25% for global aggregates (*13*) but far greater, on the order of 50%, for individual ice masses.
20. M. F. Meier, D. B. Bahr, M. B. Dyurgerov, W. T. Pfeffer, *Geophys. Res. Lett.* **32**, L17501 (2005).
21. This work was supported by NSF grants OPP 0327345, OPP 0425488, and EAR 0549566; NASA grants NGT5-155 and NAG5-13691; and a Marie Curie International Fellowship within the 6th European Community Framework Program. We thank three anonymous reviewers for their critical reading of the manuscript.

**Supporting Online Material**
www.sciencemag.org/cgi/content/full/1143906/DC1
Figs. S1 to S3
Table S1
References

17 April 2007; accepted 10 July 2007
Published online 19 July 2007;
10.1126/science.1143906
Include this information when citing this paper.

# The Southern Ocean Biological Response to Aeolian Iron Deposition

Nicolas Cassar,[1]* Michael L. Bender,[1] Bruce A. Barnett,[1] Songmiao Fan,[2] Walter J. Moxim,[2] Hiram Levy II,[2] Bronte Tilbrook[3]

Biogeochemical rate processes in the Southern Ocean have an important impact on the global environment. Here, we summarize an extensive set of published and new data that establishes the pattern of gross primary production and net community production over large areas of the Southern Ocean. We compare these rates with model estimates of dissolved iron that is added to surface waters by aerosols. This comparison shows that net community production, which is comparable to export production, is proportional to modeled input of soluble iron in aerosols. Our results strengthen the evidence that the addition of aerosol iron fertilizes export production in the Southern Ocean. The data also show that aerosol iron input particularly enhances gross primary production over the large area of the Southern Ocean downwind of dry continental areas.

The rate of organic matter export from the surface waters of the Southern Ocean has an important impact on distributed properties of the environment. First, it influences the residual nutrient burden of waters that flow northward in the subsurface to supply nutrients to much of the extrapolar ocean (*1*). Second, carbon export removes $CO_2$ from surface waters, thereby influencing the atmospheric $CO_2$ concentration over both glacial-interglacial and anthropogenic time scales. There is compelling evidence that iron supply from a number of sources (such as coastal sediments, aerosols, upwelling, ice melting, and enhanced mixing over high topography) influences rates of both gross production and carbon export by Southern Ocean ecosystems. Ocean color data, for example, show that biomass is elevated downwind of aeolian iron sources, and extraordinary "patch" experiments have shown that iron addition enhances primary production and new production in several representative regions (*2*).

To understand the potential for aeolian iron fertilization, we compared a large number of net community production (NCP) measurements in the Southern Ocean (*3*, *4*) to a modeled Fe deposition (*5*). NCP and gross primary production (GPP) are calculated as the production rates required to maintain the observed biological $O_2$ supersaturation (derived from $O_2$/Ar) and $O_2$ triple-isotope anomaly against equilibration by gas exchange (parameterized in terms of wind speed) (*6*). NCP from $O_2$ is the stoichiometrically equivalent rate of organic carbon production in excess of respiration; it approximates carbon export from the mixed layer. Our data set establishes the pattern of this fundamental rate process in the Southern Ocean at a scale heretofore accessed only for chlorophyll, which reflects biomass. We implemented these methods with samples of water from the upper-ocean mixed layer. Samples were collected by us or collaborators on cruises of opportunity and returned to the laboratory for analysis; in this way, it was possible to assemble a very large data set.

Our approach to determining NCP and GPP has distinct attributes and limitations. The method accesses production over times on the order of 1 week, corresponding to the mixed-layer depth divided by the piston velocity. We assumed steady-state mixed-layer depth and productivity (clearly a simplification). We ignored exchange between the mixed-layer and underlying waters. The analysis of Wang *et al.* (*7*) suggests that, in the Polar Front Zone and the Subantarctic Zone, this process is of minor importance in the summer and in the spring. When the flux of $O_2$ is into the ocean, we report negative values of NCP. Although we refer to the air-sea biological $O_2$ flux as NCP, we were unable to determine whether negative values reflect net heterotrophy in the mixed layer or upwelling of $O_2$-undersaturated waters.

Figure 1 shows summer NCP values superimposed on Southern Ocean properties (*8*). Most of the Southern Ocean can be considered a high-nutrient low-chlorophyll region, with the caveat that the area north of the Antarctic Polar Front (APF) is depleted in silicate during summertime. The strong westerlies around the Antarctic continent drive a northward Ekman transport of nutrient-rich circumpolar deep waters that upwell south of the APF. From the south, the Antarctic Zone lies between the Southern Boundary of the Antarctic circumpolar current and the APF, the Polar Frontal Zone stretches from the APF to the Subantarctic Front, and the Subantarctic Zone extends from the Subantarctic Front to the Subtropical Front. The Subtropical Front is the boundary between the warm and salty subtropical waters and the relatively cooler and fresher waters of the Southern Ocean. The summertime chlorophyll distribution is shown by the background colors of the map (Fig. 1).

We observed that, in general, NCP rises toward the north (Figs. 1 and 2), with considerable spatial heterogeneity. Visual inspection, along with the statistical analysis of Reuer *et al.* (*4*), shows that NCP is weakly correlated with climatological satellite chlorophyll estimates. Our results also show higher NCP and GPP in the spring than in the summer over most of the Southern Ocean (*9*) (Fig. 2). Our approach underestimates NCP in upwelling areas, where mixing to the surface of $O_2$-depleted waters lowers the biological $O_2$ supersaturation. For this reason, the apparent poleward decrease in NCP could partially be driven by upwelling of upper circum-

[1]Department of Geosciences, Princeton University, Princeton, NJ 08544, USA. [2]Geophysical Fluid Dynamics Laboratory/National Oceanic and Atmospheric Administration, Post Office Box 308, Princeton, NJ 08542, USA. [3]Commonwealth Scientific and Industrial Research Organisation (CSIRO) Marine and Atmospheric Research and Antarctic Climate and Ecosystem Cooperative Research Center, Hobart, Tasmania 7001, Australia.

*To whom correspondence should be addressed. E-mail: ncassar@princeton.edu

polar deep water south of the APF. However, we believe that part of this poleward decrease accurately reflects the gradient in mixed-layer fertility because chlorophyll concentration, as well as our $^{17}\Delta$-based estimates of GPP (which are less affected by upwelling), show a similar trend (Fig. 2).

We considered three properties that, individually and in combination, influence spatial variability of summertime Southern Ocean productivity: $Si(OH)_4$, light, and iron. $Si(OH)_4$ undoubtedly limits diatom production at certain times but cannot account for the pattern of GPP and NCP that we observed: It is replete only in southern waters, but production is highest in the north (*4*). In addition, because of diatom Si:C plasticity, limitation of $Si(OH)_4$ uptake does not necessarily entail carbon-specific growth limitation (*10*). The mixed layer is sometimes light-limited because deep mixed layers, with lower mean irradiance, are typical of the Southern Ocean. However, a comparison of our summer NCP measurements to climatological photosynthetically active radiation within the mixed layer shows no statistically significant correlation (fig. S1).

Iron might account for meridional variability in open ocean production in one of three ways. First, if the source of iron is upwelled subsurface waters, production should be elevated near the zone of upwelling—mainly around and south of the APF. Indeed, there is some evidence for higher production at the APF. However, as water upwells south of the APF and flows northward in the Ekman Drift, we do not observe the predicted decrease in production, which theoretically would be caused by removal of iron by scavenging and carbon export. Furthermore, studies from the Australian and Pacific sectors of the Southern Ocean agree that the mixed-layer Fe concentration increases, rather than decreases, toward the north (*11*–*13*). This iron increase to the north is accompanied by rising relative variable fluorescence as measured by fast repetition rate fluorometry (*14*, *15*). Relative variable fluorescence is positively correlated to in situ Fe concentration in the Southern Ocean (*14*). In addition, phytoplankton communities north of the APF do not respond as strongly in Fe enrichment experiments as the ones south of the APF (*15*).

Second, if the source of iron is seasonal or annual aerosol input, production should be correlated to long-term average Fe deposition. Given a plausible residence time on the order of 5 months (calculated for the Subantarctic Zone assuming soluble iron deposition = 0.06 μmol $m^{-2}$ $day^{-1}$, mixed-layer depth = 30 m, and mixed-layer [Fe] = 0.3 nmol $kg^{-1}$), the dissolved Fe concentration will reflect aerosol deposition somewhat upstream of the sampling point, a complication we neglect here. In Fig. 3A, we plot NCP versus the annual iron deposition rate at the sampling location computed by Fan *et al.* (*5*). Their model, driven by analyzed meteorological properties, simulates chemical changes occurring in aerosols that increase Fe solubility with atmospheric transport time (Fig. 4A). This increase in Fe solubility exerts a first-order control on aerosol Fe input to the oceans (*16*). Relative to a model assuming that a constant fraction of iron dissolves, models invoking chemical transformations predict diminished soluble Fe addition near dust sources and enhanced delivery in remote regions (Fig. 4B). Uncertainties in the entrainment rates of dust in the source areas and the fraction of soluble iron in settling aerosols introduce important errors into rates of soluble iron deposition simulated by the model. There is clearly a strong correlation between NCP and annual Fe deposition ($r$ = 0.60, df = 381; Fig. 3A).

Third, if the source of iron is synoptic-scale deposition, production should be correlated with the deposition rate during some recent period. The correlation coefficient between NCP and soluble iron deposition is a maximum when iron deposition is averaged for a period of 14 days before sampling ($r$ = 0.53, df = 381; Fig. 3B), decreasing only slightly with longer averaging times (*6*). This period may be shorter than the average residence time. Nevertheless, synoptic-scale events would lead to variability of about 25% in the ambient iron concentration given transient doublings and halvings of the soluble iron input with a 30-day cycling time. Such changes appear feasible based on the comparison of average Fe deposition at sampling sites during the 2-week period before collection and the average annual Fe deposition at the sites (fig. S2), and the variability would of course be greater if the residence time were <5 months. Fe excursions might raise NCP by inducing transient increases in phytoplankton growth that would eventually be curtailed as grazers respond. Alternatively, recently added iron might be more available to phytoplankton than iron that has resided for a longer time in the mixed layer. A large proportion of Fe in the mixed layer is organically chelated (*17*, *18*), and the bioavailability of this ligand-complexed Fe is poorly understood (*19*). Similar analyses demonstrate the influence of soluble Fe deposition on GPP as well (fig. S3).

Thus, our data are compatible with either annual iron deposition or synoptic-scale iron deposition that has a significant influence on variability of NCP, as well as GPP, in the Southern Ocean. Statistical tests confirm the link between increasing iron deposition and increasing NCP and GPP (*6*). Some of the variability in NCP versus Fe deposition can be explained by other sources of Fe (such as meltwater, sedimentary, and upwelling sources), variable phytoplankton Fe:C quotas, light and silicate limitations, parameterization of the atmospheric Fe dissolution kinetics, aeolian transport model errors, and wind parameterization of the piston velocity.

To explore the potential and nature of atmospheric Fe fertilization, we performed a model

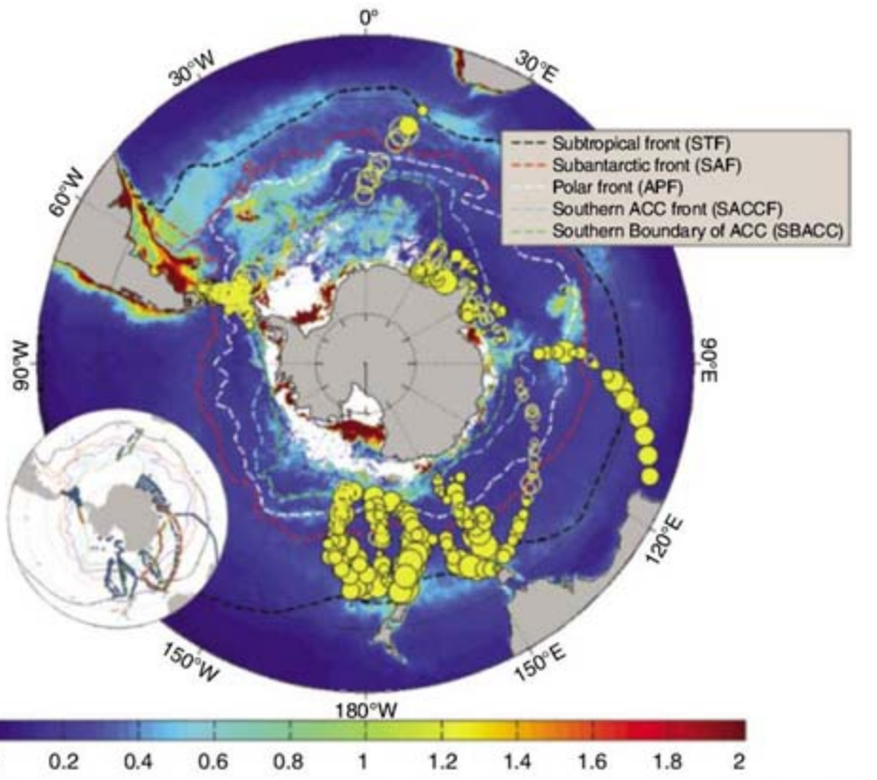


**Fig. 1.** Austral summer NCP measurements in the Southern Ocean. Yellow circles indicate locations of summertime $O_2$/Ar samples from which we calculated air-sea $O_2$ fluxes and NCP values. Open circles denote $O_2$-undersaturated waters and $O_2$ fluxes into the ocean. Closed circles reflect net autotrophy, with the circle size proportional to its magnitude. The largest filled circle represents 168 μmol $O_2$ $m^{-2}$ $day^{-1}$. Sea-Viewing Wide Field-of-View Sensor (SeaWiFS) summer chlorophyll a climatology is also shown (color bar, bottom, in mg $m^{-3}$). (Inset) Color-coded sampling sites with summer, spring, and fall in blue, green, and orange, respectively. Dashed lines indicate the climatological locations of fronts that separate the main water masses associated with the Antarctic circumpolar current (ACC) (*35*).

II least-squares bisector regression analysis (*20*) to calculate the $Fe/C_{org}$ ratio (aerosol Fe input/NCP) implied by our data (Fig. 3B). We adopted an $O_2/C$ molar photosynthetic quotient of 1.4 for NCP (i.e., NCP is assumed to be mostly nitrate-derived) (*21*). The resulting $Fe/C_{org}$ ratio for the spring and summer seasons is 2.5 μmol $mol^{-1}$. This number is markedly similar to the oceanic Fe/C ratios in Southern Ocean phytoplankton (*22*) (1.5 and 2.1 μmol $mol^{-1}$ in the Ross Sea and Drake Passage, respectively). For comparison, Fe:C in laboratory cultures of *Thalassiosira oceanica* varies between 2.5 to 34 μmol $mol^{-1}$ depending on Fe availability (*23*).

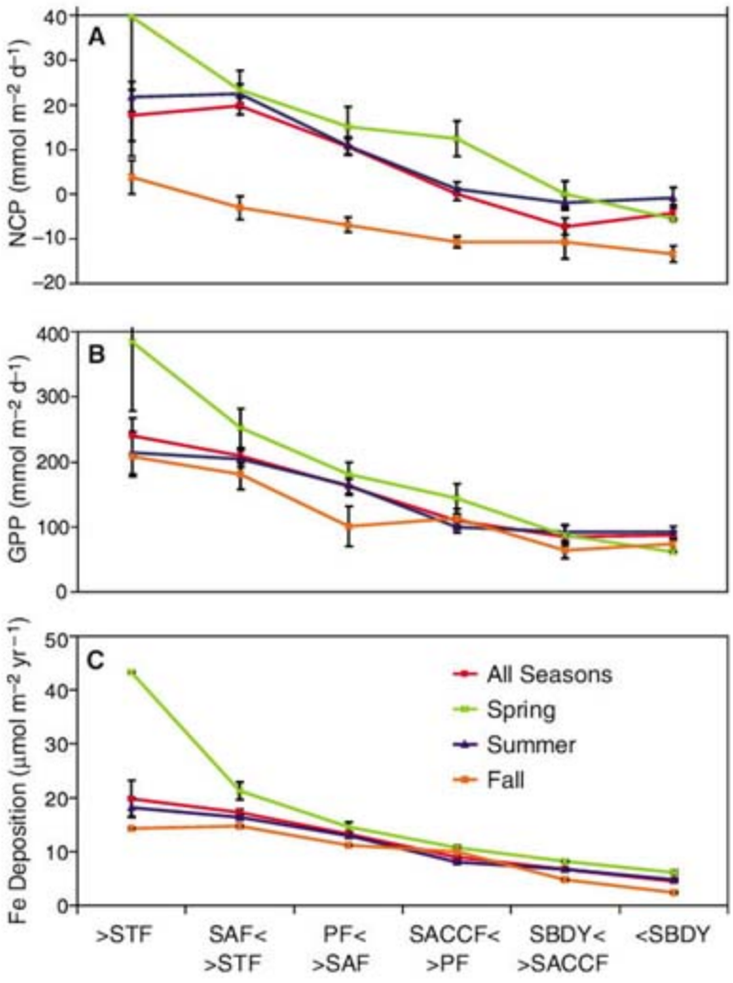


**Fig. 2.** Zonally averaged seasonal and regional gradient in (**A**) $O_2/Ar$-derived NCP, (**B**) oxygen triple isotope–derived GPP (mmol $m^{-2}$ $day^{-1}$) from available measurements, and (**C**) Fe deposition (μmol $m^{-2}$ $year^{-1}$) from corresponding model grid boxes. Standard error bars are also shown when available. STF, Subtropical Front; SAF, Subantarctic Front; PF, Antarctic Polar Front (APF); SACCF, Southern ACC Front; SBDY, southern boundary of the ACC.

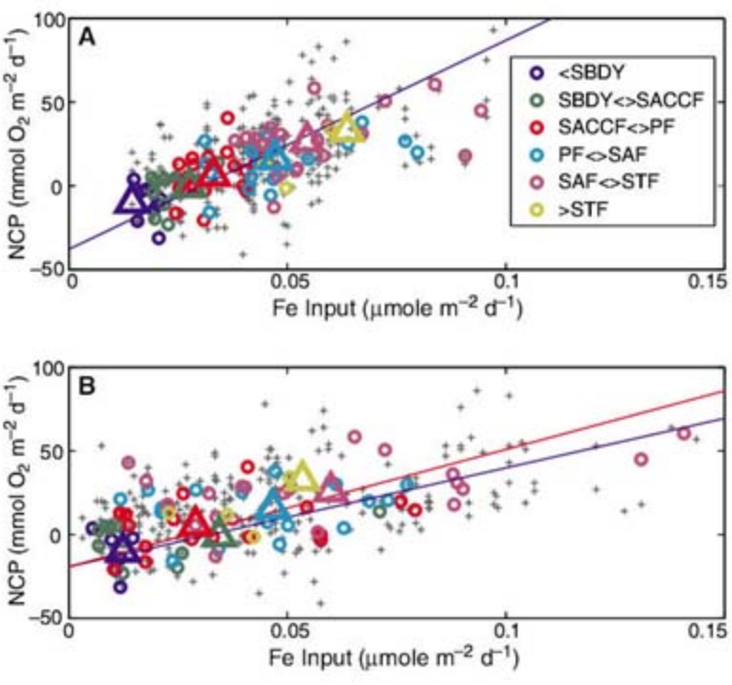


**Fig. 3.** Spring (16%) and summer (84%) NCP measurements versus corresponding modeled annual (**A**) and 2-week (**B**) Fe deposition rates. Gray pluses, circles, and triangles represent individual observations, regional averages for each transect, and regional averages of all samples, respectively. The blue line represents a model II least-squares bisector regression analysis. The red line represents an Fe requirement of 1.4 μM $Fe/MO_2$ [compatible with Sunda's (*22*) Southern Ocean phytoplankton's Fe:C ratio estimate and a photosynthetic quotient of 1.4 (*21*)].

In the Southern Ocean, where Fe is highly limiting, phytoplankton species are at the lower end of this range (*24*–*28*). Deriving our estimates for the cellular Fe quota based on NCP is reasonable if, in the mixed layer, Fe is stoichiometrically cycled along with organic carbon, rather than independently exported (*28*). Stoichiometric cycling is supported by the Fe/C remineralization ratio, which is also about 2 μmol $mol^{-1}$ (*22*). Hence, our results show that photoautotrophs may rely on aeolian input of Fe over a broad area of the Southern Ocean.

Our work, together with other recent studies, provides a comprehensive picture of the ways in which iron fertilization and iron limitation influence the biomass and fertility of Southern Ocean ecosystems. There are five sources of bioavailable iron to surface waters of the Southern Ocean. First, melting of sea ice can release accumulated iron that contributes locally to springtime blooms along the ice edge (*29*). Second, the release of dissolved iron or resuspension of sediments can supply iron to waters overlying shallow sea floor, accounting for high productivity in continental shelf environments (along the Antarctic coast, for example) (*30*). Third, upwelling supplies iron and accounts for elevated productivity in some areas of the APF (*31*) and along the continental slope. Fourth, vertical mixing, induced by rough bottom topography, supplies iron to surface waters and enhances productivity in regions such as the Scotia Sea east of the Drake Passage, and the Kerguelen Plateau in the center of the Indian Antarctic sector (*32*). Finally, as we discuss, delivery of soluble iron by aerosol deposition supplies that element to the Southern Ocean, particularly areas downwind of substantial dust sources, accounting for elevated chlorophyll and/or productivity to the east of Patagonia and to the south and southwest of Australia, New Zealand, and Africa. Regions lacking all sources are the least fertile in the Southern Ocean, despite their high burdens of $NO_3^-$, $PO_4^{3-}$, and $Si(OH)_4$. These include waters overlying the Enderby Abyssal Plain (western Indian sector), South Indian Basin (eastern Indian sector), and the Bellingshausen abyssal Plain (Pacific sector), all in the Antarctic Zone of the Southern Ocean.

Both data and models support the idea that the flux of dust to the Southern Ocean was much higher during the last ice age than during the present or preindustrial times (*33*). In the Subantarctic region, lower $\delta^{15}N$ of sedimentary nitrogen in glacial sediments (*34*), along with more rapid biogenic $SiO_2$ accumulation, indicates higher rates of export production. Increased iron delivery is certainly a plausible explanation for faster export. According to the model of Robinson *et al.* (*34*), the resulting depletion of subantarctic waters in nutrients and $TCO_2$ would have led to an atmospheric $CO_2$ drawdown of up to 40 parts per million, accounting for nearly half the glacial lowering of atmospheric $CO_2$. Our work shows that delivery of

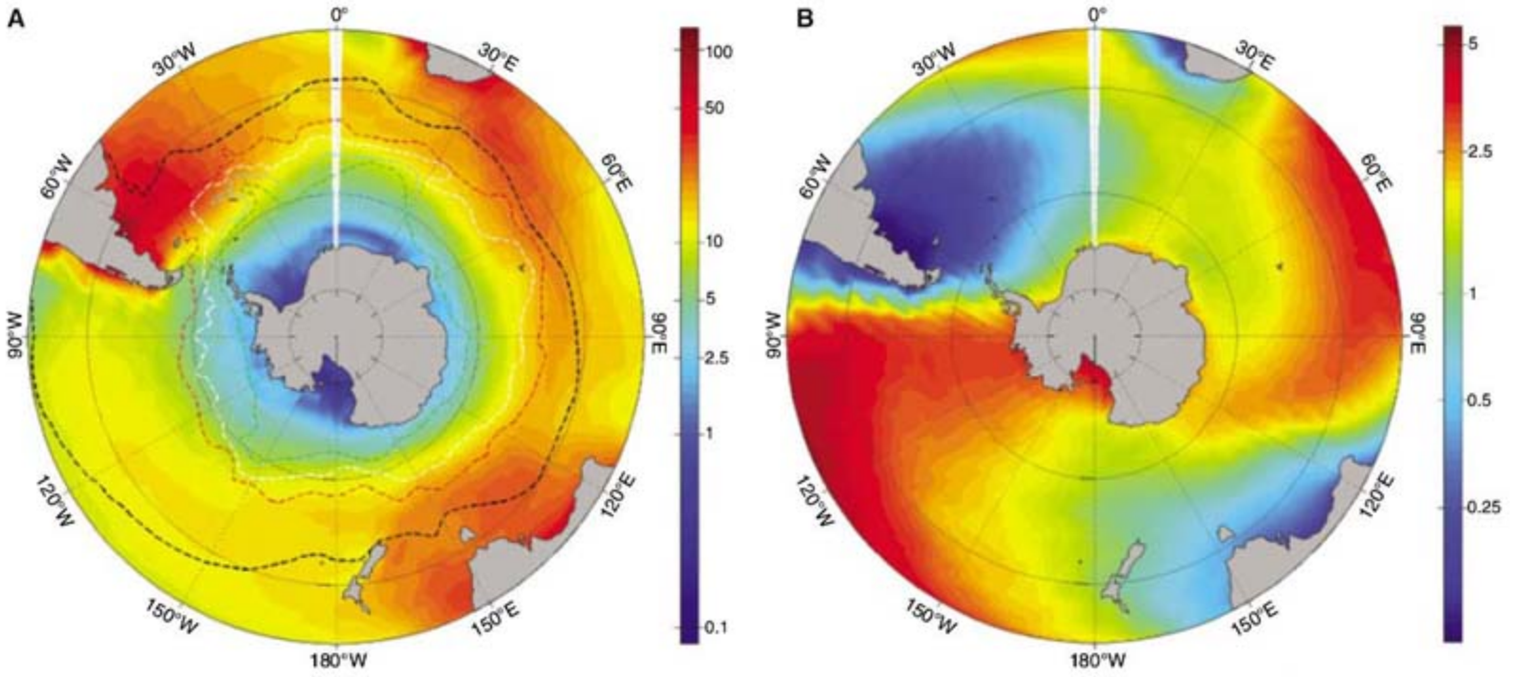


**Fig. 4.** (**A**) Annual deposition fluxes of dissolved Fe to the ocean based on the Fan *et al.* (*5*) two-step solubility process (μmol $m^{-2}$ $year^{-1}$). (**B**) Ratio of fluxes shown in (A) and a constant 5% Fe solubility model.

airborne Fe increases production of subantarctic waters, strengthening the link between enhanced Fe delivery and lower $CO_2$ during the ice ages. Our work also underscores the importance of understanding the implications of the large change in dust transport to the ocean simulated for the coming centuries (*33*).

### References and Notes


1. J. L. Sarmiento, N. Gruber, M. A. Brzezinski, J. P. Dunne, *Nature* **427**, 56 (2004).
2. P. W. Boyd *et al.*, *Science* **315**, 612 (2007).
3. M. B. Hendricks, M. L. Bender, B. A. Barnett, *Deep-Sea Res. I* **51**, 1541 (2004).
4. M. K. Reuer, B. A. Barnett, M. L. Bender, P. G. Falkowski, M. B. Hendricks, *Deep-Sea Res. I* **54**, 951 (2007).
5. S. M. Fan, W. J. Moxim, H. Levy, *Geophys. Res. Lett.* **33**, L07602 (2006).
6. Materials and methods are available as supporting material on *Science* Online.
7. X. J. Wang, R. J. Matear, T. W. Trull, *J. Geophys. Res. Oceans* **106**, 31525 (2001).
8. We include only springtime and summertime data in our discussion. Although fall data strengthen our conclusions, we omitted these results from our analysis because mixed-layer oxygen supersaturation can be influenced by entrainment of undersaturated subsurface waters.
9. M. L. Dickson, J. Orchardo, *Deep-Sea Res. II* **48**, 4101 (2001).
10. D. M. Nelson, M. A. Brzezinski, D. E. Sigmon, V. M. Franck, *Deep-Sea Res. II* **48**, 3973 (2001).
11. P. N. Sedwick, P. R. Edwards, D. J. Mackey, F. B. Griffiths, J. S. Parslow, *Deep-Sea Res. I* **44**, 1239 (1997).
12. H. J. W. de Baar *et al.*, *Mar. Chem.* **66**, 1 (1999).
13. C. I. Measures, S. Vink, *Deep-Sea Res. II* **48**, 3913 (2001).
14. H. M. Sosik, R. J. Olson, *Deep-Sea Res. I* **49**, 1195 (2002).
15. M. R. Hiscock *et al.*, *Deep-Sea Res. II* **50**, 533 (2003).
16. J. L. Hand *et al.*, *J. Geophys. Res.* **109**, D17205 (2004).
17. E. L. Rue, K. W. Bruland, *Mar. Chem.* **50**, 117 (1995).
18. J. F. Wu, G. W. Luther, *Mar. Chem.* **50**, 159 (1995).
19. D. A. Hutchins, A. E. Witter, A. Butler, G. W. Luther, *Nature* **400**, 858 (1999).
20. P. Sprent, G. R. Dolby, *Biometrics* **36**, 547 (1980).
21. E. A. Laws, *Deep-Sea Res. A* **38**, 143 (1991).
22. W. G. Sunda, *Mar. Chem.* **57**, 169 (1997).
23. W. G. Sunda, S. A. Huntsman, *Mar. Chem.* **50**, 189 (1995).
24. R. F. Strzepek *et al.*, *Global Biogeochem. Cycles* **19**, GB4526 (2005).
25. B. S. Twining, S. B. Baines, N. S. Fisher, *Limnol. Oceanogr.* **49**, 2115 (2004).
26. M. T. Maldonado *et al.*, *Limnol. Oceanogr.* **46**, 1802 (2001).
27. W. G. Sunda, S. A. Huntsman, *Nature* **390**, 389 (1997).
28. S. Blain *et al.*, *Nature* **446**, 1070 (2007).
29. P. N. Sedwick, G. R. DiTullio, *Geophys. Res. Lett.* **24**, 2515 (1997).
30. B. B. Prezelin, E. E. Hofmann, C. Mengelt, J. M. Klinck, *J. Mar. Res.* **58**, 165 (2000).
31. H. J. W. Debaar *et al.*, *Nature* **373**, 412 (1995).
32. E. Bucciarelli, S. Blain, P. Treguer, *Mar. Chem.* **73**, 21 (2001).
33. N. M. Mahowald *et al.*, *J. Geophys. Res. Atmos.* **111**, D10202 (2006).
34. R. S. Robinson *et al.*, *Paleoceanography* **20**, PA3003 (2005).
35. A. H. Orsi, T. Whitworth, W. D. Nowlin, *Deep-Sea Res. I* **42**, 641 (1995).


36. We thank P. Ginoux, M. Reuer, and P. Falkowski for helpful discussions, two anonymous reviewers for perceptive comments, and P. Schultz for providing the average climatological mixed layer PAR data-product. We gratefully acknowledge support for this work from NASA, NSF, the Gary Comer Family Foundation, and the CSIRO Climate Change Research Program.


### Supporting Online Material

www.sciencemag.org/cgi/content/full/317/5841/1067/DC1
Materials and Methods
Figs. S1 to S4
Table S1
References

3 May 2007; accepted 20 July 2007
10.1126/science.1144602

# The Evolution of Selfing in *Arabidopsis thaliana*

**Chunlao Tang,[1] Christopher Toomajian,[1] Susan Sherman-Broyles,[2] Vincent Plagnol,[1,3] Ya-Long Guo,[4] Tina T. Hu,[1] Richard M. Clark,[4] June B. Nasrallah,[2] Detlef Weigel,[4,5] Magnus Nordborg[1]***

Unlike most of its close relatives, *Arabidopsis thaliana* is capable of self-pollination. In other members of the mustard family, outcrossing is ensured by the complex self-incompatibility (*S*) locus, which harbors multiple diverged specificity haplotypes that effectively prevent selfing. We investigated the role of the *S* locus in the evolution of and transition to selfing in *A. thaliana*. We found that the *S* locus of *A. thaliana* harbored considerable diversity, which is an apparent remnant of polymorphism in the outcrossing ancestor. Thus, the fixation of a single inactivated *S*-locus allele cannot have been a key step in the transition to selfing. An analysis of the genome-wide pattern of linkage disequilibrium suggests that selfing most likely evolved roughly a million years ago or more.

The transition from outcrossing to selfing is a major theme in the evolution of flowering plants, having occurred independently in numerous lineages (*1*). Although it leads to inbreeding depression, the ability to self can be advantageous when colonizing new territory and is therefore associated with weedy and invasive species. *A. thaliana*, a member of the Brassicaceae,

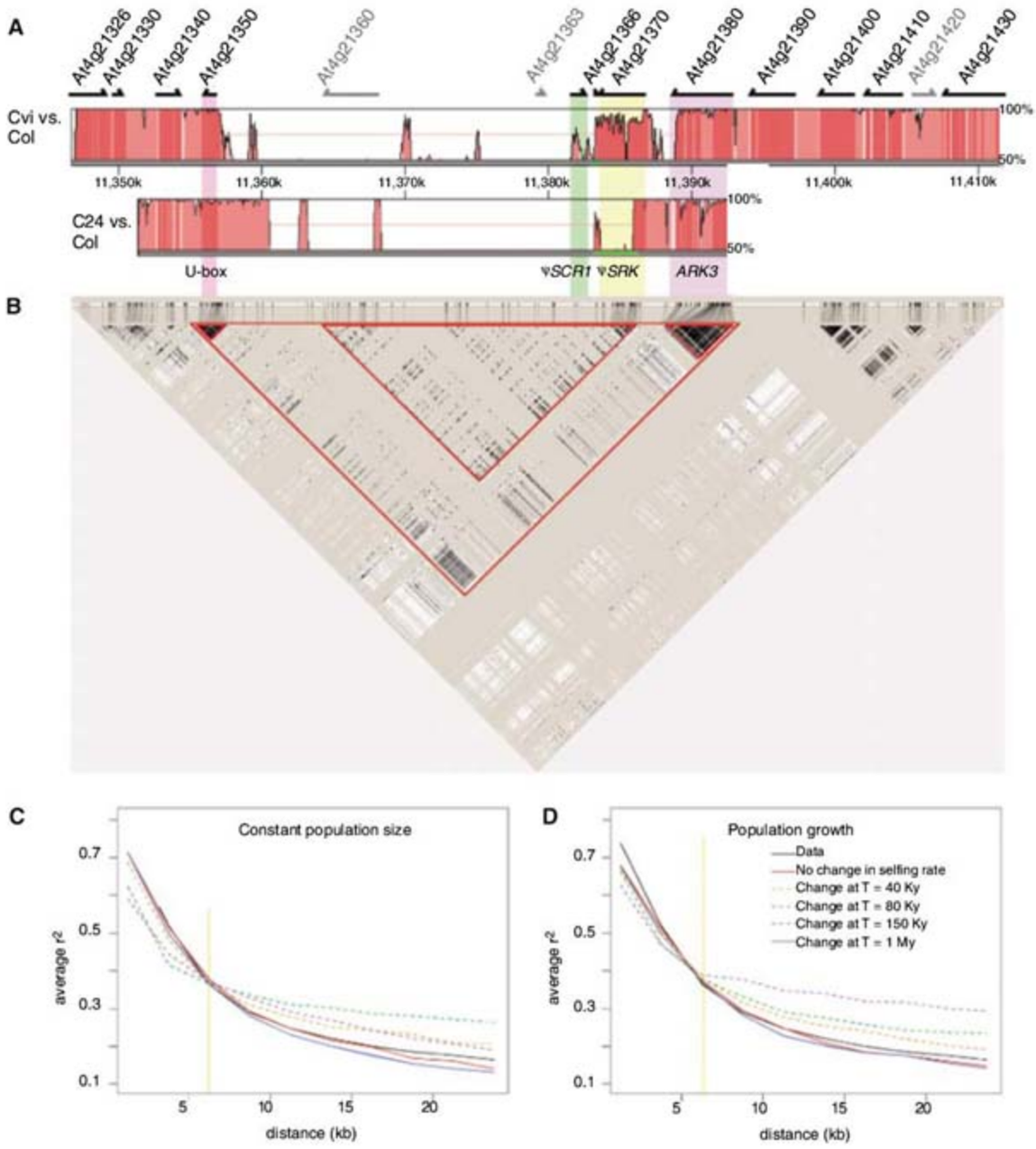


**Fig. 1.** (**A**) Plots illustrating sequence conservation (*18*) across the *S*-locus region between C24 and Col-0 (bottom plot) and between Cvi-0 and Col-0 (top plot). Colored regions designate the U-box, *ΨSCR*, *ΨSRK*, and *ARK3* loci, respectively. Sequence similarity is represented on the *y* axis. Most of the *S* locus is too diverse to be aligned for the three haplotypes. (**B**) Plot of LD [measured as $r^2$, with the darkest and lightest colors indicating complete linkage and no linkage, respectively (*19*)] across the *S*-locus region. See table S1 for a summary of investigated polymorphisms. Because the observed polymorphisms are highly clumped, the spacing in the plot is nonlinear: Thin lines connect the actual positions of polymorphism along the chromosome. The highlighted blocks illustrate strong LD not only within the U-box and *ARK3* genes but also (i) across the *S* locus from At4g21360 (a transposable element) through *ΨSRK* and (ii) across the entire region from the U-box to *ARK3*. (**C** and **D**) Observed LD decay in genome-wide single-nucleotide polymorphism data (*11*) as compared with coalescent simulation results (*10*), assuming a constant population size (C) or assuming population growth (D). The simulations fit the data only if the transition to selfing occurred so recently that no trace would be visible ("no change in selfing rate") or so long ago that the trace would have been lost ["change at $T$ = 1 million years (My)"]. Ky, thousand years.

is a highly selfing plant that is separated from its closest relative, the self-incompatible *A. lyrata*, by about 5 million years (*2*, *3*).

In the Brassicaceae, the main components of the *S* locus are the tightly linked *S*-locus cysteine-rich protein (*SCR*) and *S*-locus receptor kinase (*SRK*) genes, which encode male and female specificity determinants of self-incompatibility, respectively (*4*). The *S* locus is characterized by highly diverged haplotypes, as predicted by theory (*5*). Because *A. thaliana* is self-compatible, the self-incompatibility system must be inactive, and both *SCR* and *SRK* are pseudogenes (*ΨSCR* and *ΨSRK*) in the reference accession Col-0 (*5*). Because transformation with *S*-locus alleles from *A. lyrata* can restore self-incompatibility in *A. thaliana* (*6*), inactivation of the *S* locus could have been the key step in the transition to selfing. If this occurred only once, it should have sharply reduced variability at this locus [a so-called "selective sweep" (*7*, *8*)]. Even if such an event happened a long time ago, it should be readily detectable because the ancestral locus would have been extremely polymorphic (*5*, *9*).

We investigated variation at the *S* locus using several approaches. Polymerase chain reaction (PCR) amplification of *ΨSCR* and *ΨSRK* failed in many of 96 surveyed accessions (*10*), indicating that these genes are either very diverged in sequence or missing. These results were supported by whole-genome resequencing data for 20 accessions with oligonucleotide arrays (*11*). The *S*-locus region of many accessions did not hybridize well to the arrays, which had been designed based on the reference sequence. Several, highly diverged haplotypes extend throughout the *S*-locus region (table S1). About 35 accessions are very similar to the Col-0 reference. Cvi-0, from the extreme south of the species' range, carries a very distinctive haplotype that occurs only once in our sample. Another distinctive group includes nine accessions, with origins ranging from Kashmir (*12*) to Spain. The remaining accessions are characterized by different but consistent patterns of missing data. This latter group includes C24, which carries an extensively rearranged haplotype (see below).

We dideoxy-sequenced bacterial artificial chromosomes (BACs) covering the *S* locus from two accessions: C24, which was the only accession for which self-incompatibility was restored upon transformation by *S*-locus alleles from *A. lyrata*

[1]Molecular and Computational Biology, University of Southern California, Los Angeles, CA 90089, USA. [2]Department of Plant Biology, Cornell University, Ithaca, NY 14853, USA. [3]Juvenile Diabetes Research Foundation/Wellcome Trust Diabetes and Inflammation Laboratory, University of Cambridge, Wellcome Trust/Medical Research Council Building, Cambridge, CB2 2XY, UK. [4]Department of Molecular Biology, Max Planck Institute for Developmental Biology, 72076 Tübingen, Germany. [5]Plant Biology Laboratory, The Salk Institute for Biological Studies, La Jolla, CA 92037, USA.

*To whom correspondence should be addressed. E-mail: magnus@usc.edu

(*6*), and the highly divergent Cvi-0 (*13*). In C24, the *S* locus is extensively rearranged as compared with that of Col-0, and Ψ*SCR* is deleted (*14*), whereas in Cvi-0, the *S* locus is similar in structure to Col-0 but is highly diverged in sequence (Fig. 1A). Most of the sequence between the U-box gene and Ψ*SRK* cannot be aligned for the three haplotypes. Cvi-0 *SCR* carries no obvious null mutation, whereas Cvi-0 Ψ*SRK* has a distinctive splice-site change (fig. S1).

Because we found high variation, our data rule out the fixation of a single loss-of-function allele at the *S* locus as a key step in the transition to selfing. Instead, the ancestral balanced polymorphism at the *S* locus is gradually being eroded through genetic drift, perhaps in combination with selection for inactivity: a process that may be very slow, especially in highly structured populations. The *A. thaliana SRK* alleles are shared with closely related species (*15*). Given that linkage disequilibrium (LD) extends throughout the *S*-locus region (Fig. 1B), it seems likely that the same will be true for *SCR*. At the same time, the observation that transformation with *S*-locus alleles from *A. lyrata* does not always restore self-incompatibility (*6*) suggests multiple evolutionary routes to selfing.

Our results contradict a report of low variability at Ψ*SCR* (but not Ψ*SRK*) resulting from a recent selective sweep (*12*). The disagreement is not due to differences in the sample that was used: We were unable to replicate previously published results (*12*) using the published PCR primers and accessions (table S1 and fig. S2), and the reported Ψ*SCR* sequence in Cvi-0 disagrees with our BAC sequence, although the highly divergent Ψ*SRK* is identical in our BAC sequence and in the sequence in the previous report. We therefore conclude that the published results are erroneous. It has been noted that a selective sweep at *SCR*, but not *SRK*, seemed unlikely (*15*): Our data resolve this contradiction.

Finally, we considered when selfing might have evolved. It has been estimated that *SRK* started to become a pseudogene no more than 413,000 years ago (*15*); however, the transition to selfing could have taken place earlier if loss of *S*-locus function was not the first step [as suggested by the discovery of a modifier of self-incompatibility in *A. thaliana* (*16*)]. To obtain an alternative estimate, we examined the genome-wide pattern of LD (*11*). LD in a partially selfing organism should decay like that in an outcrosser, albeit more slowly (*17*). However, a very different pattern is expected with a recent, dramatic change in outcrossing, because recombination events that took place before the transition to selfing would have been more effective in breaking up LD. As a result, long-range LD, which reflects recent events, should be too high relative to short-range LD, which reflects more ancient events. This pattern should be detectable unless selfing evolved either a very long time ago (on the order of the coalescence time, or about $10^6$ years in *A. thaliana*) or very recently, in which case the LD pattern should still look like that of an outcrosser. The LD decay reveals no indication of a recent change in selfing (Fig. 1, C and D), and because the LD pattern is very different from that in an outcrosser, species-wide selfing most likely evolved on the order of a million years ago or more. This would also have provided ample time for the suite of selfing-associated traits that distinguish *A. thaliana* from *A. lyrata* to evolve (*3*).


**References and Notes**

1. S. C. H. Barrett, *Nat. Rev. Genet.* **3**, 274 (2002).
2. M. Koch, B. Haubold, T. Mitchell-Olds, *Am. J. Bot.* **88**, 534 (2001).
3. D. Charlesworth, X. Vekemans, *Bioessays* **27**, 472 (2005).
4. J. B. Nasrallah, *Curr. Opin. Plant Biol.* **3**, 368 (2000).
5. M. Kusaba *et al.*, *Plant Cell* **13**, 627 (2001).
6. M. E. Nasrallah, P. Liu, S. Sherman-Broyles, N. A. Boggs, J. B. Nasrallah, *Proc. Natl. Acad. Sci. U.S.A.* **101**, 16070 (2004).
7. J. Maynard Smith, J. Haigh, *Genet. Res.* **23**, 23 (1974).
8. N. L. Kaplan *et al.*, *Genetics* **123**, 887 (1989).
9. T. R. Ioerger, A. G. Clark, T.-H. Kao, *Proc. Natl. Acad. Sci. U.S.A.* **87**, 9732 (1990).
10. Materials and methods are available as supporting material on *Science* Online.
11. R. M. Clark *et al.*, *Science* **317**, 338 (2007).
12. K. K. Shimizu *et al.*, *Science* **306**, 2081 (2004).
13. M. Nordborg *et al.*, *PLoS Biol.* **3**, e196 (2005).
14. S. Sherman-Broyles *et al.*, *Plant Cell* **19**, 94 (2007).
15. J. S. Bechsgaard, V. Castric, D. Charlesworth, X. Vekemans, M. H. Schierup, *Mol. Biol. Evol.* **23**, 1741 (2006).
16. P. Liu, S. Sherman-Broyles, M. E. Nasrallah, J. B. Nasrallah, *Curr. Biol.* **17**, 734 (2007).
17. M. Nordborg, *Genetics* **154**, 923 (2000).
18. C. Mayor *et al.*, *Bioinformatics* **16**, 1046 (2000).
19. J. C. Barrett, B. Fry, J. Maller, M. J. Daly, *Bioinformatics* **21**, 263 (2005).


20. This study was funded by NSF grant DEB-0115062 to M.N., NIH Center of Excellence in Genomic Science grant P50 HG002790 to M. Waterman, NSF grant IBN-0414521 to M. E. Nasrallah and J.B.N., NIH grant GM62932 to J. Chory and D.W., and the Max Planck Society. The GenBank accession number for the Cvi-0 BAC sequence is EF637083. We thank M. Koornneef for access to the Cvi-0 BAC library.


**Supporting Online Material**

www.sciencemag.org/cgi/content/full/1143153/DC1
Materials and Methods
Figs. S1 and S2
Tables S1 and S2
References


28 March 2007; accepted 17 July 2007
Published online 26 July 2007;
10.1126/science.1143153
Include this information when citing this paper.


# Anatomy and Dynamics of a Supramolecular Membrane Protein Cluster


**Jochen J. Sieber,[1] Katrin I. Willig,[2] Carsten Kutzner,[3] Claas Gerding-Reimers,[1] Benjamin Harke,[2] Gerald Donnert,[2] Burkhard Rammner,[4] Christian Eggeling,[2] Stefan W. Hell,[2] Helmut Grubmüller,[3] Thorsten Lang[1]†**



Most plasmalemmal proteins organize in submicrometer-sized clusters whose architecture and dynamics are still enigmatic. With syntaxin 1 as an example, we applied a combination of far-field optical nanoscopy, biochemistry, fluorescence recovery after photobleaching (FRAP) analysis, and simulations to show that clustering can be explained by self-organization based on simple physical principles. On average, the syntaxin clusters exhibit a diameter of 50 to 60 nanometers and contain 75 densely crowded syntaxins that dynamically exchange with freely diffusing molecules. Self-association depends on weak homophilic protein-protein interactions. Simulations suggest that clustering immobilizes and conformationally constrains the molecules. Moreover, a balance between self-association and crowding-induced steric repulsions is sufficient to explain both the size and dynamics of syntaxin clusters and likely of many oligomerizing membrane proteins that form supramolecular structures.


The fluid mosaic model for the structure of biological membranes (*1*) proposes that individual membrane proteins diffuse freely in a sea of lipids. However, it is becoming clear that most membrane proteins are organized in clusters that are diverse. Current popular theories for membrane compartmentalization do not provide a satisfactory explanation for this degree of micropatterning. For instance, partitioning selected components into lipid rafts is supposed to organize the membrane (*2*), but whereas glycosylphosphatidyl (GPI)–anchored proteins enrich in rafts, the large majority of transmembrane proteins prefer the nonraft phase. Other models propose subplasmalemmal "fences" and "pickets" to form compartment boundaries (*3*). However, these theories can explain formation of only a limited number of different plasmalemmal compartments, what is difficult to reconcile with the large compositional diversity of membrane domains. Thus, the physical principles underlying most membrane protein clusters are not yet adequately understood.

Several observations are consistent with highly specific clustering mechanisms. Particularly striking are observations that several integral membrane protein isoforms or structurally similar family members segregate in nonoverlapping clusters, including receptors (*4*), lipid phosphate phosphatases (*5*), and members of the soluble *N*-ethylmaleimide–sensitive factor attachment pro-

tein receptor (SNARE) family [so-called syntaxins (*6*, *7*)]. Segregation of syntaxins is likely functionally important because syntaxin 1 and 4 clusters represent sites for docking and fusion of secretory granules and caveolae, respectively (*8*–*10*). In vitro, syntaxin 1 forms homo-oligomers via its SNARE motif (*11*), and, although most syntaxin clusters are also stabilized by cholesterol [for example, (*6*, *8*–*10*)], it has been shown that for specific cluster formation homophilic interactions of the SNARE motifs are essential (*7*). This renders a self-organizing system governed by protein-protein interactions, a plausible biological mechanism, explaining the high specificity of cluster formation. Unfortunately, the existence, let alone the mechanism, of such a self-organizing process could so far not be established because of limited knowledge about the size, composition, and dynamics of the clusters.

To overcome this limitation, we have combined the nanoresolving power of stimulated emission depletion (STED) fluorescence microscopy (fig. S1) (*12*–*14*) with quantitative biochemistry, fluorescence recovery after photobleaching (FRAP) analysis, and simulations to determine the physical basis of the supramolecular nanostructure formed by syntaxin 1.

[1]Department of Neurobiology, Max Planck Institute for Biophysical Chemistry, Am Fassberg 11, 37077 Göttingen, Germany. [2]Department of Nanobiophotonics, Max Planck Institute for Biophysical Chemistry, Am Fassberg 11, 37077 Göttingen, Germany. [3]Department of Theoretical and Computational Biophysics, Max Planck Institute for Biophysical Chemistry, Am Fassberg 11, 37077 Göttingen, Germany. [4]Friedensallee 92, 22763 Hamburg, Germany.

†To whom correspondence should be addressed. E-mail: tlang@gwdg.de

In neuroendocrine PC12 cells, the density of syntaxin clusters per surface area plasma membrane was quantified by STED microscopy on membrane sheets (Fig. 1A). STED microscopy reaches resolutions far below that of conventional light microscopy (*12*–*14*) and is able to separate individual clusters (Fig. 1A). Featuring a focal plane resolution of 50 nm, that is, ~5 times beyond the diffraction barrier, the STED microscope revealed an average density of 19.6 clusters per $\mu m^2$ (Fig. 1A). To estimate the total number of clusters, we further determined the average cell surface area by confocal microscopy (460 $\mu m^2$; fig. S2). Accordingly, a cell contains about 9000 clusters. Quantitative immunoblotting revealed an average of 830,000 syntaxin 1 copies per cell (fig. S3), yielding a syntaxin/cluster ratio of 90, which is an upper estimate (*15*). STED microscopy also revealed an average cluster diameter of 50 to 60 nm (Fig. 1B) (*15*), suggesting that within the cluster syntaxin molecules are densely packed.

To examine the mobility of syntaxin in the plasma membrane, we performed FRAP experiments in living PC12 cells expressing green fluorescent protein (GFP)–labeled syntaxin 1A. This method determines the overall mobility, although it is not able to differentiate between clustered and freely moving molecules. As shown in Fig. 2, fluorescence recovery times ranged from 40 to 60 s, much higher than expected for a freely diffusing protein with a single transmembrane region (TMR) [(*16*); for diffusion coefficients, see (*15*)], and full recovery was not reached in the course of the experiment. To exclude the possibility that incomplete recovery is a bleaching artifact, we performed FRAP control experiments on membrane sheets that enabled us to correct the signal for bleaching and laser fluctuations because the total fluorescence of the preparation was known. No difference in FRAP was observed between live cells and membrane sheets (fig. S4). This experiment further indicates that cytosolic factors and actin reorganization play no role in controlling syntaxin mobility.

To identify the region of the protein that is responsible for mobility restriction, we studied mutant forms and deletion constructs of syntaxin 1A. Syntaxin 1A contains a C-terminal TMR, a membrane-adjacent SNARE motif, and an independently folded N-terminal domain connected to the SNARE motif via a linker region (*17*) (Fig. 2B). It has been previously shown that syntaxin can form oligomers via its TMRs (*18*) and can adopt a closed conformation in which the N-terminal domain is folded back onto the SNARE motif (*19*). In FRAP experiments, mutations that prevent TMR oligomerization (*18*) or the closed conformation (*19*) behaved indistinguishably from wild-type syntaxin (Fig. 2B), indicating that these mechanisms have no strong influence on syntaxin mobility. However, mobility increased dramatically after deleting most of syntaxin's cytoplasmatic part, and restriction in mobility could be rescued by adding back the SNARE motif (Fig. 2C). Shortening the N-terminal part of the SNARE motif gradually increased mobility from region –5 on, with almost maximal mobility observed after deletion of region –3 (Fig. 2, D and F). Thus, the part from –5 to –3 is essential for restricted mobility. However, it is not sufficient, because construct –5Δ (Fig. 2F), containing –5 to –3 but lacking the

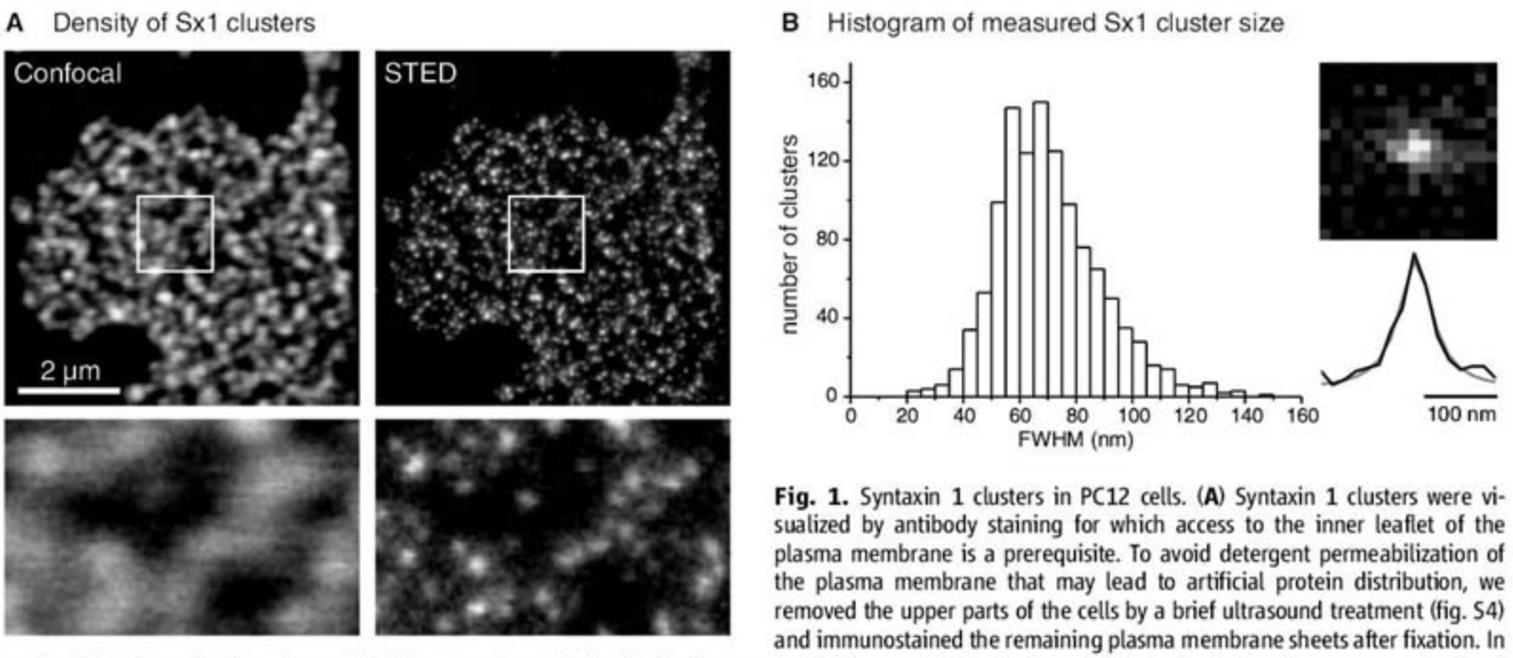


**Fig. 1.** Syntaxin 1 clusters in PC12 cells. (**A**) Syntaxin 1 clusters were visualized by antibody staining for which access to the inner leaflet of the plasma membrane is a prerequisite. To avoid detergent permeabilization of the plasma membrane that may lead to artificial protein distribution, we removed the upper parts of the cells by a brief ultrasound treatment (fig. S4) and immunostained the remaining plasma membrane sheets after fixation. In contrast to their confocal counterparts (left), nanoscale-resolution STED micrographs (right) reveal that syntaxin concentrates in clusters at an average density of 19.6 ± 5.7 per $\mu m^2$ (mean ± SD, $n$ = 47 membrane sheets). Bottom images are magnified views from boxed regions in top images. (**B**) Histogram showing the distribution of full width at half maximum (FWHM) of syntaxin 1 cluster signals obtained from STED micrographs by line scan analysis (median = 68 nm; 1166 clusters from 25 membrane sheets). The FWHM of individual clusters was determined from the Lorentzian fit (gray line) of the line scan (black line) through the corresponding cluster. From the median value of 68 nm, we estimated the real average cluster size to be between 50 and 60 nm (*15*).

subsequent part from –2 to +8, shows fast recovery (Fig. 2E). These experiments suggest that SNARE motifs associating along almost their entire length are responsible for the reduced mobility of syntaxin, whereas its closed conformation and TMRs play no role. The similarity to the mechanism that directs syntaxin into clusters (*7*) indicates that reduced mobility is caused by the assembly of syntaxin into clusters.

As discussed above, FRAP does not differentiate whether recovery results from diffusion of entire clusters or from individual syntaxin molecules (or small oligomers) exchanging between immobile clusters. To address this question, we studied the dynamics of syntaxin 1A–GFP clusters. In this experiment, diffraction-limited spots, composed of a few individual clusters, were monitored that should reorganize, move, or show intensity fluctuations if clusters are mobile. To avoid membrane motions caused by cellular dynamics as, for example, actin cortex reorganization, we used native plasma membrane sheets in which syntaxin mobility is indistinguishable compared to that of intact cells (fig. S4). Syntaxin spots did not change over minutes (Fig. 3), suggesting that fluorescence recovery occurs via exchange of syntaxin molecules between clusters. Together, these data show that free and clustered syntaxin molecules are in dynamic equilibrium with each other and all that is needed for clustering are weak homophilic interactions between plasmalemmal syntaxin molecules. Because strong overexpression of syntaxin increases cluster number rather than cluster size and does not generate a uniform syntaxin distribution (*7*), it is unlikely that other proteins are involved in the clustering mechanism. We therefore asked whether size and dynamics of such microdomains could be governed by simple physical principles rather than by elaborate layers of biological regulation. In the first scenario, clusters would form by self-organization solely depending on weak attractive forces involving homophilic SNARE motif interactions (likely supported by cholesterol) that are balanced by repulsive forces that may include steric hindrance due to crowding.

To test whether this is possible, we simulated FRAP experiments by Brownian dynamics (Fig. 4, A and B) using a simple interaction potential between individual syntaxin molecules (Fig. 4B inset, bold line). An additional repulsive component was introduced, which strengthens with cluster size (Fig. 4B inset, dashed lines showing the resulting potentials). The known concentration of syntaxin [about 1800 molecules per $\mu m^2$; see also (*15*)] was used, and syntaxin diffusion was assumed to be similar to that of the construct lacking the cytoplasmatic part, which had been shown previously not to participate in syntaxin clusters (*7*). Of the two adjustable parameters, the effective attraction and the strength of the repulsive component, only those parameter combinations were considered for which the simulations equilibrated at the experimental cluster density. For each of the allowed combinations, the sim-

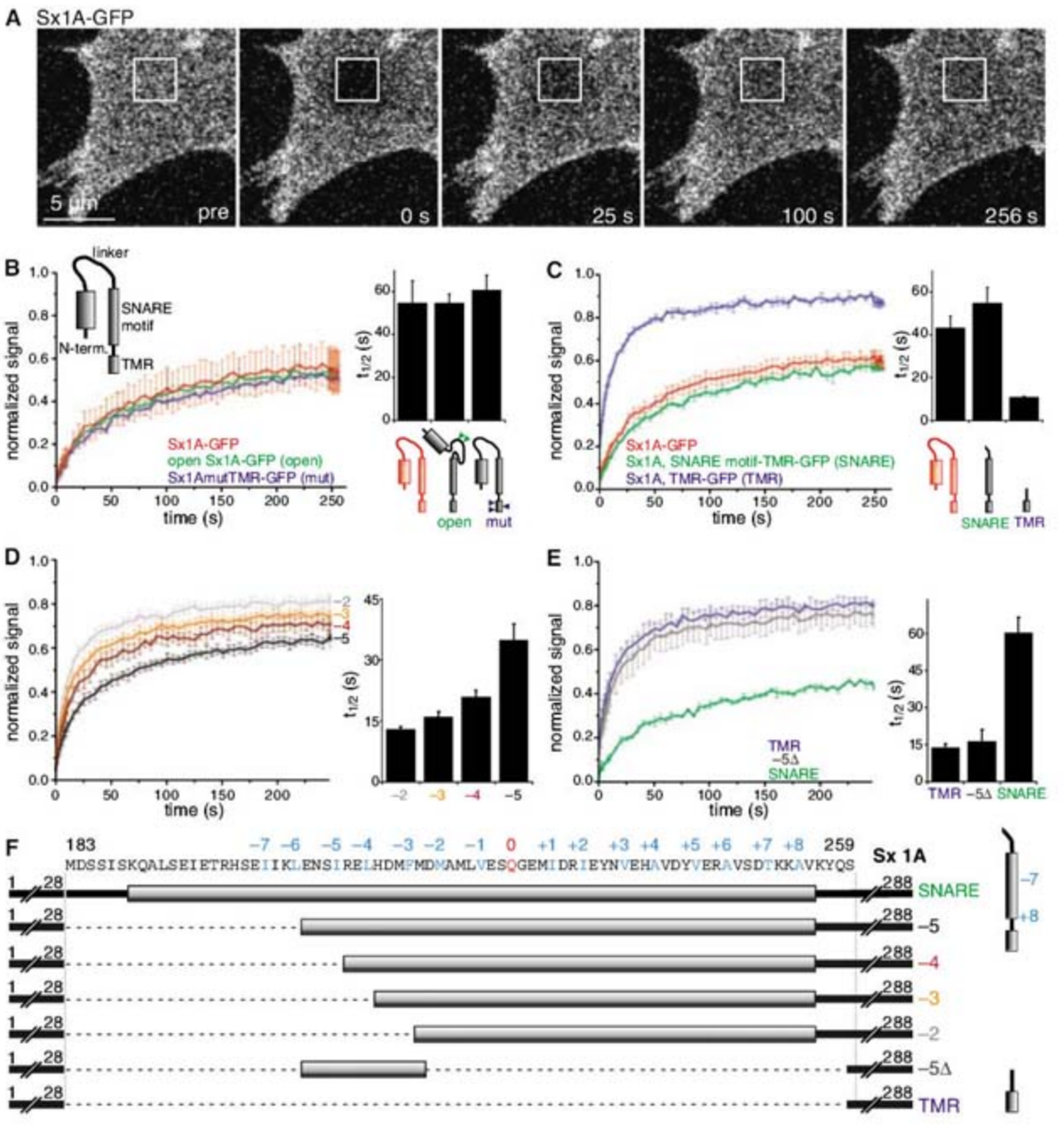


**Fig. 2.** Syntaxin 1 mobility is determined by the clustering reaction. (**A**) Confocal images from the basal plasma membrane of a PC12 cell expressing GFP-labeled syntaxin 1A. A squared region was bleached and FRAP was monitored. In one experiment, traces from individual cells (fig. S6) were averaged and fitted, and the recovery half time was determined. For each set of experiments [(B) to (E); *n* from 3 to 5 independent experiments), the means ± SEM of the recovery half times and the trace obtained by averaging the single experiments are shown. Syntaxin 1A (S × 1A) was compared to point mutants (**B**) or deletion derivates (**C**). (**D** and **E**) Testing the constructs indicated in (**F**), we studied the mechanism by which the SNARE motif controls mobility in further detail. Construct –4 is significantly different from –2, –3, and –5 ($P < 0.05$, paired *t* test, $n = 5$). (F) Numbers –7 to +8 refer to amino acids (*24*) (highlighted in blue and red) participating in layers of interaction in a hypothetical SNARE core complex (*25*).

ulation equilibrated at different amounts of syntaxin molecules per cluster and hence different fractions of free syntaxin, as indicated in Fig. 4B. With proper selection of the free syntaxin fraction, perfect agreement with the measured recovery curve was obtained (Fig. 4B, green curve). This shows that the observed self-organizing process can be explained in terms of simple interactions. Further, an average cluster size of 75 molecules is predicted by the simulation, with the remaining circa 300 molecules/$\mu m^2$ (corresponding to 16%) diffusing mostly individually between clusters. Exchange between clustered and freely diffusing molecules is governed by a distribution of dissociation time constants (fig. S5) with an average rate constant of $\langle k_{off} \rangle$ = 25,000/s. Although only a small fraction of syntaxin is freely diffusing, a much higher degree of fluorescence recovery is reached because both pools of syntaxin are in equilibrium with each other. Moreover, clusters become immobile during the simulation within diffraction-limited resolution, another characteristic that is consistent with our experimental data.

Whereas the molecular basis for attractive forces can be readily explained by homophilic interactions of the SNARE motif, the origin of repulsive forces is less obvious. An in silico model of 75 open syntaxin molecules, oligomerized tightly via their SNARE motifs (Fig. 4C, left), offers a plausible and consistent explanation. In this model, the bulky N-termini would cause syntaxins to adopt a half-closed conformation at the rim of the cluster, resulting in a bunchlike structure. The 50-nm diameter of the structure formed by the N-termini, which contain the epitope for antibody staining, agrees with the cluster dimensions measured by STED microscopy. In this structure, molecules are conformationally constrained, and steric hindrance complicates attachment of more molecules with increasing cluster size. This effect would set an upper limit for the degree of oligomerization and provides a molecular explanation for the repulsive forces in the simulation. Further, it explains the immobile fraction of syntaxins in terms of slow release of inner molecules. Lastly, the bunchlike structure predicts that overexpression

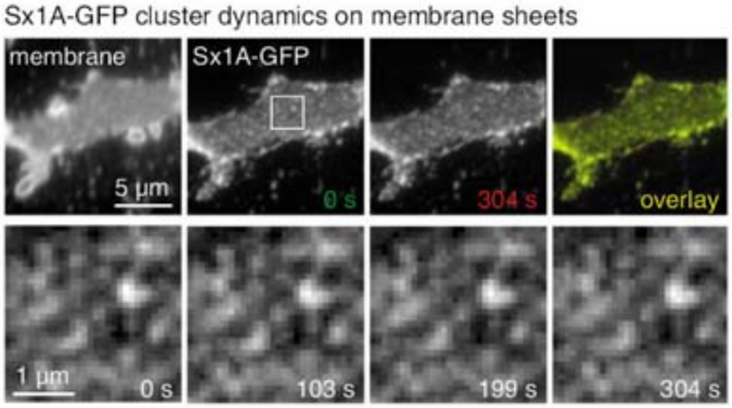


**Fig. 3.** Mobility of syntaxin clusters. Membrane sheet generated from a syntaxin 1A–GFP–expressing PC12 cell. A 5-min time-lapse experiment using epifluorescence microscopy was performed. Top left, 1-(4- trimethylammoniumphenyl)-6-phenyl-1,3,5-hexatriene (TMA-DPH) staining for phospholipids of the membrane sheet. Middle and last images, first and last images of the GFP channel and corresponding overlay. The Pearson correlation coefficient of the first and last image was calculated, indicating high similarity [0.82 ± 0.11 (mean ± SD; $n$ = 16 membrane sheets)]. Bottom images show magnified views of the boxed region (top) at indicated times.

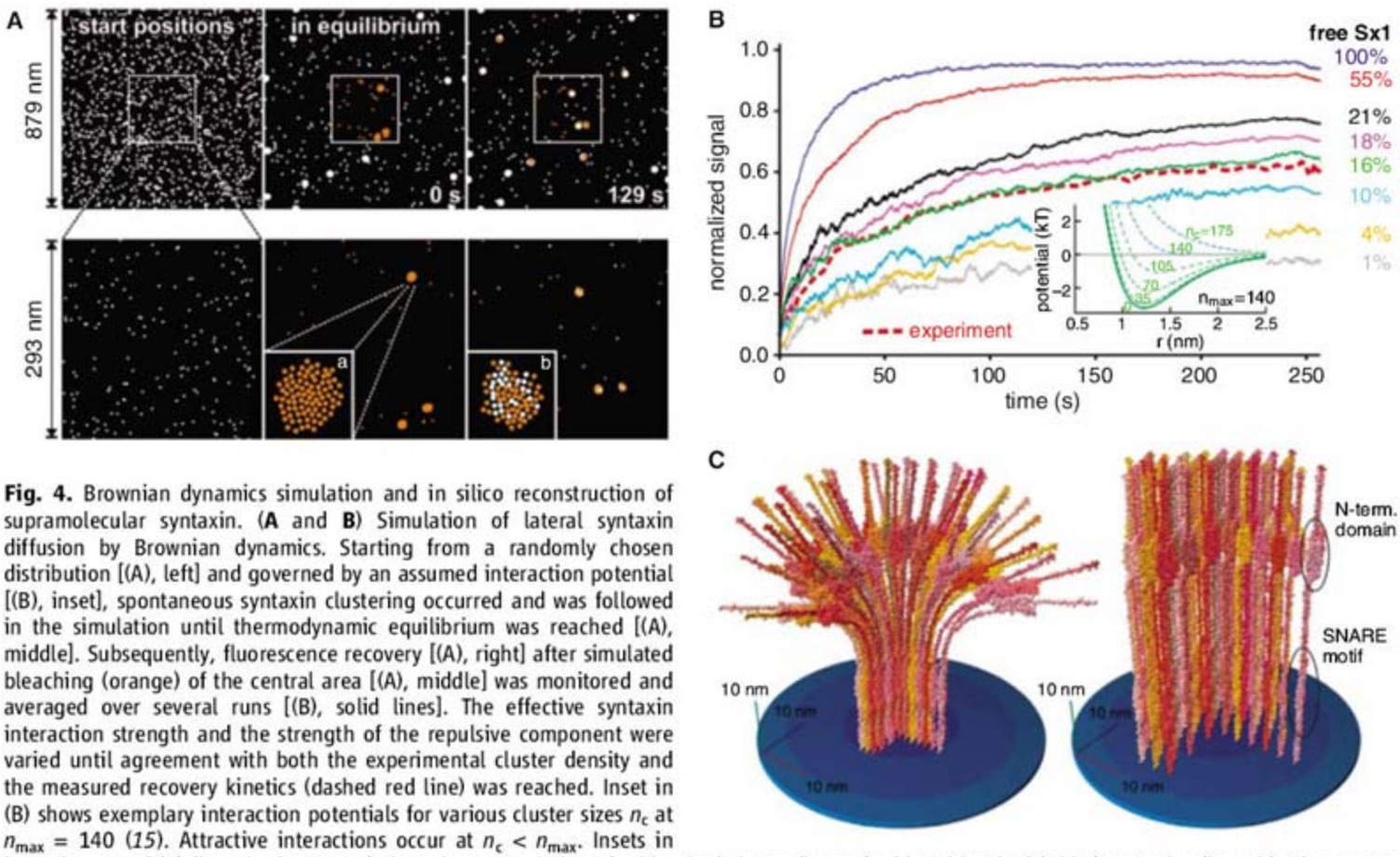


**Fig. 4.** Brownian dynamics simulation and in silico reconstruction of supramolecular syntaxin. (**A** and **B**) Simulation of lateral syntaxin diffusion by Brownian dynamics. Starting from a randomly chosen distribution [(A), left] and governed by an assumed interaction potential [(B), inset], spontaneous syntaxin clustering occurred and was followed in the simulation until thermodynamic equilibrium was reached [(A), middle]. Subsequently, fluorescence recovery [(A), right] after simulated bleaching (orange) of the central area [(A), middle] was monitored and averaged over several runs [(B), solid lines]. The effective syntaxin interaction strength and the strength of the repulsive component were varied until agreement with both the experimental cluster density and the measured recovery kinetics (dashed red line) was reached. Inset in (B) shows exemplary interaction potentials for various cluster sizes $n_c$ at $n_{max}$ = 140 (*15*). Attractive interactions occur at $n_c < n_{max}$. Insets in lower images of (A) (length of 14.7 nm) show the repopulation of a bleached cluster (inset a) with unbleached (white) syntaxins (inset b). Please note that at diffraction-limited resolution, images of the clusters appear blurred, resulting in spotty signals (Fig. 1A) with diameters of several hundred nanometers (about the size of the inset box). For this reason, in Fig. 3 cluster motions over small distances cannot be detected. (**C**) In silico reconstructions of supramolecular syntaxin.

of syntaxin increases the number of clusters rather than their size, which is in agreement with previous observations (*7*). In contrast, a hypothetical cylindrical syntaxin arrangement (Fig. 4C, right) would not explain our findings.

The self-organization model shows that a simple balance between weak homophilic interactions and a repulsive component can explain all available experimental data on the composition and the dynamics of syntaxin clusters.

Syntaxin clustering via self-assembly is likely a paradigm that applies to a variety of membrane protein clusters. Like the syntaxins, many other membrane proteins are known both to form clusters and to homo-oligomerize in vitro via their cytoplasmic domain. Examples include structurally diverse proteins such as synaptotagmins (*13*, *20*) and receptors (*4*, *21*) (containing single transmembrane domains), anion transporters [e.g., (*22*)] containing multiple transmembrane domains, and proteins such as reggie with lipid anchors [e.g., (*23*)]. The tendency to form homo-oligomers in solution would be enhanced in the plane of a membrane where membrane anchoring orients the molecules ideally for oligomerization. Hence, in the membrane self-association is enforced, leading finally to nanodomains containing many copies of the self-assembled membrane proteins. Thus, just as for the syntaxins, homo-oligomerization will likely lead to cluster formation for any membrane protein that can self-associate in solution.

The concept of clustering via self-assembly is not restricted to membrane proteins oligomerizing via their cytoplasmic domain. Rather, it can be widely applied to membrane proteins oligomerizing via their transmembrane or extracellular domains, with the only prerequisite being that in these cases there would be additional protein domains causing steric crowding or other repulsive forces, as, for example, accumulating charges.

As outlined above, the mechanisms underlying the high degree of membrane micropatterning are not well understood for most membrane proteins. With syntaxin 1 as an example, we present a conceptual framework for the description of protein domains in membranes. This biological principle is expected to explain a considerable part of the compositional variability of membrane protein clusters and hence will help to advance our understanding of membrane micropatterning.

### References and Notes


1. S. J. Singer, G. L. Nicolson, *Science* **175**, 720 (1972).
2. K. Simons, E. Ikonen, *Nature* **387**, 569 (1997).
3. A. Kusumi *et al.*, *Annu. Rev. Biophys. Biomol. Struct.* **34**, 351 (2005).
4. S. Uhles, T. Moede, B. Leibiger, P. O. Berggren, I. B. Leibiger, *J. Cell Biol.* **163**, 1327 (2003).
5. M. Kai *et al.*, *J. Biochem. (Tokyo)* **140**, 677 (2006).
6. S. H. Low *et al.*, *Mol. Biol. Cell* **17**, 977 (2006).
7. J. J. Sieber, K. I. Willig, R. Heintzmann, S. W. Hell, T. Lang, *Biophys. J.* **90**, 2843 (2006).
8. T. Lang *et al.*, *EMBO J.* **20**, 2202 (2001).
9. M. Ohara-Imaizumi *et al.*, *J. Biol. Chem.* **279**, 8403 (2004).
10. S. A. Predescu, D. N. Predescu, K. Shimizu, I. K. Klein, A. B. Malik, *J. Biol. Chem.* **280**, 37130 (2005).
11. J. C. Lerman, J. Robblee, R. Fairman, F. M. Hughson, *Biochemistry* **39**, 8470 (2000).
12. S. W. Hell, J. Wichmann, *Opt. Lett.* **19**, 780 (1994).
13. K. I. Willig, S. O. Rizzoli, V. Westphal, R. Jahn, S. W. Hell, *Nature* **440**, 935 (2006).
14. G. Donnert *et al.*, *Proc. Natl. Acad. Sci. U.S.A.* **103**, 11440 (2006).
15. Materials and methods are available on *Science* Online.
16. A. K. Kenworthy *et al.*, *J. Cell Biol.* **165**, 735 (2004).
17. A. T. Brunger, *Q. Rev. Biophys.* **38**, 1 (2005).
18. R. Laage, J. Rohde, B. Brosig, D. Langosch, *J. Biol. Chem.* **275**, 17481 (2000).
19. I. Dulubova *et al.*, *EMBO J.* **18**, 4372 (1999).
20. M. Fukuda, E. Kanno, Y. Ogata, K. Mikoshiba, *J. Biol. Chem.* **276**, 40319 (2001).
21. K. Kanazawa, A. Kudo, *J. Bone Miner. Res.* **20**, 2053 (2005).
22. D. Navaratnam, J. P. Bai, H. Samaranayake, J. Santos-Sacchi, *Biophys. J.* **89**, 3345 (2005).
23. C. Neumann-Giesen *et al.*, *Biochem. J.* **378**, 509 (2004).
24. Single-letter abbreviations for the amino acid residues are as follows: A, Ala; C, Cys; D, Asp; E, Glu; F, Phe; G, Gly; H, His; I, Ile; K, Lys; L, Leu; M, Met; N, Asn; P, Pro; Q, Gln; R, Arg; S, Ser; T, Thr; V, Val; W, Trp; and Y, Tyr.
25. R. B. Sutton, D. Fasshauer, R. Jahn, A. T. Brunger, *Nature* **395**, 347 (1998).


26. The authors thank R. Jahn and S. O. Rizzoli for helpful suggestions on the manuscript, V. Westphal and J. Keller for help with analysis software, K.-H. Drexhage for providing the dyes Atto532 and Atto647N, and F. E. Zilly and M. G. Holt for gifts of a plasmid and a recombinant protein, respectively. T.L. was supported by a grant from the Deutsche Forschungsgemeinschaft (LA1272/2). S.W.H. consults for Leica Microsystems CMS, Gmbh, Mannheim, Germany.


### Supporting Online Material

www.sciencemag.org/cgi/content/full/317/5841/1072/DC1
Materials and Methods
Figs. S1 to S7
References

23 February 2007; accepted 13 July 2007
10.1126/science.1141727

# Domain Architecture of Pyruvate Carboxylase, a Biotin-Dependent Multifunctional Enzyme

**Martin St. Maurice,[1] Laurie Reinhardt,[1] Kathy H. Surinya,[2] Paul V. Attwood,[3] John C. Wallace,[2] W. Wallace Cleland,[1] Ivan Rayment[1]***

**Biotin-dependent multifunctional enzymes carry out metabolically important carboxyl group transfer reactions and are potential targets for the treatment of obesity and type 2 diabetes. These enzymes use a tethered biotin cofactor to carry an activated carboxyl group between distantly spaced active sites. The mechanism of this transfer has remained poorly understood. Here we report the complete structure of pyruvate carboxylase at 2.0 angstroms resolution, which shows its domain arrangement. The structure, when combined with mutagenic analysis, shows that intermediate transfer occurs between active sites on separate polypeptide chains. In addition, domain rearrangements associated with activator binding decrease the distance between active-site pairs, providing a mechanism for allosteric activation. This description provides insight into the function of biotin-dependent enzymes and presents a new paradigm for multifunctional enzyme catalysis.**

In biochemical pathways, metabolites must be efficiently transferred between enzymes to avoid the energetic penalty associated with their loss to diffusion, degradation, or competing side-reactions. Particularly efficient transfer is afforded by multifunctional enzymes that directly transfer products from one reactive site to the next through tunnels and channels (*1*) or through the use of covalently attached prosthetic groups (*2*). Although the reactions catalyzed at the individual active sites of many multifunctional enzymes are well understood, few studies have detailed their complete domain architecture. Consequently, descriptions of intermediate transfer between active sites in multifunctional enzymes remain largely incomplete.

The multifunctional enzymes of the biotin-dependent family use a covalently attached biotin prosthetic group to directly transfer an activated $CO_2^-$ intermediate between distinct active sites in several essential metabolic reactions (*3*). Some members of this enzyme family, including acetyl–coenzyme A carboxylase (ACC) and pyruvate carboxylase (PC), have recently attracted interest as potential targets in the treatment of obesity and type 2 diabetes (*4*, *5*). Although several individual domain structures have been determined for various family members (*6*–*9*), the relative arrangement of these domains in a complete multifunctional enzyme remains unknown. PC is typically composed of three distinct functional domains arranged on a single 120- to 130-kD polypeptide chain. The three domains are an N-terminal biotin carboxylase (BC) domain, a central carboxyltransferase (CT)

[1]Department of Biochemistry, University of Wisconsin, Madison, WI 53706, USA. [2]School of Molecular and Biomedical Science, University of Adelaide, SA 5005, Australia. [3]School of Biomedical, Biomolecular, and Chemical Sciences, University of Western Australia, Crawley, WA 6009, Australia.

*To whom correspondence should be addressed. E-mail: Ivan_Rayment@biochem.wisc.edu

domain, and a C-terminal biotin carboxyl carrier protein (BCCP) domain (Fig. 1A). The enzyme uses a covalently attached biotin cofactor to catalyze the adenosine triphosphate (ATP)–dependent carboxylation of pyruvate to oxaloacetate in two steps (*10*). Biotin is initially carboxylated at the BC active site by ATP and bicarbonate. The carboxyl group is subsequently transferred by carboxybiotin to a second active site in the CT domain, where pyruvate is carboxylated to generate oxaloacetate. The BCCP domain transfers the tethered cofactor between the two remote active sites. To discover what distance is traversed by the BCCP domain and what domain motions facilitate the transfer of biotin between active sites, we have determined the crystal structure of the complete PC enzyme.

The crystal structure of PC from *Rhizobium etli* (RePC) was determined by single-wavelength anomalous diffraction and solvent flattening, followed by molecular replacement (*11*). The final model was refined to a resolution of 2.0 Å (see table S1 for refinement statistics and fig. S1 for representative electron density). The crystals contain a dimer in the asymmetric unit. Monomer A includes the complete polypeptide chain, composed of the three functional domains [BC (blue), CT (yellow), and BCCP (red)], and a central allosteric domain (green) that has not been previously described (Fig. 1B). Monomer B is nearly complete except for the C-terminal BCCP domain, which was disordered and could not be modeled (model completeness is described in table S2). The dimer is asymmetric, and the notable differences in the position and orientation of the BC domain between the two monomers have important implications in the mechanism of PC catalysis and regulation.

The two active sites of RePC were identified through structural homology with related enzyme subunits and from the position of bound ligands. The nonhydrolyzable ATP analog, adenosine 5′-*O*-(3-thiotriphosphate) (ATP-γ-S), is bound at the active site of the BC domain (Fig. 2A). The binding site consists of an ATP-grasp fold (*12*), typical of the arrangement reported for orthologous enzymes (*6*, *13*). The overall BC domain fold is very similar [1.1 to 1.2 Å root mean square deviation (RMSD)] to the BC subunits from other family members (fig. S2A). However, the position of ATP-γ-S in the binding site of RePC reveals differences with the position of ATP in the BC subunit of ACC (*13*) (fig. S3). The position of ATP-γ-S in RePC is much more typical of other ATP-grasp binding sites (*14*, *15*) [supporting online material (SOM) text]. The CT domain of RePC also shares high structural similarity (1.1 to 1.5 Å RMSD) with the equivalent subunits from orthologous enzymes (*7*, *9*) (fig. S2B). This domain consists of a core $\alpha_8\beta_8$ barrel capped by a funnel that centers on a structurally conserved metal ion at the active site. The metal ion in RePC superimposes closely with the active-site metal ions of orthologous enzymes. Metal-ion analysis indicates that $Zn^{2+}$ is the active-site metal in RePC, which is consistent with the observed electron density. Mutations of residues directly ligating this $Zn^{2+}$ ion either eliminate or substantially reduce the catalytic activity of PC (*16*).

PC is subject to a variety of allosteric control mechanisms (*5*), and acetyl–coenzyme A (acetyl-CoA) is an allosteric activator for PC enzymes from many species (*17*). Both acetyl-CoA and the nonhydrolyzable analog, ethyl-CoA, are activators of RePC, with activation constant $K_A$ values of 30.4 and 360 μM, respectively (table S3). RePC was cocrystallized with ethyl-CoA, and the partial electron density allowed the nucleotide portion of the activator to be modeled into the structure, revealing the location of the allosteric binding site. The binding site is located in a previously unrecognized domain that serves as a mediator among the BC, CT, and BCCP domains. The allosteric domain consists of four antiparallel β strands bracketing a central α helix (Fig. 1B, green) and superficially resembles the protein fold and acetyl-CoA binding of the GCN-5–related acetyltransferases (*18*) [secondary structure matching (*19*) gives a weak *Q* score of 0.053 with a GCN-5–related aminoglycoside 3-*N*-acetyltransferase, 1bo4]. The central α helix

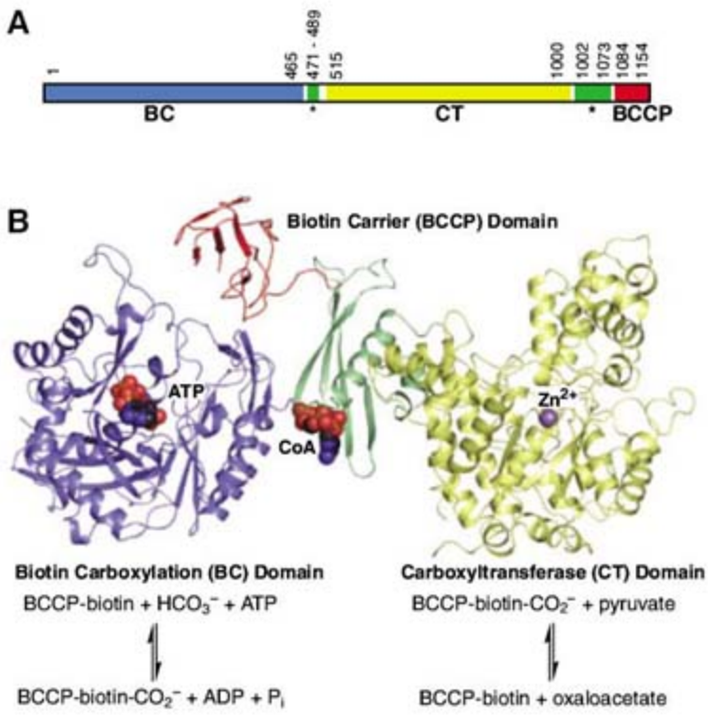


**Fig. 1.** (**A**) Schematic drawing of the primary structure arrangement for the multidomain PC from *R. etli*. The allosteric domain, indicated with asterisks, includes residues 471 to 489 and 1002 to 1073. (**B**) The structure of the *R. etli* PC monomer A. The BC, CT, BCCP, and allosteric domains are colored blue, yellow, red, and green, respectively. The chemical reactions catalyzed in the individual domains are illustrated below the corresponding domain structure. ADP, adenosine diphosphate; $P_i$, inorganic phosphate.

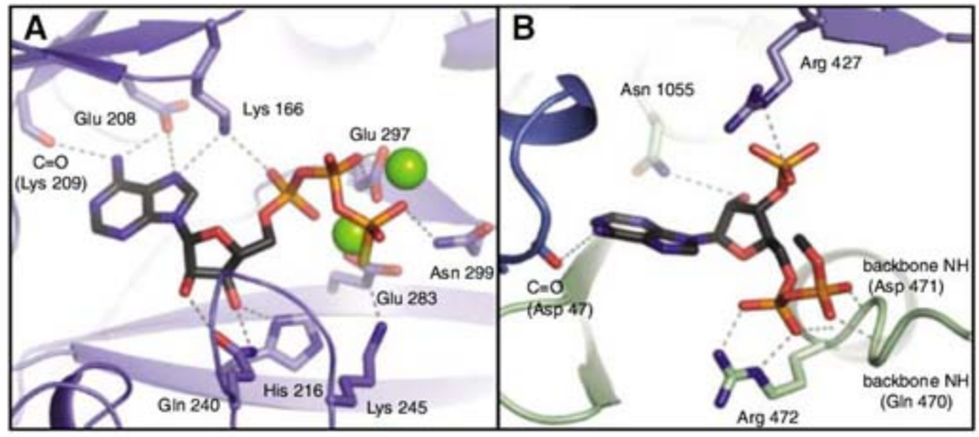


**Fig. 2.** (**A**) The ATP binding site. The revised definition of the precise ATP binding site reveals several interacting residues not previously noted in the structure of the BC subunit from ACC. In particular, the interaction of $Lys^{245}$ with the γ-phosphate of ATP is consistent with substrate-labeling studies that suggest that this residue directly interacts with ATP (*30*). Several previously unrecognized residues, including $Glu^{283}$, $Glu^{297}$, and $Asn^{299}$, are now seen to be important for coordinating the two essential $Mg^{2+}$ ions (depicted as green spheres) and ATP binding. (**B**) The ethyl-CoA binding site. Interactions with the nucleotide portion of ethyl-CoA include residues from both BC subunits and from the allosteric domain. Most notably, $Arg^{472}$ of the allosteric domain creates a strong interaction with the 5′ α-phosphate of ethyl-CoA.

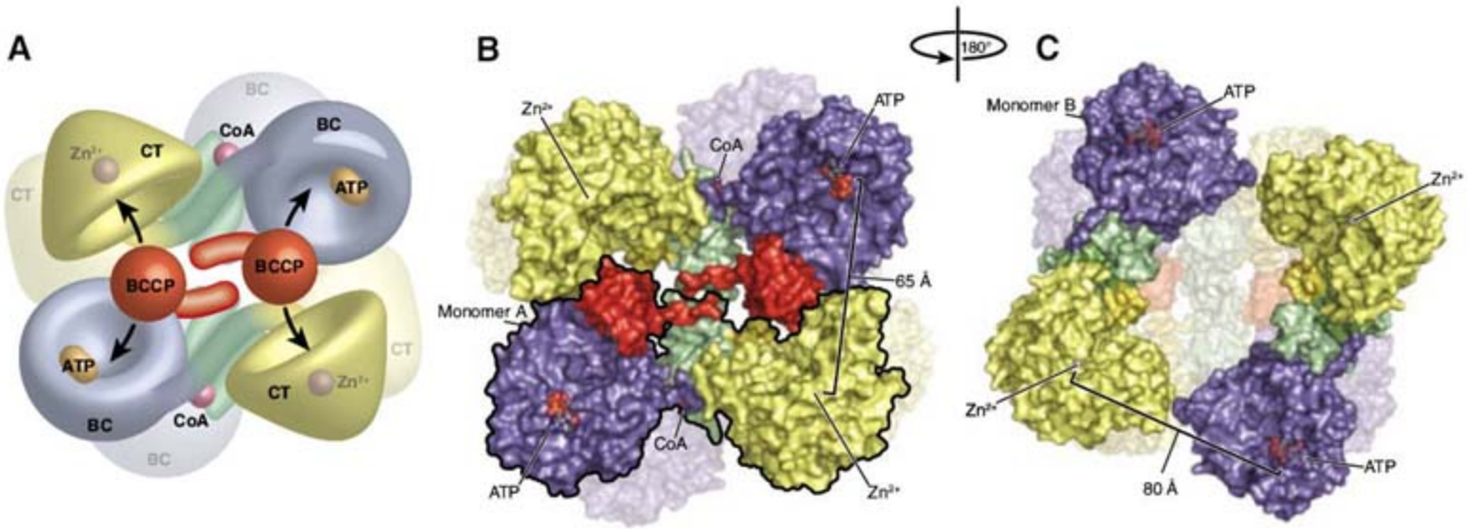


**Fig. 3.** (**A**) Model of the RePC tetramer showing the movement of the BCCP domain between neighboring active sites on opposing polypeptide chains. (**B**) Surface representation of the top face of the tetramer. For clarity, one of the two individual monomers has been outlined in black. The distance between ATP-γ-S in the BC active site and $Zn^{2+}$ in the CT active site of the opposing polypeptide chain is 65 Å. (**C**) Surface representation of the bottom face of the tetramer, after a 180° rotation about the *y* axis. The BCCP domain is disordered in these monomers and could not be modeled. The distance between ATP-γ-S in the BC active site and $Zn^{2+}$ in the CT active site of the opposing polypeptide chain increases to 80 Å as a result of the altered orientation of the BC domain.

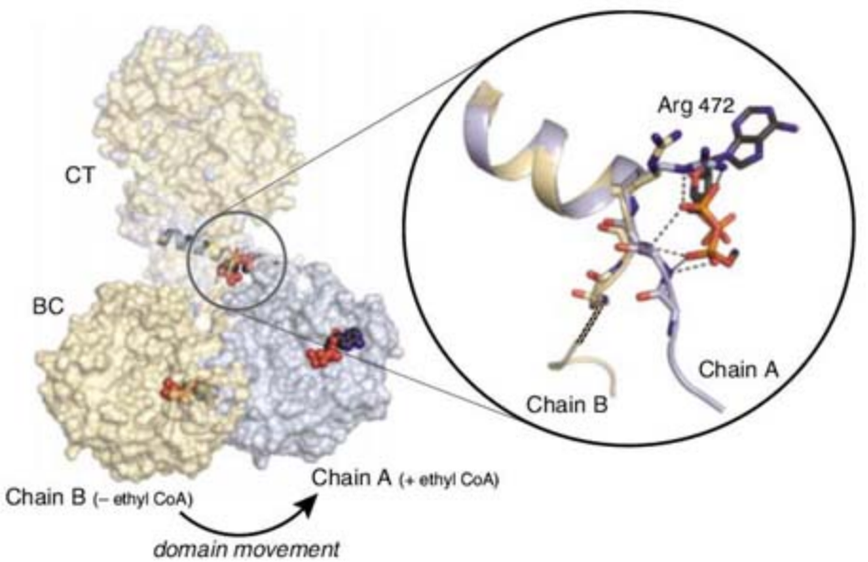


**Fig. 4.** Ethyl-CoA binding alters the position and orientation of the BC domain. The allosteric domain of monomer A was aligned with the allosteric domain of monomer B. The superposition shows minor deviations in the CT domain but substantial deviations in the BC domain. The BC domain begins to deviate precisely at the three residues forming tight hydrogen-bonding interactions with the 5′ α- and β-phosphates of ethyl-CoA: $Arg^{472}$ and the backbone amides of $Gln^{470}$ and $Asp^{471}$. Where ethyl-CoA is unbound in monomer B, the side chain of $Arg^{472}$ is pointed away from the position occupied by the activator, and the backbone of $Gln^{470}$ and $Asp^{471}$ threads from a radically different direction.

includes $Asp^{471}$ to $His^{488}$ and connects the BC and CT domains, whereas $Asp^{1018}$ to $Asp^{1065}$ fold around this helix in an antiparallel ($\beta_4$) sheet and connect the CT domain to the BCCP domain. The allosteric domain displays no sequence similarity with other members of the biotin-dependent enzyme family, suggesting that it is specific to PC. Ethyl-CoA is bound at the N-terminal end of the central α helix, near the BC-BC dimer interface (Fig. 2B). Residues interacting with the nucleotide portion of CoA are highly conserved among PC enzymes, explaining why PC from *Corynebacterium* (*20*) and subunit-type PCs (*17*) that have mutations or deletions in these residues are not activated by acetyl-CoA.

A critical feature of multifunctional enzyme catalysis is the requisite transfer of intermediates between remote active sites. The structure of RePC monomer A includes a complete BCCP domain relative to the individual catalytic domains of the enzyme, which advances our understanding of intermediate transfer. Although the electron density for the biotin cofactor was disordered, the global position and structure of the BCCP domain provide a powerful restraint on the arrangement of the prosthetic group carrier (SOM text). It is clear from the structure that the distance between active sites greatly exceeds the ~16 Å length of the biotin arm. Thus, the BCCP domain itself must move as it carries biotin between the active sites. The 34 Å linker connecting BCCP to the allosteric domain is highly flexible (*8*, *21*), facilitating domain movement. The linker is similar to those described for the lipoyl domains of 2-oxo acid dehydrogenase (*22*). If the BCCP domain were to transfer carboxybiotin between active sites on the same polypeptide chain, a dramatic domain movement would be required. Alternatively, serving between active sites on opposing polypeptide chains necessitates substantially less motion. The quaternary structure and kinetic evidence described below support the latter scenario.

The RePC crystal lattice contains a tetramer, composed of a dimer of dimers. The tetramer is stabilized by conserved dimerization interfaces between neighboring BC domains and between neighboring CT domains. PC exists predominantly as a tetramer in solution, and only the tetramer catalyzes the overall reaction (*23*). The tetramer is asymmetric, with ethyl-CoA bound to each of the two (monomer A) monomers on the top face, whereas the two (monomer B) monomers on the bottom face are unbound. On the top face, the BC active site is positioned ~65 Å from the CT active site of an opposing polypeptide chain, with the biotinylated BCCP domain positioned equidistant between the two. Based on the distance and orientation between these opposing active sites, the BCCP domain is predicted to swing between active-site pairs on opposing polypeptide chains rather than between active sites on the same chain (Fig. 3).

To confirm this prediction, we created two RePC mutants. In one construct, the biotinylated $Lys^{1119}$ residue was mutated to prevent biotinylation of the BCCP domain, and, in the second construct, a carbamylated $Lys^{718}$ in the CT active site was mutated to impair the second half-reaction.

When assayed individually, the mutant enzymes $Lys^{1119}$→$Gln^{1119}$ (K1119Q) and K718Q exhibited 0.1 and 4% wild-type activity, respectively (table S4). Hybrid tetramers were created by mixing and diluting the mutants together before assaying for enzyme activity. Dilution of PC promotes equilibration among monomers, dimers, and tetramers (*23*) and allows a mixed heterotetramer population to reassociate. The mixed population of heterotetramers exhibited 20% wild-type activity (table S3), nearly five times as much as that observed with either mutant homotetramer and near to the maximum predicted activity of 26% (fig. S4). The recovery of activity on reassociation is possible only if the hybrid tetramers recombine to restore a functional pair of neighboring active sites, capable of transferring the tethered carboxybiotin intermediate between two opposing chains. The transfer of a carboxybiotin intermediate between active sites on separate polypeptide chains is a previously unrecognized feature of PC catalysis. Several multifunctional enzymes have similarly been shown to transfer their tethered intermediates between active sites on opposing polypeptide chains (*24*, *25*), suggesting that intermolecular intermediate transfer is a common and essential feature of catalysis.

Ethyl-CoA is bound to only one monomer of the RePC asymmetric dimer, permitting a direct comparison of the consequences of activator binding on domain arrangement and orientation. A superposition of the two monomers reveals a 40° rotation and a translocation of nearly 40 Å in the BC active site, centered at the ethyl-CoA binding site of the allosteric domain (Fig. 4). In the tetramer, ethyl-CoA is bound to both monomers on the top face, and the BC active site is positioned ~65 Å from its opposing CT active-site pair (Fig. 3B). On the bottom face of the tetramer, ethyl-CoA is unbound, and the distance between the opposing active-site pairs increases to ~80 Å (Fig. 3C). The rotation in the BC domain inhibits acetyl-CoA binding on the bottom face of the tetramer. Thus, only two binding sites are available per tetramer, which is consistent with the Hill coefficient observed for yeast PC (*26*) and with the observation that only 50% of acetyl-CoA binding sites are occupied in yeast PC (*27*). The structure suggests that acetyl-CoA activates PC by decreasing the distance between neighboring active sites. While the active-site pairs on the top face of the tetramer are pushed closer together, the active-site pairs on the bottom face are pulled farther apart. This is a rare example of allosteric activation paired with negative cooperativity and implies that half of the active-site pairs are more active than the others. Recent kinetic studies and numerical simulations support half-sites reactivity for the BC subunit of ACC (*28*), suggesting that this mechanism is conserved among enzymes of the biotin-dependent family. Such half-sites reactivity may permit PC to affect efficient catalysis while maintaining its in vivo association with other metabolic enzymes (*29*).

The allosteric binding site in PC offers a target for modifiers of activity that may be useful in the treatment of obesity or type 2 diabetes, and the mechanistic insights gained from the complete structural description of RePC permit detailed investigations into the individual catalytic and regulatory sites of the enzyme. Furthermore, as a consequence of its fully defined domain architecture, PC represents a paradigm for understanding interdomain arrangement and allosteric regulation in multifunctional enzymes.

### References and Notes


1. F. M. Raushel, J. B. Thoden, H. M. Holden, *Acc. Chem. Res.* **36**, 539 (2003).
2. R. N. Perham, *Annu. Rev. Biochem.* **69**, 961 (2000).
3. S. Jitrapakdee, J. C. Wallace, *Curr. Protein Pept. Sci.* **4**, 217 (2003).
4. L. Tong, *Cell. Mol. Life Sci.* **62**, 1784 (2005).
5. S. Jitrapakdee, A. Vidal-Puig, J. C. Wallace, *Cell. Mol. Life Sci.* **63**, 843 (2006).
6. S. Kondo *et al.*, *Acta Crystallogr. D* **60**, 486 (2004).
7. P. R. Hall *et al.*, *EMBO J.* **23**, 3621 (2004).
8. E. L. Roberts *et al.*, *Biochemistry* **38**, 5045 (1999).
9. R. Studer *et al.*, *J. Mol. Biol.* **367**, 547 (2007).
10. P. V. Attwood, J. C. Wallace, *Acc. Chem. Res.* **35**, 113 (2002).
11. Materials and methods are available as supporting material on *Science* Online.
12. M. Y. Galperin, E. V. Koonin, *Protein Sci.* **6**, 2639 (1997).
13. J. B. Thoden, C. Z. Blanchard, H. M. Holden, G. L. Waldrop, *J. Biol. Chem.* **275**, 16183 (2000).
14. J. B. Thoden, G. Wesenberg, F. M. Raushel, H. M. Holden, *Biochemistry* **38**, 2347 (1999).
15. J. B. Thoden, S. Firestine, A. Nixon, S. J. Benkovic, H. M. Holden, *Biochemistry* **39**, 8791 (2000).
16. J. Yong-Biao, M. N. Islam, S. Sueda, H. Kondo, *Biochemistry* **43**, 5912 (2004).
17. S. Jitrapakdee, J. C. Wallace, *Biochem. J.* **340**, 1 (1999).
18. F. Dyda, D. C. Klein, A. B. Hickman, *Annu. Rev. Biophys. Biomol. Struct.* **29**, 81 (2000).
19. E. Krissinel, K. Henrick, *Acta Crystallogr. D* **60**, 2256 (2004).
20. P. G. Peters-Wendisch, V. F. Wendisch, S. Paul, B. J. Eikmanns, H. Sahm, *Microbiology* **143**, 1095 (1997).
21. D. V. Reddy, S. Rothemund, B. C. Shenoy, P. R. Carey, F. D. Sonnichsen, *Protein Sci.* **7**, 2156 (1998).
22. R. N. Perham, *Biochemistry* **30**, 8501 (1991).
23. P. V. Attwood, W. Johannssen, A. Chapman-Smith, J. C. Wallace, *Biochem. J.* **290**, 583 (1993).
24. V. S. Rangan, A. K. Joshi, S. Smith, *J. Biol. Chem.* **273**, 34949 (1998).
25. Y. Tang, C. Y. Kim, I. I. Mathews, D. E. Cane, C. Khosla, *Proc. Natl. Acad. Sci. U.S.A.* **103**, 11124 (2006).
26. J. J. Cazzulo, A. O. Stoppani, *Arch. Biochem. Biophys.* **127**, 563 (1968).
27. A. Chapman-Smith, G. W. Booker, P. R. Clements, J. C. Wallace, D. B. Keech, *Biochem. J.* **276**, 759 (1991).
28. M. S. de Queiroz, G. L. Waldrop, *J. Theor. Biol.* **246**, 167 (2007).
29. L. A. Fahien, J. W. Davis, J. Laboy, *J. Biol. Chem.* **268**, 17935 (1993).
30. Y. Kazuta, E. Tokunaga, E. Aramaki, H. Kondo, *FEBS Lett.* **427**, 377 (1998).


31. This work was supported by grants to W.W.C., J.C.W., and P.V.A. from NIH (GM070455) and to I.R. from NIH (AR35186). M.St.M. was supported in part by a fellowship from the Natural Science and Engineering Research Council of Canada. Use of the Structural Biology BM19 beamline Argonne National Laboratory Advanced Photon Source was supported by the U.S. Department of Energy, Office of Energy Research, under contract number W-31-109-ENG-38. We thank M. Dunn for providing the *R. etli* PC clone; V. Klenchin for helpful discussions and critical reading of the manuscript; J. B. Thoden and H. M. Holden for preliminary crystallography trials; A. Netting (Adelaide Microscopy) for technical assistance with metal-ion analysis; and A. Steinberg for his assistance in generating the illustrations. Coordinates and structure factors have been deposited in the Protein Data Bank (www.rcsb.org) with the accession number 2QF7.


### Supporting Online Material

www.sciencemag.org/cgi/content/full/317/5841/1076/DC1
Materials and Methods
SOM Text
Figs. S1 to S4
Tables S1 to S4
References

1 May 2007; accepted 5 July 2007
10.1126/science.1144504

# When Fear Is Near: Threat Imminence Elicits Prefrontal–Periaqueductal Gray Shifts in Humans

**Dean Mobbs,* Predrag Petrovic, Jennifer L. Marchant, Demis Hassabis, Nikolaus Weiskopf, Ben Seymour, Raymond J. Dolan, Christopher D. Frith**

Humans, like other animals, alter their behavior depending on whether a threat is close or distant. We investigated spatial imminence of threat by developing an active avoidance paradigm in which volunteers were pursued through a maze by a virtual predator endowed with an ability to chase, capture, and inflict pain. Using functional magnetic resonance imaging, we found that as the virtual predator grew closer, brain activity shifted from the ventromedial prefrontal cortex to the periaqueductal gray. This shift showed maximal expression when a high degree of pain was anticipated. Moreover, imminence-driven periaqueductal gray activity correlated with increased subjective degree of dread and decreased confidence of escape. Our findings cast light on the neural dynamics of threat anticipation and have implications for the neurobiology of human anxiety-related disorders.

Critical to an organism's survival is the ability to switch flexibly between defensive states in response to threat. Within behavioral ecology, a key component of defensive switching is the "predatory imminence continuum" where distinct threat states are configured according to whether a predator is distal or proximal to the prey (*1*–*5*). This continuum

encompasses three core stages: "pre-encounter," where there is risk in the absence of immediate danger; "post-encounter," where the threat is detected; and "circa-strike," defined as distal or proximal interaction with the threat stimulus (*2*).

These stages, relating to the distance from a threat, are associated with distinct patterns of activity at the neurobiological level (*6*–*8*). For example, distal threat elicits activity in the prefrontal cortices, which possibly reflects the complex planning of avoidance strategies. As threat becomes proximal, midbrain structures such as the periaqueductal gray (PAG) dominate (*3*, *6*). This shift to phylogenetically older midbrain regions has adaptive value because these structures control fast reflexive behaviors (e.g., fight, flight, or freeze) as well as fear-induced analgesia. The parallel neural dynamics of threat in humans have yet to be identified.

We hypothesized that brain activity associated with threat detection and distal and proximal distance to threat in humans would mirror those derived from defense systems models developed in rodents. We tested a prediction that detection of distal threat would elicit activity in brain regions associated with value-based and complex decision making, such as the anterior cingulate and ventromedial prefrontal cortex (vmPFC), whereas proximal threat would engage low-level midbrain regions implicated in reflexive escape behavior (i.e., PAG). To test this model, we used high-resolution functional magnetic resonance imaging (fMRI) to examine brain activity in 14 healthy subjects while they performed an active "escape-pain" task within a two-dimensional maze. The paradigm involved the subject trying to avoid a "virtual predator" that had the capacity to chase, capture, and cause pain of high (three shocks: $AI_{high}^{predator}$) or low (one shock: $AI_{low}^{predator}$) intensity (Fig. 1).

Avoidance time in the maze was significantly longer for $AI_{high}^{predator}$ (mean ± SD: 24.2 ± 1.6 s) relative to $AI_{low}^{predator}$ (19.4 ± 2.0 s) on escaped conditions ($t_{13} = -9.59$, $P < 0.0005$), suggesting that players were more motivated to escape the $AI_{high}^{predator}$. Speed, defined as number of squares per second, was significantly different between the first half and second half of the conditions ($AI_{high}^{predator}$ $t_{13} = -5.86$, $P < 0.0005$; $AI_{low}^{predator}$ $t_{13} = -5.984$, $P < 0.0005$). However, no significant difference was found for speed between the proximal $AI_{high}^{predator}$ and $AI_{low}^{predator}$ ($t_{13} = -2.94$, $P < 0.773$) conditions. A trend toward significance was evident for the number of times the subjects were captured in the $AI_{high}^{predator}$ (62.5 ± 15.9%) versus the $AI_{low}^{predator}$ condition (67.0 ± 16.4%; $t_{13} = -1.5$, $P < 0.14$). Together these results sug-

Wellcome Trust Centre for Neuroimaging, Functional Imaging Laboratory, University College London, London WC1N 3BG, UK.

*To whom correspondence should be addressed. E-mail: d.mobbs@fil.ion.ucl.ac.uk

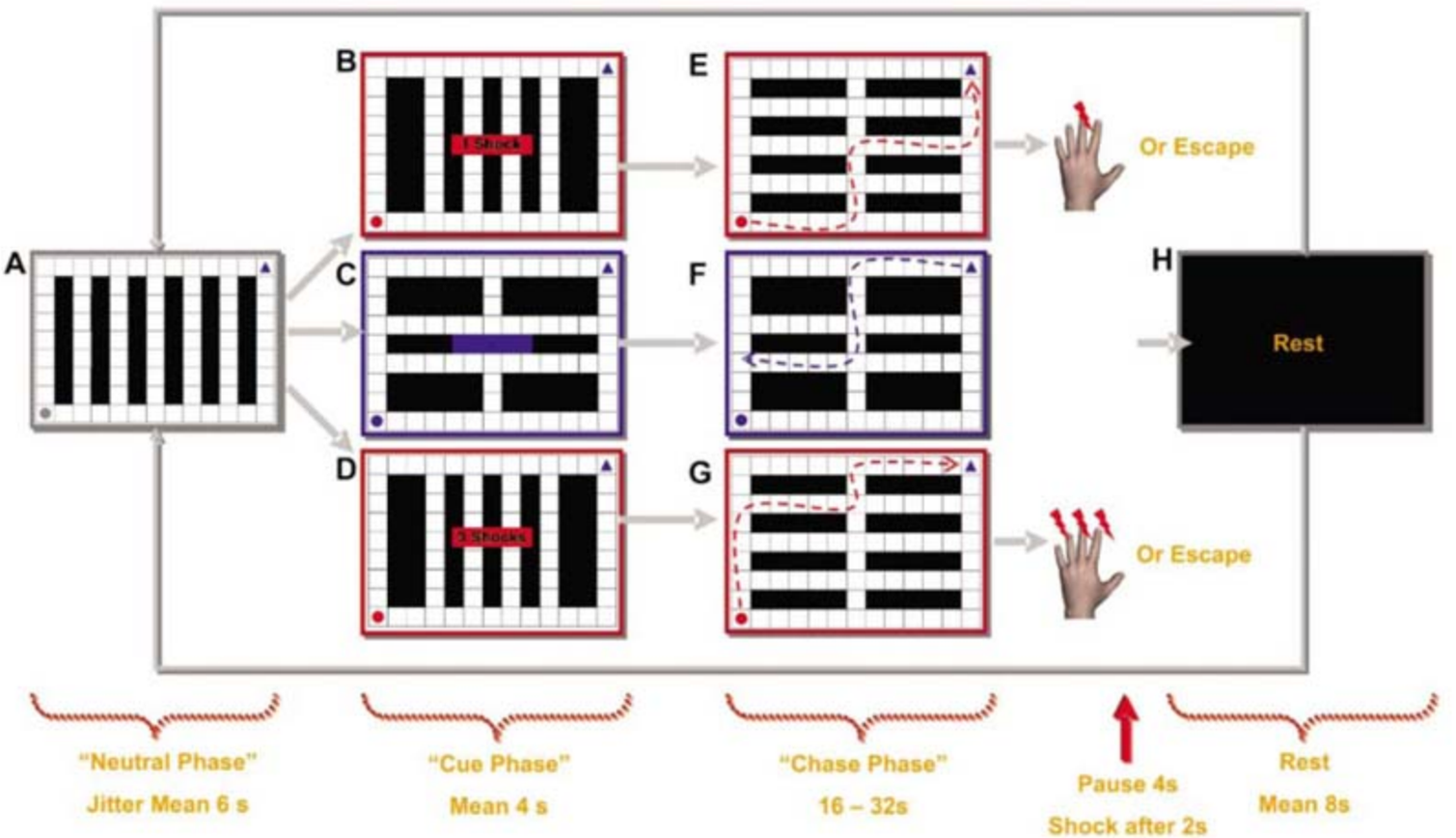


**Fig. 1.** The virtual predator and prey paradigm. Subjects were presented with a two-dimensional maze containing a 9 × 13 rectangle grid of walls (black squares) and paths (white squares). All experimental conditions commenced with a "neutral phase" where a preprogrammed artificially intelligent (AI) gray circle ($AI_{neutral}$) appeared at the left-bottom side of the maze (**A**). The $AI_{neutral}$ was presented on average for 6 s (jitter ± 2 s) and programmed to wander the maze indiscriminately. After this, the "cue phase" commenced with the $AI_{neutral}$ changed into a predator ($AI_{predator}$) or a yoked control condition. The change from $AI_{neutral}$ to $AI_{predator}$ was signaled by the circle flashing between red and gray. The flashing $AI_{predator}$ appeared for 2 s, and during this time it wandered the maze indiscriminately. Directly after this, subjects were also informed for 2 s of the amount of cutaneous electrical shock they would receive if the $AI_{predator}$ captured them: (**B**) one shock ($AI_{low}^{predator}$), (**C**) no shock, or (**D**) three shocks ($AI_{high}^{predator}$). During the cue phase, subjects were passive and unable to move the blue triangle situated in the upper right corner of the maze. The "chase phase" began with the $AI_{predator}$ ceasing to flash and the subject moving the blue triangle to (**E**) escape the $AI_{low}^{predator}$, (**F**) mimic the movements of the triangle in a replay of a previous experimental condition, or (**G**) escape the $AI_{high}^{predator}$. (**H**) After escape or capture, a rest period was presented before the onset of the next trial. To ensure that subjects would not anticipate the end of the chase, we randomly varied the time each $AI_{predator}$ encounter was played (e.g., 16, 20, 24, 28, 32 s). The subjects were not informed that the length of trials varied or given any indication of how much time they had on each trial. To enhance the feelings of spatial distance, mazes were intentionally designed so that chases were long unimpeded runs with no dead-ends. Each block was interleaved with 8, 10, or 12 s of black screen. Further details can be found in the supporting online material.

gest that subjects were more efficient in movement planning and execution when escaping the $AI_{high}^{predator}$.

For the analysis of brain activity, we first examined the evoked blood oxygenation level–dependent (BOLD) responses to the 2-s cue that indicated participants would encounter the $AI_{predator}$ (Fig. 1A and table S1) as compared to the yoked control cue (Fig. 1C). We found enhanced activity in the rostral anterior cingulate cortex [rACC; MNI space coordinates ($x$, $y$, $z$): –6, 41, 22; $Z = 3.85$; $P < 0.0005$] and medial orbitofrontal cortex (mObfc; 6, 49, –19; $Z = 3.42$; $P < 0.0005$), ventral anterior cingulate cortex (vACC; 13, 32, –14; $Z = 4.56$; $P < 0.0005$ uncorrected), and the vmPFC (–4, 39, –13; $Z = 3.48$; $P < 0.0005$).

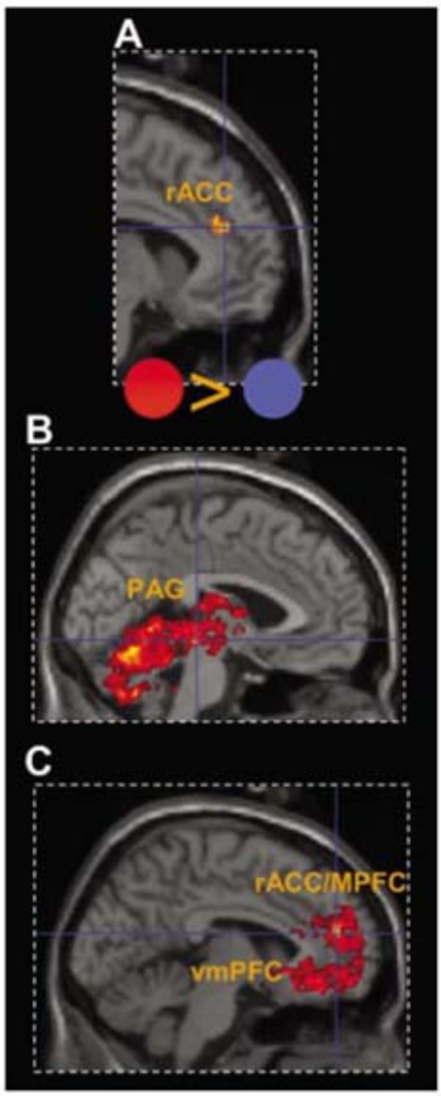


**Fig. 2.** Statistical parametric maps illustrating BOLD responses to the aversive cues and activation for the $AI_{predator}$ conditions collapsed across blocks. Mean activity is shown for regions within 4 mm of peak. (**A** and **B**) Activity for the $AI_{predator}$ (red circle) minus the $AI_{neutral}$ (blue circle) cue in (A) rACC and (B) periaqueductal gray (PAG) activity increased during all $AI_{predator}$ blocks minus yoked blocks. (**C**) Activity in the rACC/mPFC and vmPFC (table S2) for yoked blocks minus $AI_{predator}$ blocks.

For the "chase phase," we first collapsed activity across all $AI_{predator}$ blocks (i.e., $AI_{high}^{predator}$ and $AI_{low}^{predator}$ conditions) and compared them to the yoked blocks. For the $AI_{predator}$ condition, we found increased activity that peaked in the cerebellum (–5, –63, –13; $Z = 5.48$) but extended across the entire PAG (right: 3, –25, –7; $Z = 4.87$; left: –2, –28, –8; $Z = 4.94$) and posterior thalamus including the pulvinar (3, –22, 11; $Z = 4.63$) (Fig. 2B). A different pattern was observed for the yoked minus the $AI_{predator}$ blocks, where activity peaked in the medial PFC (mPFC) (–5, 48, 17; $Z = 5.50$), extending to the right vmPFC (3, 37, –9; $Z = 4.63$) and amygdala (22, –2, –18; $Z = 4.94$) (Fig. 2C and table S2).

We next asked whether there was a relationship between distal and proximal threat and brain activity for the "chase phase" of $AI_{predator}$ (Fig. 3 and table S3). We used a parametric regression between predator distance and BOLD signal, excluding the period in which the shock was administered. Thus, these effects were independent of whether shocks were actually received. Distal threat was associated with increased activity in the vmPFC, including the subgenual ACC, for both $AI_{high}^{predator}$ (–8, 35, –13; $Z = 3.66$; Fig. 3A) and $AI_{low}^{predator}$ (–10, 38, –11; $Z = 3.93$; Fig. 3B) conditions. Proximal threat was associated with increased activity in the PAG for both $AI_{high}^{predator}$ (left: –3, –33, –15; $Z = 3.58$; right: 8, –32, –21; $Z = 3.73$; Fig. 3C) and $AI_{low}^{predator}$ (6, –33, –14; $Z = 3.02$; fig. S2) conditions. Proximal $AI_{high}^{predator}$ condition also elicited activity in the right dorsal amygdala corresponding with the central nucleus (CeA)/bed nucleus of the stria terminalis (BNST) (32, 4, –13; $Z = 4.78$), whereas the distal $AI_{high}^{predator}$ elicited activity in the right lateral amygdala corresponding to the basolateral amygdala (BLA; 32, –4, –24; $Z = 3.77$). Direct subtraction showed that the $AI_{high}^{predator}$ activated the PAG to a greater extent than did the $AI_{low}^{predator}$ condition (–3, –32, –15; $Z = 3.33$). Conversely, the $AI_{low}^{predator}$ activated the anterior vmPFC (–1, 51, –1; $Z = 3.81$) and BLA (31, –4, –23; $Z = 4.09$) to a greater extent than did the $AI_{high}^{predator}$ condition (fig. S4).

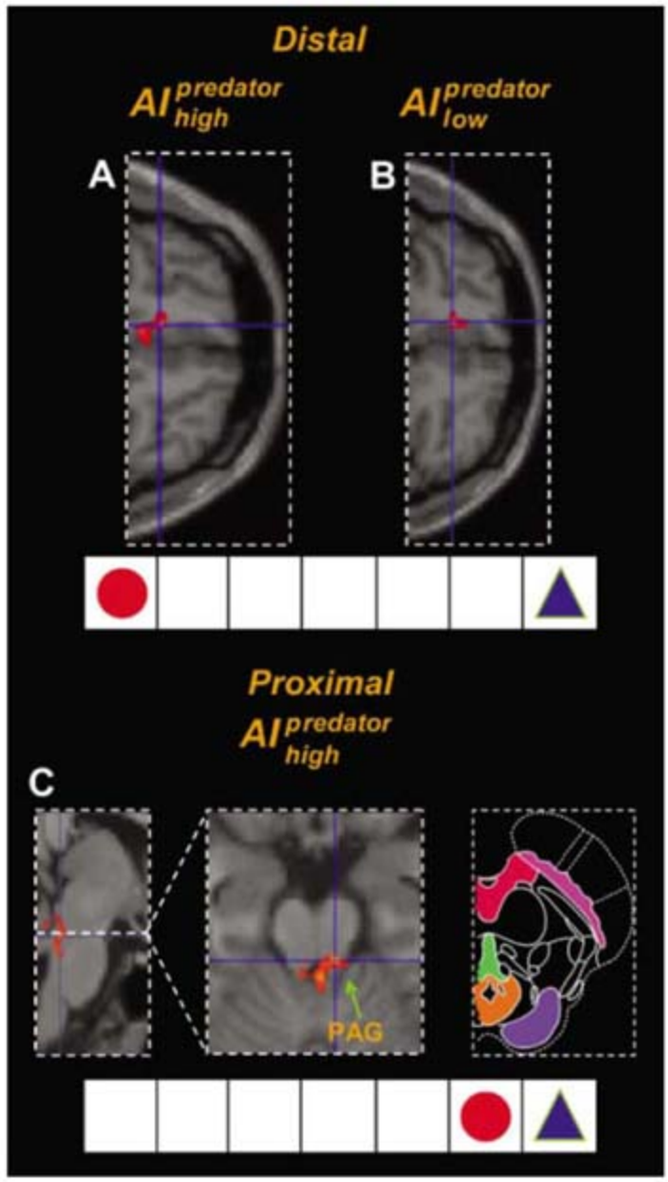


**Fig. 3.** fMRI results illustrating the imminence effect in the predator condition. For distal threat there was greater activity in vmPFC (horizontal view) for both (**A**) $AI_{high}^{predator}$ and (**B**) $AI_{low}^{predator}$ shock expectation. (**C**) For proximal threat there was greater activity in the PAG for $AI_{high}^{predator}$ [left panel, sagittal view; center panel, horizontal view; right panel, schematic depiction of the midbrain with PAG shown in orange; modified from (*27*)]. See fig. S2 for images of the PAG activity for the $AI_{low}^{predator}$ imminence. See fig. S4 for coronal view of the PAG activity.

If this forebrain-midbrain threat circuit is mediated by both geographical-temporal and psychological distance, as predicted by theorists (*4*, *5*), we would then expect subject-specific differences in psychological indices of threat to be correlated with PAG activity. We regressed post-scan reports of dread of being chased by the $AI_{predator}$ (*9*) and confidence of escaping capture with the imminence-driven BOLD signal (Fig. 4). Subjective scores of dread and confidence did not correlate (Pearson $r = -0.016$; $P < 0.96$), which suggests that they tap distinct traits.

Dread of capture correlated with enhanced activity in the PAG (11, –32, –18; $Z = 3.14$), but peaking in the vicinity of the dorsal raphe nuclei (DRN; –1, –26, –19; $Z = 4.65$), for the $AI_{high}^{predator}$ condition. A similar pattern was observed for PAG (–5, –32, –18; $Z = 3.33$) and DRN (0, –28, –19; $Z = 4.29$; fig. S5) activity in the $AI_{low}^{predator}$ condition (Fig. 4). Decreased dread was associated with medial PFC activity (–3, 48, 24; $Z = 3.56$) for the $AI_{low}^{predator}$ condition and ventral PFC activity (3, 38, –17; $Z = 3.37$) for the $AI_{high}^{predator}$ condition (table S4). Likewise, decreased confidence of escape was associated with increased activity in the PAG for both the $AI_{high}^{predator}$ (2, –29, –19; $Z = 3.19$), and $AI_{low}^{predator}$ (–3, –37, –20; $Z = 2.63$) conditions. Increased confidence of escape was associated with increased activity in the vmPFC for both conditions (table S5).

Our results show a dynamic configuration of threat responses that include the PAG and are akin to what might be predicted from animal models of defensive avoidance (*6*, *7*) and fear (*10*). When threat was detected, we observed enhanced activity in the rACC and mObfc. The rACC activation encompassed the cytoarchitectonic subdivisions of Brodmann areas 32 and 24c, which have known connections to the amygdala, mObfc, PAG, and brainstem reticular formation; these regions are critical to autonomic, visceromotor, and opioidergic functioning (*11*). One interpretation is that the rACC activity is associated with the response conflict between fleeing or staying (*3*), whereas mObfc activity represents the threat value of the $AI_{predator}$ (*12*). It has been suggested that post-encounter anticipatory anxiety promotes behavior that reduces an aversive state (e.g., avoidance) and may recruit the rACC for this purpose (*5*, *13*). The ACC markedly increases in activity with increased dread of pain (*9*) and supports our findings of a positive correlation between dread ratings and rACC activity when the $AI_{high}^{predator}$ was proximal (table S4). Notably, the ACC produces glutamatergic aversive teaching signals (*14*) that may regulate avoidance behaviors (*15*).

As hypothesized, distal threat elicited increased vmPFC activity during the chase phase. It might be argued that this prefrontal activity represents processes where different alternative goal-directed behaviors are compared in order to choose the most effective strategy to avoid the threat or distress (*16*–*18*). However, the functions of the vmPFC may also be understood by its connections to the amygdala. The BLA has direct connections with the vmPFC and mObfc and is important in determining the motivational importance of the stimuli (e.g., the degree of threat), whereas the CeA/BNST of the amygdala are major entryways into the PAG and are important for controlling a repertoire of behavioral and neurovegative defensive states (*3*, *5*, *17*, *19*). In this framework, the BLA may be more involved in active responses in the form of guidance or gating of behavior, whereas the CeA/BNST is involved in aversive conditioning and reflexive responding through its descending connections to the PAG (*3*, *6*).

When threat became proximal, we observed increased PAG activity. This forebrain-to-midbrain switch is anatomically credible in light of descending connections between the vmPFC/amygdala and PAG in the primate brain (*16*, *20*, *21*). Electrical stimulation of the human PAG can result in heightened fear and anxiety (*22*). In rats, stimulation of the ventrolateral PAG and dorsolateral PAG promotes passive (e.g., freezing) and active (e.g., escape) coping, respectively (*21*, *23*). The PAG is further divisible along the rostral-caudal axis, implicated in flight and fight (*21*). Although the functional territories of the human PAG are difficult to dissociate and should be interpreted with caution, our study shows that both the ventral and dorsal portions of the PAG were active during the $AI_{high}^{predator}$ condition. Moreover, both the $AI_{high}^{predator}$ and the $AI_{high}^{predator}$ minus $AI_{low}^{predator}$ comparisons were active in the dorsal PAG, supporting the putative role of this region in active avoidance (*21*).

Activity in the PAG was conspicuously increased during the $AI_{high}^{predator}$ condition and for participants with increased dread and decreased confidence of escape. Previous studies have shown that this forebrain-midbrain circuit is abnormal in panic and chronic anxiety patients who show decreased vmPFC but increased gray matter volume and activity in the midbrain encompassing the PAG (*24*, *25*). Intriguingly, the infralimbic vmPFC inhibits stress-induced neural activity in the rodent brainstem and is important in facilitating escape and extinction learning (*18*, *26*). Note also that the vmPFC and mObfc project directly into the dorsolateral PAG (*17*). Our results therefore support the hypothesis that the PAG is critical during immediate proximal threat, yet may be suppressed or promoted by higher prefrontal regions (*16*–*18*).

Our observations concur with the proposition of a hardwired forebrain-midbrain network, which includes the vmPFC at the lowest level of threat and interacts with the midbrain PAG as the threat level increases. From an evolutionary viewpoint, higher cortical systems control behavior when the degree of threat is appraised as non–life-endangering and guides the organism to choose the most effective and resourceful strategy for instrumental avoidance. At extreme levels of threat, the PAG may in turn inhibit more complex control processes when a fast and indeed obligatory response is required, preparing the organism for survival and possible tissue

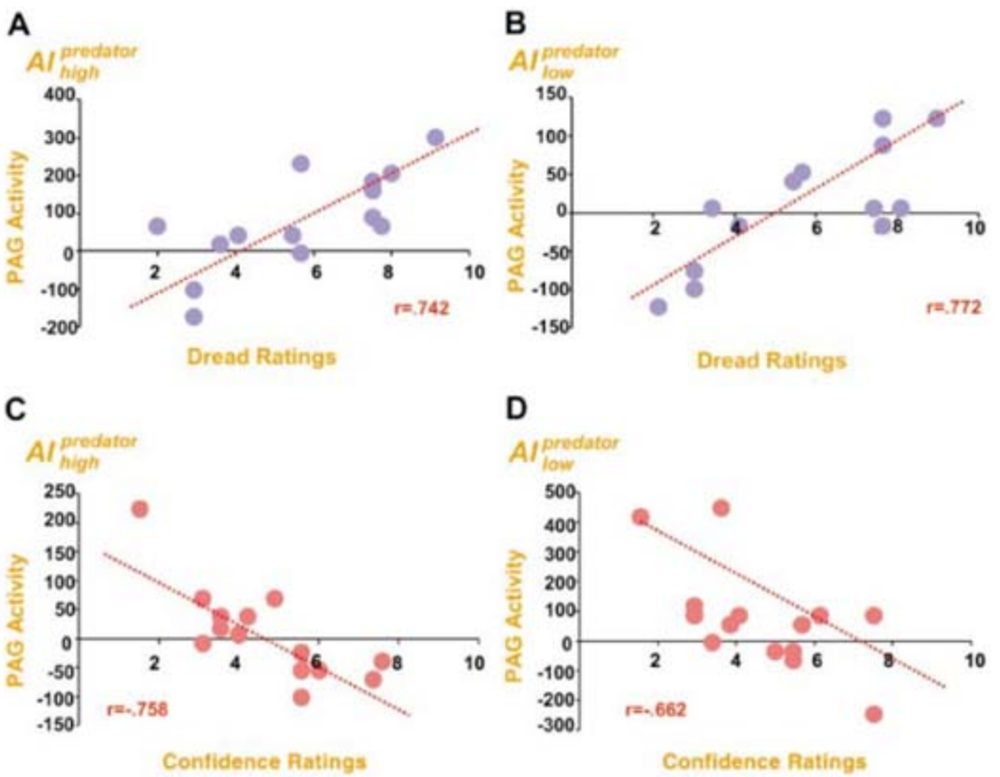


**Fig. 4.** Subject-specific differences in dread of capture and confidence of escape. (**A** and **B**) Scatterplots of regions of the PAG that correlated with threat distance and increased dread of being caught by the (A) $AI_{high}^{predator}$ and (B) $AI_{low}^{predator}$. (**C** and **D**) Regions associated with threat distance and decreased confidence of escaping the (C) $AI_{high}^{predator}$ and (D) $AI_{low}^{predator}$. Each point represents an individual's response on post-scan questionnaire.

damage (*3*, *16*–*18*, *21*). Understanding the balance between forebrain and midbrain responses to threat might illuminate the pathophysiology of neuropsychiatric disturbances, including chronic anxiety and panic disorder, where brainstem involvement has long been suspected.

### References and Notes


1. R. J. Blanchard, D. C. Blanchard, in *Fear and Defence*, P. F. Brain, R. J. Blanchard, S. Parmigiani, Eds. (Harwood Academic, London, 1990), pp. 89–108.
2. M. S. Fanselow, L. S. Lester, in *Evolution and Learning*, R. C. Bolles, M. D. Beecher, Eds. (Erlbaum, Hillsdale, NJ, 1988), pp. 185–211.
3. M. S. Fanselow, *Psychon. Bull. Rev.* **1**, 429 (1994).
4. M. G. Craske, *Anxiety Disorders: Psychological Approaches to Theory and Treatment* (Westview, Boulder, CO, 1999).
5. V. Rau, M. S. Fanselow, in *Understanding Trauma: Integrating Biological, Clinical, and Cultural Perspectives* L. J. Kirmayer, R. Lemelson, M. Barad, Eds. (Cambridge Univ. Press, New York, 2007), pp. 27–40.
6. N. McNaughton, P. J. Corr, *Neurosci. Biobehav. Rev.* **28**, 285 (2004).
7. J. F. W. Deakin, F. G. Graeff, *J. Psychopharmacol.* **5**, 305 (1991).
8. P. J. Lang, M. Davis, *Prog. Brain Res.* **156**, 3 (2006).
9. G. S. Berns *et al.*, *Science* **312**, 754 (2006).
10. J. M. Gorman, J. M. Kent, G. M. Sullivan, J. D. Coplan, *Am. J. Psychiatry* **157**, 493 (2000).
11. O. Devinsky, M. J. Morrell, B. A. Vogt, *Brain* **118**, 279 (1995).
12. P. H. Rudebeck, M. J. Buckley, M. E. Walton, M. F. Rushworth, *Science* **313**, 1310 (2006).
13. J. C. Hsieh, S. Stone-Elander, M. Ingvar, *Neurosci. Lett.* **262**, 61 (1999).
14. J. P. Johansen, H. L. Fields, *Nat. Neurosci.* **7**, 398 (2004).
15. K. Shima, J. Tanji, *Science* **282**, 1335 (1998).
16. G. Hadjipavlou, P. Dunckley, T. E. Behrens, I. Tracey, *Pain* **123**, 169 (2006).
17. J. L. Price, *J. Comp. Neurol.* **493**, 132 (2005).
18. J. Amat *et al.*, *Nat. Neurosci.* **8**, 365 (2005).
19. F. G. Graeff, *Neurosci. Biobehav. Rev.* **28**, 239 (2004).
20. N. S. Floyd, J. L. Price, A. T. Ferry, K. A. Keay, R. Bandler, *J. Comp. Neurol.* **422**, 556 (2000).
21. R. Bandler, K. A. Keay, N. Floyd, J. Price, *Brain Res. Bull.* **53**, 95 (2000).
22. B. S. Nashold, W. P. Wilson, D. G. Slaughter, *J. Neurosurg.* **30**, 14 (1969).
23. M. R. Vianna *et al.*, *Braz. J. Med. Biol. Res.* **34**, 233 (2001).
24. X. Protopopescu *et al.*, *Neuroreport* **17**, 361 (2006).
25. E. M. Reiman *et al.*, *Arch. Gen. Psychiatry* **46**, 493 (1989).
26. E. A. Phelps, M. R. Delgado, K. I. Nearing, J. E. LeDoux, *Neuron* **43**, 897 (2004).
27. H. M. Duvernoy, *The Human Brain Stem and Cerebellum* (Springer, New York, 1995).


28. We thank C. Hagan and U. Frith for helpful comments. Supported by a Brain Research Trust Prize studentship (D.M.) and by the Wellcome Trust.


### Supporting Online Material

www.sciencemag.org/cgi/content/full/317/5841/1079/DC1
Materials and Methods
Figs. S1 to S5
Tables S1 to S5
References

26 April 2007; accepted 10 July 2007
10.1126/science.1144298

# Astrocytes Potentiate Transmitter Release at Single Hippocampal Synapses

**Gertrudis Perea and Alfonso Araque***

Astrocytes play active roles in brain physiology. They respond to neurotransmitters and modulate neuronal excitability and synaptic function. However, the influence of astrocytes on synaptic transmission and plasticity at the single synapse level is unknown. $Ca^{2+}$ elevation in astrocytes transiently increased the probability of transmitter release at hippocampal area CA3-CA1 synapses, without affecting the amplitude of synaptic events. This form of short-term plasticity was due to the release of glutamate from astrocytes, a process that depended on $Ca^{2+}$ and soluble *N*-ethylmaleimide–sensitive factor attachment protein receptor (SNARE) protein and that activated metabotropic glutamate receptors (mGluRs). The transient potentiation of transmitter release became persistent when the astrocytic signal was temporally coincident with postsynaptic depolarization. This persistent plasticity was mGluR-mediated but *N*-methyl-D-aspartate receptor–independent. These results indicate that astrocytes are actively involved in the transfer and storage of synaptic information.

Recent data have demonstrated the existence of bidirectional communication between astrocytes and neurons (*1*). In addition to responding to synaptic activity, astrocytes release gliotransmitters (*2*), which modulate neuronal excitability and neurotransmission (*3*). To investigate the consequences of astrocyte $Ca^{2+}$ elevations on evoked synaptic transmission at single hippocampal synapses, we performed paired recordings from CA1 pyramidal neurons and single astrocytes (*4*). Astrocytes were loaded with the $Ca^{2+}$-cage *o*-nitrophenyl-EGTA (NP-EGTA) to be selectively stimulated by ultraviolet (UV)–flash photolysis, while we stimulated Schaffer collaterals using the minimal stimulation method that activates single, or very few synapses (*5*, *6*).

First, we established that single synapses were stimulated in our experimental model by quantifying the synaptic transmission properties of the excitatory postsynaptic currents (EPSCs) (Fig. 1). Synaptic responses showed failures and successes in neurotransmitter release [probability of release (Pr) was 0.34 ± 0.02; range, 0.13 to 0.54; $n = 34$]; regular amplitude of successful responses (termed "synaptic potency"; 20.9 ± 1.3 pA; range, 8.5 to 37.5 pA; $n = 34$); and relatively low synaptic efficacy {i.e., the mean amplitude of all responses including failures: 6.9 ± 0.5 pA [range, 2.8 to 10.2 pA; $n = 34$ (fig. S1)]}. Paired-pulse stimulation facilitated the second EPSC relative to the first EPSC [paired-pulse facilitation (PPF) index was 0.48 ± 0.05; $n = 20$ (fig. S1)]. To stimulate astrocytes, we patch-clamped single passive astrocytes located in the stratum radiatum near (<50 μm from) the stimulating pipette. We included NP-EGTA and fluo-4 in the recording pipette to selectively activate single astrocytes and to monitor their $Ca^{2+}$ levels, respectively (Fig. 1A). UV-flash trains evoked astrocyte $Ca^{2+}$ elevations that were reliably repeated by successive stimuli [15 out of 15 astrocytes (fig. S2)].

After the control recording of EPSCs, NP-EGTA–loaded astrocytes were photo-stimulated. In 18 out of 38 neuron-astrocyte pairs [47% (Fig. 1D)] astrocytic $Ca^{2+}$ elevations transiently (~2 min) increased the synaptic efficacy (from 4.8 ± 0.6 pA to 6.2 ± 1.0 pA; $n = 18$; $P < 0.05$). This was due to a transient enhancement of Pr rather than a postsynaptic modulation (Fig. 1, F and G). Indeed, although Pr increased after astrocyte stimulation (from 0.24 ± 0.03 to 0.33 ± 0.04; $n = 18$; $P < 0.001$), the synaptic potency was unchanged (from 15.2 ± 1.3 pA to 15.7 ± 1.9 pA; $n = 18$; $P = 0.96$). Moreover, the PPF index changed from 0.64 ± 0.06 to 0.33 ± 0.10 after astrocyte stimulation [(fig. S3) $n = 18$; $P < 0.01$], which is consistent with a presynaptic mechanism of action. Furthermore, the kinetic properties of EPSCs were unaffected (respective rise and decay time constants before and after astrocyte stimulation were $\tau_{on}$ = 1.48 ± 0.22 ms and 1.45 ± 0.23 ms; $P = 0.34$; $\tau_{off}$ = 9.80 ± 0.94 ms and 10.31 ± 1.77 ms; $P = 0.43$; $n = 6$). These effects were reliably evoked by successive astrocyte stimulation (Fig. 2A).

In the absence of NP-EGTA or with the NP-EGTA–filled pipette placed outside the cell, UV flashes did not modify synaptic transmission (fig. S4), which indicated that the effects were not due to photo-stimulation of synaptic terminals and that $Ca^{2+}$ elevation in astrocytes is necessary and sufficient to potentiate the synaptic transmission.

We further analyzed whether the astrocyte-induced neuromodulation could also be evoked by stimuli that elevate astrocyte $Ca^{2+}$ through transmitter receptor activation. We used adeno-

Instituto Cajal, Consejo Superior de Investigaciones Científicas, Madrid, Spain.

*To whom correspondence should be addressed. E-mail: araque@cajal.csic.es

sine 5′-triphosphate (ATP) because, although it may act on neuronal and astrocytic receptors, it is highly effective in elevating astrocytic $Ca^{2+}$ (*3*, *7*). While recording synaptic currents, we locally applied ATP by microionophoresis (from pipette placed in the stratum radiatum >150 μm away from the synapse-stimulating pipette), which elevated $Ca^{2+}$ in a large number of astrocytes (Fig. 2B). Because ATP is converted to adenosine by extracellular adenosine triphosphatases (ATPases), these experiments were performed in the presence of the A1 purinergic receptor antagonist 8-cyclopentyltheophylline (CPT; 2 μM), which increases synaptic transmission (fig. S5), but prevents adenosine-dependent

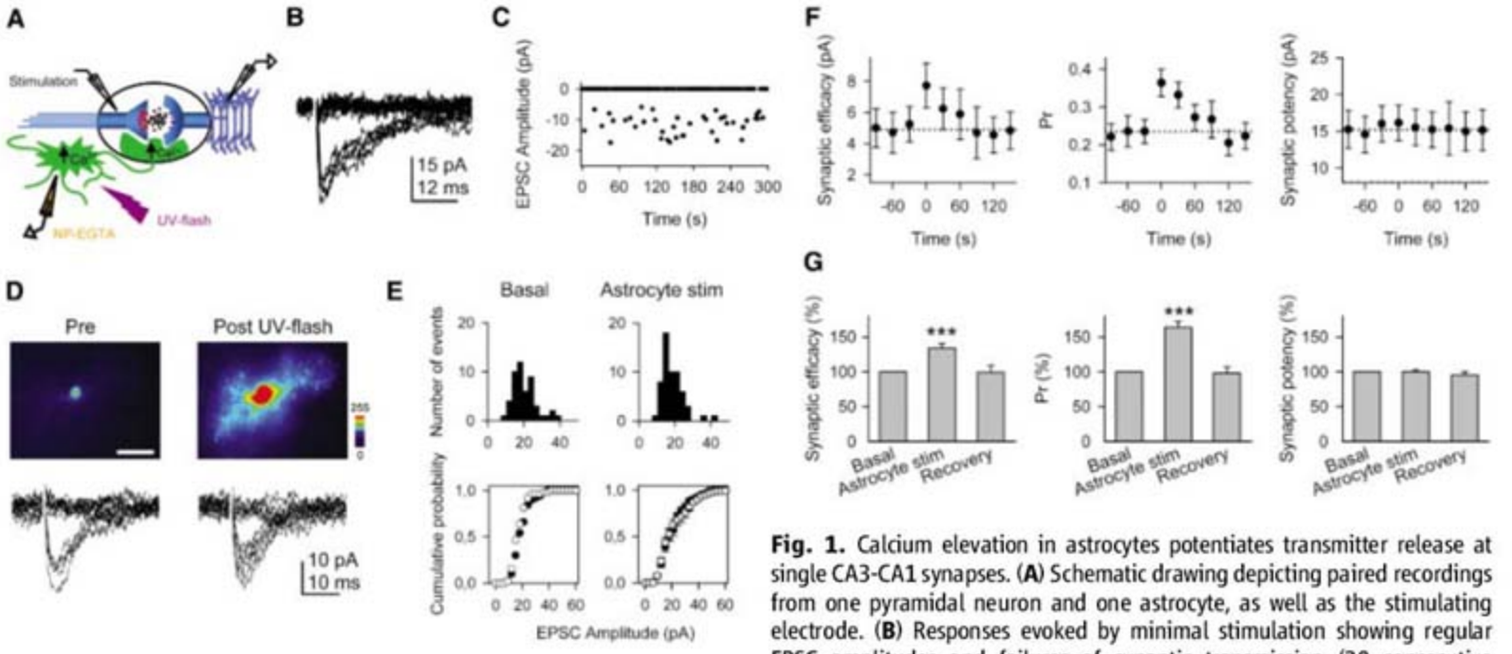


**Fig. 1.** Calcium elevation in astrocytes potentiates transmitter release at single CA3-CA1 synapses. (**A**) Schematic drawing depicting paired recordings from one pyramidal neuron and one astrocyte, as well as the stimulating electrode. (**B**) Responses evoked by minimal stimulation showing regular EPSC amplitudes and failures of synaptic transmission (20 consecutive stimuli). (**C**) EPSC amplitudes from a representative synapse. (**D**) Pseudocolor images representing fluorescence intensity of a NP-EGTA– and fluo-4–filled astrocyte (top) and synaptic responses [(bottom) 15 consecutive stimuli] obtained from paired whole-cell recordings before and after UV-flash astrocyte stimulation. Scale bar, 20 μm. (**E**) EPSC amplitude histograms (bin width, 3 pA) (top); corresponding cumulative probability plot (bottom, left); and average ($n$ = 7 astrocyte-neuron pairs) cumulative probability plots (bottom, right) of EPSC amplitudes before and after astrocyte stimulation (filled and open circles, respectively). (**F**) Synaptic efficacy (i.e., mean amplitude of responses including successes and failures of neurotransmission); probability of neurotransmitter release (Pr); and synaptic potency (i.e., mean EPSC amplitude excluding failures) (bin width, 33 s; $n$ = 18 astrocyte-neuron pairs). Zero time corresponds to the time of astrocyte stimulation. (**G**) Relative changes of synaptic parameters in the control state, after astrocyte stimulation, and 2 min later (recovery) ($n$ = 18). $^{***}P < 0.001$. Error bars indicate SEM.

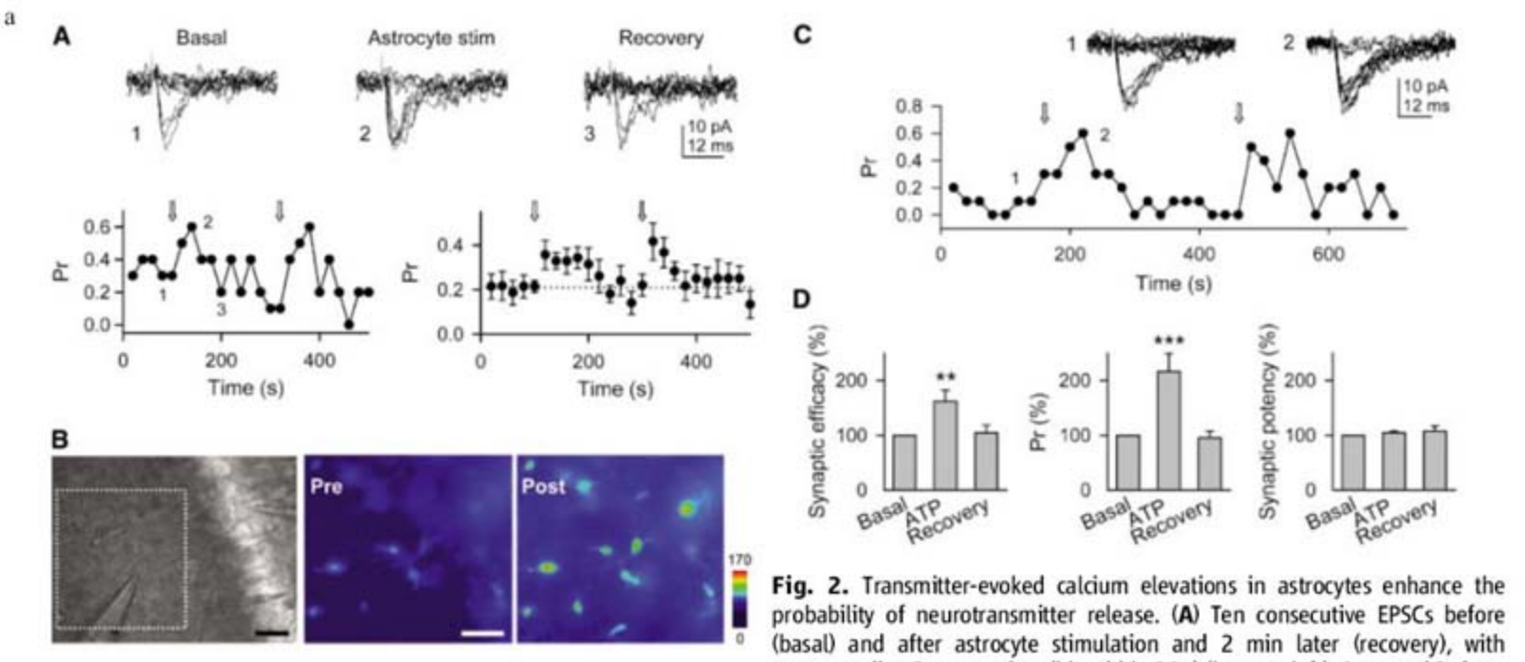


**Fig. 2.** Transmitter-evoked calcium elevations in astrocytes enhance the probability of neurotransmitter release. (**A**) Ten consecutive EPSCs before (basal) and after astrocyte stimulation and 2 min later (recovery), with corresponding Pr versus time (bin width, 20 s) (bottom, left). Averaged Pr from seven neuron-astrocyte pairs (bottom, right). Arrows indicate astrocyte stimulation. (**B**) Infrared differential interference contrast image showing the recorded pyramidal neuron and the stimulation electrode (left). Pseudocolor images representing fluorescence intensity of fluo-4–filled astrocytes before (pre) and after (post) ATP application through a pipette placed out of the image. Scale bar, 30 μm. (**C**) Ten consecutive EPSCs before (1) and after (2) ATP-evoked astrocyte $Ca^{2+}$ elevations, with corresponding Pr versus time. (**D**) Relative changes of synaptic parameters in the control state, induced by ATP-evoked astrocyte stimulation, and after recovery (2 min later) ($n$ = 16). $^{**}P < 0.01$, $^{***}P < 0.001$. Error bars indicate SEM.

neuromodulation (*8–11*). Under these conditions, ATP-evoked astrocyte $Ca^{2+}$ elevations transiently potentiated synaptic transmission in 43% of the synapses (16 out of 37) (Fig. 2C). The analysis of synaptic responses showed an increase of Pr [(Fig. 2, C and D) from 0.30 ± 0.03 to 0.41 ± 0.03 after astrocyte stimulation; $n = 16$; $P < 0.001$], without changes of synaptic potency (from 17.3 ± 1.1 pA to 17.8 ± 1.1 pA; $n = 16$; $P = 0.47$). Consequently, the synaptic efficacy was increased [(Fig. 3D) from 6.0 ± 0.6 pA to 8.0 ± 0.7 pA; $n = 16$; $P < 0.01$]. Because ATP is not a specific agonist for astrocytes, a direct effect on neurons cannot be totally excluded. However, the comparable effects of astrocyte $Ca^{2+}$ elevations evoked by photo-stimulation or ATP, as well as their equal sensitivity to metabotropic glutamate receptor (mGluR) antagonists (see below), indicate that these effects were not likely due to nonspecific actions of the stimuli.

We next investigated the mechanisms responsible for the astrocyte-induced neuromodulation. Passive astrocytes release gliotransmitters that influence neurotransmission (*7–18*). Because some gliotransmitters are released through soluble *N*-ethylmaleimide–sensitive factor attachment protein receptor (SNARE) protein–dependent mechanisms (*19–21*), we asked if the cleavage of synaptobrevin 2 by tetanus toxin (TeNT) affected the astrocyte-induced neuromodulation. When the light chain of TeNT was included in the recording astrocyte, photo-stimulation of the NP-EGTA–loaded astrocyte increased its intracellular $Ca^{2+}$ but did not affect the synaptic properties [(Fig. 3A) $n = 13$]. Therefore, the neuromodulation requires the SNARE protein–dependent gliotransmitter release from astrocytes.

Because glutamate is released by astrocytes through $Ca^{2+}$- and SNARE protein–dependent mechanisms (*19–21*) and can facilitate neurotransmitter release by activation of presynaptic group I mGluRs (*13*, *22*, *23*), we investigated their participation in the synaptic transmission potentiation. After assessing that UV-flash astrocyte stimulation transiently increased Pr, we perfused the group I mGluR antagonists 2-methyl-6-(phenylethynyl)-pyridine (MPEP, 50 μM) and (+)-2-methyl-4-carboxyphenylglycine (LY367385, 100 μM), which are mGluR subtype 5 and mGluR subtype 1 antagonists, respectively. These antagonists blocked the transient potentiation of transmitter release without affecting the astrocyte $Ca^{2+}$ signal [(Fig. 3, B and C) Pr = 0.41 ± 0.11 and 0.37 ± 0.12 before and after astrocyte stimulation; $n = 8$; $P = 0.28$). Likewise, the synaptic potentiation induced by ATP-evoked astrocyte $Ca^{2+}$ elevations was inhibited by those antagonists [$n = 7$ (fig. S6)].

One of the most-studied forms of synaptic plasticity is long-term potentiation (LTP), characterized by a long-lasting increase of synaptic strength caused by the coincidence of pre- and postsynaptic activity (*24*). The results above indicate that astrocytes evoke a short-term potentiation of neurotransmitter release. We then investigated whether the temporal coincidence of the astrocytic signal and the postsynaptic activity could induce a long-lasting modulation of synaptic transmission. We analyzed the long-term effects of pairing the astrocyte $Ca^{2+}$ uncaging with a transient mild depolarization (to –30 mV) of the postsynaptic neuron. We first established that in the absence of astrocyte stimulation, the postsynaptic depolarization per se did not modify the synaptic parameters [$n = 6$ (Fig. 4, D and E)]. However, when astrocytes were photo-stimulated during the postsynaptic depolarization, both the synaptic efficacy and the probability of transmitter release were persistently (≥60 min) increased in 41% of the synapses ($n = 7$ out of 17) [(Fig. 4, A, B, and E); synaptic efficacy: 5.1 ± 0.5 pA and 15.5 ± 2.1 pA ($P < 0.01$) and Pr = 0.28 ± 0.04 and 0.71 ± 0.08 ($P < 0.001$), before and 60 min after astrocyte stimulation, respectively; $n = 7$]. Although two out of seven synapses showed a potentiation of the synaptic potency, on average the synaptic efficacy increase was not accompanied by synaptic potency changes (18.1 ± 1.3 pA and 21.0 ± 2.7 pA, before and 60 min after astrocyte stimulation, respectively; $n = 7$; $P = 0.17$). The astrocyte-induced LTP was also evoked by receptor-mediated astrocyte $Ca^{2+}$ signaling because pairing the neuronal depolarization with the ATP-evoked astrocyte stimulation (in the presence of CPT) caused a long-lasting potentiation of synaptic transmission in 46% of the synapses (6 out of 13) (Fig. 4C). This astrocyte-induced LTP was independent of *N*-methyl-D-aspartate receptor (NMDAR) activation because it was unaffected by D-2-amino-5 phosphonopentanoic acid (D-AP5; 50 μM) [(Fig. 4, C and E); 42% of synapses showed persistent potentiation; $n = 5$ out of 12].

This form of LTP was associated with the astrocyte-induced transient increase of Pr be-

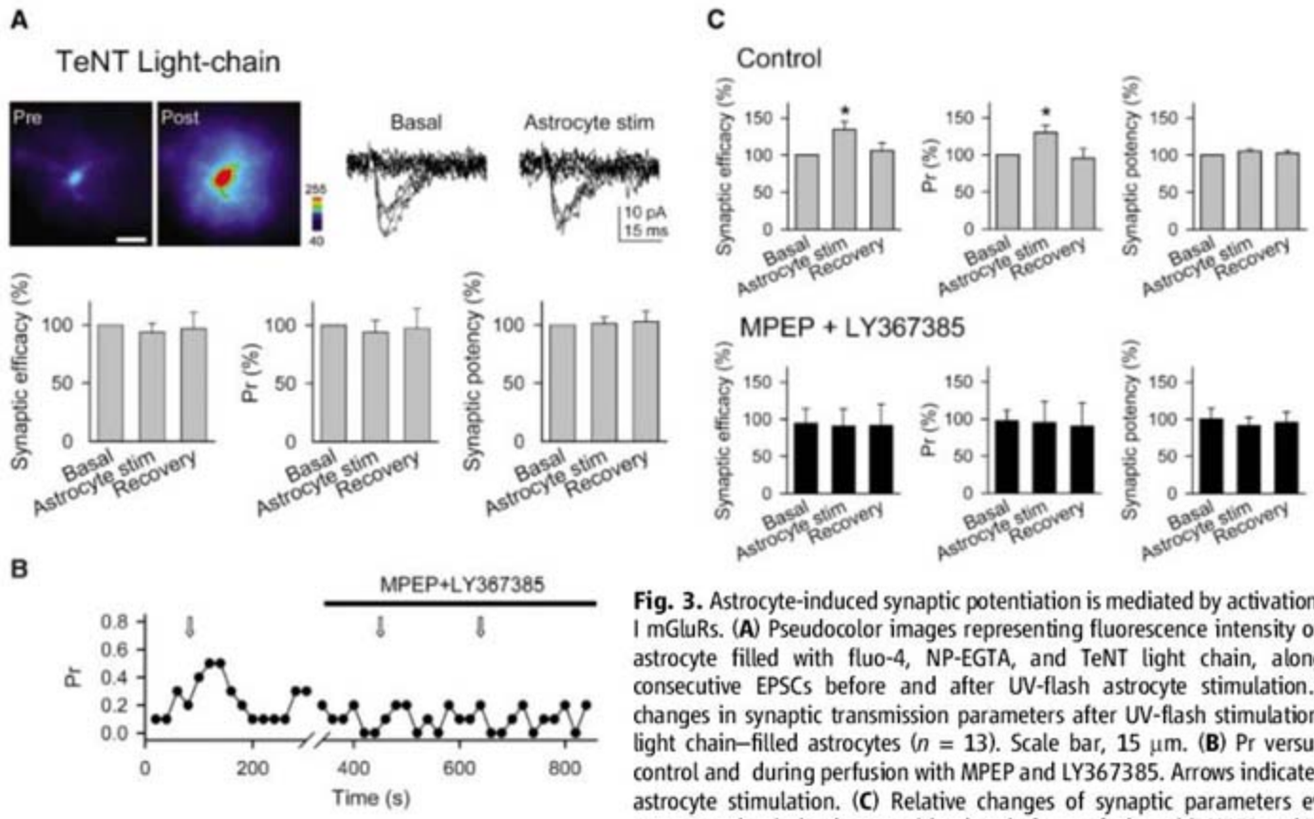


**Fig. 3.** Astrocyte-induced synaptic potentiation is mediated by activation of group I mGluRs. (**A**) Pseudocolor images representing fluorescence intensity of a single astrocyte filled with fluo-4, NP-EGTA, and TeNT light chain, alongside 12 consecutive EPSCs before and after UV-flash astrocyte stimulation. Relative changes in synaptic transmission parameters after UV-flash stimulation of TeNT light chain–filled astrocytes ($n = 13$). Scale bar, 15 μm. (**B**) Pr versus time in control and during perfusion with MPEP and LY367385. Arrows indicate UV-flash astrocyte stimulation. (**C**) Relative changes of synaptic parameters evoked by astrocyte stimulation in control (top) and after perfusion with MPEP and LY367385 (bottom) ($n = 8$). *$P < 0.05$. Error bars indicate SEM.

cause 7 out of 17 synapses showed both transient and long-lasting increase in Pr and no synapses underwent persistent potentiation without transient modulation ($n = 10$). Therefore, we studied whether astrocyte-induced LTP depended on activation of group I mGluRs. In the presence of the antagonists MPEP and LY367385, astrocyte stimulation did not modify the synaptic parameters [$n = 6$ (Fig. 4, D and E)].

Our results show that $Ca^{2+}$ elevation in astrocytes modulates transmitter release probability and evokes long-term synaptic plasticity at single hippocampal synapses without affecting the postsynaptic sensitivity. Although the astrocyte-induced transient synaptic modulation is in agreement with reports of mGluR-dependent neuromodulation [compare (*13*, *22*, *23*)], the NMDAR-independent long-lasting effects are more challenging to our vision of the classical LTP in the CA1 region, where postsynaptic changes underlie its expression [(*25*), but see (*26*)].

These data extend the classical Hebbian model for LTP, which results from concurrent pre- and postneuronal activity, to include astrocytes activity, so that the temporal coincidence the temporal coincidence of astrocyte and postsynaptic activities evokes long-term changes in synaptic efficacy. Therefore, astrocytes are directly involved in the synaptic information transfer and storage by the nervous system.

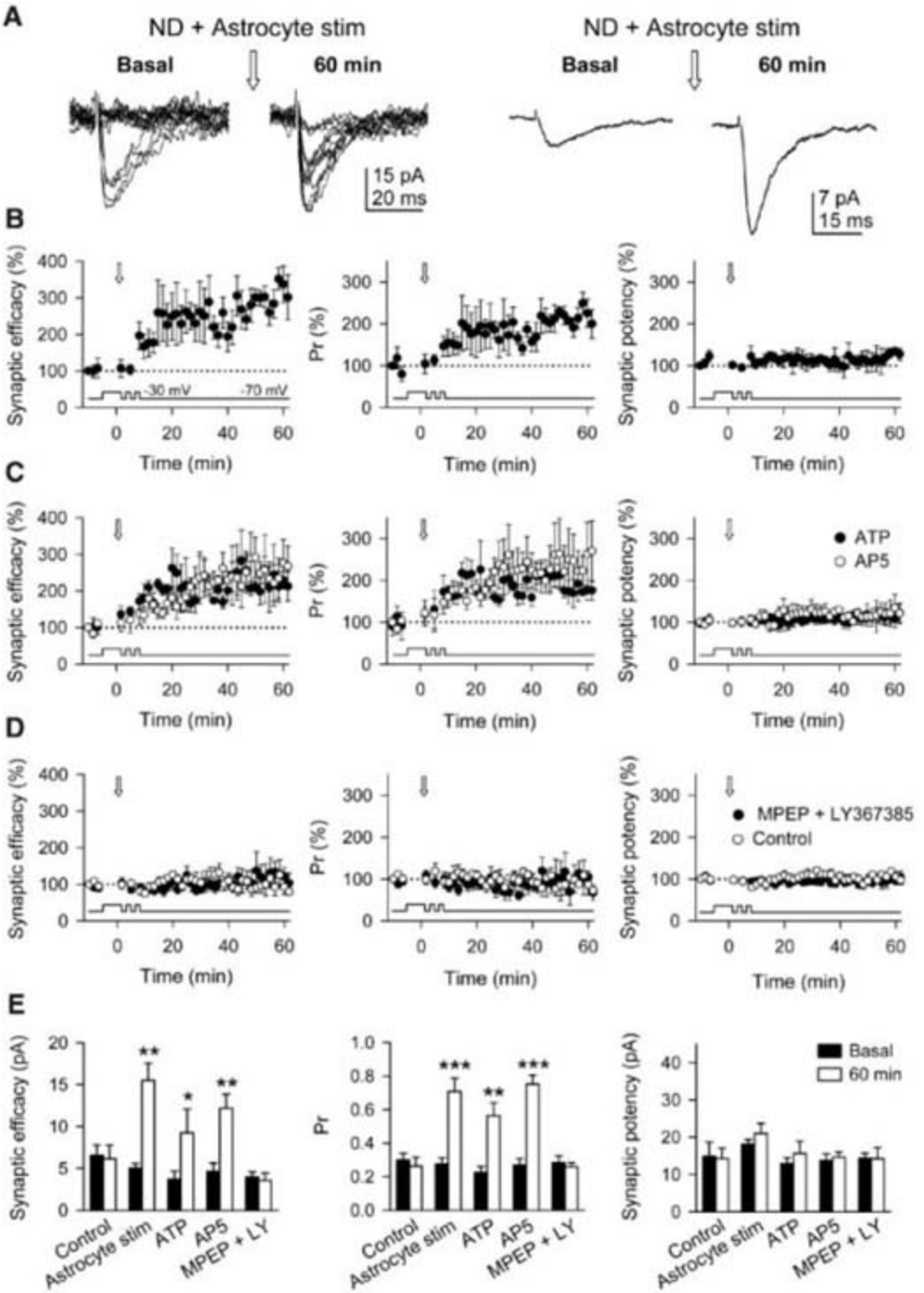


**Fig. 4.** Temporal coincidence of astrocyte and neuronal signals evoke LTP of synaptic transmission. (**A**) Fifteen consecutive EPSCs (left) and average EPSCs ($n = 50$ trials including failures) (right) before (basal) and 60 min after pairing neuronal depolarization (ND) and UV-flash astrocyte stimulation. (**B** to **D**) Synaptic parameters normalized to baseline and plotted over time. Arrows indicate astrocyte stimulation. (B) Pairing of UV-flash astrocyte stimulation and ND ($n = 7$ astrocyte-neuron pairs). (C) Pairing of ATP-evoked astrocyte stimulation and ND in control (black circles, $n = 6$) and after administering 50 μM D-AP5 (white circles, $n = 5$). (D) Pairing of UV-flash astrocyte stimulation and ND after administering MPEP and LY367385 (black circles); and ND with no astrocyte stimulation (control; white circles); ($n = 6$ for each case). (**E**) Synaptic parameters before and after 60 min under different conditions. $^*P < 0.05$, $^{**}P < 0.01$, $^{***}P < 0.001$. Error bars indicate SEM.


**References and Notes**

1. A. Araque, V. Parpura, R. P. Sanzgiri, P. G. Haydon, *Trends Neurosci.* **22**, 208 (1999).
2. A. Volterra, J. Meldolesi, in *Neuroglia*, H. Kettenmann, E. Ransom, Eds. (Oxford Univ. Press, New York, 2005), pp. 190–201.
3. E. A. Newman, *Trends Neurosci.* **26**, 536 (2003).
4. Materials and methods are available as supporting material on *Science* Online.
5. L. E. Dobrunz, C. F. Stevens, *Neuron* **18**, 995 (1997).
6. J. T. Isaac, G. O. Hjelmstad, R. A. Nicoll, R. C. Malenka, *Proc. Natl. Acad. Sci. U.S.A.* **93**, 8710 (1996).
7. G. Perea, A. Araque, *J. Neurosci.* **25**, 2192 (2005).
8. O. Pascual *et al.*, *Science* **310**, 113 (2005).
9. A. Serrano, N. Haddjeri, J. C. Lacaille, R. Robitaille, *J. Neurosci.* **26**, 5370 (2006).
10. J. M. Zhang *et al.*, *Neuron* **40**, 971 (2003).
11. E. D. Martín *et al.*, *Glia* **55**, 36 (2007).
12. E. C. Beattie *et al.*, *Science* **295**, 2282 (2002).
13. T. A. Fiacco, K. D. McCarthy, *J. Neurosci.* **24**, 722 (2004).
14. J. Kang, L. Jiang, S. A. Goldman, M. Nedergaard, *Nat. Neurosci.* **1**, 683 (1998).
15. Q. S. Liu, Q. Xu, G. Arcuino, J. Kang, M. Nedergaard, *Proc. Natl. Acad. Sci. U.S.A.* **101**, 3172 (2004).
16. A. Panatier *et al.*, *Cell* **125**, 775 (2006).
17. Y. Yang *et al.*, *Proc. Natl. Acad. Sci. U.S.A.* **100**, 15194 (2003).
18. P. Jourdain *et al.*, *Nat. Neurosci.* **10**, 331 (2007).
19. A. Araque, N. Li, R. T. Doyle, P. G. Haydon, *J. Neurosci.* **20**, 666 (2000).
20. J. P. Mothet *et al.*, *Proc. Natl. Acad. Sci. U.S.A.* **102**, 5606 (2005).
21. P. Bezzi *et al.*, *Nat. Neurosci.* **7**, 613 (2004).
22. A. Rodriguez-Moreno, A. Sistiaga, J. Lerma, J. Sanchez-Prieto, *Neuron* **21**, 1477 (1998).
23. N. E. Schwartz, S. Alford, *J. Neurophysiol.* **84**, 415 (2000).
24. R. C. Malenka, M. F. Bear, *Neuron* **44**, 5 (2004).
25. G. L. Collingridge, J. T. Isaac, Y. T. Wang, *Nat. Rev. Neurosci.* **5**, 952 (2004).
26. S. S. Zakharenko, L. Zablow, S. A. Siegelbaum, *Nat. Neurosci.* **4**, 711 (2001).


27. Supported by grants from the Ministry of Education and Science of Spain (BFU2004-00448) and Comunidad de Madrid–Consejo Superior de Investigaciones Científicas (CAM-CSIC), Spain. We thank W. Buño, M. Navarrete, E. Martin, D. Fernández de Sevilla and C. Cabezas for helpful suggestions.


**Supporting Online Material**

www.sciencemag.org/cgi/content/full/317/5841/1083/DC1
Materials and Methods
Figs. S1 to S6
References


4 May 2007; accepted 17 July 2007
10.1126/science.1144640

# CHD1 Motor Protein Is Required for Deposition of Histone Variant H3.3 into Chromatin in Vivo

Alexander Y. Konev,[1] Martin Tribus,[2] Sung Yeon Park,[3] Valerie Podhraski,[2] Chin Yan Lim,[4*] Alexander V. Emelyanov,[1] Elena Vershilova,[1] Vincenzo Pirrotta,[3] James T. Kadonaga,[4] Alexandra Lusser,[2]† Dmitry V. Fyodorov[1]†

The organization of chromatin affects all aspects of nuclear DNA metabolism in eukaryotes. H3.3 is an evolutionarily conserved histone variant and a key substrate for replication-independent chromatin assembly. Elimination of chromatin remodeling factor CHD1 in *Drosophila* embryos abolishes incorporation of H3.3 into the male pronucleus, renders the paternal genome unable to participate in zygotic mitoses, and leads to the development of haploid embryos. Furthermore, CHD1, but not ISWI, interacts with HIRA in cytoplasmic extracts. Our findings establish CHD1 as a major factor in replacement histone metabolism in the nucleus and reveal a critical role for CHD1 in the earliest developmental instances of genome-scale, replication-independent nucleosome assembly. Furthermore, our results point to the general requirement of adenosine triphosphate (ATP)–utilizing motor proteins for histone deposition in vivo.

Histone-DNA interactions constantly change during various processes of DNA metabolism. Recent studies have highlighted the importance of histone variants, such as H3.3, CENP-A (centromere protein A), or H2A.Z, in chromatin dynamics (*1*, *2*). Incorporation of replacement histones into chromatin occurs throughout the cell cycle, whereas nucleosomes containing canonical histones are assembled exclusively during DNA replication. A thorough understanding of the replication-independent mechanisms of chromatin assembly, however, is lacking.

In vitro, chromatin assembly requires the action of histone chaperones and adenosine triphosphate (ATP)–utilizing factors (*3*). Histone chaperones may specialize for certain histone variants. For example, H3.3 associates with a complex containing HIRA, whereas canonical H3 is in a complex with CAF-1 (chromatin assembly factor 1) (*4*). The molecular motors known to assemble nucleosomes are ACF (ATP-utilizing chromatin assembly and remodeling factor), CHRAC (chromatin accessibility complex), and RSF (nucleosome-remodeling and spacing factor), which contain the Snf2 family member ISWI as the catalytic subunit (*5*–*7*), and CHD1, which belongs to the CHD subfamily of Snf2-like adenosine triphosphatases (ATPases) (*8*). These factors have not been shown to mediate deposition of histones in vivo. We previously demonstrated that CHD1, together with the chaperone NAP-1, assembles nucleosome arrays from DNA and histones in vitro (*9*). Here, we investigated the role of CHD1 in chromatin assembly in vivo in *Drosophila*.

We generated *Chd1* alleles by P element–mediated mutagenesis (Fig. 1A) (*10*). Two excisions, *Df(2L)Chd1[1]* and *Df(2L)Chd1[2]*, deleted fragments of the *Chd1* gene and fragments of unrelated adjacent genes. Heterozygous combinations, however, of *Chd1[1]* or *Chd1[2]* with *Df(2L)Exel7014* affect both copies of the *Chd1* gene only (Fig. 1B). We also identified a single point mutation that results in premature translation termination of *Chd1* (Q1394*) in a previously described lethal allele, *l(2)23Cd[A7-4]* (*11*). Hence, *l(2)23Cd[A7-4]* was renamed *Chd1[3]*.

Analysis of Western blots of embryos from heterozygous *Chd1[3]* fruit flies revealed the presence of a truncated polypeptide besides full-length CHD1 (Fig. 1C). No truncated polypeptides were detected in heterozygous *Chd1[1]* or *Chd1[2]* embryos. Therefore, the corresponding deficiencies result in null mutations of *Chd1*. Crosses of heterozygous *Chd1* mutant alleles with *Df(2L)JS17/CyO* or *Df(2L)Exel7014/CyO* produced subviable adult homozygous mutant progeny (fig. S1). Both males and females were sterile. Homozygous null females mated to wild-type males laid fertilized eggs that died before hatching. Therefore, maternal CHD1 is essential for embryonic development.

When we examined the chromosome structure of 0- to 4-hour-old embryos laid by *Chd1*-null females, we observed that, during syncytial mitoses (cycles 3 to 13), the nuclei appeared to be abnormally small. The observed numbers of anaphase chromosomes suggested that they were

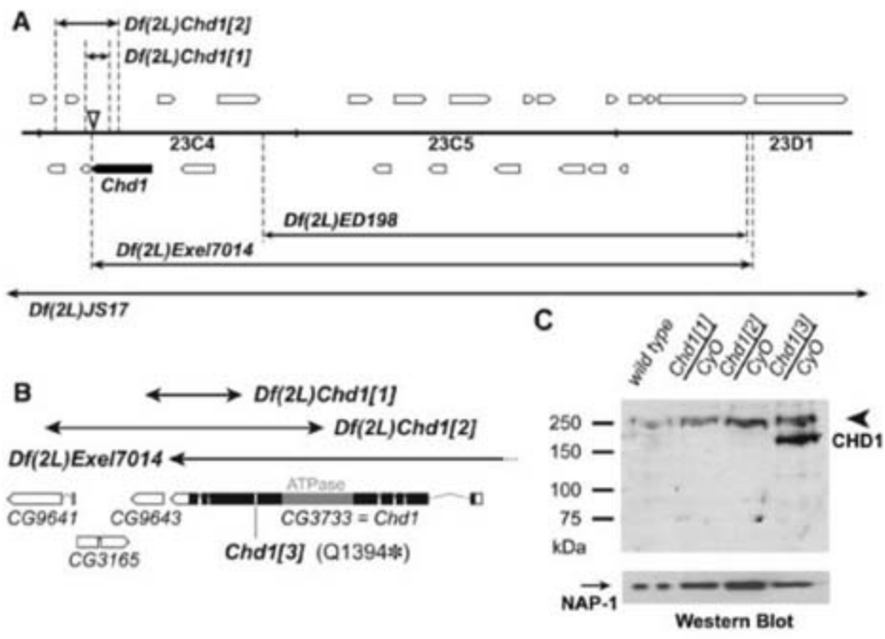


**Fig. 1.** Characterization of *Chd1* mutant alleles. (**A**) Genomic structure of the *Chd1* locus. *Df(2L)JS17* and *Df(2L)Exel7014* uncover *Chd1*. White boxes, predicted genes; black box, *Chd1*; black arrows, chromosome deficiencies; dashed lines, deficiency breakpoints; triangle, *P{EPgy2}EY07345* insertion that was used for excisions. (**B**) The *Chd1[1]* and *Chd1[2]* excisions delete 296 and 958 amino acids, respectively, from the C terminus of CHD1. *Chd1[3]* has a nonsense mutation resulting in a stop at glutamine 1394. The distal breakpoint of *Df(2L)Exel7014* is located immediately downstream of the *Chd1* 3′ untranslated region. White boxes, predicted genes; black box, *Chd1* coding sequence; gray box, *Chd1* ATPase domain. (**C**) Western blot of heterozygous mutant embryos. Truncated CHD1 polypeptides are not detected in heterozygous *Chd1[1]* or *Chd1[2]* embryos. Heterozygous *Chd1[3]* embryos express a truncated (residues 1 to 1394) CHD1 polypeptide. Arrowhead, wild-type CHD1 (250 kD); arrow, left, NAP-1 (loading control); *CyO*, second-chromosome balancer.

[1]Department of Cell Biology, Albert Einstein College of Medicine, 1300 Morris Park Avenue, Bronx, NY 10461, USA. [2]Division of Molecular Biology, Biocenter, Innsbruck Medical University, Fritz-Pregl Strasse 3, A-6020 Innsbruck, Austria. [3]Department of Molecular Biology and Biochemistry, Rutgers University, 604 Allison Road, Piscataway, NJ 08854, USA. [4]Section of Molecular Biology, University of California at San Diego, La Jolla, CA 92093, USA.

*Present address: Stem Cell and Developmental Biology Group, Genome Institute of Singapore, 60 Biopolis Street, S138672, Singapore.

†To whom correspondence should be addressed. E-mail: dfyodoro@aecom.yu.edu, alexandra.lusser@i-med.ac.at

haploid (Fig. 2A). To confirm this observation, we mated wild-type or *Chd1*-null females with males that carried a green fluorescent protein (GFP) transgene. Embryonic DNA was amplified with primers detecting male-specific GFP and a reference gene, Asf1. In wild-type embryos, both primer pairs produced polymerase chain reaction (PCR)–amplified products, whereas only the Asf1 fragment was amplified in the mutants (Fig. 2B). Thus, *Chd1* embryos develop with haploid, maternally derived chromosome content.

To investigate the causes of haploidy in mutant animals, we compared distributions of various developmental stages in samples of wild-type and *Chd1*-null embryos (table S1). The lack of maternal CHD1 dramatically changed this distribution. Most notably, at 0 to 4 hours after egg deposition, the majority of *Chd1* embryos (56%) remained at a very early stage of development in contrast to the wild type (24%) (table S1).

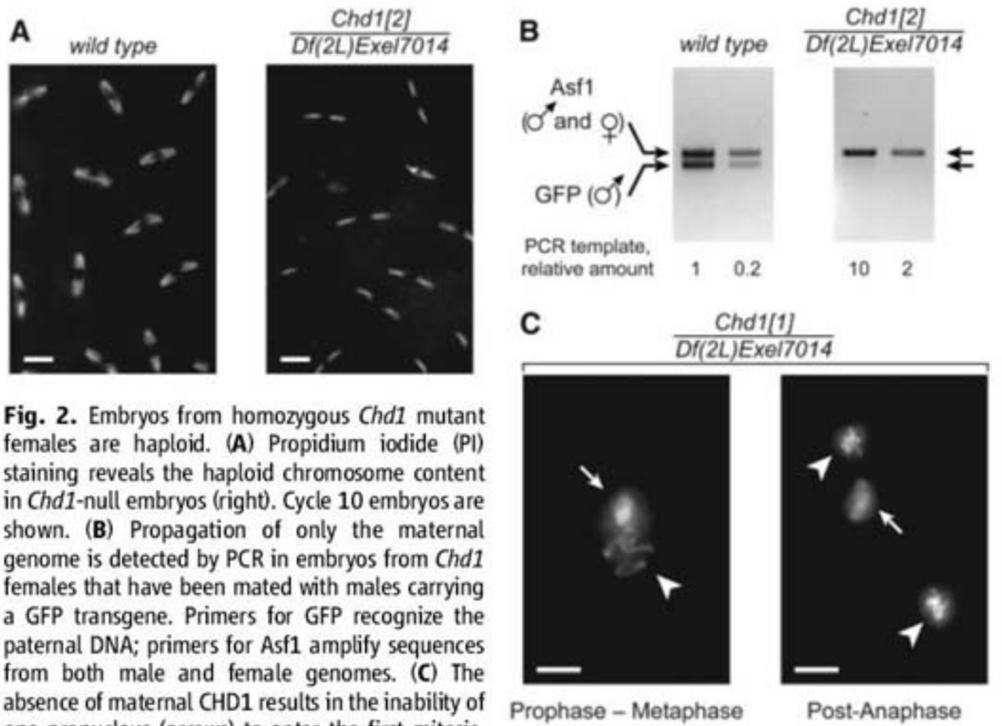


**Fig. 2.** Embryos from homozygous *Chd1* mutant females are haploid. (**A**) Propidium iodide (PI) staining reveals the haploid chromosome content in *Chd1*-null embryos (right). Cycle 10 embryos are shown. (**B**) Propagation of only the maternal genome is detected by PCR in embryos from *Chd1* females that have been mated with males carrying a GFP transgene. Primers for GFP recognize the paternal DNA; primers for Asf1 amplify sequences from both male and female genomes. (**C**) The absence of maternal CHD1 results in the inability of one pronucleus (arrows) to enter the first mitosis. The other pronucleus (arrowheads) continues with divisions (left, prophase to metaphase; right, post anaphase). Labeling above the panels refers to genotypes of mothers. Scale bars, 10 μm.

In *Drosophila* eggs, meiosis gives rise to four haploid nuclei. When the egg is fertilized, one of them is selected as a female pronucleus; the remaining three form the polar body. After breakdown of the sperm nuclear envelope, the compacted sperm chromatin is decondensed, and sperm-specific protamines are replaced with maternal histones. The male and female pronuclei juxtapose in the middle of the embryo and undergo one round of separate haploid mitoses. The resulting products fuse with their counterparts to give two diploid nuclei (*12*). In the majority of *Chd1* embryos, we observed partial decondensation of the sperm chromatin and normal apposition of parental pronuclei. Then, however, one pronucleus underwent mitosis; the other one did not (Fig. 2C). Considering the subsequent loss of paternal DNA (Fig. 2B), we conclude that mitotic progression of the male pronucleus is hindered in *Chd1* embryos.

Because CHD1 can assemble nucleosomes in vitro, we asked whether the absence of CHD1 affects histone incorporation into the male pronucleus. Embryos from wild-type or *Chd1*-null females were stained with an antibody against histone H3. In wild-type embryos, we observed uniform staining in both parental pronuclei (Fig. 3A). In contrast, in *Chd1*-null embryos only the

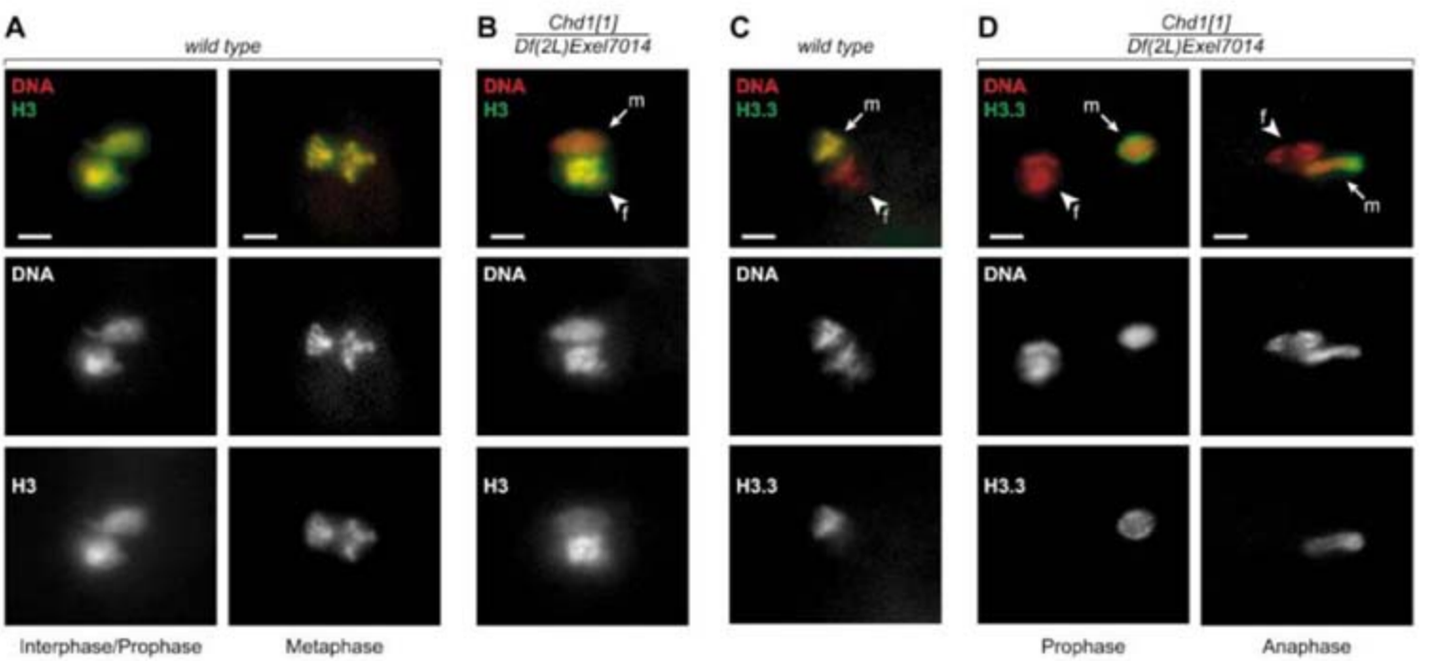


**Fig. 3.** CHD1 is required for incorporation of histones into decondensing sperm chromatin. (**A**) H3 colocalizes with DNA in both parental pronuclei of wild-type embryos (left, interphase or prophase; right, metaphase). (**B**) In *Chd1* mutant embryos, the male pronucleus fails to undergo mitosis and accumulates abnormally little H3. (**C**) H3.3-FLAG is incorporated into chromosomes of the male pronucleus in wild-type embryos. Panels show the first metaphase. (**D**) In *Chd1* mutant eggs, H3.3-FLAG accumulates in the periphery of the male pronucleus. The female pronucleus proceeds with mitosis (left, prophase; right, anaphase). (B, C, and D) Arrows, male pronuclei (m); arrowheads, female pronuclei (f). Labeling above the panels refers to genotype of mothers. Red, PI; green, H3 (A and B) or H3.3-FLAG (C and D). Scale bars, 10 μm.

female chromatin was brightly stained. The male pronucleus contained considerably less histone H3 (Fig. 3B). These observations indicate that CHD1 is necessary for nucleosome assembly during sperm decondensation.

Sperm DNA does not replicate during decondensation, and histones are deposited by replication-independent assembly mechanisms, which involve the variant histone H3.3 but not canonical H3 (*13*). It has been shown in *Drosophila* and mice that H3.3 is specifically present in the male pronucleus (*14*, *15*). We analyzed the distribution of H3.3 in embryos derived from *Chd1*-null females that carry a FLAG-tagged H3.3 transgene. In wild-type embryos, we observed colocalization of the H3.3-FLAG signal with male pronuclear DNA during migration and apposition. No H3.3-FLAG was detectable in the maternal pronucleus (Fig. 3C). In *Chd1*-null embryos, the male pronucleus showed altered H3.3-FLAG staining. The signal did not co-localize with the DNA but remained constrained to the nuclear periphery in a sac-shaped pattern (Fig. 3D).

These findings suggest that in the earliest phases of *Drosophila* development CHD1 is essential for the incorporation of H3.3 and normal assembly of paternal chromatin. In contrast, CHD1 does not appear to affect the organization of maternal chromatin. We conclude that CHD1 is required for replication-independent nucleosome assembly in the decondensing male pronucleus, but is dispensable for replication-coupled incorporation of H3.

It was shown recently that the *sèsame* (*ssm*) mutation of *Drosophila* histone chaperone HIRA caused the development of haploid embryos and abolished H3.3 deposition into the male pronucleus (*14*). *Chd1* and *ssm* mutants, however, differ profoundly in the manifestation of this phenotype. In *ssm* embryos, H3.3 is absent from the male pronucleus. In contrast, in *Chd1*-null embryos, H3.3 delivery to the male pronucleus appears to be unaffected. Thus, our observations allow us to mechanistically discern the roles of CHD1 and HIRA. Whereas HIRA is essential for histone delivery to the sites of nucleosome assembly, CHD1 directly facilitates histone deposition (fig. S3). Our findings are consistent with observations in vitro that histone chaperones either do not assemble nucleosomes or assemble them at a greatly reduced rate in the absence of ATP-utilizing factors. Our data provide evidence that histone deposition in vivo also transpires through an ATP-dependent mechanism.

CHD1 has been implicated in transcription elongation–related chromatin remodeling (*16*). We demonstrate that CHD1 functions in nucleosome assembly in the early *Drosophila* embryo, which is transcriptionally silent. The biological role of CHD1, therefore, is not confined to transcription-related processes. The *Schizosaccharomyces pombe* homolog of CHD1, Hrp1, has been shown to function in loading of the centromere-specific H3 variant CENP-A (*17*). Similarly to H3.3, incorporation of CENP-A into chromatin is not restricted to S phase. Therefore, CHD1 may have a general role in replication-independent nucleosome assembly.

Sperm decondensation involves not only histone incorporation, but also eviction of protamines. To discern whether CHD1 has a role in this process, we analyzed the fate of protamine B (Mst35Bb) in *Chd1*-null embryos. Although we detected GFP-tagged Mst35Bb in the sperm head immediately upon fertilization, we did not observe Mst35Bb-GFP signal in the male pronucleus (fig. S2). Thus, like HIRA (*18*), CHD1 is dispensable for protamine removal. We have shown that the male pronucleus in *Chd1*-null embryos contains very low amounts of histones (Fig. 3), yet the DNA is not packaged with protamines. It remains an open question whether other DNA-protein complexes exist in the male pronucleus.

*Drosophila* eggs contain stores of both known chromatin assembly factors CHD1 and ISWI (fig. S4A) (*19*). Nevertheless, ISWI is unable to substitute for CHD1 in the deposition of H3.3. To examine whether CHD1 and ISWI differ in their ability to interact with the H3.3 chaperone HIRA, we performed coimmunoprecipitation experiments with extracts from embryos expressing FLAG-HIRA. CHD1 signal was readily detected in FLAG-specific immunoprecipitates, whereas ISWI did not co-immunoprecipitate with HIRA (fig. S4B). Thus, a fraction of CHD1, but not ISWI, physically associates with HIRA. This property of CHD1 may account for its unique function in the H3.3 deposition process.

A subpopulation of *Chd1* mutant haploid embryos survives beyond apposition stage (table S1). Therefore, we asked whether H3.3 deposition is altered in *Chd1* mutant embryos during later developmental stages. In wild-type nuclei, the H3.3-FLAG signal originating from the male pronucleus becomes undetectable after 2 to 3 divisions. Most maternal H3.3 remains distributed diffusely throughout the syncytium. After cycle 11 (roughly correlating with the onset of zygotic transcription) H3.3-FLAG is redistributed into the nuclei, where it colocalizes with the DNA (Fig. 4A). In contrast, incorporation of H3.3 into *Chd1* mutant nuclei was impaired. H3.3-FLAG produced a speckled staining with numerous bright dots that poorly overlapped with the maxima of DNA staining (Fig. 4B). It is important to note that, in the *ssm* (HIRA) mutant, H3.3 incorporation defects in tissues or developmental stages other than the apposition stage were not observed. This result is consistent with the idea that misincorporation of H3.3 in *Chd1* embryos is a direct effect of CHD1 deletion rather than a consequence of haploid development. We also conclude that CHD1 functions in H3.3 deposition during later stages of embryonic development, possibly in a HIRA-independent fashion.

This study provides evidence that ATP-dependent mechanisms are used for histone deposition during chromatin assembly in vivo. Thus, molecular motor proteins, such as CHD1, function not only in remodeling of existing nucleosomes but also in de novo nucleosome assembly from DNA and histones. Finally, our work identifies CHD1 as a specific factor in the assembly of nucleosomes that contain variant histone H3.3.

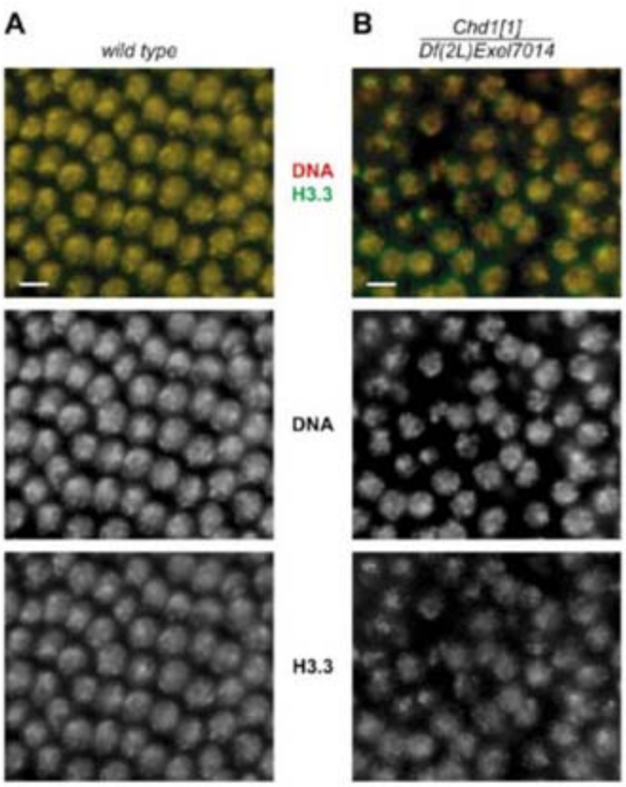


**Fig. 4.** Deposition of H3.3 into chromatin during syncytial blastoderm is compromised in *Chd1* mutants. (**A**) H3.3-FLAG overlaps with DNA in syncytial nuclei of a cycle 14 wild-type embryo. (**B**) H3.3-FLAG colocalizes poorly with DNA in *Chd1* mutant embryos. Labeling above the panels refers to genotypes of mothers. Red, PI; green, H3.3-FLAG. Scale bars, 10 μm.

**References and Notes**

1. J. Jin *et al.*, *Trends Biochem. Sci.* **30**, 680 (2005).
2. S. Henikoff, K. Ahmad, *Annu. Rev. Cell Dev. Biol.* **21**, 133 (2005).

3. D. V. Fyodorov, J. T. Kadonaga, *Cell* **106**, 523 (2001).
4. H. Tagami, D. Ray-Gallet, G. Almouzni, Y. Nakatani, *Cell* **116**, 51 (2004).
5. T. Ito *et al.*, *Genes Dev.* **13**, 1529 (1999).
6. P. D. Varga-Weisz *et al.*, *Nature* **388**, 598 (1997).
7. A. Loyola *et al.*, *Mol. Cell. Biol.* **23**, 6759 (2003).
8. T. Woodage, M. A. Basrai, A. D. Baxevanis, P. Hieter, F. S. Collins, *Proc. Natl. Acad. Sci. U.S.A.* **94**, 11472 (1997).
9. A. Lusser, D. L. Urwin, J. T. Kadonaga, *Nat. Struct. Mol. Biol.* **12**, 160 (2005).
10. Materials and methods are available as supporting material on *Science* Online.
11. For *Drosophila* genetics information, see FlyBase.org.
12. G. Callaini, M. G. Riparbelli, *Dev. Biol.* **176**, 199 (1996).
13. K. Ahmad, S. Henikoff, *Mol. Cell* **9**, 1191 (2002).
14. B. Loppin *et al.*, *Nature* **437**, 1386 (2005).
15. M. E. Torres-Padilla, A. J. Bannister, P. J. Hurd, T. Kouzarides, M. Zernicka-Goetz, *Int. J. Dev. Biol.* **50**, 455 (2006).
16. R. J. Sims 3rd, R. Belotserkovskaya, D. Reinberg, *Genes Dev.* **18**, 2437 (2004).
17. J. Walfridsson *et al.*, *Nucleic Acids Res.* **33**, 2868 (2005).
18. S. Jayaramaiah Raja, R. Renkawitz-Pohl, *Mol. Cell. Biol.* **25**, 6165 (2005).
19. R. Deuring *et al.*, *Mol. Cell* **5**, 355 (2000).
20. We thank M. Goralik-Schramel for technical assistance; B. Loppin and R. Renkawitz-Pohl for fly lines; and R. Perry for antibodies. We thank K. Beirit, B. Birshtein, V. Elagin, T. Juven-Gershon, M.-C. Keogh, P. Loidl, S. Morettini, M. Scharff, D. Sharp, and A. Skoultchi for critical reading of the manuscript and A. Tokareva for discussions and advice. This work was supported by grants from the National Institutes of Health to D.V.F. (GM74233) and J.T.K. (GM58272), the Austrian Science Foundation (Y275-B12) and Tyrolean Science Foundation to A.L., and the Swiss National Science Foundation to V.P. D.V.F is a Scholar of the Sidney Kimmel Foundation for Cancer Research.

**Supporting Online Material**

www.sciencemag.org/cgi/content/full/317/5841/1087/DC1
Materials and Methods
Figs. S1 to S5
Table S1
References

17 May 2007; accepted 13 July 2007
10.1126/science.1145339

# Blue-Light–Activated Histidine Kinases: Two-Component Sensors in Bacteria

**Trevor E. Swartz,[1]* Tong-Seung Tseng,[2] Marcus A. Frederickson,[1] Gastón Paris,[3] Diego J. Comerci,[6] Gireesh Rajashekara,[4,7] Jung-Gun Kim,[5] Mary Beth Mudgett,[5] Gary A. Splitter,[4] Rodolfo A. Ugalde,[6] Fernando A. Goldbaum,[3] Winslow R. Briggs,[2] Roberto A. Bogomolni[1]†**

Histidine kinases, used for environmental sensing by bacterial two-component systems, are involved in regulation of bacterial gene expression, chemotaxis, phototaxis, and virulence. Flavin-containing domains function as light-sensory modules in plant and algal phototropins and in fungal blue-light receptors. We have discovered that the prokaryotes *Brucella melitensis*, *Brucella abortus*, *Erythrobacter litoralis*, and *Pseudomonas syringae* contain light-activated histidine kinases that bind a flavin chromophore and undergo photochemistry indicative of cysteinyl-flavin adduct formation. Infection of macrophages by *B. abortus* was stimulated by light in the wild type but was limited in photochemically inactive and null mutants, indicating that the flavin-containing histidine kinase functions as a photoreceptor regulating *B. abortus* virulence.

LOV (light, oxygen, or voltage) domains are distributed in the three kingdoms of life (Eukarya, Archaea, and Bacteria) (*1*, *2*). In most cases, the LOV domain is the primary sensory module that conveys a signal to protein domains with known or putative functions as diverse as regulation of gene expression, regulation of protein catabolism, and activation of serine/threonine kinases in eukaryotes and histidine kinases in prokaryotes (*3*, *4*). The only two LOV-domain proteins from bacteria that have been studied are YtvA—a LOV-STAS (LOV–sulfate transporter and anti-sigma factor antagonist) protein from *Bacillus subtilis*—and a LOV protein (containing no other known domains) from *Pseudomonas putida* (*5*–*8*).

The best-characterized LOV domains belong to the plant blue-light receptors, the phototropins, and the closely related photoreceptor neochrome (*9*). The LOV-domain x-ray structure shows the flavin mononucleotide (FMN) chromophore noncovalently bound to the protein through hydrogen bonding and hydrophobic interactions, and the sulfur atom of a reactive cysteine to be within 4.2 Å of the C(4a) carbon of FMN (*10*). Light absorption by the LOV-domain flavin chromophore results in formation of a cysteinyl-flavin adduct in which the sulfur of the reactive cysteine forms a covalent bond with the C(4a) carbon of FMN. In the phototropin LOV domains, this stable bond spontaneously breaks in the dark (in many seconds), completing a photocycle (*11*). This process has been proposed to be base catalyzed (*12*–*14*). Cysteinyl adduct formation in the phototropins produces protein conformational changes (*15*, *16*) that activate a serine/threonine kinase domain, resulting in autophosphorylation (*9*). The activated phototropins mediate several blue-light responses in plants, including phototropism, chloroplast relocation, leaf expansion, and stomatal opening (*17*).

Sequence analysis predicts that the genomes of the human/animal facultative intracellular pathogen *Brucella melitensis* (*18*, *19*), the plant pathogen *Pseudomonas syringae* (*3*, *4*), and the marine bacterium *Erythrobacter litoralis* code for proteins that contain a LOV domain at their N terminus, with a histidine kinase occupying the C terminus (LOV-HK). Protein sequence and structural modeling [Swiss model (*20*)] of these bacterial LOV domains predict that all four LOV-HK proteins will bind a flavin and that all contain a cysteine within a few angstroms of the chromophore. Analysis of published genomes indicates 24 different sequenced bacteria contain genes that code for putative LOV-HKs (*1*, *4*).

The full-length proteins (489 amino acids) from *B. melitensis* (BM-LOV-HK) and *B. abortus* (BA-LOV-HK) contain three distinct domains: a LOV domain at the N terminus, followed by a PAS (Per- Arnt- Sim) domain in the intervening sequence, and a histidine kinase at the C terminus (Fig. 1). Although there are some silent mutations in the genes that encode the LOV-HK in the various *Brucella* species, the protein sequence is identical in *B. melitensis*, *B. abortus*, and *B. suis*. The two LOV-HK proteins from *E. litoralis* (346 amino acids and 368 amino acids in length for EL346-LOV-HK and


**Fig. 1.** Domain alignment of LOV histidine kinase proteins (LOV-HK).

[1]Department of Chemistry and Biochemistry, University of California, Santa Cruz, Santa Cruz, CA, USA. [2]Department of Plant Biology, Carnegie Institution of Washington, Stanford, CA, USA. [3]Fundación Instituto Leloir, Instituto de Investigaciones Bioquímicas Buenos Aires–Consejo Nacional de Investigaciones Científicas y Técnicas (IIBBA-CONICET), Buenos Aires, Argentina. [4]Department of Animal Health and Biomedical Sciences, University of Wisconsin, Madison, WI, USA. [5]Department of Biological Sciences, Stanford University, Stanford, CA, USA. [6]Instituto de Investigaciones Biotecnológicas, Universidad Nacional de San Martín, CONICET, San Martín, Argentina. [7]Food Animal Health Research Program–Ohio Agricultural Research and Development Center (FAHRP-OARDC), Ohio State University, Wooster, OH, USA.

*Present address: Early Stage Pharmaceutical Development, Genentech, Inc., South San Francisco, CA, USA.
†To whom correspondence should be addressed. E-mail: bogo@chemistry.ucsc.edu

EL368-LOV-HK, respectively) contain only a LOV domain followed by a linking sequence and a C-terminal histidine kinase domain (Fig. 1). The LOV-domain protein from the plant pathogen *P. syringae* (PS-LOV-HK) (534 amino acids) contains a LOV domain at the N terminus, followed by a histidine kinase and a putative C-terminal receiver (Rec) domain (i.e., response regulator) (Fig. 1). All of these sensor/histidine kinase proteins are hypothesized to be involved in two-component signaling at some stage in the organism's life cycle.

We have cloned the genes encoding BM-LOV-HK, EL368-LOV-HK, EL346-LOV-HK and PS-LOV-HK, expressed them in *Escherichia coli,* and affinity-purified their full-length proteins. The four proteins exhibit characteristic LOV-domain absorption, with two broad absorption bands (450 nm and 370 nm) with secondary spectral peaks indicative of flavin in a tight-binding pocket (*16*) (Fig. 2A). The flavin chromophore was extracted from the four LOV-HKs and analyzed by thin-layer chromatography (TLC). All four LOV-HKs expressed in *E. coli* bind FMN as the flavin chromophore (table S1).

Light-induced absorption changes were measured to study the photochemistry of the isolated LOV-HKs. Illumination of the LOV-HKs with a 1-ms camera strobe flash produced a difference spectrum that indicates a loss of absorption from the 450-nm band, with some increase in absorption in the ultraviolet A (UVA) region (Fig. 2B). These difference absorption changes are characteristic of the formation of a flavin cysteinyl adduct that has a broad absorption band around 390 nm (*11*, *12*).

The BM-LOV-HK adduct state is extremely stable and does not decay measurably in 2 hours (Fig. 2C). This stability is unlike that of the other three LOV-domain proteins presented here, in which the cysteinyl adduct breaks spontaneously, with the chromophore/protein thermally returning to the ground state in the dark. The other three LOV-HKs complete a photocycle in which they decay thermally from the adduct state back to the ground state in the dark with half-lives of 28 (EL346-LOV-HK), 32 (EL368-LOV-HK), and 22 (PS-LOV-HK) min (Fig. 2C). In the phototropin LOV domains, the spontaneous adduct decay is thought to be base-catalyzed (*12*–*14*), possibly initiated by abstraction of the N5 proton. However, the putative proton acceptor has not been identified; sequence comparisons of the various LOV domains do not provide information about the residues controlling the relative rates of dark decay.

The four LOV-HKs incorporated $^{32}P$ from [$\gamma$-$^{32}P$]ATP (adenosine triphosphate) in a light-dependent manner at $T$ = 0 min (Fig. 3 A-D), confirming that each functions as a light-activated kinase. The BM-LOV-HK-C69A mutant, which binds FMN but cannot form the cysteinyl adduct, did not activate the kinase in response to illumination (Fig. 3E). In addition, an assay testing the alkali and acid stability of the phosphate bond indicated that, in all the proteins, a phosphohistidine bond most likely formed upon kinase activation (fig. S1) (*21*).

The LOV-HKs we examined all contain a sensor/histidine kinase and therefore are presumably involved in two-component signaling. When activated, the histidine kinases operate by transiently phosphorylating a histidine residue on the kinase, and the phosphate from the activated kinase is transferred to an aspartate of a response regulator (*22*, *23*). The activated response regulators are generally involved in control of gene expression or, in the case of chemotaxis, in flagellar motor control (*22*, *23*). The PS-LOV-HK is unique among these four LOV kinases because its putative receiver (Rec) domain is covalently linked to the histidine ki-

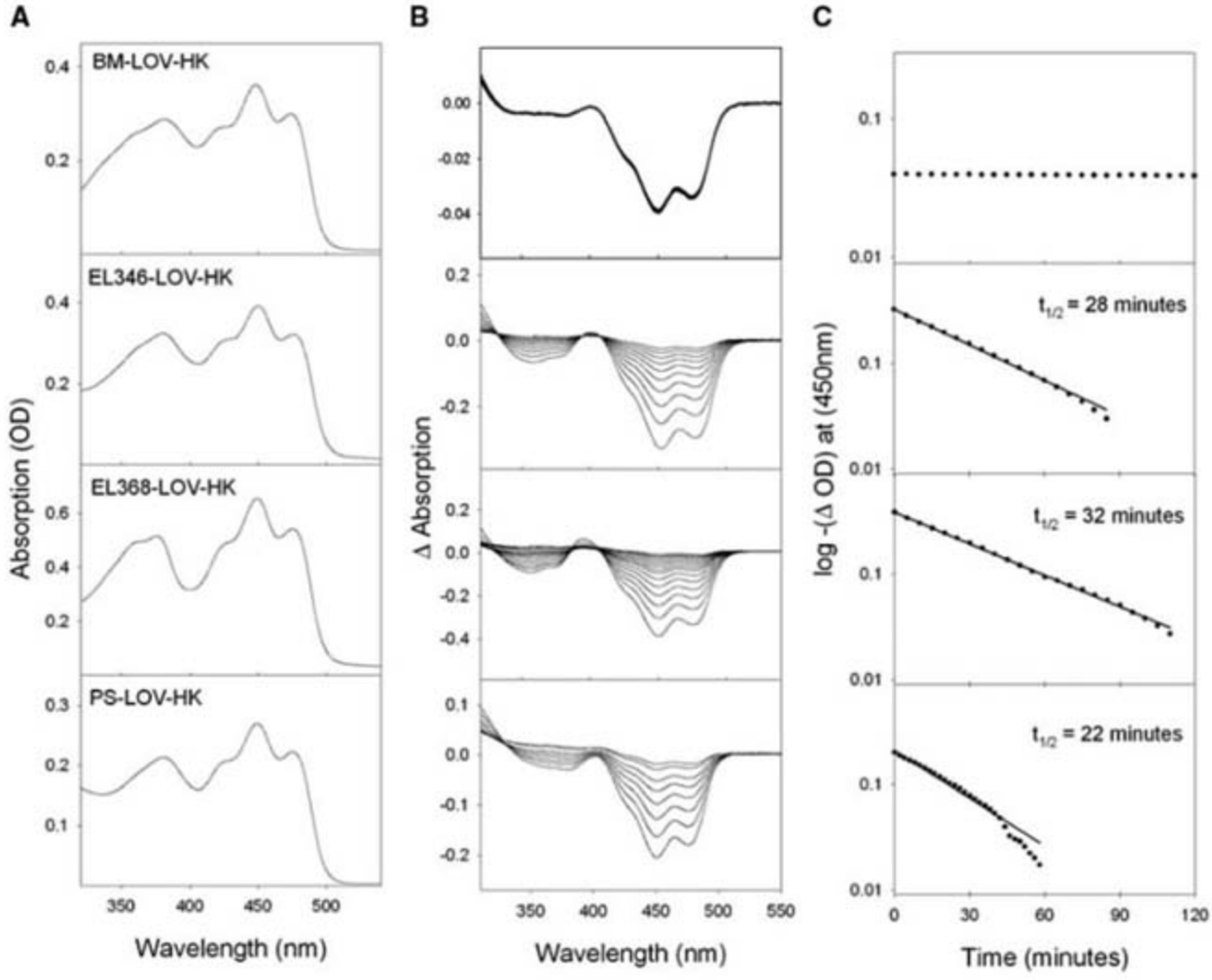


**Fig. 2.** Absorption spectra and absorption changes for full-length LOV-HKs. (**A**) Absorption of LOV-HKs showing flavin binding and characteristic LOV-domain absorption spectra. (**B**) Light-induced absorption difference spectra. BM-LOV-HK data collected every 5 min for 2 hours after light excitation. EL346-LOV-HK, EL368-LOV-HK, and PS-LOV-HK spectra collected every 10 min after light excitation. Difference spectra are typical of cysteinyl adduct formation characteristic of LOV-domain photosensory module photochemistry. (**C**) Absorption changes after light excitation measured at 450 nm. Decay is fit to a single exponential with the half-life shown on the graphs. Samples were all in phosphorylation buffer.

nase at the C terminus (Fig. 1). In two-component signaling, the Rec should be the final acceptor of the phospho-relay chain. However, our in vitro activity assay (fig. S1) indicated that the histidine of the sensor kinase and not the aspartate on the response regulator domain was phosphorylated, because treatment of phosphorylated PS-LOV-HK with alkaline buffer to hydrolize phospho-aspartates (*21*) did not significantly reduce phosphorylation.

After irradiation, the BM-LOV-HK kinase activity correlates with the presence of the flavin cysteinyl adduct state (Fig. 3A). For the other three kinases, the amount of radioactive phosphate incorporated decreased with time in darkness (Fig. 3, B to D) corresponding to the breakage of the cysteinyl adduct (Fig. 2B), indicating that the LOV-domain adduct state is the signaling state that triggers activation of the histidine kinase. When a second light pulse was given 180 min after the first, phosphorylation was as strong as that from the initial light pulse, indicating that the decrease in phosphorylation over time after the initial light pulse was not due to protein degradation.

The kinase-domain activation results presumably from intramolecular propagation of a local structural perturbation generated by adduct formation. We do not know whether the LOV domains in microorganisms use a common intramolecular signaling mechanism that has been adapted to allow for simple exchanging of sensory modules to different output signaling domains. In the plant receptor phototropin, it seems that LOV-domain activation disrupts an adjacent amphipathic alpha helix (Jα), which then activates the kinase domain (*16*). Although protein modeling with the Swiss-model program (*20*) predicts a close resemblance to phototropin LOV domains, it does not predict an amphipathic Jα helix, which suggests that different intramolecular signaling mechanisms occur.

LOV domain photoactivity implies that light responses are important for these microorganisms (*3*, *4*) and possibly required for virulence (*24*). We found that the PS-LOV-HK gene was constitutively expressed in the *P. syringae* pathovar *syringae* strain DC3000 grown in minimal media (fig. S2), a condition known to induce the type III secretion/pathogenicity island (*25*). Conversely, we did find about a twofold increase in transcription of the BM-LOV-HK (BMEII0679) gene from *B. melitensis* at a pH (*26*) similar to that within infected macrophages (table S2).

Two-component signal transduction systems are involved in bacterial virulence (*24*); hence, we investigated the role of BA-LOV-HK in virulence by constructing an insertion-knockout mutant strain by the introduction of a kanamycin-resistant cassette into the gene (*27*). To determine whether the *B. abortus* LOV-HK mutant is able to replicate inside mammalian host cells, we infected J774A.1 murine macrophages with the wild type and the knockout bacteria and counted intracellular bacteria after infection

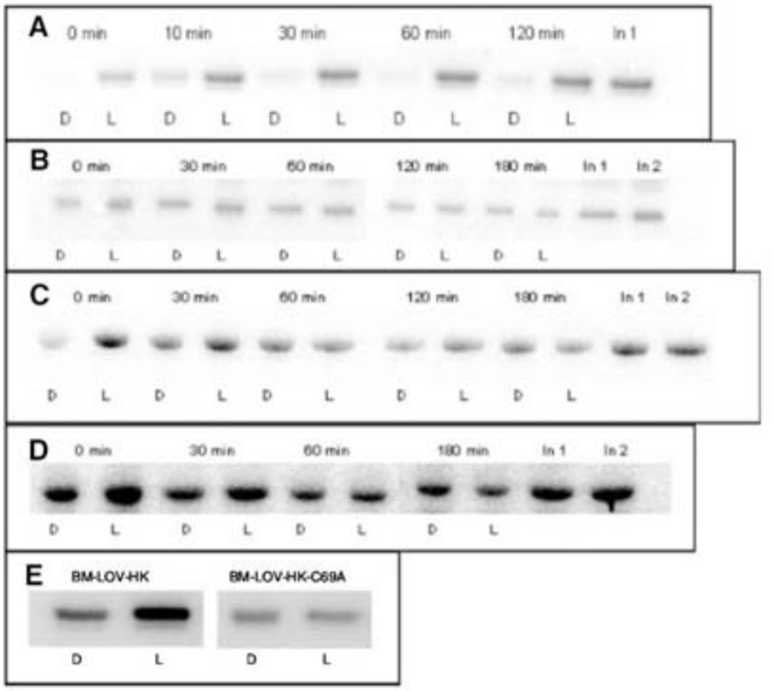


**Fig. 3.** LOV-HKs function as light-activated kinases. Autoradiogram showing the light-dependent phosphorylation of LOV-HKs. Samples were given a mock irradiation (D) or irradiated with a 1-min white light (L) pulse at a fluence of 2000 μmol $m^{-2}$ $s^{-2}$. [γ-$^{32}$P]ATP was added 0, 30, 60, 120, and 180 min after the light pulse, and the samples were incubated for 4 min at room temperature. Samples were then fractionated with SDS–polyacrylamide gel electrophoresis (PAGE), and the gels were exposed to film. (In 1 indicates a sample in darkness for 180 min followed by a light pulse and addition of [γ-$^{32}$P]ATP. In 2 indicates a sample given light pulse followed by 180 min in darkness, followed by a second light pulse and immediate addition of [γ-$^{32}$P]ATP). All manipulations were carried out under dim red light. (**A**) BM-LOV-HK. (**B**) EL346-LOV-HK. (**C**) EL368-LOV-HK. (**D**) PS-LOV-HK. (**E**) BM-LOV-HK-C69A shows no light-induced activation of the kinase domain, consistent with the absence of light-induced photochemistry.

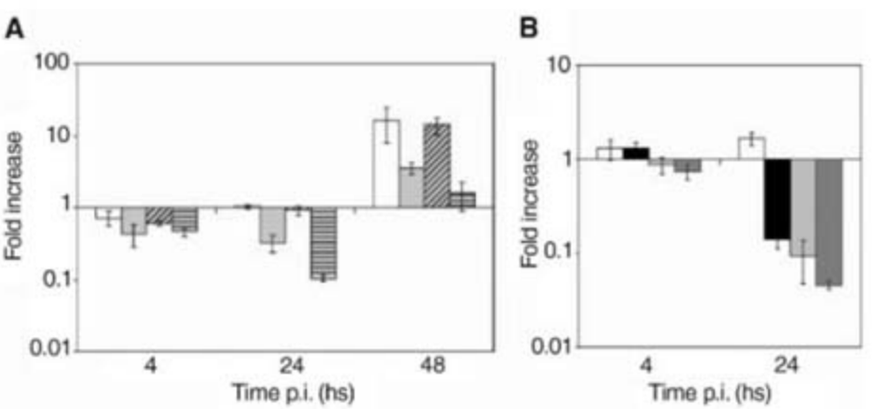


**Fig. 4.** LOV-HK protein from *B. abortus* is involved in virulence. Infectivity of *B. abortus* 2308 and *B. abortus* LOV-HK null mutant was tested in the J774A.1 murine macrophage cell line (**A**). At the indicated times (4, 24 and 48 hours), cells were lysed and the number of intracellular bacteria was determined by plating on tryptic soy agar. *B. abortus* 2308 (white), LOV-HK mutant (light gray), LOV-HK mutant complemented with plasmid pBBR-BaLOV expressing LOV-HK protein (diagonal hatched) and *B. abortus* LOV-HK mutant transformed with pBBR-BaLOV C69A expressing LOV-HK-C69A mutant protein (horizontal hatched). Data (mean ± standard deviation of duplicates) shown are representative of three independent experiments performed. Light affects *B. abortus* infection (**B**). *B. abortus* 2308 and LOV-HK bacteria given either dark or light treatment were used to infect macrophage cell line J774A.1. At the indicated times, the number of intracellular bacteria was determined by plating in tryptic soy agar. *B. abortus* 2308 light treatment (white) and dark treatment (black); LOV-HK knockout mutant light treated (light gray) and dark treated (dark gray). Data shown (mean ± standard deviation of duplicates) are representative of two independent experiments. In both graphs, data are presented as relative increase over 1-hour data. All CFU/ml (colony forming units) values were divided by the corresponding one-hour data.

(Fig. 4A). Replication of the *B. abortus* LOV-HK mutant strain was less than the wild-type strain as early as 4 hours after infection. To confirm that this defect in replication was only due to the absence of the BA-LOV-HK gene, the LOV-HK mutant was complemented with a plasmid expressing the wild-type BA-LOV-HK gene. The complemented strain was able to rescue the mutant phenotype (Fig. 4A), confirming that the BA-LOV-HK gene is required for optimal replication of *B. abortus* in macrophages.

Light activation of the LOV-HK requires a reactive cysteine (C69). A C69A mutant in a *B. abortus* LOV-HK knockout background did not return the replication rate to the wild-type level (Fig. 4A), indicating that formation of the covalent adduct between FMN and the LOV protein is essential to restore kinase function. Thus, the biological role of the LOV-HK protein is associated with its capacity to sense light and transduce the signal to the output kinase domain. The number of intracellular bacteria increased slightly after 24 hours in culture in the light (Fig. 4B); however, in the dark, roughly an order of magnitude fewer bacteria survived, a survival rate no better than that of the BA-LOV-HK knockout mutant, which suggests clearly that the BA-LOV-HK photoreceptor serves as a virulence factor in *Brucella* spp. and that light may prepare the bacteria present in the aborted placenta for infection of the next host (*28*).

We have shown that four bacterial LOV-HKs bind a flavin chromophore that, upon illumination, forms the cysteinyl adduct characteristic of LOV domain photochemistry. Unexpectedly, the cysteinyl adduct in *Brucella* LOV-HK does not break spontaneously in the dark as it does in the other bacterial LOV-HK proteins and the plant phototropin LOV domains (*17*). Upon illumination in the presence of ATP, the kinases of all four LOV-HKs undergo autophosphorylation, likely on a conserved histidine, and are activated. The close correlation between cysteinyl-flavin adduct lifetime and kinase activity indicates that the adduct is the signaling state that activates the histidine kinase. Furthermore, the BA-LOV-HK appears to function as a photoreceptor that is directly related to *Brucella* survival and replication within macrophages.

### References and Notes


1. S. Crosson, in *Handbook of Photosensory Receptors*, W. Briggs, J. L. Spudich, Eds. (Wiley VCH, Weinheim, 2005), pp. 323–336.
2. A. Losi, in *Flavins: Photochemistry and Photobiology*, E. Silva, A. M. Edwards, Eds. (Royal Society of Chemistry, Cambridge, 2006), pp. 217–269.
3. S. Crosson, S. Rajagopal, K. Moffat, *Biochemistry* **42**, 2 (2003).
4. A. Losi, *Photochem. Photobiol. Sci.* **3**, 566 (2004).
5. T. A. Gaidenko, T. J. Kim, A. L. Weigel, M. S. Brody, C. W. Price, *J. Bacteriol.* **188**, 6387 (2006).
6. M. Avila-Perez, K. J. Hellingwerf, R. Kort, *J. Bacteriol.* **188**, 6411 (2006).
7. U. Krauss, A. Losi, W. Gartner, K. E. Jaeger, T. Eggert, *Phys. Chem. Chem. Phys.* **7**, 2804 (2005).
8. A. Losi, E. Polverini, B. Quest, W. Gartner, *Biophys. J.* **82**, 2627 (2002).
9. J. M. Christie, *Annu. Rev. Plant Biol.* **58**, 21 (2007).
10. S. Crosson, K. Moffat, *Proc. Natl. Acad. Sci. U.S.A.* **98**, 2995 (2001).
11. M. Salomon, J. Christie, E. Knieb, U. Lempert, W. Briggs, *Biochemistry* **39**, 9401 (2000).
12. T. E. Swartz *et al.*, *J. Biol. Chem.* **276**, 36493 (2001).
13. M. T. Alexandre, J. Arents, R. Van Grondelle, K. Hellingwerf, J. Kennis, *Biochemistry* **46**, 3129 (2007).
14. T. Kottke, J. Heberle, D. Hehn, B. Dick, P. Hegemann, *Biophys. J.* **84**, 1192 (2003).
15. S. B. Corchnoy *et al.*, *J. Biol. Chem.* **278**, 724 (2003).
16. S. M. Harper, L. Neil, K. Gardner, *Science* **301**, 1541 (2003).
17. W. R. Briggs, J. Christie, *Trends Plant Sci.* **7**, 204 (2002).
18. V. G. DelVecchio *et al.*, *Proc. Natl. Acad. Sci. U.S.A.* **99**, 443 (2002).
19. S. M. Halling *et al.*, *J. Bacteriol.* **187**, 2715 (2005).
20. T. Schwede, J. Kopp, N. Guex, M. C. Peitsch, *Nucleic Acids Res.* **31**, 3381 (2003).
21. S. Klumpp, J. Krieglstein, *Eur. J. Biochem.* **269**, 1067 (2002).
22. A. H. West, A. M. Stock, *Trends Biochem. Sci.* **26**, 369 (2001).
23. A. M. Stock, V. L. Robinson, P. N. Goudreau, *Annu. Rev. Biochem.* **69**, 183 (2000).
24. J. A. Hoch, *Curr. Opin. Microbiol.* **3**, 165 (2000).
25. J. R. Alfano, A. Collmer, *Annu. Rev. Phytopathol.* **42**, 385 (2004).
26. F. Porte, J. P. Liautard, S. Kohler, *Infect. Immun.* **67**, 4041 (1999).
27. R. A. Ugalde, *Microbes Infect.* **1**, 1211 (1999).
28. P. H. Elzer, S. D. Hagius, D. S. Davis, V. G. DelVecchio, F. M. Enright, *Vet. Microbiol.* **90**, 425 (2002).


29. We are grateful to W.-O. Ng for experimental advice and to S. Zulman for critical reading of the manuscript. Work in the authors' laboratories was supported by NSF grants MCB 0444390 (R.A.B.) and MCB 0091384 and 0444504 (W.R. B.); NIH 1.U54-AI-057153, Binational Agricultural Research and Development Fund US-3829-06, and USDA 35204-14856 (G.S.); and NIH RO1-GM068886 (M.B.M.), ANPCyT PICT2004-20408 (R.A.U.), and PICT2005-38272 (D.J.C.). The research of F.A.G. was supported in part by an International Research Scholars' grant from the Howard Hughes Medical Institute and by Agencia Nacional de Promoción Científica y Tecnológica–Proyectos de Investigación Científica y Tecnológica (ANPCYT-PICT2004-21193). We thank S. Giovannoni and his laboratory and the J. Craig Venter Institute (JCVI) for the *E. litoralis* HTCC2594 genome sequence, which was determined and deposited in GenBank (CP000157) with support from the Gordon and Betty Moore Foundation. We are indebted to S. Kravitz and S. Ferriera of JCVI and J. Kitner, J. Tripp, S. Givan, and K. Vergin of Oregon State University for their work on the *E. litoralis* genome sequence and for the DNA used to clone the *E. litoralis* LOV domains.


### Supporting Online Material

www.sciencemag.org/cgi/content/full/317/5841/1090/DC1
Materials and Methods
Figs. S1 and S2
Tables S1 and S2
References

26 April 2007; accepted 27 June 2007
10.1126/science.1144306

# Temporal Fragmentation of Speciation in Bacteria

**Adam C. Retchless and Jeffrey G. Lawrence***

Because bacterial recombination involves the occasional transfer of small DNA fragments between strains, different sets of niche-specific genes may be maintained in populations that freely recombine at other loci. Therefore, genetic isolation may be established at different times for different chromosomal regions during speciation as recombination at niche-specific genes is curtailed. To test this model, we separated sequence divergence into rate and time components, revealing that different regions of the *Escherichia coli* and *Salmonella enterica* chromosomes diverged over a ~70-million-year period. Genetic isolation first occurred at regions carrying species-specific genes, indicating that physiological distinctiveness between the nascent *Escherichia* and *Salmonella* lineages was maintained for tens of millions of years before the complete genetic isolation of their chromosomes.

The proper identification and delineation of bacterial species play critical roles in medical diagnosis, food safety, epidemiology, and bioterrorism mitigation. Human responses are guided by perceptions of the biological properties and capabilities of a named species, as well as by an understanding of its natural variability and potential to change. The biological species concept (BSC) considers a species to be a group of organisms that readily exchange genetic information only with each other (*1*). In eukaryotes, recombination—here defined as allelic exchange—is often tied to reproduction, whereby meiosis is followed by the karyogamy of two entire haploid genomes. Consequently, as new species arise, genetic isolation would occur simultaneously for all loci, meaning that all pairs of orthologous genes would be diverging for about the same amount of time. Whereas bacterial speciation is a complex process (*2*–*4*), the BSC has also been applied to bacteria such as *E. coli* (*5*). Bacterial recombination involves the occasional, unidirectional transfer of small DNA fragments from one strain into the homologous locus of another strain. Because only a small portion of

Department of Biological Sciences, University of Pittsburgh, Pittsburgh, PA 15260, USA.

*To whom correspondence should be addressed. E-mail: jlawrenc@pitt.edu

the genome is transferred, orthologs would have diverged for differing amounts of time (fig. S1, A and B). Interspecies transfer is limited by mechanisms that increasingly reject recombination as donor and recipient sequences become more divergent (*6*, *7*). Yet this process does not speak to how recombination ceases within a group of recombining strains (wherein allelic differences are few), thereby allowing two genetically distinct groups to form.

Given the vast range of recombination rates seen for bacterial populations (*8*, *9*), we propose two models for lineage separation after the emergence of and selection for a differentially adapted genotype. First, nucleotide substitutions and lineage-specific loci could be acquired quickly, relative to the rate of recombination (*10*). In this model, genetic isolation would be established almost simultaneously for all orthologs (fig. S1A). Alternatively, niche-specific changes may be acquired more slowly, relative to the rate of recombination (fig. S1B), and gene conversion events would continue at loci unlinked to niche-defining genes (*11*). In this case, between-population selective sweeps (*12*) would occur freely at loci that are unlinked to genes imparting ecological distinctiveness; in contrast, recombinants losing niche-specific functions would be poorly adapted to either environment and would be counterselected (*4*). Thus, alleles may undergo selective sweeps across "species" boundaries when not proximate to niche-specific loci; over time, all loci would become genetically isolated as mismatches accumulate and the number of niche-specific loci increases. This fragmented speciation model further predicts that early-diverging genes will be linked to loci that interfered with effective interlineage recombination, such as those encoding niche-specific traits or those subject to diversifying or frequency-dependent selection (*13*, *14*). As a caveat, regions of strongly dissimilar DNA can interfere with recombination at highly similar flanking regions, independent of selection against recombinants (*7*); the consequences of this issue are beyond the scope of this work.

To detect temporal fragmentation of speciation, we must first distinguish between early- and late-diverging orthologs. Because divergence is a function of both time and evolutionary rate, time may be estimated from divergence once the evolutionary rate is determined (fig. S1C). At synonymous sites, evolutionary rate can be estimated from the codon adaptation index (CAI), an intragenomic, time-independent measure of selection (*15*). Divergence is measured as the number of synonymous substitutions per synonymous site ($K_s$); because $K_s$ decreases as CAI increases (fig. S1C), CAI can generate the expected value of $K_s$ if divergence times are uniform among genes (*16*). Early-diverging orthologs will have larger than expected $K_s$ values because more time has elapsed since their divergence, and late-diverging orthologs will have smaller than expected values (fig. S1C).

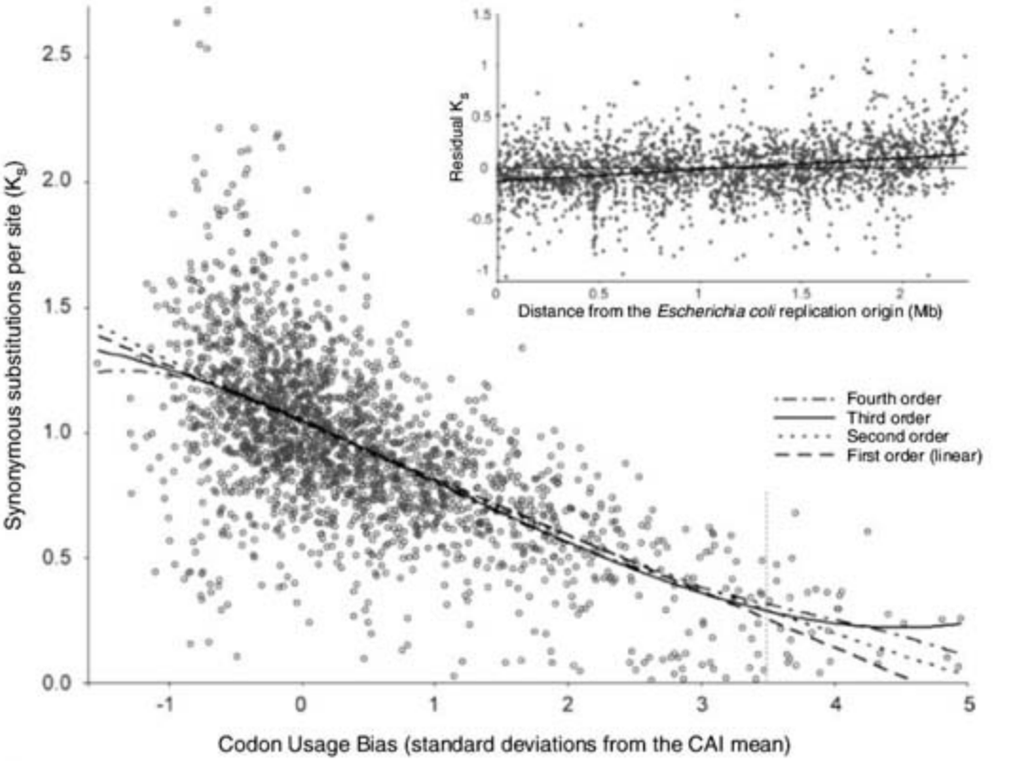


**Fig. 1.** Influences on synonymous substitution rate. Synonymous substitutions as a function of mean codon bias of the open reading frames are shown, with polynomial least-squares regression lines. The dashed vertical line indicates the value of CAI above which the relationship between CAI on $K_s$ was unclear. (**Inset**) Scatter plot of third-order regression residuals as a function of distance from the *E. coli* K12-MG1655 origin, with a linear least-squares regression line. Mb, megabase.

We applied this method to the genomes of *E. coli* and *S. enterica*; recombination is common within either taxon (*8*, *10*, *17*), whereas interspecies recombination is inhibited (*18*). We analyzed genes with orthologs present in each of three different *E. coli* and *S. enterica* genomes representing the most diverse available sequences (*16*). These six strains share a chromosomal backbone of 2677 sets of orthologs (table S1). CAI and between-species $K_s$ were computed for protein-coding genes, and the relationship was fit by polynomial regression (Fig. 1). As expected, increasing selection for preferred codons (high CAI) is generally reflected by lower divergence (low $K_s$). We ignored 527 pairs of genes with <50 synonymous sites, either because their $K_s$ values were in saturation or because the relationship between CAI and $K_s$ was unclear (Fig. 1). The effect of map position on $K_s$ (*19*) was estimated by treating CAI-corrected $K_s$ as a linear function of the gene's distance from the *E. coli* K12 replication origin (Fig. 1, inset). Ultimately, relative divergences of 2150 genes along the chromosomal backbone (Fig. 2) were calculated as the ratio of observed $K_s$ to that expected from CAI and map position (*16*).

Although stochastic variation in the accumulation of substitutions will account for much of the variability in relative divergence, genes that have recombined more recently should have lower $K_s$ values. To detect this footprint of recombination, we rely on a mechanistic constraint of bacterial gene exchange: Physically proximate genes will be transferred in the same recombination events. As a result, early- and late-diverging genes will not be randomly distributed throughout the genome but will cluster in regions defined by the most recent interlineage exchange. Therefore, physical association among genes with $K_s$ values higher or lower than expected can be taken as evidence for recombination. The scale of recombination regions was estimated from the correlation of relative divergence values for pairs of orthologs (solid line in Fig. 2, inset). Adjacent genes showed a strong intraclass correlation [intraclass correlation coefficient (ICC) = 24%, $P < 10^{-24}$, F test] that decreased as pairs of orthologs became more distantly situated on the chromosomal backbone, becoming undetectable when separated by more than 20 genes (~32 kb). These results are consistent with the boundary of recombination interference observed for the *rfb* locus (*20*, *21*). To remove any correlation in $K_s$ resulting from transcription-associated repair or selection for mRNA stability, we recalculated ICCs, having excluded comparisons between consecutive genes transcribed in the same direction. Despite the decreased sample size, a significant correlation (ICC = 11%, $P < 10^{-2}$, F test) extended to the same distance (dashed line in Fig. 2, inset). Thus, genes within the *Escherichia* and *Salmonella* chromosomes diverged at significantly different times at different locations.

Potential recombination events were delineated with an agglomerative clustering algorithm

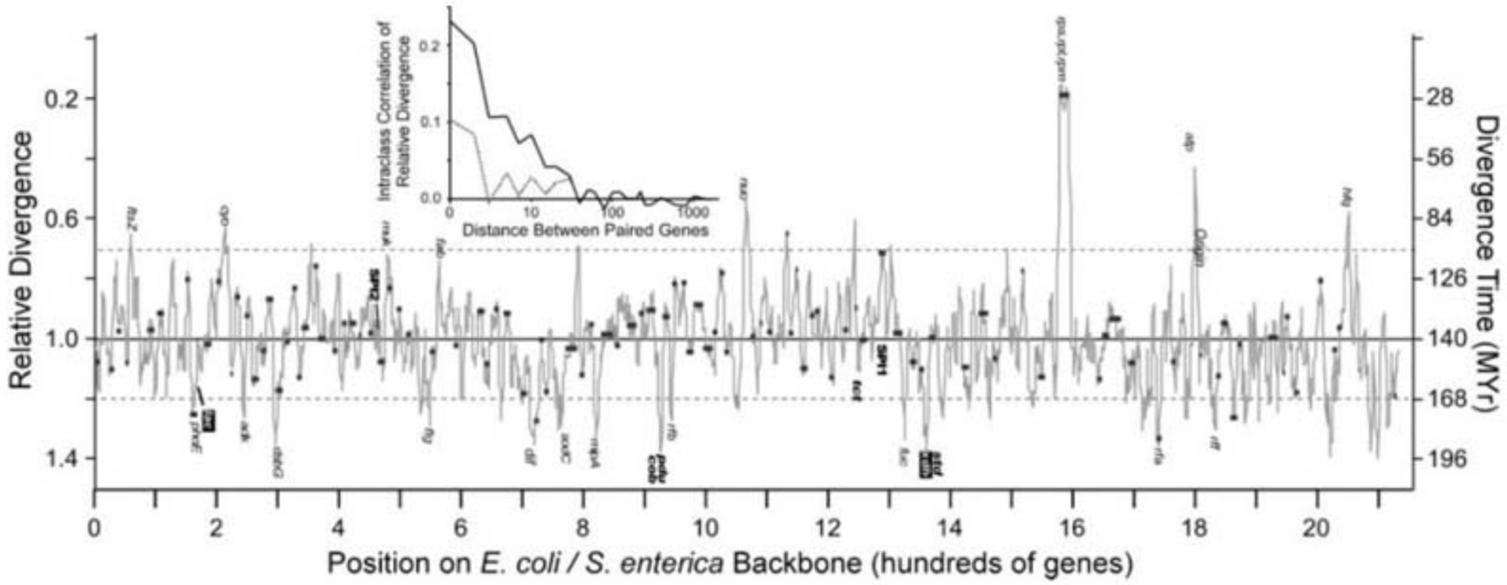


**Fig. 2.** Time of divergence of chromosomal regions. Relative divergence for orthologs is plotted against *E. coli* K12-MG1655 chromosomal position, averaged across a seven-gene window. Dark gray bars indicate divergence times of regions longer than six genes. Dashed lines delineate 95% of the range of divergence values. Shared loci are indicated in italics; *Escherichia*- and *Salmonella*-specific loci are indicated at their corresponding location on the backbone in inverse and bold-faced type. (**Inset**) Intraclass correlations of relative divergence for gene pairs as a function of distance. The solid line indicates all gene pairs, whereas the dotted line indicates gene pairs not within runs of consecutive genes transcribed in the same direction.

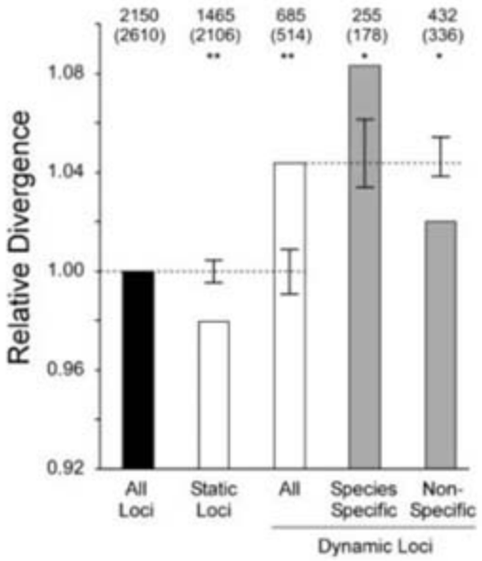


**Fig. 3.** Relative divergence based on region character. Bars show the mean relative divergence of sets of orthologs classified according to adjacency to loci that distinguish genomes; above the bars are the number of orthologs (top row) and the number of loci (bottom row in parentheses). Dashed lines show the average value for the entire set. Error bars show 1 SE for the distribution of randomized samples. *, $P < 0.01$; **, $P < 0.000001$.

that minimized variability of relative divergence within clusters (*16*); the algorithm terminated when the distribution of cluster sizes most closely reflected the magnitude of ICCs across segments of differing length. The most robust segments (SE < 0.013; each longer than six genes, covering 49% of genes) appear as dark gray bars in Fig. 2. If *Escherichia* and *Salmonella* genes have been diverging for ~140 million years on average (*22*), the distribution of divergence times shows that genetic isolation developed over a period of ~70 My (region between the dashed lines in Fig. 2). As expected, among the first regions to diverge were those containing genes producing surface structures, such as the *rfa*, *rfb*, *rff*, *flg*, *mipA*, and *phoE* loci, which are often subject to frequency-dependent or diversifying selection. Other early-diverging regions are associated with differences in gene content, such as those adjacent to (i) the *Salmonella cbi*, *pdu*, *std*, and *tct* operons and (ii) the *Escherichia lac* and *xdh* operons (Fig. 2), most of which encode physiological functions that distinguish the two species (*23*). In contrast, the regions flanking *Salmonella* Pathogenicity Islands 1 and 2 (SPI1 and SPI2) diverged more recently, suggesting that they did not promote the separation of *Escherichia* and *Salmonella*. Even though relative divergence was corrected for evolutionary rate, the major peaks in Fig. 2 consistently represent clusters of genes with high CAI values. These slowly evolving regions may offer longer stretches of DNA with high similarity, thereby postponing the establishment of recombination barriers.

As a control, we compared the genomes of *Buchnera aphidicola* strains APS and Sg, whose 489 conserved protein-coding genes show divergence similar to those of *Escherichia-Salmonella* comparison. *Buchnera* are *recA*-deficient intracellular endosymbionts believed to recombine rarely (*24*). We would expect lineage diversification to affect all loci simultaneously, and analysis of these genomes showed no significant correlation in relative divergence for adjacent genes (fig. S2). To control for the lower sample size, we examined all regions of the *Escherichia-Salmonella* comparative backbone with equal gene numbers; these regions showed significant ICC values that were invariably stronger than the *Buchnera* ICC value, suggesting that the lack of correlation for *Buchnera* reflects a lack of recombination.

The fragmented speciation model (fig. S1B) predicts that genetic and ecological differentiation developed even as recombination continued at loci not conferring ecological distinctiveness. Niche-specific traits often arise by gene gain or loss, where altered physiology allows cells to thrive in conditions that are hostile to parental strains (*25*). If recombination between incipient *Escherichia* and *Salmonella* lineages continued at some loci even after lineage-specific loci had arisen, then shared regions around the lineage-specific genes should have been among the first to become genetically isolated, because recombination in those regions would have eliminated the gene-content differences at those loci. Conversely, if the differences in gene content developed only after interlineage recombination had effectively ceased, then these genes should be distributed without regard to the divergence time of the surrounding region.

We defined a locus as a pair of genes in the *Escherichia-Salmonella* comparative backbone. There were 514 dynamic loci (685 genes; some genes contributed to 2 loci; table S2), at which a pair of conserved genes was separated by at least one gene that had been gained or lost in any genome (*16*); the remaining 2106 static loci showed no insertion or deletion events (white bars in Fig. 3). Genes at static loci have an average divergence time that is 4.4% younger than the average for the entire genome ($P < 10^{-5}$ by randomization), which is likely because longer stretches of uninterruptible, slowly evolving genes allow for continued recombination.

A fraction of dynamic loci (178 loci, table S2) show species-specific differences, whereat the conserved gene pair was interrupted in the three strains of one species by genes absent from the three strains of the other species. These loci would include sites whereat differences arose while the *Escherichia* and *Salmonella* lineages were diverging. Other dynamic loci (e.g., those where only a single strain shows a difference) would have arisen only after recombination had effectively ceased between the two lineages. Genes adjacent to species-specific loci are 6.2% older than genes adjacent to other dynamic loci ($P < 10^{-2}$ by randomization; gray bars in Fig. 3); thus, species-specific genes are not randomly distributed but are found preferentially in the older regions, indicating that the incipient *Escherichia* and *Salmonella* lineages continued to participate in recombination at loci unlinked to lineage-specific genes.

In contrast to the rapid formation of eukaryotic species boundaries, the ~70-My time frame over which genetic isolation evolved between *Escherichia* and *Salmonella* represents a temporal fragmentation of speciation. Because separate lineages arise within populations that continue to recombine at some loci for tens of millions of years, relationships among species inferred from few loci may underestimate their underlying complexity. Taxa may show different relationships depending on the genes compared. Long periods of partial genetic isolation allow extant, named species (such as *E. coli*) to contain multiple nascent species. Although one can observe recombination at some genes within *E. coli* as a whole, strains also have niche-specific loci that may act as genetic progenitors for the creation of new species. That is, it may not possible to make a clear distinction between intraspecific and interspecific variability (*26*), and clearly defined species cannot represent newly formed lineages. Therefore, the species concept proposed by Dykhuizen and Green [in which gene phylogenies are congruent among representatives of different species but are incongruent among members of the same species (*5*)] works to delineate long-established species but fails to recognize incipient species.

### References and Notes


1. E. Mayr, *Systematics and the Origin of Species from the Viewpoint of a Zoologist* (Columbia Univ. Press, New York, 1942).
2. F. M. Cohan, *Syst. Biol.* **50**, 513 (2001).
3. D. Gevers *et al.*, *Nat. Rev. Microbiol.* **3**, 733 (2005).
4. J. G. Lawrence, *Theor. Popul. Biol.* **61**, 449 (2002).
5. D. E. Dykhuizen, L. Green, *J. Bacteriol.* **173**, 7257 (1991).
6. M. Vulić, F. Dionisio, F. Taddei, M. Radman, *Proc. Natl. Acad. Sci. U.S.A.* **94**, 9763 (1997).
7. P. Shen, H. V. Huang, *Genetics* **112**, 441 (1986).
8. E. J. Feil *et al.*, *Proc. Natl. Acad. Sci. U.S.A.* **98**, 182 (2001).
9. W. P. Hanage, C. Fraser, B. G. Spratt, *J. Theor. Biol.* **239**, 210 (2006).
10. D. Falush *et al.*, *Philos. Trans. R. Soc. London Ser. B* **361**, 2045 (2006).
11. C. Fraser, W. P. Hanage, B. G. Spratt, *Science* **315**, 476 (2007).
12. D. S. Guttman, D. E. Dykhuizen, *Genetics* **138**, 993 (1994).
13. H. Wildschutte, D. M. Wolfe, A. Tamewitz, J. G. Lawrence, *Proc. Natl. Acad. Sci. U.S.A.* **101**, 10644 (2004).
14. R. Milkman, *Genetics* **146**, 745 (1997).
15. P. M. Sharp, W. H. Li, *Nucleic Acids Res.* **15**, 1281 (1987).
16. Materials and methods are available as supporting material on *Science* Online.
17. D. S. Guttman, D. E. Dykhuizen, *Science* **266**, 1380 (1994).
18. V. Daubin, N. A. Moran, H. Ochman, *Science* **301**, 829 (2003).
19. P. M. Sharp, D. C. Shields, K. H. Wolfe, W. H. Li, *Science* **246**, 808 (1989).
20. R. Milkman, M. M. Bridges, *Genetics* **133**, 455 (1993).
21. R. Milkman, E. Jaeger, R. D. McBride, *Genetics* **163**, 475 (2003).
22. H. Ochman, A. C. Wilson, *J. Mol. Evol.* **26**, 74 (1987).
23. A. Rambach, *Appl. Environ. Microbiol.* **56**, 301 (1990).
24. I. Tamas *et al.*, *Science* **296**, 2376 (2002).
25. H. Ochman, J. G. Lawrence, E. Groisman, *Nature* **405**, 299 (2000).
26. W. P. Hanage, C. Fraser, B. G. Spratt, *BMC Biol.* **3**, 6 (2005).


27. This work was supported by grant GM078092 from the NIH. We thank B. Siegler Retchless and H. Hendrickson for helpful discussions and comments on the manuscript.


### Supporting Online Material

www.sciencemag.org/cgi/content/full/317/5841/1093/DC1
Materials and Methods
Figs. S1 to S3
Tables S1 to S3
References

9 May 2007; accepted 27 July 2007
10.1126/science.1144876

# Video Ergo Sum: Manipulating Bodily Self-Consciousness

**Bigna Lenggenhager,[1] Tej Tadi,[1] Thomas Metzinger,[2,3] Olaf Blanke[1,4]***

Humans normally experience the conscious self as localized within their bodily borders. This spatial unity may break down in certain neurological conditions such as out-of-body experiences, leading to a striking disturbance of bodily self-consciousness. On the basis of these clinical data, we designed an experiment that uses conflicting visual-somatosensory input in virtual reality to disrupt the spatial unity between the self and the body. We found that during multisensory conflict, participants felt as if a virtual body seen in front of them was their own body and mislocalized themselves toward the virtual body, to a position outside their bodily borders. Our results indicate that spatial unity and bodily self-consciousness can be studied experimentally and are based on multisensory and cognitive processing of bodily information.

Ever since William James categorized different aspects of self-consciousness at the end of the 19th century, these aspects have been continuously refined and expanded, including many different sensory, emotional, or cognitive layers. This has led to an excess of definitions, in the absence of a widely accepted model of self-consciousness that is based on empirical neurobiological data (*1*). More recent philosophical and neurological theories converge on the relevance of bodily self-consciousness (i.e., the nonconceptual and prereflective processing and representation of body-related information) as one promising approach for the development of a comprehensive neurobiological model of self-consciousness (*1*–*4*).

We investigated bodily self-consciousness experimentally, and we now describe an illusion during which healthy participants experienced a virtual body as if it were their own and localized their "selves" outside of their body borders at a different position in space. We modified the so-called "rubber-hand illusion" (RHI), during which synchronous stroking of a seen fake hand and one's own unseen hand causes the fake hand to be attributed to one's body (to "feel like it is my hand"; misattribution). Under such conditions of multisensory conflict, vision typically dominates over proprioception and touch (*5*). Several studies have demonstrated that the RHI also induces a mislocalization of one's hand toward the fake hand, which is often referred to as "proprioceptive drift" (*6*–*8*). Brain-imaging studies associated the RHI mainly with the activation of the multisensory premotor cortex, posterior parietal areas (*7*), and right posterior insula (*9*); these areas have also been implicated in the integration of visual and somatosensory signals in nonhuman primates (*10*). These experimental findings corroborate anecdotal clinical data in neurological patients with right temporo-parietal damage leading to somatoparaphrenia, during which patients misattribute their own hand or foot as belonging to another person (*11*). The data on the RHI shows that important subglobal aspects of bodily experience, such as self-attribution and self-localization

[1]Laboratory of Cognitive Neuroscience, Ecole Polytechnique Fédérale de Lausanne, Station 15, 1015 Lausanne, Switzerland. [2]Philosophical Seminar, Johannes Gutenberg-Universität Mainz, 55099 Mainz, Germany. [3]Frankfurt Institute for Advanced Studies, Johann Wolfgang Goethe-Universität, 60438 Frankfurt am Main, Germany. [4]Department of Neurology, University Hospital, 1214 Geneva, Switzerland.

*To whom correspondence should be addressed. E-mail: olaf.blanke@epfl.ch

of body parts, can be manipulated experimentally (*12*).

Yet, the fundamental sense of selfhood (*2*, *13*, *14*) that is associated with bodily self-consciousness (but not with cognitive or emotional layers of self-consciousness) is experienced as the transparent content of a single, coherent whole-body representation, rather than as multiple representations of separate body parts. Accordingly, the latter have been referred to as the sense of body-part ownership, whereas whole-body representations or global ownership are directly associated with the sense of selfhood (*2*). Studies on the RHI and somatoparaphrenia thus investigated only body-part ownership or the attribution and localization of a body part with respect to the global bodily self; i.e., a part-to-whole relationship. Thus, these studies did not experimentally manipulate selfhood per se.

To manipulate attribution and localization of the entire body and to study selfhood, we designed an experiment based on clinical data in neurological patients with out-of-body experiences. These data suggest that the spatial unity between self and body may be disrupted (*15*–*17*), leading in some cases to the striking experience that the global self is localized at an extracorporeal position (*15*, *17*). The aim of the present experiments was to induce out-of-body experiences in healthy participants to investigate selfhood. We hypothesized that, under adequate experimental conditions, participants would experience a visually presented body as if it were their own, inducing a drift of the subjectively experienced bodily self to a position outside one's bodily borders. Evidence for this conjecture stems not just from out-of-body experiences, but also from early anecdotal mirror-induced whole-body illusions (*18*) and the phenomenon of "presence" in virtual-reality environments (*19*, *20*).

We applied virtual reality to examine the possible induction of out-of-body experiences by using multisensory conflict. In the first experiment, participants viewed the backs of their bodies filmed from a distance of 2 m and projected onto a three-dimensional (3D)–video head-mounted display (HMD) (Fig. 1A). The participants' backs were stroked for 1 min, either synchronously or asynchronously with respect to the virtually seen body. Global self-attribution of the virtual character was measured by a questionnaire that was adapted from the RHI (*6*). Global self-localization was measured by passively displacing the blind-folded participants immediately after the stroking and asking them to return to their initial position (*21*).

As predicted, participants showed a drift toward the virtual body (anterior-posterior axis) in the synchronous condition [24.1 ± 9.0 cm (mean ± SEM)]. This position differed significantly from the initial position ($P = 0.02$, Student's $t$ test = 2.67) (*21*). In the asynchronous condition, the drift was smaller (12. ± 8.5 cm) and no longer significant ($P = 0.17$, $t = 1.45$) (Fig. 2A). No significant drift was measured along the left-to-right axis (fig. S1). Global illusory self-localization was corroborated by high–self-attribution scores on the three relevant questionnaire items (Q1 to Q3) (*21*) also showing significant differences between synchronous and asynchronous conditions (all $P$ values < 0.001) (Fig. 2B). Participants reported varied feelings of "weirdness" or "strangeness," and some found the experiment irritating. None of the participants reported sensations of overt disembodiment or a change in visuospatial perspective.

In a second study, we examined whether this illusion depends on cognitive knowledge about bodies and whether the drift toward the virtual body was not due to a general motor bias to overshoot the target position. With the use of a constant time delay in asynchronous conditions, we either presented the participant's own body (as in study I) (Fig. 1A), a fake body (Fig. 1B), or an object (Fig. 1C) being stroked synchronously or not. Compared to a motor-control condition [no visual scene was shown (*21*)], we found a significant drift toward the virtual own body ($P = 0.02$, $t = 2.78$) and the fake body ($P = 0.01$, $t = 3.02$) (*21*). This drift was weaker and no longer significant in the case with a noncorporeal object ($P = 0.07$, $t = 1.95$) and absent when the stroking was asynchronous (all $P$ values > 0.11) (Fig. 3). There was no drift in further control conditions or for the left-to-right axis (*21*). Yet, self-attribution differed between

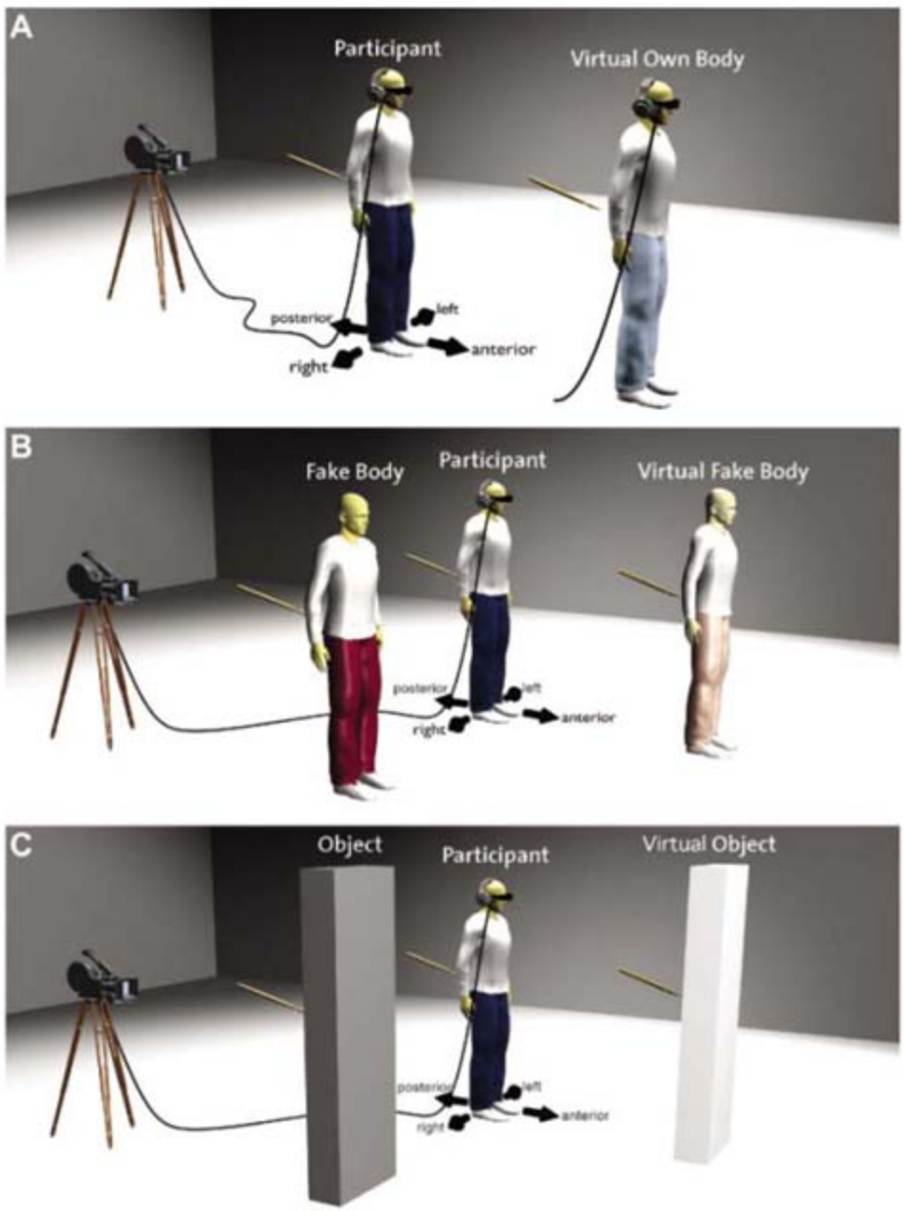


**Fig. 1.** (**A**) Participant (dark blue trousers) sees through a HMD his own virtual body (light blue trousers) in 3D, standing 2 m in front of him and being stroked synchronously or asynchronously at the participant's back. In other conditions (study II), the participant sees either (**B**) a virtual fake body (light red trousers) or (**C**) a virtual noncorporeal object (light gray) being stroked synchronously or asynchronously at the back. Dark colors indicate the actual location of the physical body or object, whereas light colors represent the virtual body or object seen on the HMD. [Illustration by M. Boyer]

the bodily conditions and the object condition. The first two questions of the questionnaire (Q1 and Q2) were answered positively in all of the synchronous conditions (own body, fake body, and object) and were significantly different and answered negatively in the asynchronous conditions ($P < 0.01$, $t > 2.56$). However, the third question (Q3: "It felt as if the virtual character was my body") led to different results. Whereas in both bodily conditions (own body and fake body) the result was the same as in Q1 and Q2 ($P < 0.05$, $t > 2.40$), this was not the case in the object condition where participants gave negative scores in the synchronous condition, revealing no significant difference between synchronous and asynchronous stroking ($P > 0.05$, $t = 1.55$) (fig. S2). This suggests that Q3 is important to evaluate self-identification with virtual bodily and nonbodily characters, whereas the first two questions seem more related to the feeling and location of touch.

With the use of virtual reality and multisensory conflict, we induced an illusion that makes it possible to quantify selfhood by manipulating attribution and localization of the entire body. Our results show that humans systematically experience a virtual body as if it were their own when visually presented in their anterior extrapersonal space and stroked synchronously. This finding was corroborated by the participants' mislocalization of their own bodies to a position outside their bodies, showing that self-attribution and localization of the entire body rely, at least partly, on similar visual-somatosensory integrative mechanisms to those of body parts (*6*–*8*). Although research of visual-somatosensory integration has mostly investigated directly visible body parts, comparable interactions have also been found for body parts that humans cannot see directly, such as the back (*22*). The overall pattern of the data from studies I and II suggests that, under appropriate conditions of multisensory conflict between visual signals conveying information about a virtual body (on a HMD) and tactile, proprioceptive, and vestibular signals conveying information from the participant's body, visual capture is still present. There were also differences between both studies. Asynchrony in study II was more predictable (*21*), and the relation between felt and seen events might have been perceived as stronger, leading to larger drifts in the asynchronous conditions in study II. This might have led to the diminished effect of synchrony on the drift in the own-body condition, which is compatible with higher questionnaire scores for the asynchronous conditions from study II as compared with those from study I (Q1 to Q3) (Fig. 2C and fig. S2A) (*21*).

By manipulating visual input in the RHI, controversial data have been reported concerning the influence of cognitive constraints on multisensory integration, self-localization, and self-attribution. Whereas some authors argue that multisensory correlation is a sufficient condition for self-attribution (*23*), others argue for additional cognitive constraints in terms of higher-level knowledge about the body (*8*). We found evidence for higher-level knowledge by revealing in study II a weaker drift toward the object as compared with the fake-body condition, as well as a selective effect of synchrony in the fake-body condition. Because the fake-body and object conditions are completely comparable concerning the experimental setup (*21*), and given the pattern of results, we suggest that in order to investigate the influence of cognitive knowledge on self-localization, the comparison between the fake-body and object conditions is more relevant than that between the own-body and object conditions. These effects on illusory self-localization were corroborated by illusory self-attribution. When asked whether it felt as if the virtual character or object was their body (Q3), participants self-identified with both bodily stimuli but not with the object during synchronous stroking. Collectively, these findings speak in favor of bottom-up mechanisms as well as cognitive constraint (*8*), rejecting a pure Bayesian account (*23*) for self-attribution and self-localization of the entire body.

Illusory self-localization to a position outside one's body shows that bodily self-consciousness and selfhood can be dissociated from one's physical body position. This finding differs from the RHI, in which this aspect of selfhood remained constant and only the attribution and localization of the stimulated hand was manipulated. Does illusory self-localization to a position outside one's body mean that we have experimentally induced full-blown out-of-body experiences? Out-of-body experiences are characterized by a disembodiment of the self to an extracorporeal location, an extracorporeal visuospatial perspective, and the sight of one's own body from this self-location. Because the present illusion was neither associated with overt disembodiment nor with a change in visuospatial perspective, we argue that we have induced only some aspects of out-of-body experiences or rather the closely related experience of heautoscopy that has also been observed in neurological patients (*15*–*17*). During heautoscopy, patients either constantly or intermittently experience as if they were seeing from and were localized at the position of an illusory body, their physical body, or at an intermediate position (*15*, *24*). Such patients may also see themselves from behind (*17*) and often identify with the illusory body and partly transfer selfhood to the illusory body, even if visual bodily detail is lacking (*17*). Yet, they never report the overt disembodiment that is the most characteristic feature of out-of-body experiences (*25*, *26*). Because our healthy participants did not report feelings of overt disembodiment, the present data suggest that other mechanisms in addition to conflicting visual-somatosensory information, such as visual-vestibular disintegration, are involved in generating full-blown out-of-body experiences and a more complete transfer of selfhood to an illusory body. These findings are compatible with clinical data (*15*, *17*). Damage to or electrical stimulation of the temporo-parietal junction may lead to out-of-body experiences and heautoscopy (*15*, *27*), and healthy participants activate the same region when employing extracorporeal self-locations in mental imagery (*28*, *29*). Although other important aspects of self-consciousness are likely to involve additional brain areas such as the amygdala and the right frontal cortex (*3*) as well as multisensory areas in premotor and parietal cortices [representing both

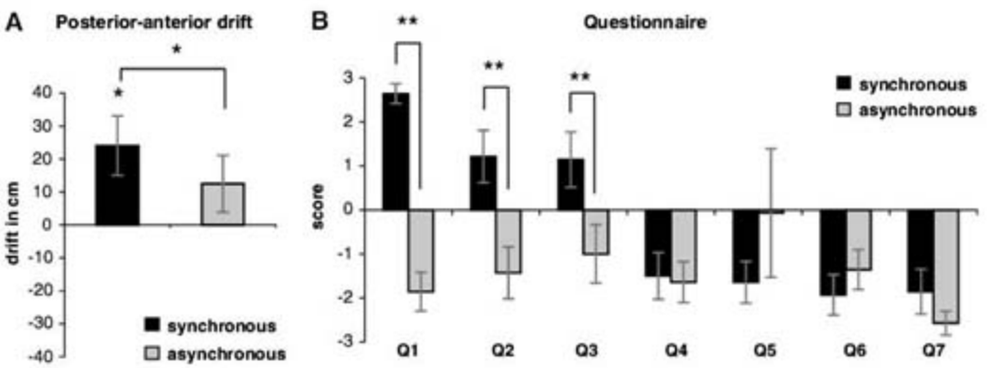


**Fig. 2.** (**A**) Drift measured in centimeters [mean ± SEM (error bars)] in the synchronous (black) and asynchronous stroking conditions (gray) on the posterior-anterior axis. Participants showed a significantly stronger drift in the direction of the virtual body in the synchronous condition. *$P < 0.05$. (**B**) Score (mean ± SEM) on the "self-attribution questionnaire" as adapted from (*6*). **$P < 0.01$.

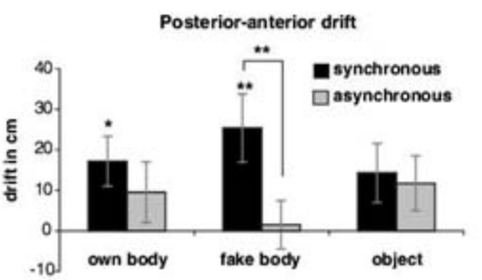


**Fig. 3.** Drift measured in centimeters, relative to the pure motor-control condition [mean ± SEM (error bars)] in the synchronous (black) and asynchronous stroking conditions (gray) for the different experiments: own body, object, and fake body. Only posterior-anterior drift is shown. *$P < 0.05$, **$P < 0.01$.

the seen and felt positions of one's arm (*10*) and correlating with the RHI (*7*), we speculate that humans' daily experience of an embodied self and selfhood, as well as the illusion reported here, relies on brain mechanisms at the temporo-parietal junction. Experimentally creating illusions of the globalized, multisensory awareness of selfhood in a controlled manner with virtual-reality technology opens a new avenue for the investigation of the neurobiological, functional, and representational aspects of embodied self-consciousness. Further research should include the entire spectrum of disturbed global own-body perceptions, ranging from autoscopic hallucinations and heautoscopy to full-blown disembodied states such as out-of-body experiences.

### References and Notes


1. S. Gallagher, *Trends Cogn. Sci.* **4**, 14 (2000).
2. T. Metzinger, *Being No One: The Self-Model Theory of Subjectivity* (MIT Press, Cambridge, MA, 2003).
3. A. R. Damasio, *Descartes' Error: Emotion, Reason, and the Human Brain* (Grosset/Putnam, New York, 1994).
4. O. Blanke, *Nature Rev. Neurosci.* **5**, 243 (2004).
5. A. Maravita, C. Spence, J. Driver, *Curr. Biol.* **13**, R531 (2003).
6. M. Botvinick, J. Cohen, *Nature* **391**, 756 (1998).
7. H. H. Ehrsson, C. Spence, R. E. Passingham, *Science* **305**, 875 (2004).
8. M. Tsakiris, P. Haggard, *J. Exp. Psychol. Hum. Percept. Perform.* **31**, 80 (2005).
9. M. Tsakiris, M. D. Hesse, C. Boy, P. Haggard, G. R. Fink, *Cereb. Cortex* 10.1093/cercor/bhl131 (2006).
10. M. S. A. Graziano, D. F. Cooke, C. S. R. Taylor, *Science* **290**, 1782 (2000).
11. P. W. Halligan, J. C. Marshall, D. T. Wade, *Cortex* **31**, 173 (1995).
12. S. Gallagher, *How the Body Shapes the Mind* (Oxford Univ. Press, Oxford, 2005).
13. F. Macknik, A. Reeves, *Science* **302**, 61 (2003).
14. T. Metzinger, *Mind Matter* **3**, 37 (2005).
15. O. Blanke, T. Landis, L. Spinelli, M. Seeck, *Brain* **127**, 243 (2004).
16. P. Brugger, *Cognit. Neuropsychiatr.* **7**, 179 (2002).
17. O. Blanke, C. Mohr, *Brain Res. Rev.* **50**, 184 (2005).
18. C. M. Stoffler, *Mind* **8**, 492 (1899).
19. "Doppelgängers," *Science* **291**, 619 (2001).
20. M. V. Sanchez-Vives, M. Slater, *Nat. Rev. Neurosci.* **6**, 332 (2005).
21. Material and methods, as well as detailed statistical analysis and results, are available as supporting material on *Science* Online.
22. L. P. Tigue *et al.*, *Exp. Brain Res.* **159**, 160 (2004).
23. K. C. Armel, V. S. Ramachandran, *Proc. Biol. Sci.* **270**, 1499 (2003).
24. P. Brugger, R. Agosti, M. Regard, H. G. Wieser, T. Landis, *J. Neurol. Neurosurg. Psychiatry* **57**, 838 (1994).
25. S. Blackmore, *Beyond the Body: An Investigation of Out-Of-Body Experiences* (Heinemann, London, 1982).
26. H. Irwin, *Flight of Mind: A Psychological Study of the Out-Of-Body Experience* (Scarecrow, Metuchen, NJ, 1985).
27. O. Blanke, S. Ortigue, T. Landis, M. Seeck, *Nature* **419**, 269 (2002).
28. S. Arzy, G. Thut, C. Mohr, C. M. Michel, O. Blanke, *J. Neurosci.* **26**, 8074 (2006).
29. O. Blanke *et al.*, *J. Neurosci.* **25**, 550 (2005).


30. This work was supported by the Gelbin Foundation, the Fondation de Famille Sandoz, the Fondation Defitech, and the Swiss National Science Foundation. We thank S. Arzy, A. Bertrand, S. Dieguez, and M. Steiger for their helpful comments on a previous version of the manuscript and M. Bayer for the illustrations in Fig. 1.


### Supporting Online Material

www.sciencemag.org/cgi/content/full/317/5841/1096/DC1
Materials and Methods
SOM Text
Figs. S1 to S3
Table S1
References


4 April 2007; accepted 19 July 2007
10.1126/science.1143959

## BRAIN INJURY RESEARCH GRANT AVAILABILITY

Three-Year Individual Research Grant,
maximum of $165,000 per year.

Three-Year Multi-Investigator Project Grant,
maximum of $660,000 per year.

Application form and details contact:
**www.nj.gov/health/njcbir**

**New Jersey Commission on**
**Brain Injury Research**
**PO Box 360**
**Market and Warren Streets**
**Trenton, New Jersey 08625-0360**

**Tel: 609-633-6465**
**E-mail: njcbir@doh.state.nj.us**

Letters of Intent deadline: **October 4, 2007**
Closing date for applications: **November 2, 2007**

## The Linda and Jack Gill Center for Biomolecular Science

### Gill Prizes for Outstanding Neuroscience Research - Call for Nominations

The Linda and Jack Gill Center for Biomolecular Science at Indiana University seeks nominations for the 2008 Distinguished Neuroscience Investigator Award and Young Neuroscience Investigator Award. These annual awards recognize individuals who have made significant contributions to cellular or molecular neuroscience. Prizes of $25,000 and $5,000, respectively, will be presented at the 2008 Gill Symposium on the campus of Indiana University, Bloomington, in May, 2008.

Past recipients include Richard Tsien, Benjamin Cravatt, Carla Schatz and Eric Nestler. Award recipients will present lectures on their research during the 2008 Gill Symposium, and the winners will be announced in prominent scientific publications. Nominations, including self nominations, should include a *curriculum vitae* and a brief account that highlights the contributions of the nominee.

***Deadline for submission is November 15, 2007***

Please submit nominations to:
**Gill Center for Biomolecular Science**
ATTN: Misty Theodore
Indiana University
1101 East Tenth Street
Bloomington, IN 47405
**E-mail:** gillctr@indiana.edu

**http://www.indiana.edu/~gillctr**

**INDIANA UNIVERSITY**
**BLOOMINGTON**

Held Concurrently
September 24-26, 2007 Waltham, Massachusetts

# Cell Culture Scale-Up

*Mammalian Cell Line Development, Scale-Up and Productivity*

Conference Co-Chairs
Greg Dean, Ph.D. - *Cambridge Antibody Technology*
Geoffrey Hodge - *Xcellerex, Inc.*

Sponsored By: PALL Life Sciences

*The Williamsburg BioProcessing Foundation*
P.O. Box 1229
Virginia Beach, VA 23451
757.423.8823 / fax 757.423.2065
www.wilbio.com
info@wilbio.t

WilBio

Conference Speakers
Celina de la Cruz Edmonds, *Merck & Co., Inc.* • Greg Dean, Ph.D., *Cambridge Antibody Technology*
Lewis Ho, Ph.D., *IDL Bioservices LLC* • Abdul Wajid, Ph.D., *XOMA Corporation, LLC*
Wenlin Zeng, Ph.D., *MedImmune Vaccines* • Ronald Fedechko, Ph.D., *Pfizer, Inc.*
John Fann, Ph.D., *Abbott Bioresearch Center* • Victor Saucedo, *Genentech, Inc.*
Jamal Meghrous, *Protein Sciences Corporation* • S. Edward Lee, Ph.D., *Pfizer Global R & D*
Phillip Madeira, *Genzyme Corporation* • Cori Gorman, Ph.D., *Selexis USA*
Ailsa Shepherd, *BioReliance Corporation* • John Carvell, Ph.D., *Aber Instruments*
Christian Kaisermayer, Ph.D., *University of Natural Resources and Applied Life Sciences*

genzyme
*Featuring a tour of the Genzyme facility in Allston Landing, MA*

# Purification of Biological Products

*Optimizing Recovery and Purity While Minimizing Cost*

Conference Co-Chairs
Pete Gagnon - *Validated Biosystems, Inc.*

Conference Speakers
Judy Glynn, *Pfizer, Inc.* • Missag Parseghian, Ph.D., *Peregrine Pharmaceuticals*
Jonathan Romero, Ph.D., *Biogen Idec, Inc.* • Nihal Tugcu, Ph.D., *Merck & Co., Inc.*
Andrew Baird, *Fluor Daniel* • Jonathan Lawrence, *Eli Lilly & Company*
Jin-an Jiao, Ph.D., *Hematech, Inc.* • José Arnau, Ph.D., *UNIZYME Laboratories AS*
Michael DiLeo, *Dyax Corporation* • Dan Carter, *New Century Pharmaceuticals*
Canping Jiang, *Bristol-Myers Squibb* • Wenjie Cheng, *ImmunoGen, Inc.*
Les Beadling, *Rational Affinity Devices, LLC* • Ned Watson, Ph.D., *SAFC Biosciences*
Peter Gagnon, *Validated Biosystems, Inc.* • Norbert Schuelke, Ph.D., *Millennium Pharmaceuticals, Inc.*
Elisabeth Maurer, *Green Hills Biotechnology AG* • Cyrus Karakaria, Ph.D., *CuraGen Corporation*

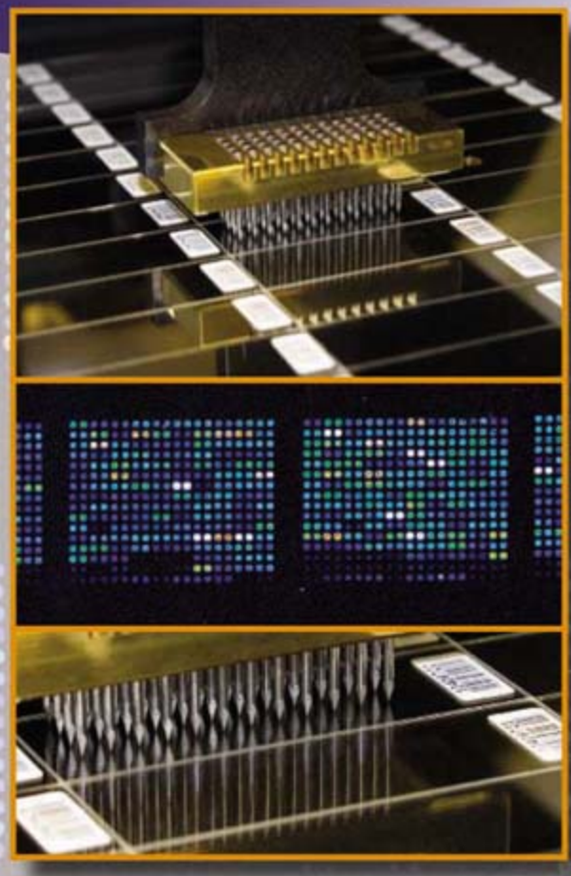

# MICROARRAY TECHNOLOGIES:

## BENCH TO BEDSIDE

DNA microarray technology has matured to the point where some applications are deemed reliable enough for use in patient care. At the same time, microarrays are evolving to help expand the understanding of transcriptome complexity: single nucleotide polymorphisms, copy number variation, CpG methylations, microRNAs—so many genetic and epigenetic variations and a slew of microarrays to investigate each one. Furthermore, newer DNA sequencing technologies now threaten to do to microarray technology what automobiles did to the horse and buggy. For now, however, the two approaches appear to coexist happily, and microarrays remain a perfectly reasonable way to get around the genome.

**By Emma Hitt**

The first report on microarray technology appeared in *Science* barely more than a decade ago, and since its inception, microarray technology has been burdened with issues of reproducibility and standardization. Recently, however, the technology has received a vote of confidence in the form of US Food and Drug Administration approval, laying the groundwork for its broader application in a clinical setting. The newly approved test, the MammaPrint assay, was developed by **Agendia** in the Netherlands and measures the expression of 70 genes that predict the likelihood of breast cancer metastasis. Several such tests have already received the "CE mark" for clinical use in Europe, and a handful of tests that analyze DNA polymorphisms (as opposed to gene expression) have been available clinically in the United States since 2004, when **Roche's** AmpliChip CYP450 assay became the first to receive approval.

As is the case for most biological paradigms, the entire transcriptome within a given cell has turned out to be much more complicated than ever imagined. As a result, tools to study epigenetic variations and other regulatory mechanisms within the cell have proliferated. Microarrays can now measure changes in gene copy number (copy number variation, CNV), changes in the expression levels of microRNAs (miRNAs), contributions from gene splice variants, and changes in methylation patterns. "There are really a plethora of new assay types, and each of these is complementary to one another and informs from a different perspective," notes Kevin Meldrum, director of genomics marketing for **Agilent**.

### DNA Sequencing Technologies

Perhaps one of the most exciting new developments in the microarray field is one that—paradoxically—may render the technology obsolete. DNA sequencing—the remarkably robust kind that has allowed a pioneer like James Watson to obtain his personal genome sequence on a DVD in about two months—is becoming the five-lane superhighway of genomic analysis. A 454 Life Sciences (now a part of Roche Diagnostics) sequencer was used to complete Watson's analysis, but several other companies now have their own sequencing approaches including **Illumina's** Solexa technology, **Applied Biosystems'** SOLiD System, **Helicos BioSciences'** True Single Molecule Sequencing (tSMS), and others.

"An interesting paradigm shift is taking place," says Steve Lombardi, chief operating officer and executive vice president with Helicos BioSciences. "You can do virtually any genetic analysis with sequencing technology—ranging from quantification of DNA, RNA, or cDNA, to measuring copy number variation and methylation," he says. "Microarrays, which require probes with known sequences, have limitations that simply do not exist with sequencing technology." continued ›

> "There are really a plethora of new assay types, and each of these is complementary to one another and informs from a different perspective."

Look for these **Upcoming** Articles

Genomics: SNPs — October 19

RNAi: Therapeutic Applications — November 2

Protein-Protein Interaction — November 30

*Inclusion of companies in this article does not indicate endorsement by either AAAS or* Science, *nor is it meant to imply that their products or services are superior to those of other companies.*

Microarray Technologies

"What this massively parallel approach to sequencing allows us to do is to generate about a hundred-fold more data for about 1 percent of the cost of current technology."

According to Lombardi, True Single Molecule Sequencing has the advantage of a simple sample preparation process that does not require amplification, and the image processing software and informatics will be open source allowing users to innovate.

A popular application of sequencing technology is to replace classic microarray chromatin immunoprecipitation (ChIP)-chip analyses. Microarrays to measure protein binding to DNA surfaced about five years ago and involve the placement of immunoprecipitated DNA fragments as probes on a DNA microarray. There is a wide range of products from Agilent, **Affymetrix,** Illumina, **Aviva Systems Biology, Nimblegen Systems,** and others for this purpose. With sequencing technology, the whole process becomes scaled up and digitized. First, binding proteins are cross-linked in place to DNA, the chromatin is isolated and fragmented, a protein-specific antibody is added, and the protein-DNA complexes are purified. The binding proteins are then chemically removed, and the remaining DNA is isolated. The DNA strands are then size selected, a process that isolates short sequences of, say, 25 bases—millions and millions of them. Finally, binding sequences are identified by virtue of the fact that their sequences are enriched several-fold relative to other sequences.

"What this massively parallel approach to sequencing allows us to do is to generate about a hundred-fold more data for about 1 percent of the cost of current technology," notes Omead Ostadan vice president of marketing with Illumina. Some proponents suggest that the sequencing approach will ultimately replace microarrays. "Microarrays are most popular for performing gene expression and genotyping applications, and in some cases, for sequencing applications such as ChIP-chip analysis. Over time some of these applications may migrate over to a sequencing platform because of the added power and quality you get from sequencing. However, we see these two approaches as complementary, offering researchers the broadest solutions for studies," says Todd Dickinson, director of product marketing at Illumina.

It may not be prudent to throw out the array chips just yet, however. "Sequencing technology is young, and issues regarding cost and ease of use still need to be worked out," notes Steven Bodovitz, an industry analyst with **BioPerspectives**. "Nonetheless, sequencing is certainly more comprehensive than microarray technology, and getting a sequence without knowing what you are looking for ahead of time is a big advantage," he says. "It will be interesting to see how the two approaches play out—the technologies are likely to both complement and compete with one another."

Still, microarrays remain ideally suited for experiments that require analysis of large numbers of samples against known sequences—and will likely remain the predominant approach in diagnostic applications. "Not all companies are jumping on board with the sequencing approach," says Bodovitz.

## Optimizing Arrays

Of late, developments in gene expression arrays have focused on optimizing coverage of the entire human genome, which includes well over 30,000 genes, processed into hundreds of thousands of different variations. Newer arrays are aiming to capture that variability. Affymetrix's GeneChip Human Gene 1.0 ST Array released this year measures the overall expression of all transcripts derived from a gene, in contrast to traditional arrays that measure only the 3′ end of a gene. "More than 60 percent of human genes undergo alternative splicing, resulting in multiple transcript variants with potentially distinct functions," says Yan Zhang, associate director of product marketing with Affymetrix. Each of 28,869 genes is represented on the array by approximately 26 probes per gene directed at the full length of the gene. "We estimate that the accuracy is greater compared with the previous generation's 3′ approach, and the format is smaller, which reduces cost without reducing content," Zhang says.

Illumina's whole-genome expression arrays employ the BeadArray technology, which uses 50-mer oligos attached to 3 μm beads, allowing six or eight samples to be profiled per BeadChip simultaneously. This multisample approach provides increased throughput and decreased cost per sample. Also allowing for higher throughput and lower costs, Nimblegen's Human Whole Genome Expression Microarrays include 60-mer oligo probes for all human genes, eight per gene, including 47,633 different targets, and Agilent has a whole human genome chip containing 60-mer oligonucleotide probes arranged as microarrays in the format of 1 x 244K, 2 x 105K, 4 x 44K, or 8 x 15K on individual glass slides.

## Microarray Manufacture

Arrays can be loosely classified into ready-made versions and custom "home-brew" forms that contain DNA spotted onto slides. Custom microarrays are fabricated largely by pin-based direct deposition printers.

UK-based company **Arrayjet** recently launched its benchtop Sprint Inkjet Microarrayer. The new machine can handle 20 microarray slides and allows printing from two microtiter plates (96- or 384-well) simultaneously.

"Due to their contact with the surface, pin printers can have problems with speed, quality, and reproducibility," notes Howard Manning, Arrayjet founder and technical director. "With the ink jet approach, the Jetspyder enables the inkjet print head to draw in multiple samples before arraying spots are printed on the slide without the print head stopping and without making contact," says Manning. Another advantage of inkjet printing is that spotting pins may damage some of the newer substrates used for arrays, such as membrane-coated substrates and hydrogels.

The processes utilized to manufacture arrays are also being enhanced. "Updates to the Agilent SurePrint technology were implemented last year," Meldrum said, "enabling us to manufacture arrays with up to 244,000 unique features. We have also improved the efficiency of the nucleic acid synthesis process, signficantly reducing depurination side reactions." **Nanogen** NanoChip arrays use a proprietary technology consisting of individually controllable microelectrodes that, when positively charged, can attract negatively charged DNA and RNA molecules. "The use of electronics to drive the concentration reaction mitigates the variability arising from spotting small volumes onto a surface," says Nanogen's Elaine Weidenhammer. "Consequently, the Nanogen system is subject to less variability than some other formats," she claims.

## SNPs and CNV

A recent publication from The ENCyclopedia Of DNA Elements (ENCODE), an international research consortium organized by the National Human Genome Research Institute (NHGRI) indicates that the DNA-makes-RNA-makes-protein paradigm is too simplistic and that 99 percent of the genome is not, in fact, junk. continued ›

IMAGE: ILLUMINA, INC.

# BIOMICRO | BUILDING BLOCKS FOR TOMORROW'S MICROARRAY RESEARCH.


Microarray research is today's hero. That won't last unless researchers stay ahead of growing expectations for the science and demands from industry. That's the test.

BioMicro® Systems takes on these challenges with products that increase the accuracy, consistency, productivity and cost-effectiveness of your microarray research.

Just as the BioMicro MAUI® Systems revolutionized hybridization, we now offer new ways to boost the quality of your results:

**PROVEN!** MAUI Hybridization Systems and MAUI Mixer Hybridization Chambers. The highest quality hybridization systems on the market with over 450 installations worldwide.

**NEW!** Arrayjet Microarray Printers. Rapid and reliable microarray printing with the flexibility of inkjet technology.

**NEW!** Kreatech ULS Labeling Kits. Fast and consistent labeling results made easy.

Great reputations are built on great technology. That's why scientists looking for innovations to improve their chances for future success look to BioMicro Systems. And why every day more microarray research gets done with BioMicro products.

**Spot. Label. Hyb. Achieve!**

**biomicro.com | 1.800.454.1485**

MAUI 4-Bay
Hybridization System

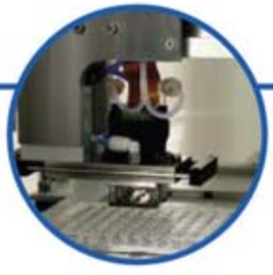

Arrayjet
Microarray Printers

MAUI 12-Bay
Hybridization System

MAUI Mixer
Hybridization
Chambers

Kreatech ULS™
Labeling Kits

BioMicro® SYSTEMS

**Spot-On Solutions™ for Microarray Research**

VISIT US AT
**D-2-D 2007**
BOOTH #511

Gene transcripts appear to overlap, and genes, regulatory elements, and other types of DNA sequences interact as a network in a nonlinear fashion. New technologies are now evolving to define this complex variability.

This year, Affymetrix introduced the Genome-Wide Human SNP Array 6.0, which includes about 1.8 million markers that can be used to detect genetic variation in whole-genome association studies. Specifically, the newest SNP Array 6.0 contains 906,600 single nucleotide polymorphisms (SNPs) and about 946,000 nonpolymorphic probes that "will aim to detect CNVs in both known and unknown regions," says Jessica Tonani, Genotyping Specialist with Affymetrix. "The array tiles known CNVs very heavily, with an average of about 61 probes per known CNV region. For the remainder of the genome we have tiled probes at a resolution of about a probe every 700 bases."

"Our overall hope is to identify the part of the genome that has previously been considered a 'genomic wasteland,' or junk DNA, but may in fact be involved in regulating gene expression," she says, "although we are reaching a point where there is more to be gained by studying more samples as opposed to putting more SNPs on an array."

Newest to Illumina's Infinium portfolio is the Human 1M BeadChip, which provides expanded genomic coverage for whole-genome association studies. This chip adds several hundred thousand individually selected SNPs in genes and functional areas as well as CNV content not available on any other platform, according to Illumina. Tag SNPs represent a group of SNPs that tend to be inherited together. "By targeting tag SNPs, we can vastly increase the power of the study by looking at the genotype of one SNP, which effectively represents the genotype of many," Dickinson says. "The power of this array is increased dramatically because of this coverage and has reduced costs for researchers conducting genome-wide association studies," he adds. "For example, in 2000, genotyping a single SNP cost $1 or more. Today, the cost is less than $0.001 per SNP."

## Featured Participants

**Affymetrix**
www.affymetrix.com

**Agendia**
www.agendia.com

**Agilent**
www.agilent.com

**Almac Diagnostics**
www.almacgroup.com/diagnostics

**Applied Biosystems**
www.appliedbiosystems.com

**Arrayjet Ltd.**
www.arrayjet.co.uk

**Aviva Systems Biology**
www.avivasysbio.com

**BioMerieux**
www.biomerieux.com

**BioPerspectives**
www.bioperspectives.com

**Helicos BioSciences Corporation**
www.helicosbio.com

**Illumina**
www.illumina.com

**Kreatech Biotechnology**
www.kreatech.com

**MicroArray Quality Control (MAQC)**
www.fda.gov/nctr/science/centers/toxicoinformatics/maqc

**Minimal Information about Microarray Experiment (MIAME)**
www.mged.org/Workgroups/MIAME/miame.html

**Nanogen**
www.nanogen.com

**Nimblegen Systems**
www.nimblegen.com

**Pathwork Diagnostics**
www.pathworkdx.com

**Roche**
www.roche.com

**Veridex**
www.veridex.com

## Regulatory miRNA

MiRNAs have recently been shown to play an important role in regulating gene expression. Over 500 human miRNAs have already been identified and validated, and are thought to regulate about one-third of all human genes. Several companies now make kits for labeling and detection of miRNAs utilizing array platforms. Agilent recently introduced its miRNA assay which uses a direct labeling protocol on as little as 100 ng of total RNA. "Because miRNAs are typically 25–30 nucleotides in length and have high sequence homology, utilization of conventional probe design methods results in significant cross-hybridization of RNAs within the sample," notes Agilent's Meldrum, "but we have developed novel probe design algorithms that enable us to achieve extremely high specificity for each unique sequence."

**Kreatech Biotechnology** in the Netherlands recently introduced its miRacULS II Kit labeling technology, which uses a nonenzymatic labeling reaction independent of fragment size. The kit enables isolation and labeling of miRNAs from samples of less than 105 cells or 5 mg tissue as well as samples with a low miRNA expression level.

## Ready for Prime Time?

Efforts are ongoing to standardize data input and reporting of microarray experimental data. **Minimal Information about Microarray Experiment (MAIME)** standards for microarray experiments have been put in place to define the minimal amount of information needed to interpret and reproduce a microarray experiment.

The first phase of the **MicroArray Quality Control** (MAQC) project, with participants from academia, government, and industry, recently concluded that results mostly were reproducible among labs; the second phase of the MAQC is under way and will try to establish the applicability of microarray data to clinical settings, with results expected in about a year. "When moving something from the bench to medical practice, there is an absolute requirement that the consistency of the performance of the test system can be guaranteed in different people's hands," says Uwe Scherf, with the FDA's Center for Devices and Radiological Health. "The MAQC studies were one of the first indications that microarrays could be suitable for medical evaluation."

The External RNA Controls Consortium (ERCC), established in 2003, is developing a set of external RNA spike-in controls for use in all microarray platforms and quantitative polymerase chain reaction (PCR) assays. If successful, this will allow a reliable comparison of expression profiling among more than 10 microarray and PCR platforms.

According to Affymetrix, at least 20 diagnostic tests are being developed for use on its platform—mostly expression-based tests evaluating tumors—and they are partnering with several companies, including Roche, **Almac Diagnostics**, **Veridex**, **BioMerieux**, and **Pathwork Diagnostics**, for the development of molecular diagnostic tests that use its platform. VeraCode, a new technology introduced by Illumina earlier this year, is available for researchers conducting low- and midplex biomarker validation studies. Using digital holographic codes embedded in cylindrical glass beads, VeraCode allows for efficient and cost-effective screening of hundreds to thousands of samples against panels of one to 384 biomarkers.

"It will be important to develop tools that can be utilized to analyze data sets for different applications and start to merge that information together," Agilent's Meldrum says. "Within the next few years the field is going to go from one-dimensional [e.g., gene expression profiling] to a multidimensional view, offering a richer picture of what's really happening in the cell."

*Emma Hitt is a freelance medical and science writer living in Marietta, Georgia.*

New Products

## Multiplexed Assay System

The BeadXpress System is a high throughput, dual color laser detection system that enables scanning of a broad range of multiplexed assays developed using the VeraCode digital microbead technology. VeraCode technology features uniquely inscribed digital microbeads that provide high-quality data, broad multiplexing capability, and assay flexibility. The instrument scans the VeraCode microbeads for their code and fluorescent signals, generating data quickly and efficiently. Using the system, researchers can assay tens to hundreds of analytes in a single sample at one time. Application areas include biomarker research and validation, pharmaceutical development, industrial testing, agriculture, clinical research, and the development of molecular diagnostic assays. For example, BeadXpress technology can be used to develop screening assays that profile inherited and complex diseases. Drug discovery researchers can use it to validate RNA and protein biomarkers. Genetic researchers can use it to replicate single nucleotide polymorphism studies from large disease association studies to their own populations, for example, quickly retesting the top 50 or 100 polymorphisms in very large sample sizes. The system can scan assays ranging from a single-plex to 384-plex in a single well.

Illumina
For information 312-997-2436
www.illumina.com

## DNA Methylation Arrays

NimbleGen DNA methylation analysis arrays allow researchers to rapidly identify methylated regions in a high throughput manner. These arrays can be used to correlate promoter and genic methylation with gene expression and phenotype and detect differential DNA methylation between normal tissues and tumor samples as potential diagnostic and prognostic markers. Whole-genome DNA methylation arrays are available for human, mouse, rat, dog, and chicken genomes, tiling at an average probe spacing of 100 bp to provide an unbiased approach to DNA methylation analysis. These arrays survey not only regions surrounding known genes but also intergenic regions, allowing distal regulatory elements to be surveyed and providing the maximum opportunity to discover relevant biomarkers. For studies focusing on promoter regions, one- and two-array sets are available for surveying promoter regions of all known genes in human, mouse, rat, and *Arabidopsis*.

NimbleGen Systems
For information 608-218-7623
www.nimblegen.com

## Network Analysis Tools

The integration of Oncomine Professional and Ingenuity Pathways Analysis (IPA) will allow users to navigate directly from cancer gene signatures discovered in Oncomine Professional to the curated pathway information available from IPA. Oncomine Professional is a rapidly growing compendium of transcriptome profiles coupled with analysis functions and a web application for data mining and visualization. Comprised of thousands of profiles representing every major type of cancer, Oncomine Professional was developed to exploit these data for therapeutic target discovery, validation, and prioritization. IPA is software that enables biologists and bioinformaticians to identify the biological mechanisms, pathways, and functions most relevant to their experimental datasets or genes of interest. The integrated workflow based on IPA's capabilities for rapid and reliable biological interpretations of Oncomine's high-quality cancer transcriptome profiles is expected to provide a powerful tool for oncology researchers focused on understanding mechanisms of disease, and on the discovery and validation of cancer biomarkers.

Compendia Bioscience and Ingenuity Systems
For information 650-381-5150
www.compendiabio.com and www.ingenuity.com

## Human Genomewide SpliceArray

The SpliceArray provides a unique approach to detecting all known and novel expressed transcripts. The Human GW SpliceArray monitors more than 23,000 human genes covering more than 130,000 expressed transcripts and requires more than 6 million probes to help elucidate the enormous diversity of the human proteome. This new design, manufactured on the Affymetrix platform, provides researchers the opportunity to obtain gene expression results at a resolution previously unattainable on a single microarray by interrogating both exons and splice junctions.

ExonHit Therapeutics
For information +33 1 58 05 47 00
www.exonhit.com

## Dynamic Light Scattering Instrument

The DynaPro Plate Reader is a temperature controlled, high throughput dynamic light scattering (DLS) plate reader. It allows researchers to perform classical thermal DLS studies automatically on a large number of therapeutic macromolecules over a wide range of solution conditions. Conventional DLS studies are laborious and time consuming, with each solution condition studied manually, one at a time, over several hours. In contrast, the DynaPro controls the temperature for hundreds of samples simultaneously, capturing DLS data quickly, easily, and directly from standard microplates (96-well, 384-well, and 1,536-well formats) without perturbing precious samples. As little as 5 µl of sample per well is required in the 1,536-well format. The instrument includes an array of state-of-the-art technologies, including software controlled, Peltier-based temperature systems; compact digital attenuators; precision mechanical stages; proprietary multimode optical fibers; and novel software control and processing algorithms.

Wyatt Technology
For information 805-681-9009
www.wyatt.com

## Microarray Data Analysis

TMA Foresight is a statistical tool for tissue microarray data analysis. Users can explore the relatedness of prognostic marker expression and clinicopathological variates with the outcome. Cox's Proportional Hazard analysis can be used for prognostic marker identification. Hierarchical clustering can be used to group patients on the basis of clinicopathological parameters and biomarkers. Kaplan-Meier plots and log-rank tests are used to identify prognostically significant clusters.

Premier Biosoft International
For information 650-856-2703
www.premierbiosoft.com

### *Correction*

*Life Science Technologies Feature:*
*"Cell Signaling: Phosphorylation, Kinases, and Kinase Inhibitors" (6 April 2007, p. 125). The trademark for the homogeneous time-resolved fluorescence (HTRF) technology was incorrectly attributed to Millipore Corporation. The HTRF trademark is held by Cisbio International of Gif-sur-Yvette, France.*

## POSITIONS OPEN

### ASSISTANT/ASSOCIATE PROFESSOR
**Pharmacology**

Applications are invited for a tenure-track position at the Assistant/Associate Professor level. Applicants should have a Ph.D. or equivalent degree and evidence of research productivity and creativity. Applicants are sought with demonstrated research expertise, including but not limited to molecular and cellular biology, genomics, ransgenesis and gene targeting, receptor signal transduction mechanisms, and proteomics. The successful candidate will be expected to participate in graduate and medical student teaching and to develop a strong, independent research program. He or she will join an interactive faculty with research interests in molecular biology of ion channels, biochemistry, biophysics, and molecular biology of cardiac, smooth and skeletal muscle cells, and cellular and molecular aspects of neuropharmacology **(website: http://www.unr.edu/med/dept/Pharmacology/index.html).** The Department consists of fifteen active faculty members, ranks in the top 50th percentile of NIH awards to U.S. medical school pharmacology departments, and also receives generous support from the Department of Defense. Opportunities exist for a variety of collaborative interactions throughout the University including possible adjunct appointment in the interdisciplinary Center of Biomedical Research Excellence. Competitive salaries, startup, and state-of-the-art instrumentation and facilities are available. In addition to participating in our growing Medical School, northern Nevada also offers great natural beauty, with Lake Tahoe a short drive away, the Truckee River offering kayaking and fishing, and our beautiful mountainous high desert environment. Reno also has wonderful cultural activities, including our own symphony, chamber orchestra, opera, and rich community theatre offerings. The State of Nevada has no state income tax. Review of applications will begin October 1, 2007, and will continue until the position is filled. Visit **website: http://www.unrsearch.com/applicants/Central?quickFind=52473** for complete position announcement and requirements and to apply online. *Affirmative Action/Equal Employment Opportunity Women and underrepresented groups are encouraged to apply.*

---

### ASSISTANT PROFESSOR

The Department of Biological Sciences at the State University of New York at Cortland seeks applications for a tenure-track Assistant Professor starting August 2008. Requirements include a Ph.D., demonstrated scholarly productivity, and teaching experience. The Department welcomes all qualified applicants but is especially interested in those whose specialization is in neurobiology, immunology, endocrinology, or other areas of animal physiology. Teaching responsibilities include anatomy and physiology, mammalian physiology, and an upper-level course in the candidate's area of expertise. The successful candidate will be committed to excellence in teaching, develop an active research program involving undergraduates, seek external funding, and contribute to our major in biomedical sciences.

For consideration, apply online at **website: https://jobs.cortland.edu/applicants/Central?quickFind=51506** and attach a letter of application, curriculum vitae, and the names, addresses, and telephone numbers of three professional references. In addition, please mail hard copies of statements of teaching and research interests, three letters of reference, and unofficial transcripts to: **Dr. Louis A. Gatto, Chair, Department of Biological Sciences, State University of New York Cortland, P.O. Box 2000, Cortland, NY 13045.** Review of application materials will begin October 12, 2007, and continues until the position is filled.

*SUNY Cortland is an Affirmative Action/Equal Employment Opportunity/ADA Employer. We have a strong commitment to the affirmation of diversity and have interdisciplinary degree programs in the area of multicultural studies.*

## POSITIONS OPEN

TEXAS A&M
HEALTH SCIENCE CENTER
COLLEGE OF MEDICINE

### FACULTY POSITIONS

The Department of Molecular and Cellular Medicine (MCM) in the Texas A&M College of Medicine invites applications from individuals with Ph.D, M.D., or equivalent degrees for several tenure-track faculty positions at the **ASSISTANT, ASSOCIATE, or FULL PROFESSOR** rank, including the potential for an endowed position at the senior level. Applications for couples or groups of individuals are encouraged. The Department is principally located on the Texas A&M campus in College Station and is expanding in concert with the significant growth of the entire College. Research in the Department spans from the structure and function of biomolecules to cell physiology, including many areas of biochemistry, genetics, and cell and molecular biology. Senior applicants should have a vigorous extramurally funded research program and junior applicants will need to develop such a program. Applicants for junior positions should submit their curriculum vitae and descriptions of research plans and teaching philosophy and have three letters of recommendation e-mailed or sent to: **Molecular and Cellular Medicine Junior Faculty Search, 440 Reynolds Building, College Station, TX 77843-1114.** Applicants for the senior position are invited to send their portfolio to **Senior Faculty Search** at the same address. Electronic applications are preferred. Our review of applicants will begin immediately and continue through the fall. **E-mail: mcm@medicine.tamhsc.edu. Website: http://medicine.tamhsc.edu/basic_sciences/MCM.** *The Texas A&M Health Science Center is an Affirmative Action/Equal Opportunity Employer.*

---

### ASSISTANT PROFESSOR
**Cellular Biophysics**
**Department of Biological Sciences**

The Department of Biological Sciences invites applicants for a tenure-track faculty position at the Assistant Professor level to begin September 1, 2008. We are seeking candidates with research interests in cellular biophysics that include but are not limited to the study of cytoskeleton and motor proteins, intracellular signaling, intracellular trafficking, excitation-contraction coupling, and excitation-secretion coupling. Individuals applying electrophysiology or advanced fluorescence imaging are encouraged to apply. The successful candidate will have a Ph.D. and postdoctoral experience in an appropriate field, will develop an extramurally funded research program, will supervise Ph.D. and M.S. students and undergraduate research projects, and will teach undergraduate and graduate courses in area of expertise. This position is one of five tenure-track positions created for the Integrated Molecular Life Sciences and Biophysics Program (IMLSB; **website: http://www.biochem.du.edu/IMLSB),** a multidepartmental program between the Departments of Biological Sciences, Chemistry and Biochemistry, and Physics and Astronomy, that will feature emphases in biophysics, biochemistry, and neuroscience. All candidates must submit their application through **website: https://www.dujobs.org.** The application should include curriculum vitae and statements of teaching philosophy and research interests. Under separate cover please send two recent publications and three letters of recommendations to: **Biological Sciences Biophysics Faculty Search, University of Denver, Department of Biological Sciences, Denver, CO 80208.** The review of applications will begin October 15, 2007, and continue until the position is filled. Contact **Professor Joseph Angleson (e-mail: jangleso@du.edu)** if you have any questions. *The University of Denver is committed to enhancing the diversity of its faculty and staff and encourages applications from women, minorities, people with disabilities and veterans. DU is an Equal Employment Opportunity/Affirmative Action Employer.*

# Positions @ NIH

## THE NATIONAL INSTITUTES OF HEALTH

## Investigator Recruitment in Cancer Genetics

### National Human Genome Research Institute

The Cancer Genetics Branch (CGB) of the National Human Genome Research Institute (NHGRI) is seeking to recruit an outstanding tenure-track investigator to pursue innovative, independent research in cancer genetics. General areas of interest include, but are not limited to:

- Cancer Gene Discovery
- Comparative Cancer Genomics
- Genetic Epidemiology
- Molecular Profiling of Tumors
- Functional Genomics of Cancer
- Genome Instability in Cancer
- Markers for Early Detection
- Genetics of Tumor Progression

The successful candidate will be able to take advantage of interactions with a highly collegial group of scientists within NHGRI and the NIH campus as a whole. In addition, they will have access to NHGRI's outstanding core laboratories, as well as the unparalleled resources of the NIH Clinical Center.

Candidates must have a Ph.D., M.D., or equivalent degree, as well as comprehensive, advanced training and a record of accomplishment in one of the targeted areas. This position includes generous start-up funds, an ongoing commitment of research space, laboratory resources, and positions for personnel and trainees.

Interested applicants should submit a *curriculum vitae*, a three-page description of their proposed research, and three letters of recommendation through our online application system at http://research.nhgri.nih.gov/apply. The closing date for applications is November 16, 2007.

For more information on CGB and NHGRI's Intramural Program, please see http://www.genome.gov/DIR. Specific questions regarding the recruitment may be directed to Dr. Larry Brody, the Search Chair, at lbrody@helix.nih.gov. Questions may also be directed to Dr. Elaine Ostrander, the CGB Branch Chief, at eostrand@mail.nih.gov.

Interested applicants should also be aware of two concurrent tenure-track faculty searches being conducted by NHGRI's Genetics and Molecular Biology Branch (GMBB) and Genetic Disease Research Branch (GDRB). Information on these searches may be found at http://genome.gov/11509039. Qualified candidates are welcome to apply for multiple searches; please note that a separate application must be filed for each search for which you wish to be considered.

DHHS and NIH are Equal Opportunity Employers and encourage applications from women and minorities.

NATIONAL HUMAN GENOME INSTITUTE Divison of Intramural Research

U.S. DEPARTMENT OF HEALTH AND HUMAN SERVICES | NATIONAL INSTITUTES OF HEALTH | genome.gov/DIR

## Investigator Recruitment in Genetics and Molecular Biology

### National Human Genome Research Institute

The Genetics and Molecular Biology Branch (GMBB) of the National Human Genome Research Institute (NHGRI) is seeking to recruit outstanding tenure-track investigators to pursue innovative, independent research. The faculty within GMBB are highly interactive and use a variety of approaches to understand and develop new treatments for genetic and complex diseases. Current areas of research include hematopoiesis, the genetic disorders of red blood cells, cellular immunology, gene therapy, leukemogenesis, genomic instability in disease, the genetics of skin diseases, and the genomics of the skin microbiome. Of particular interest are candidates with research interests in the following areas:

- Clinical genetics
- Application of genomics tools to understanding human disease
- Clinical/translational research
- Basic genetic/genomics research

The successful candidate will be able to take advantage of interactions with a highly collegial group of scientists within NHGRI and the NIH campus as a whole. In addition, the successful candidate will have access to NHGRI's outstanding core laboratories, as well as the unparalleled resources of the NIH Clinical Center.

Candidates must have a Ph.D., M.D., or equivalent degree, as well as comprehensive, advanced training and a record of accomplishment in one of the targeted areas. This position includes a generous start-up allowance, an ongoing commitment of research space, laboratory resources, and positions for personnel and trainees.

Interested applicants should submit a *curriculum vitae*, a three-page description of proposed research, and three letters of recommendation through our online application system, at http://research.nhgri.nih.gov/apply. The closing date for applications is November 16, 2007.

For more information on GMBB and NHGRI's Intramural Program, please see http://genome.gov/DIR. Specific questions regarding the recruitment may be directed to Dr. Fabio Candotti, the Search Chair, at fabio@nhgri.nih.gov. Questions may also be directed to Dr. David Bodine, the GMBB Branch Chief, at tedyaz@nhgri.nih.gov. Interested applicants should also be aware of two concurrent tenure-track faculty searches being conducted by NHGRI's Cancer Genetics Branch (CGB) and Genetic Disease Research Branch (GDRB). Information on these searches may be found at http://genome.gov/11509039. Qualified candidates are welcome to apply for multiple searches; please note that a separate application must be filed for each search for which you wish to be considered.

DHHS and NIH are Equal Opportunity Employers and encourage applications from women and minorities.

NATIONAL HUMAN GENOME INSTITUTE Divison of Intramural Research

U.S. DEPARTMENT OF HEALTH AND HUMAN SERVICES | NATIONAL INSTITUTES OF HEALTH | genome.gov/DIR

THE NIH IS DEDICATED TO BUILDING A DIVERSE COMMUNITY IN ITS TRAINING AND EMPLOYMENT PROGRAMS

WWW.NIH.GOV

## Investigator Recruitment in Genetic Disease Research

National Human Genome Research Institute

The Genetic Disease Research Branch (GDRB) of the National Human Genome Research Institute (NHGRI) is seeking to recruit outstanding tenure-track or tenured investigators to pursue innovative, independent research. GDRB faculty members are highly interactive and use a variety of approaches to study the genes and proteins involved in normal development and related disease processes. Investigators in the Branch are currently engaged in studies of limb and skeletal development, pigment cell development and neurocristopathies, T-cell development, function, and defects in host defense; and the role of rare variants in common disease. Of particular interest are candidates with backgrounds in one or more of the following areas:

- Clinical or translational research
- Molecular and genomic approaches to understanding the mechanisms of disease
- Basic genetic or genomic research

The successful candidate will be able to take advantage of interactions with a highly collegial group of scientists within NHGRI and the NIH campus as a whole. In addition, the successful candidate will have access to NHGRI's outstanding core laboratories, as well as the unparalleled resources of the NIH Clinical Center. Candidates must have a Ph.D., M.D., or equivalent degree, as well as comprehensive, advanced training and a record of accomplishment in one of the targeted areas. This position includes a generous start-up allowance, an ongoing commitment of research space, laboratory resources, and positions for personnel and trainees. Interested applicants should submit a *curriculum vitae*, a three-page description of proposed research, and three letters of recommendation through our online application system, at http://research.nhgri.nih.gov/apply. The closing date for applications is November 16, 2007.

For more information on GDRB and NHGRI's Intramural Program, please see http://genome.gov/DIR. Specific questions regarding the recruitment may be directed to Dr. William Pavan, the Search Chair, at bpavan@nhgri.nih.gov. Questions may also be directed to Dr. Leslie Biesecker, the GDRB Branch Chief, at leslieb@nhgri.nih.gov. Interested applicants should also be aware of two concurrent tenure-track faculty searches being conducted by NHGRI's Cancer Genetics Branch (CGB) and Genetics and Molecular Biology Branch (GMBB). Information on these searches may be found at http://genome.gov/11509039. Qualified candidates are welcome to apply for multiple searches; please note that a separate application must be filed for each search for which you wish to be considered.

DHHS and NIH are Equal Opportunity Employers and encourage applications from women and minorities.

NATIONAL HUMAN GENOME INSTITUTE Divison of Intramural Research

U.S. DEPARTMENT OF HEALTH AND HUMAN SERVICES | NATIONAL INSTITUTES OF HEALTH | genome.gov/DIR

## Tenure-Track Position
## Vascular Medicine Branch

The Vascular Medicine Branch within the Division of Intramural Research of the National Heart, Lung and Blood Institute is seeking an individual to direct an independent research program in lipoprotein metabolism and vascular therapeutics. Demonstrated research accomplishment and excellence in the area of lipoprotein metabolism will be considered, however, preference will be given to those working in the area of HDL metabolism and potential therapeutic approaches. The candidate may have an M.D., Ph.D. or both and have an outstanding record of research accomplishments as evidenced by publications in major peer-reviewed journals. The position is tenure-track and comes with generous start up support. Also available is open access to various core facilities, including transgenic and knockout mouse facility, confocal and electron microscopy cores, multi-modality non-invasive mouse imaging facility, siRNA resources, fluorescent activated cell sorting facility and state of the art genomics, microarray and proteomics facilities.

The successful candidate will be offered a competitive salary commensurate with experience and qualifications. Appointees must be US citizens, resident aliens or non-resident alien with a valid employment visa. Applications must be received by October 31, 2007. Please submit a curriculum vitae and brief statement of research interests along with three letters of reference to Ross Heffer at hefferr@mail.nih.gov or mail to:

Robert S. Balaban, Ph.D., Scientific Director, NHLBI, c/o Mr. Ross Heffer, Administrative Officer, NHLBI, 10, Center Drive, MSC 1670, Building 10, Room 7N220, Bethesda, MD 20892-1670.

NIEHS
National Institute of Environmental Health Sciences
National Institutes of Health

## Chemist
Research Triangle Park, NC

**Chemist** to design, oversee, and report rodent ADME studies conducted through contracts; evaluate metabolism data from literature or other sources; and serve as Program expert on biotransformation.

Apply online at www.USAJOBS.gov, Announcement Number HHS/NIH-2007-0739 for position title Chemist, GS-1320-13/14 (NIEHS-DE) by **September 7, 2007**.
For additional information contact Angela Heard, Office of Human Resources, at hearda@mail.nih.gov

***DHHS and NIH are Equal Opportunity Employers***

## FACULTY POSITION IN GENE EXPRESSION AND REGULATION

### UNIVERSITY OF CALIFORNIA, IRVINE

The Department of Molecular Biology and Biochemistry in the School of Biological Sciences announces the availability of a tenure-track position in the field of Gene Expression, at the **ASSISTANT PROFESSOR** level. Applicants should hold a Ph.D., M.D. or equivalent degree, and will be expected to establish a vigorous and internationally competitive research program in any area from genome organization to post-translational control. The successful candidate will be expected to teach at the undergraduate and graduate levels.

Applicants should upload a description of their research accomplishments including future plans, a Curriculum Vitae, and a list of at least four references. Please see the URL: **http://jobs.bio.uci.edu/showopenjobs_tenure.cfm** for application instructions under "Department of Molecular Biology and Biochemistry."

**DEADLINE FOR RECEIPT OF APPLICATIONS:** Review of applications will begin **September 30, 2007** and the recruitment will remain open until the position is filled.

*The University of California, Irvine is an Equal Opportunity Employer committed to excellence through diversity and strongly encourages applications from all qualified applicants including women and minorities.*

---

MAYO CLINIC

**For more information, visit our website:** www.mayo.edu

## Postdoctoral Position

**Department of Molecular Pharmacology and Experimental Therapeutics Rochester, Minnesota**

A postdoctoral research fellow position is immediately available in pharmacogenomics and pharmacogenetics lab at Mayo Clinic Rochester. Candidate should be highly motivated with experience in pharmacogenomics and pharmacogenetics of cancer chemotherapy. The laboratory focus is primarily on investigating the pharmacogenetics of chemotherapeutic drugs used as first and second line treatment in colorectal, breast and lung cancers. This laboratory utilizes a multitude of molecular biology techniques. Studies conducted include the molecular mechanisms (genetic and epigenetic) involved in sensitivity and resistance to chemotherapeutic agents and small molecules, and the expression analysis and sequence variations of genes involved in the anabolic and catabolic pathways of chemotherapeutic drugs. Minimum requirements for this position are a Ph.D., previous research experience with publications and familiarity with molecular biology techniques.

Mayo Clinic College of Medicine is a not-for-profit organization that integrates research with clinical practices and education in a multi-campus environment. Mayo offers an attractive benefit package. Salary will be determined by the successful candidate's experience. For further information, please visit **http://www.mayo.edu/**.

Applications, including curriculum vitae and bibliography, summary of past accomplishments and three signed reference letters, should be sent to:

**Ms. Karen J. Hanson**
Research Operations Coordinator
***Mayo Clinic***
Gonda 19-461, 200 1st St. SW, Rochester, MN 55905
Email: hanson.karen3@mayo.edu
Phone: 507-266-7619

Mayo Clinic College of Medicine is an affirmative action and equal opportunity employer.

---

**U.S. Department of Energy**
**Associate Director**
**Office of Science for**
**Biological and Environmental Research**
**Announcement # SES-SC-HQ-014 (kd)**

The U.S. Department of Energy's (DOE's) Office of Science is seeking qualified candidates to lead its Biological and Environmental Research (BER) Program. With an annual budget of more than $500 million, the BER Program is the nation's leading program devoted to applications of biology to bio-energy production and use and to environmental remediation. The BER Program supports major research programs in genomics, proteomics, systems biology, and environmental remediation. The Program is also one of the nation's leading contributors to understanding the effects of greenhouse gas emissions, aerosols, and atmospheric particulates on global climate change.

The Director of Biological and Environmental Research is responsible for all strategic program planning in the BER Program; budget formulation and execution; management of the BER office including a federal workforce of more than 30 technical and administrative staff; program integration with other Office of Science activities and with the DOE technology offices; and interagency integration. The position is within the ranks of the U.S. government's Senior Executive Service (SES); members of the SES serve in key positions just below the top Presidential appointees. For more information on the program please go to **http://www.sc.doe.gov/ober/**.

For further information about this position and the instructions on how to apply and submit an application, please go to the following website: **http://jobsearch.usajobs.opm.gov/getjob.asp?JobID=58520806&AVSDM=2007%2D06%2D06+13%3A44%3A02&Logo=0&q=SES-SC-HQ-014+(kd)&FedEmp=N&sort=rv&vw=d&brd=3876&ss=0&FedPub=Y&SUBMIT1.x=47&SUBMIT1.y=18**. To be considered for this position you must apply online. It is important that you follow the instructions as stated on the announcement **SES-SC-HQ-014 (kd)** located at the website above.

---

MICHIGAN STATE UNIVERSITY

**Tenure-track Assistant Professor**

**Departments of Crop and Soil Sciences and Geological Sciences and the Environmental Science and Policy Program**

The Departments of Crop and Soil Sciences and Geological Sciences and the Environmental Science and Policy Program at Michigan State University invite applications for a new tenure-track assistant professor position in soil physics and hydrology with emphasis on unsaturated flow and transport.

This research and teaching position will emphasize water and solute transport processes in the unsaturated and capillary zones. The ideal candidate will combine experiments with quantitative models to explore the complex physical, chemical, and biological processes that govern unsaturated flow and transport across multiple scales. The candidate will be expected to teach an undergraduate and graduate course, train graduate students, and establish an extramurally funded multidisciplinary research program.

Additional information for submitting complete applications is available online at: **http://www.css.msu.edu/soilphysics/**. Nominations and inquiries are encouraged and should be forwarded to **Alvin Smucker, Search Committee Chair, by email: smucker@msu.edu.**

Michigan State University is committed to achieving excellence through cultural diversity. The university actively encourages applications and/or nominations from women, persons of color, veterans and persons with disabilities.

MSU IS AN AFFIRMATIVE ACTION, EQUAL OPPORTUNITY EMPLOYER.

**The GKSS Research Centre is located in Geesthacht near Hamburg, Germany, with a further centre in Teltow close to Berlin. It is a member of the Helmholtz Association of German Research Centres. With its approximately 700 employees it undertakes, in collaboration with universities and industry, research and development in the areas of coastal research, materials research, regenerative medicine, and structure research with neutrons and synchrotron radiation.**

The GKSS Research Centre is running a centre for materials research based on the complementary use of synchrotron radiation and neutron radiation operating the Geesthacht Neutron Facility GeNF (http://genf.gkss.de) in Geesthacht and a growing outstation at DESY in Hamburg. As a collaborating research group we are operating the high energy beamline HARWI II at DORIS III and are building a High Energy Materials Science Beamline (HEMS) and an Imaging Beamline at the new high-brilliance synchrotron radiation source PETRA III at DESY.

In this framework we are looking for a

## Scientist (permanent position) - Code-No. W 12 (Hamburg)

who will strengthen and further develop our activities in residual stress analysis with diffraction methods using synchrotron radiation. You will participate in the technical and scientific development of the new state of the art undulator beamline HEMS which will have a main energy of 120 keV, tunable in the range 50 to 300 keV and will be optimized for sub-micrometer focusing (http://hasylab.desy.de/site_petra3/content/beamlines/work_packages/e1036/e1557/index_eng.html), offering unique opportunities in the fields of Material Science and Physics. You will be responsible for the design and maintenance of a specialized 3D-XRD microscope at HEMS for the characterization of the microstructure and strain of polycrystalline materials and assist external users in preparing and running their experiments there. You are expected to develop an innovative in-house research program for grain mapping which should exploit the unique features of the beamline and its various sample environments (fatigue loading, furnace, welding, cryostat etc.) and strong sample preparation and analysis support from its home institute in Geesthacht near Hamburg. For this position good skills in instrumentation and experience in high energy X-ray scattering methods at 3rd generation synchrotron radiation sources are essential. In addition you are expected to provide support to external users also of other experiments at HEMS and of the Wiggler beamline HARWI-II, which is complementary to HEMS. For specific inquiries please contact Dr. Norbert Schell (norbert.schell@gkss.de)

In addition we are looking for a

## Scientist (Postdoc) - Code-No. W 13 (Geesthacht/Hamburg)

for an initial 3 years in the field of residual stress analysis who will take part in performing experiments at the GKSS high-energy materials science beamlines HARWI and HEMS at DESY in Hamburg as well as at the neutron strain scanner ARES-2 at GeNF in Geesthacht. In this position you will deal with fundamental problems of diffraction-based stress analysis, you will take part in operating and further developing the above mentioned instruments and you will support internal and external users in this field. Ideally, you already have knowledge in the mechanics of materials and experience with diffraction methods for residual stress analysis. For specific inquiries please contact Dr. Peter Staron (peter.staron@gkss.de).

Furthermore we are looking for a

## Scientist (Postdoc) - Code-No. W 14 (Geesthacht/Hamburg)

for an initial three years who will support the radiography and tomography activities in our rapidly growing tomography group. You will perform experiments at the state of the art tomography instruments at the GKSS beamlines HARWI and the new Imaging Beamline at DESY in Hamburg as well as at the neutron radiography/tomography instrument Genra-3 at GeNF in Geesthacht. In this position you will take part in operating and further developing these methods and you will support internal and external users during their experiments. For specific inquiries please contact Dr. Felix Beckmann (felix.beckmann@gkss.de).

All three positions will allow you to continue and develop your own scientific research program using synchrotron radiation and neutrons. You will support external users during the experiment, including evaluation and publication of results, and deal with orders from industry. Within this context, international collaborations as well as cooperation with staff members and other scientists at GKSS are highly encouraged. Opportunities for gaining additional qualifications by cooperation with internal partners, especially in the field of joining techniques, are available. Current topics in this field are e.g. friction stir welding as well as laser beam welding for aircraft construction.

For all three positions a Ph.D. or equivalent in materials science and engineering, physics, chemistry or a related field is mandatory. Beside good communication skills, the positions require excellent experience in the respective scattering techniques using synchrotron radiation or neutrons, ideally in the field of materials research. We expect good English language skills; German language skills are an asset.

A fast familiarization with new topics is a personal challenge for you. You should be familiar with complex experiments and control software. You have adopted a purposeful and result-oriented way of working and are able to realize this in a team. You are flexible and communicative in your approach with collaborators and you give priority to the success of a project and your team. You are familiar with publishing the results of your work and presenting them at international conferences.

The first position is a permanent appointment and the other two will initially be for 3 years with the possibility of extension. We offer an appropriate salary, related to TV-AVH, as well as the usual public sector social benefits.

The GKSS is an equal opportunity/affirmative action employer seeking to increase the proportion of female staff members. Qualified women are therefore especially encouraged to apply. Handicapped persons with equal qualifications will be preferred.

For general inquiries please contact Dr. Klaus Pranzas (pranzas@gkss.de).

Please send your application with the corresponding code, CV and references to pranzas@gkss.de or to our Personnel-Division. The closing date for applications is four weeks after publication of this advertisement.

**GKSS • FORSCHUNGSZENTRUM GEESTHACHT**
**MAX-PLANCK-STRASSE 1 • 21502 GEESTHACHT • GERMANY**

PENNSTATE Department of Chemistry

## THE PENNSYLVANIA STATE UNIVERSITY DEPARTMENT OF CHEMISTRY

### FACULTY POSITIONS IN ORGANIC CHEMISTRY AND BIOMOLECULAR/ MACROMOLECULAR NMR

Several faculty positions are available for Fall, 2008 at the junior or senior level in the areas of organic chemistry and biomolecular/ macromolecular structure and function with an emphasis on NMR spectroscopy. The Chemistry Department has recently moved into a new state-of-the-art building. Departmental research spans both traditional and non-traditional areas. Faculty members have opportunities to participate in university-wide life sciences, materials, environmental, and computational institutes. Appointees are expected to establish an exceptionally strong and highly visible research program that incorporates excellence in undergraduate and graduate education. Senior appointments should have a previous record of national and international distinction.

Applicants should submit curriculum vitae, list of publications, and research plans to: **Chair of the Search Committee, Box C, Department of Chemistry, 104 Chemistry Building, The Pennsylvania State University, University Park, PA 16802**. Junior applicants should also arrange to have three letters of recommendation sent to this address. Review of applications will begin on **October 1, 2007** and continue until the positions are filled.

To view this position:
**http://www.chem.psu.edu/faculty/facultyad.html**

*Penn State is committed to Affirmative Action, Equal Opportunity and the diversity of its workforce.*

## Chair • Department of Biochemistry and Cell Biology

Stony Brook University's Department of Biochemistry and Cell Biology is an internationally recognized interdisciplinary research and education department with an outstanding record of research achievement. Currently, the Department has 20 tenured/tenure-track faculty having research interests covering the broad areas of biochemical and cell biological sciences. The Department also has close relationships with faculty at Brookhaven National Laboratory and Cold Spring Harbor Laboratory. We are seeking an outstanding scientific leader to direct the future growth of the Department. The candidate must also be committed to the Department's undergraduate, graduate, and medical education programs. **Required:** Ph.D. or equivalent degree, the academic rank of Professor and a vigorous research program that is recognized at both the national and international level, as judged by extramural funding, scholarly publications, and invited presentations. The successful candidate must have an eagerness to promote multidisciplinary interactions and a demonstrated record of success in graduate student and/or postdoctoral training. Substantial start-up package for the Chair with resources for the expansion of the Department in both research and teaching will be provided through the College of Arts and Sciences and the School of Medicine.

The review of applications will begin September 1, 2007, and will continue until the position is filled. For more information, please visit: *http://www.sunysb.edu/biochem/*

**Interested individuals can apply online at *www.stonybrook.edu/cjo* (Reference number: F-4196-07-07) or forward a curriculum vitae to:**
Biochemistry and Cell Biology Chair Search Committee, c/o Carol Galdi
Department of Biochemistry and Cell Biology
450 Life Sciences Building
Stony Brook University, SUNY
Stony Brook, NY 11794-5215

Equal Opportunity/Affirmative Action Employer.

STONY BROOK

VirginiaTech
*Invent the Future*

### Molecular Microbiologist

### Department of Biological Sciences

The Department of Biological Sciences (**www.biol.vt.edu**) is recruiting a Molecular Microbiologist for a tenure track assistant professor faculty position. Competitive salary and start-up package will be provided. The department is interested in hiring an individual from one of several research areas, including but not limited to: (1) Infectious disease; (2) Microbial interactions with the environment; (3) Signal transduction; and (4) Prokaryotic development. The hire may become affiliated with the Institute for Biomedical and Public Health Sciences or the Institute for Critical Technology and Applied Science, which were created to increase research training and research funding through interdisciplinary initiatives. Core laboratory facilities are available for DNA sequencing, microarrays, proteomics, protein structure analysis and high speed computation.

Applicants should submit a cover letter, curriculum vitae, and a statement of research and teaching interests emphasizing career goals using our on-line system (**https://jobs.vt.edu**, search posting **070798**). Three reference letters should be sent to the chair of the search committee, **Dr. Ann Stevens; Department of Biological Sciences; 2119 Derring Hall MC0406; Virginia Tech; Blacksburg, VA 24061**. Inquiries concerning the position or application process should be directed to the chair of the search committee (**ams@vt.edu**; **540-231-9378**). Review of applications will begin **October 12, 2007** and continue until position is filled.

*Virginia Tech is an NSF Advance Institution and has a strong commitment to the principle of diversity and, in that spirit, seeks a broad spectrum of candidates, including women, minorities, veterans and people with disabilities.*

## WEST VIRGINIA UNIVERSITY
### Eberly College of Arts and Sciences
### Position in Applied Mathematics (bioinformatics)

West Virginia University's Department of Mathematics invites applications for a tenure-track assistant professor in the general area of **BIOLOGICAL MATHEMATICS** in support of multidisciplinary efforts in the **BIOMEDICAL** and **LIFE SCIENCES**, involving faculty from the Eberly College of Arts and Sciences, the Robert C. Byrd Health Sciences Center, the College of Engineering and Mineral Resources, and the Davis College of Agriculture, Forestry, and Consumer Sciences. The starting date for this position will be August 16, 2008. Applicants must have a Ph.D. degree, and should have demonstrated research potential in systems biology, computational genomics, data analysis, and/or discrete optimization/algorithm design related to bioinformatics. Excellence in teaching at the undergraduate and graduate levels and the development of a vigorous and externally funded research program are expected.

West Virginia University is a Research-High Activity University enrolling over 25,000 students. The University is located in Morgantown, an award winning "small" city with a metropolitan population of about 50,000 in easy travel distance of Pittsburgh, PA, Baltimore, MD and Washington, DC.

Applicant should submit a curriculum vitae, a description of research plans, a detailed start-up budget, and a brief description of teaching interests, and arrange for three letters of recommendation to be sent to: **Math-Bio Position, Department of Mathematics, West Virginia University, P.O. Box 6310, Morgantown, WV 26506-6310, (biomathjob@math.wvu.edu)**. Priority will be given to applications received by **November 14, 2007**.

*West Virginia University is an Equal Opportunity/Affirmative Action Employer. Women and protected class individuals are encouraged to apply.*

School of Biological Sciences

## Postdoctoral Research Officer

**Project: The evolution of parasitic sex ratio distortion**

**Starting Salary: £24,478 - £28,363 (on R&A Grade 1A) p.a.**

A 3-year NERC-funded postdoctoral position is available immediately to work on proteomic or cell biology and cell signal pathway analyses of host parasite interaction of intracellular reproductive parasites in Bangor in a collaborative project with groups at University of Leeds and Liverpool and University of Poitiers. The study might involve feminisation, male killing and cytoplasmic incompatibility. Previous experience as a postdoc in cell biology or microbiology is preferable but not essential.

The successful candidate will be expected to start as soon as possible.

Application forms and further particulars should be obtained by contacting Human Resources, University of Wales, Bangor; tel: (01248) 382926/388132; e-mail: personnel@bangor.ac.uk; web: http://www.bangor.ac.uk

Please quote reference number 07-7/16 when applying.

Closing date for applications: Monday 3 September, 2007.

Informal enquiries can be made by contacting Dr Henk R. Braig, e-mail: h.braig@bangor.ac.uk

PRIFYSGOL CYMRU UNIVERSITY OF WALES BANGOR

Wedi Ymrwymo i Gyfle Cyfartal • Committed To Equal Opportunities

## Structural Biology Faculty

Stony Brook University's Department of Pharmacological Sciences seeks scientists working in the area of structural biology/X-ray crystallography to apply for a faculty position at the level of Assistant, Associate, or Full Professor. The candidate will be expected to have or develop and sustain an independent research program in structural biology and to contribute to the teaching responsibilities of the Department (*www.pharm.stonybrook.edu*). State-of-the-art equipment for X-ray crystallography is available at the Center for Structural Biology and ready access to the NSLS at Brookhaven National Laboratory is guaranteed. Many opportunities are available for collaborative research. Stony Brook has strong graduate programs in molecular, chemical, and computational biology that include researchers at the Cold Spring Harbor and Brookhaven National Laboratories.

**Required:** An M.D. or Ph.D. degree (or equivalent) with at least two years of additional research experience. The position offers a generous startup-package and salary support. Review of applications will commence immediately and will continue until the position is filled.

**To apply, please submit an application electronically to *www.stonybrook.edu/jobs*.** Application should consist of a single pdf file containing (1) a C.V. (2) synopsis of major research accomplishments and future research plans of no more than three pages, (3) names, addresses, and Email addresses for three individuals who have agreed to write letters of recommendation, and (4) a cover letter indicating whether the applicant wishes to be considered for appointment at the Assistant, Associate, or Full Professor level. Applicants at the Associate or Full Professor level should include a summary of past and current research funding, administrative, and teaching experience.

Equal Opportunity/Affirmative Action Employer.

STONY BROOK

FLORIDA STATE UNIVERSITY

### Epigenetics and Evolutionary Genetics

The Department of Biological Science invites applications for tenure-track faculty positions at any rank in our Integrating Genotype and Phenotype cluster hire of eight positions. This coincides with new construction and an aggressive expansion of faculty at FSU. For more information see **http://www.bio.fsu.edu/genphensearch/**.

**Epigenetics:** Researchers investigating **fundamental aspects of chromatin or RNA–mediated regulation of phenotypic variation, the role of epigenetics in evolution, and those using genomics or computational approaches.**

**Evolutionary Genetics:** Researchers using experimental, computational, or theoretical approaches to study the genotype-phenotype map, including, but not limited to, **evolution of development, epigenetic systems, genomics, genetic regulatory networks, or quantitative genetics.**

Please submit one electronic application (PDF files preferred) consisting of a cover letter, curriculum vitae, statements of research and teaching interests, and have four letters of reference sent to **genphensearch@bio.fsu.edu**. Review of applications will begin **October 1, 2007**, but will continue until the positions are filled.

*FSU is an AA/EO Employer. Applications from minority and female candidates are especially encouraged.*

BIODURO

BioDuro is a US-based, fully-integrated, global life science outsourcing services company. Our priority is providing the highest quality, FDA-compliant services at an affordable cost. Our customers are over 30 pharmaceutical and biotechnology companies, and our services span the entire range of drug discovery and development, from discovery chemistry, through pharmacology and drug safety and evaluation, to clinical trials.

BioDuro has openings in Biology and Chemistry in Beijing, and it is actively seeking a Group Leader/Associate Director position in Biology for our Beijing Laboratory, a newly constructed state-of-the-art facility comprising approximately 300 scientists.

The successful candidate must have a Ph.D. with > 7 years experience in assay development in the Pharmaceutical industry or Biotechnology. They also must have:

- experience in independently developing, optimizing, and validating assays,
- in-depth theoretical and practical knowledge in assay development,
- familiarity with standard assay technologies including radiometric, flouorescence, and chemiluminescence,
- familiarity with analytical software for data analysis and presentation,
- good team management skills and ability to lead projects efficiently,
- good presentation skills and ability to communicate in English.

We will offer the successful candidate competitive salary and the standard benefit package such as pension, medical insurance and vacation etc. according to his/her nationality. Please go to our website for more information **www.bioduro.com**. Please send application to:

**BioDuro, Inc.**
**4350 La Jolla Village Drive, Suite 450**
**San Diego, CA 92122**

**info@bioduro.com**
or email your application to **paul.conlon@bioduro.com**

*7542, Onna, Onna Village, Okinawa Japan 904-0411*
*Tel: +81 98 966 8711 Fax: +81 98 966 8717*
*URL: www.oist.jp*

## Principal Investigator Positions
## Okinawa Institute of Science and Technology (OIST)

The Okinawa Institute of Science and Technology (OIST: **http://www.oist.jp**) is inviting applications for Principal Investigator positions in the fields of Primate Brain Research and Functional Brain Imaging. OIST will open its brand new campus, overlooking tropical beaches in Onna Village, Okinawa, Japan in 2009. The major facilities will include a non-human primate laboratory compatible with cutting edge molecular technologies and high field MRI scanners for both non-human primates and humans. MEG, PET and other imaging facilities are future options.

Appointment is for five years and is renewable upon successful evaluation. Temporary offices near the new campus will be available until the completion of the new facilities in 2009. An appointee will be able to perform joint research based in another institute while facilities are being completed at the new campus.

### Principal Investigator Position in Primate Brain Research

A successful applicant will play a major role in planning the non-human primate research facilities, including decisions on the floor plan and major equipment. Candidates should have a doctoral degree, a strong publication record, deep practical knowledge in non-human primate research, and fresh ideas. Good communication skills and the ability to work collegially will be required for organizing this new research facility.

For the first round of reviews, candidates should send CV, statement of on-going and future research intentions, the names and contact information of five references, and up to five representative papers in electronic format to **pbr07@oist.jp** by September 28, 2007. The search will remain open until the position is filled.

### Principal Investigator Position in Functional Brain Imaging

A successful applicant will play a major role in planning the brain imaging facilities, including decisions on the floor plan and major equipment. Candidates should have a doctoral degree, a strong publication record, deep practical knowledge in functional brain imaging, and fresh ideas. Good communication skills and the ability to work collegially will be required for organizing this new research facility.

For the first round of reviews, candidates should send CV, statement of on-going and future research intentions, the names and contact information of five references, and up to five representative papers in electronic format to **fbi07@oist.jp** by September 28, 2007. The search will remain open until the position is filled.

---

## ASSISTANT PROFESSOR
## DEPARTMENT OF GENETICS
## HARVARD MEDICAL SCHOOL

The Department of Genetics invites applicants for the tenure-track position of Assistant Professor. We are searching for individuals with a strong potential for imaginative research in any area of modern genetic or genomic analysis. This position offers significant scholarly and scientific resources as well as the opportunity to teach graduate and medical students.

For further information about our Department, please see our Web Page:

**http://genetics.med.harvard.edu**

Applicants should submit electronic copies of curriculum vitae, bibliography, a brief description of research accomplishments and future research interests (limit to 500 words) by **October 31, 2007**, and ask three references to provide letters of recommendation. These materials should be sent to the following email address:

**faculty_search@genetics.med.harvard.edu**

*Harvard University is an Equal Opportunity/Affirmative Action Employer and encourages the applications of qualified women and minorities.*

---

## NORTHWESTERN UNIVERSITY
**EVANSTON AND CHICAGO, ILLINOIS**

## VICE PRESIDENT FOR RESEARCH

Northwestern University seeks nominations and applications for the position of Vice President for Research. The Vice President for Research is a senior central administrator with primary responsibility for the quality and vitality of Northwestern University's research enterprise. The Vice President for Research develops and implements strategies for achieving the University's research goals; capitalizes on the interdisciplinary strength of University research centers; oversees compliance with regulatory mandates; and ensures that the research infrastructure is robust and responsive to the needs of Northwestern University investigators. Northwestern's research awards exceed $380 million annually. The Vice President's broad portfolio includes 20 University research centers and the offices and facilities providing University-wide research services. The Office for Research comprises 450 administrative and research staff and a budget of over $100 million. The Vice President reports to the Provost and serves as a member of the President's Staff. For full consideration, nominations and applications should be received by September 28, 2007, and should be sent to:

vpsearch@northwestern.edu
or
Secretary, Search Committee for the VP for Research
Northwestern University
633 Clark Street
Evanston, IL 60208-1119

Northwestern is an affirmative action, equal opportunity educator and employer.

## Mekong River Commission

The role of MRC is to co-ordinate and promote co-operation in all fields of sustainable development, utilisation, management and conservation of the water and related resources of the Mekong Basin. MRC is seeking qualified candidates for two positions for the Environment Programme, Environment Division:

1. **CHIEF TECHNICAL ADVISOR**
2. **SENIOR ENVIRONMENT SPECIALIST**

The above positions are at level L-05, based in Vientiane, Lao PDR

The Environment Division generates data, information and knowledge in order to balance economic development and environmental conservation in decision-making. In addition to establishing systems for monitoring the Basin's environmental health, improving policies and legislation, and encouraging co-operation among the riparian countries, the programme is also charged with increasing environmental awareness amongst the public.

For information, job description and application details, please visit MRC's web site at **www.mrcmekong.org** or send an email to **mrcs@mrcmekong.org.**
Closing date for applications: **10 SEPTEMBER 2007**

## Northwestern University Feinberg School of Medicine
## Director of Clinical Pathology

The Department of Pathology at Northwestern University Feinberg School of Medicine, Chicago, invites applications for a full-time faculty position as Director of Clinical Pathology. The successful applicant will be an established investigator/clinician with a national and international reputation for excellence in clinical pathology. In addition, the applicant will have excellent interpersonal and leadership skills, and experience training Residents and Fellows. S/he will oversee the growth and operation of the clinical laboratories at Northwestern Memorial Hospital and play a major role in furthering the development of the Department into a world-class center for academic pathology.

The medical school and its main teaching hospital, Northwestern Memorial, are located in the heart of Chicago's magnificent "gold coast." The environment for hypothesis driven basic research, and for translational and collaborative research at Northwestern University and the Northwestern Memorial Hospital is outstanding. Applicants must hold MD or MD/PhD degrees, be certified in Clinical Pathology by the American Board of Pathology, as well as eligible for an unrestricted medical license in the State of Illinois.

We expect the successful candidate will be qualified to be appointed as a full professor. If professional experience warrants, this individual will also hold the position of Vice-Chair. A very generous salary and benefits package will be provided, in addition to funds for moving and expanding a research laboratory. In order to effectively evaluate candidates for the proposed starting date of January 1, 2008, interested applicants should submit a letter of interest, *curriculum vitae*, and names of three references via e-mail to **nstarks@northwestern.edu** by **October 1, 2007**. Additional questions may be submitted to: **William A. Muller, MD, PhD, Magerstadt Professor and Chairman, Northwestern University, Feinberg School of Medicine, Ward Building 6-204, 300 East Chicago Avenue, Chicago, IL 60611-3008; wamuller@northwestern.edu.**

*Northwestern University is an Equal Opportunity/Affirmative Action Employer. Women and minority candidates are encouraged to apply. Hiring is contingent upon eligibility to work in the United States.*

*WORKING AT THE UNIVERSITY OF GENEVA*

**The FACULTY OF SCIENCE seeks an**

**ASSISTANT or ASSOCIATE or FULL PROFESSOR**
**in Molecular Biology**

**(www.molbio.unige.ch)**

**POST:** Full-time research and teaching position in the general area of molecular biology. Special consideration given to scientists studying important biological problems using novel chemical, genetic or biophysical approaches.

**REQUIREMENTS:** Ph.D. degree or equivalent. Experience in teaching and leading an independent research project.

**STARTING DATE:** 1st July 2008 at the earliest.

Candidate files must be addressed before **November 15th, 2007** to : Décanat de la Faculté des sciences, 30, Quai Ernest-Ansermet, CH-1211 Genève 4, from whom additional information can be obtained regarding the responsibilities of the post and other conditions.

The University of Geneva is an equal opportunity employer and encourages applications from female candidates.

UNIVERSITÉ DE GENÈVE

## BASIC SCIENCE FACULTY POSITIONS AVAILABLE

**Institute of Human Virology**
**University of Maryland**
**School of Medicine**
**Baltimore, Maryland**

The Institute of Human Virology at the University of Maryland, Baltimore School of Medicine (**http://www.ihv.org**) is recruiting highly qualified individuals with established research programs at ranks of tenure-track **Assistant, Associate** and **Full Professor.** Candidates with NIH (R01 and/or P01) funded research programs with expertise in one or more of the following are encouraged to apply: cell biology, structural biology, basic immunology, or systems biology with interest in chronic human viral diseases such as HIV-1. These programs will complement the existing institute programs in molecular pathogenesis, innate immunity, vaccine development, and translational clinical research that focus on chronic viral diseases. The Institute of Human Virology offers excellent laboratory facilities, competitive salary and startup packages, and access to numerous core facilities including state-of-the-art BSL3 and ABSL3 facilities in a rapidly growing academic environment. The level of appointment will be commensurate with the candidate's experience.

Interested applicants are requested to forward a CV in .pdf format to: **Chairperson, c/o Beth Peterson, IHV Faculty Search Committee, Institute of Human Virology, 725 W. Lombard Street, Baltimore, Maryland, 21201.**

*The University of Maryland, Baltimore is an Equal Opportunity, Affirmative Action Employer.*

## INSTITUTE OF HUMAN VIROLOGY

**University of Maryland**
**School of Medicine**
**Baltimore, Maryland**

The Institute of Human Virology at the University of Maryland, Baltimore School of Medicine (**http://www.ihv.org**) is seeking to fill a **tenure-track faculty position** with an investigator with the ability to establish an independent research program centering on the molecular biology/virology of human papilloma virus and its interactions with host cell factors, especially those relevant to cancer. The successful candidate will have a demonstrable track record of relevant publications in peer-reviewed journals and of attracting peer-reviewed funding, preferably related to cancer. The level of appointment will be commensurate with the candidate's experience.

Interested applicants are requested to forward a CV in .pdf format to:

**Chairperson**
**c/o Beth Peterson**
**IHV Faculty Search Committee**
**Institute of Human Virology**
**725 W. Lombard Street**
**Baltimore, Maryland, 21201**

*The University of Maryland, Baltimore is an Equal Opportunity, Affirmative Action Employer.*

THE UNIVERSITY of WISCONSIN MADISON

The University of Wisconsin-Madison School of Pharmacy, invites applications for ***two tenure-track Assistant Professor positions*** in areas of drug discovery and drug delivery. Applicants must have a Ph.D. and demonstrate ability to establish an externally funded research program of high quality. The successful candidates should also have 2-4 years of postdoctoral experience and be willing to engage in productive interdisciplinary research, committed to effective teaching in undergraduate, professional, and graduate programs that serve a diverse student body, and be active in university service.

Successful candidate will join a world-class academic institution that encourages, values and supports basic, applied, and interdisciplinary research and attracts scholars and students from around the world. The School of Pharmacy is committed to excellence in teaching and research and its faculty, staff, and students reflect the global population represented within the university. We encourage applications from candidates whose skills and/or background prepare them to work effectively across socially diverse atmosphere and economic classes. Visit http://www.wisc.edu/employment/madison.php for working and living in Madison.

**Drug Discovery: PVL# 057141, http://www.ohr.wisc.edu/pvl/pv_057141.html**: Applicants for this position must hold a Ph.D. in chemistry or a related field and possess a strong background in natural products chemistry (isolation, structure elucidation, semi-synthetic modification), rational drug design, and/or the application of chemical tools for drug target identification (chemical biology) and will be expected to engage in productive interdisciplinary drug discovery and development research at the interface of chemistry and biology. Send materials to: **Prof. Jon S. Thorson, Chair, Drug Discovery Search Committee, 608-262-3829, jsthorson@pharmacy.wisc.edu**.

**Drug Delivery: PVL# 054752, http://www.ohr.wisc.edu/pvl/pv_054752.html**: Applicants for this position must hold a Ph.D. in pharmaceutical sciences, biomedical sciences or biomedical engineering and engage in creative research in the areas of biopharmaceutics, pharmacokinetics, or biological transport phenomena; innovative drug or gene targeting strategies; molecular imaging; or drug delivery to the CNS. Send materials to: **Prof. Glen Kwon, Chair, Drug Delivery Search Committee, 608-265-5183; gskwon@pharmacy.wisc.edu**.

Applications must be received by **November 2, 2007** to ensure full consideration with the appointment starting on or around July 1, 2008. Send a letter, curriculum vitae, names of three references, a statement of teaching interests, and a summary of the current and planned research to the named **Chair, School of Pharmacy, 777 Highland Avenue, Madison, WI 53705-2222**. If submitting by e-mail, please indicate **"Application for PVL# 05…"** in the subject line. The search will continue until the positions are filled.

*UW-Madison is an Equal Opportunity/ Affirmative Action Employer. Women and underrepresented minority groups are especially encouraged to apply. We promote excellence through diversity and encourage all qualified individuals to apply.*

FACULTY OF MEDICINE
GREAT MINDS FOR A GREAT FUTURE
*University of Toronto*

## Assistant Professor
## Laboratory Medicine and Pathobiology

The Department of Laboratory Medicine and Pathobiology, Faculty of Medicine, University of Toronto is seeking applicants for one full-time faculty position, academic microbiologist, either non-tenure or tenure-stream. The appointment will commence on 1 April, 2008 and will remain open until filled.

Excellence and recognized expertise in the areas of molecular and biochemical mechanisms of microbial disease, with preference to virology. Candidates must have an MD or a PhD degree or equivalent, have completed significant postdoctoral training, and have an established track record of high quality research accomplishment. Exceptional candidates with established funded research programs and a rank of Associate or Full Professor may be considered as well.

The successful candidate is expected to participate actively in graduate and undergraduate teaching programs, mount an original, competitive, and well-funded independent research program and interact with other investigators at the University of Toronto campus and the major affiliated hospitals. Rank and salary will commensurate with qualifications and experience. Additional information on the Department of Laboratory Medicine and Pathobiology can be obtained through the World Wide Web at: **http:///www.lmp.facmed.utoronto.ca**.

Interested applicants should include with their application: C.V., a description of their research accomplishments and the focus of their planned research program, together with the names of three references by **October 31, 2007** to: **Professor Avrum Gotlieb, Professor and Chair, Department of Laboratory Medicine and Pathobiology, Faculty of Medicine, University of Toronto, 100 College Street, Room 108, Toronto, Ontario M5G 1L5; E-mail: avrum.gotlieb@utoronto.ca**.

*The University of Toronto is strongly committed to diversity within its community and especially welcomes applications from visible minority group members, women, Aboriginal persons, persons with disabilities, members of sexual minority groups, and others who may contribute to the further diversification of ideas. All qualified candidates are encouraged to apply. However, Canadians and permanent residents will be given priority.*

## Nagasaki University
## Positions open for:
## Strategy for Fostering Young Scientists at a Local University (Assistant Professor)

Nagasaki University in Japan is now actively recruiting about 17 academic researchers as assistant professors for the "Strategy for Fostering Young Scientists at a Local University".

An assistant professor recruited by this program shall be expected to participate in any of the following nine major research projects designed by the University, for five years. During a project, the assistant professor will be able to work on his/her independent research supported by research space, facilities, funding, and a respectable salary. If the research achievements are deemed excellent at the end of the determined period, he/she will be promoted to associate professor following an examination.

- Global Strategic Center for Radiation Health Risk Control
- Global Control Strategy of Tropical and Emerging Infectious Diseases
- Restoration of Environment and Resources in East Asian Estuaries
- Establishment of the Center for Skeletal Basic Research
- Research Promotion regarding Drug Development for Infectious Diseases
- Chronic Pain Research and Control
- Interdisciplinary Research on Communication between Adult and Child, and between Children
- Materials Science Based on Nano-Dynamics
- Technology Integration Using Real-time Information Processing

* For detailed application information of each project, please refer to our official website at **http://www.nagasaki-u.ac.jp/wakate/index_e.html**

**Scheduled Research Period:**
**From December 1, 2007 to March 31, 2012**

**Application Deadline:**
**5:00 p.m. on Friday, September 28, 2007**

After a preliminary documentary examination, successful applicants will be expected to come to Nagasaki University around mid-October to attend a seminar in which the applicants give a lecture and undergo an oral examination on their current research. The University will cover airfare and transportation fees in Japan. In the case of international applicants, a visiting schedule may be arranged with the University.

* Please refer to our official website below for requested documents, qualifications, contact information, and address for submitting application.
**http://www.nagasaki-u.ac.jp/wakate/index_e.html**

COLUMBIA UNIVERSITY

## Biomechanics Faculty Search

2007–2008

The Department of Biomedical Engineering in the Fu Foundation School of Engineering and Applied Science at Columbia University is seeking to fill a tenure-track faculty position at the Assistant or Associate Professor level but exceptionally qualified candidates will be considered for a higher-level position. Applicants should have a doctoral degree in biomedical engineering or a closely related discipline, and should be prepared to establish a vigorous and independent research program in any of the broadly defined areas of biomechanics such as cellular or molecular biomechanics, biomechanics of growth and remodeling, biofluid mechanics, tissue mechanics. Successful candidates will have demonstrated a strong background in mechanics applied to biological systems.

Applicants should send a complete curriculum vitae, three publication reprints, a statement of research interests, a statement of teaching interests and names of four references by March 1, 2008 to:

**Professor Barclay Morrison III**
**Chair of the Biomechanics Faculty Search**
**Department of Biomedical Engineering**
**Columbia University**
**351 Engineering Terrace, Mail Code 8904**
**1210 Amsterdam Avenue**
**New York, NY 10027**

The search will remain open until the position has been filled.

Columbia University is an affirmative action/equal opportunity employer. Women and minorities are encouraged to apply.

## Senior Program Officer

The **Howard Hughes Medical Institute (HHMI)**, a national and international philanthropy devoted to biomedical research and science education, is seeking an experienced professional to oversee medical education programs. This position will be located in **Bethesda, MD**.

The HHMI-NIH Research Scholars program (or Cloister Program) is a residential program for medical, dental, and veterinary students who are housed at the Cloister (Building 60) on the campus of the National Institutes of Health in Bethesda, Maryland. The Research Training Fellowship for Medical Students Program makes awards to individuals to conduct research at institutions other than NIH.

In this key position, the Senior Program Officer will be responsible for the daily operations of the medical research training programs, the development and administration of budgets, the oversight of program policy compliance and information system applications, as well as management of staff members and contractors.

The ideal candidate must possess a Ph.D. (or M.D.) in biological sciences with laboratory research experience in a medical school environment, along with at least two years of experience in administration related to biomedical research or science education, excellent communication skills, and demonstrated skill in managing programs and people.

HHMI is an intellectually demanding, results-oriented organization with excellent salaries and benefits. Responses should include your present position, and a brief summary of your scientific interests and accomplishments. Please send your resume to Ms. Christine Leonhardt, Howard Hughes Medical Institute via e-mail at: **jobs@hhmi.org**. Please include the job title in the subject line. All applications must be received by September 17, 2007. To learn more about HHMI and this position, visit our Web site at **www.hhmi.org**.

The Howard Hughes Medical Institute is an Equal Opportunity Employer.

HHMI
HOWARD HUGHES MEDICAL INSTITUTE

## NEUROSCIENCE FACULTY POSITIONS
## THE UNIVERSITY OF IOWA
## CARVER COLLEGE OF MEDICINE

The Department of Molecular Physiology and Biophysics is seeking outstanding candidates for tenure- track positions. Successful candidates are expected to develop an extramurally funded, high quality, and independent research program. We are particularly interested in neuroscientists who would complement existing strengths in basic research. This recruitment is open to all ranks, but we are especially interested in individuals with an established research program, to be appointed to the Associate or Full Professor rank.

Candidates should have a Ph.D. or M.D. degree, at least two years of relevant postdoctoral training, and a strong record of research accomplishment. Substantial startup funds for equipment, personnel support, and supplies are available. The University of Iowa is located on the rolling hills along the Iowa River in Iowa City, an affordable university community with many cultural and recreational amenities.

Applicants are asked to submit curriculum vitae, a one page summary of research accomplishments, and a one page description of future plans and copies of major publications. Applicants should arrange to have three letters of recommendation sent to the search committee. Review of applications will begin **November 1, 2007**. Send all materials to:

**Dr. Kevin P. Campbell, Chair**
**Department of Molecular Physiology and Biophysics**
**Roy J. and Lucille A. Carver College of Medicine**
**The University of Iowa**
**5-660 Bowen Science Building**
**Iowa City, IA 52242**
**http://www.physiology.uiowa.edu/**

Electronic applications may be sent to:
**physiology-recruitment@uiowa.edu**

*The University of Iowa is an Equal Opportunity/Affirmative Action Employer. Women and minorities are encouraged to apply.*

### Northwestern University Feinberg School of Medicine
## Director of Anatomic Pathology

The Department of Pathology at Northwestern University Feinberg School of Medicine, Chicago, invites applications for a full-time faculty position as Director of Anatomic Pathology. The successful applicant will be an established investigator/clinician with a national and international reputation for excellence in surgical pathology and/or cytopathology. In addition, the applicant will have excellent interpersonal and leadership skills, and experience training Residents and Fellows. S/he will oversee the growth and operation of Anatomic Pathology at Northwestern Memorial Hospital and play a major role in furthering the development of the Department into a world-class center for academic pathology. This will include expansion of our fellowship programs, developing subspecialty areas of excellence in surgical pathology, and helping to catalyze translational research at the medical center.

The medical school and its main teaching hospital, Northwestern Memorial, are located in the heart of Chicago's magnificent "gold coast." The environment for hypothesis driven basic research, and for translational and collaborative research at Northwestern University and the Northwestern Memorial Hospital is outstanding. Applicants must hold MD or MD/PhD degrees, be certified in Anatomic Pathology by the American Board of Pathology, as well as eligible for an unrestricted medical license in the State of Illinois.

We expect the successful candidate will be qualified to be appointed as a full professor. If professional experience warrants, this individual will also hold the position of Vice-Chair. A very generous salary and benefits package will be provided, in addition to funds for moving and expanding a research laboratory, if appropriate. In order to effectively evaluate candidates for the proposed starting date of January 1, 2008, interested applicants should submit a letter of interest, *curriculum vitae*, and names of three references via e-mail to **nstarks@northwestern.edu** by **October 1, 2007**. Additional questions may be submitted to: **William A. Muller, MD, PhD, Magerstadt Professor and Chairman, Northwestern University, Feinberg School of Medicine, Ward Building 6-204, 300 East Chicago Avenue, Chicago, IL 60611-3008; wamuller@northwestern.edu.**

*Northwestern University is an Equal Opportunity/Affirmative Action Employer. Women and minority candidates are encouraged to apply. Hiring is contingent upon eligibility to work in the United States.*

# Take your next career step.

## Informatics Director
## (Assistant/Associate/Full Professor)
## Clinical and Translational Science Program
## The University of Vermont

The University of Vermont is recruiting for an Informatics Director for the Clinical and Translational Science Program. The qualified candidate will have an advanced degree and/or significant experience in the use of sophisticated informatics systems in translational and/or clinical research. Preferred candidates will have experience working at the interfaces of different IT systems in different institutions with an emphasis on interconnectivity; experience with an electronic medical record would be an advantage. The candidate will also be expected to have a track record and continue to publish in academic journals in aspects conjoining IT and clinical and/or translational research. The appointment will be made at the appropriate Professorial level with or without tenure in the Clinical and Translational Science Program and in the appropriate primary department, depending on discipline. Applications will be accepted until the position is filled; however, we strongly encourage the submission of materials by **September 30, 2007**. Applicants should send a copy of their CV, a letter outlining their interests and three letters of recommendation to: **Richard Galbraith, M.D., Ph.D., Chair of the Search Committee, Associate Dean for Patient Oriented Research, MCHV/Baird 727A, 111 Colchester Avenue, Burlington, VT 05401** or by applying at **www.uvmjobs.com**. *Applications are encouraged from women and individuals of diverse racial, ethnic and cultural backgrounds. AN EQUAL OPPORTUNITY/AFFIRMATIVE ACTION EMPLOYER.*

## Faculty Position in Cardiovascular Diseases
## Columbia University
## College of Physicians and Surgeons
### Department of Physiology and Cellular Biophysics
### Department of Medicine/Cardiology

We invite applications for tenure-track Assistant Professor or Associate Professor faculty position in the Department of Physiology and Cellular Biophysics and the Department of Medicine, focusing on Cardiovascular Diseases. We seek candidates with research interests including cellular and/or animal electrophysiology, muscle biology, cardiovascular development, stem cells and heart failure, which will complement a substantial interdisciplinary program. Applicants should have a PhD, MD or MD/PhD, or equivalent degree and postdoctoral experience. In addition to a generous start-up package, an endowed chair is available for a senior or an exceptional junior candidate. Successful candidates are expected to develop/maintain an innovative, externally funded research program, as well as participate in graduate and medical student teaching. Applicants should include a curriculum vitae, representative reprints, a statement of current and future research interests, as well as three letters of recommendation. All material should be sent to: **Sheba R. Edwards, Department of Physiology and Cellular Biophysics, Columbia University College of Physicians and Surgeons; 630 W168th Street, New York, NY 10032.** Tel: **212-342-4766.** Fax: **212-305-3690.** E-mail: **se71@columbia.edu**.

*Columbia University is an Affirmative Action/ Equal Opportunity Employer and welcomes applications from women and minorities.*

# POSITIONS OPEN

## CHEMISTRY/ENVIRONMENTAL STUDIES
### at Transylvania University

Transylvania University **(website: http://www.transy.edu/)**, an independent, residential, liberal arts college of 1,100, invites applications for a full-time, tenure-track position at the **ASSISTANT PROFESSOR** level in chemistry/environmental studies beginning September 1, 2008. Ph.D. required. Classes to be taught include general chemistry, and courses to support an environmental studies minor. Possible specialty areas include geochemistry, environmental toxicology, or environmental biochemistry. Teaching opportunities may also include periodic contribution to the College's Foundations of the Liberal Arts Program. Bingham Awards for Excellence in Teaching may provide substantial salary supplements for exceptional candidates or smaller startup awards for recent Ph.D.s. Applications including curriculum vitae, graduate and undergraduate transcripts, and three letters of recommendation should be sent to: **Dr. Alan Goren, e-mail: agoren@transy.edu** or **300 North Broadway, Lexington, KY 40508.** In your cover letter please identify and describe two specialty courses you would like to teach and how you plan to actively engage undergraduates through your teaching and research. This position is open until filled; but to assure full consideration, applications should be received no later than October 8, 2007. *Transylvania University is an Equal Opportunity Employer and is committed to building a faculty that reflects the diversity of American society.*

## ASSISTANT PROFESSOR, MICROBIOLOGY
### University of Denver

The Department of Biological Sciences, University of Denver invites applications for a tenure-track position at the Assistant Professor level to begin September 1, 2008. We are particularly interested in **MICROBIOLOGISTS** with expertise in ecology, evolution, or (preferably) both. The successful candidate will have Ph.D. and postdoctoral experience in appropriate fields. S/he will be expected to develop a funded research program, supervise Ph.D. and M.S. students, and teach undergraduate and graduate courses in areas related to her/his specialty. All candidates must submit their application through **website: https://www.dujobs.org.** The application should include curriculum vitae and statements of teaching philosophy and research interests. Under separate cover please send two recent publications and three letters of recommendation to: **Biological Sciences Microbiology Faculty Search, University of Denver, Department of Biological Sciences, Denver, CO 80208**. The review of applications will begin October 15, 2007, and continue until the position is filled. Contact **Professor Robert L. Sanford (e-mail: rsanford@du.edu)** if you have any questions. *The University of Denver is committed to enhancing the diversity of its faculty and staff and encourages applications from women, minorities, people with disabilities, and veterans. DU is an Equal Employment Opportunity /Affirmative Action Employer.*

## FACULTY POSITIONS: BIOCHEMIST, INORGANIC CHEMIST

The Department of Chemistry and Biochemistry at California State University, Long Beach, invites applications for two tenure-track positions (Inorganic Chemist, Biochemist) at the **ASSISTANT/ ASSOCIATE PROFESSOR** level to begin 25 August 2008. Excellence in teaching, scholarly activity, and service are expected at undergraduate and Master's degree levels. For complete position descriptions and application instructions, go to **website: http://chemistry.csulb.edu/.** For general information, contact **Dr. Douglas McAbee (e-mail: dmcabee@csulb.edu; telephone: 562-985-1558).** Review of applications begins 15 October 2007. *CSU, Long Beach, actively encourages applications and nominations of all qualified individuals, and welcomes candidates who support diversity.*

# POSITIONS OPEN

The Department of Biological Sciences at Dartmouth seeks applicants for a tenure-track **ASSISTANT PROFESSORSHIP** in the areas of molecular evolution, population genetics, comparative and evolutionary genomics, or quantitative paleobiology. We seek candidates who are taking empirical, theoretical, and/or statistical approaches to major questions in these areas. The successful candidate will be expected to supervise an independent research program that will attract extramural funding, to provide research training for graduate and undergraduate students, and to teach at the undergraduate and graduate levels. Application materials should include curriculum vitae, representative publications, statements of research and teaching interests, and at least three letters of reference. Please send materials either electronically to **e-mail: evosearch@mac.dartmouth.edu** or as hard copies to:

**Mark A. McPeek, Chair**
**Evolutionary Biology Search Committee**
**Department of Biological Sciences**
**Dartmouth College**
**Hanover, NH 03755-3576**

Application review will begin on October 1, 2007, and continue until the position is filled. For further information about the Department and graduate programs, see **website: http://www.dartmouth.edu/~biology/.**

*With an even distribution of male and female students and over a quarter of the undergraduate student population members of minority groups, Dartmouth is committed to diversity and encourages applications from women and minorities. Dartmouth College is an Equal Opportunity and Affirmative Action Employer.*

## ORGANIC CHEMISTRY
### Dartmouth College

Applications are invited for a faculty position at the **ASSISTANT PROFESSOR** level starting July 2008. The Chemistry Department seeks an individual who will establish a nationally recognized research program in organic chemistry at Dartmouth, and who will excel at teaching in our undergraduate and Ph.D. curriculum. We are particularly interested in individuals with a strong background in the organic chemistry of materials or biomaterials. Candidates will be expected to be able to teach introductory and advanced courses in organic chemistry, as well as graduate courses in their area of research. Applicants should submit curriculum vitae, a description of their research plans, and a brief statement about their teaching interests. Applicants should also arrange to have three letters of recommendation sent on their behalf. All inquiries and applications will be treated confidentially. The Committee will begin to consider completed applications on October 15, 2007. Application materials should be sent to: **Chair, Organic Chemist Search Committee, Department of Chemistry, 6128 Burke Laboratory, Dartmouth College, Hanover, NH 03755-3564.** *With an even distribution of male and female students and over a quarter of the undergraduate student population members of minority groups, Dartmouth is committed to diversity and encourages applications from women and minorities. Dartmouth College is an Equal Opportunity and Affirmative Action Employer.*

**ASSISTANT PROFESSOR, TENURE TRACK, MEDICAL ENTOMOLOGIST.** The Entomology Department at Texas A&M University seeks applicants with a Ph.D. in entomology or related field, with expertise in field-level studies of mosquito vectors of human disease. A full description and instructions for submission of applications are at **website: http://insects.tamu.edu.** Closing date for applications is September 15, 2007.


## POSITIONS OPEN

### Faculty Positions in HIV Virology and NeuroAIDS
### Center for AIDS Research
### Indiana University School of Medicine

The Center for AIDS Research is seeking outstanding candidates with a Ph.D. or M.D./Ph.D. degree for faculty positions at the rank of tenure-track Assistant Professor, Associate Professor, and non-tenure-track Research Assistant/Associate Professor in the areas of HIV virology and pathogenesis. Preference will be given to those with research interests in HIV neuropathogenesis, although all areas of HIV research will be considered. Academic credentials and experience will determine faculty rank and appropriate departments for joint appointments.

For tenure-track positions, external peer-reviewed funding and peer-reviewed publications in high ranking journals are absolutely required, and the faculty member will be expected to pursue independent programs in original basic research, continue to secure external grant support, and participate in teaching graduate and medical students. For non-tenure-track positions, highly productive postdoctoral training of a minimum of 3 years is required, and the faculty member will be expected to establish independent and externally funded research program and transition to tenure-track positions within 2-3 years.

A competitive start-up package is available including new laboratory space. The environment is highly interactive and productive with close ties on campus to all Basic Science and Medical Departments, and Research Centers.

Interested candidates should email their curriculum vitae, description of research goals and names, addresses, phone, fax numbers, and e-mail addresses of three references (in one PDF file) to **jjhe@iupui.edu - Johnny J. He, Ph.D., Professor and Director, Center for AIDS Research, Indiana University School of Medicine, R2-302, Indianapolis, IN 46202-5120, USA**, or to his assistant, **Ms. Cynthia Booth** at **cbooth@iupui.edu**.

*Indiana University is an Affirmative Action/Equal Opportunity Employer. M/F/D.*

## CONFERENCE

EUROPEAN SCIENCE FOUNDATION
SETTING SCIENCE AGENDAS FOR EUROPE

UNIVERSITAT DE BARCELONA

**RESEARCH CONFERENCES**

ESF-UB Conference in Biomedicine

### European Conference on Synthetic Biology (ECSB): Design, Programming and Optimisation of Biological Systems

Sant Feliu de Guixols – Spain
**24-29 November 2007**

Synthetic Biology lies at the interface of a variety of disciplines ranging from biology through chemistry, physics, computer science, mathematics and engineering. Although undeniably multi-disciplinary, this nascent field of research has tended to be locked within the narrow remits of each of its constitutive disciplines. The specific overarching aim of this conference is to generate new vigorous interactions between the disciplines that impinge (and contribute to) Synthetic Biology.
ECSB 2007 will draw on international expertise from, on the one hand, Biological disciplines (e.g. Genomics, Proteomics, Metabolomics, etc.), and on the other hand, Computational and Engineering experts to present a balanced overview of the very latest key technologies and research advances as pertaining to Synthetic Biology in general and the quest for minimal living forms in particular.

Conference Programme and further information available from
**www.esf.org/conferences/07241**
Closing Date for Applications: **7 September 2007**

European Science Foundation | Research Conferences Unit
149 avenue Louise | Box 14 | Tour Generali, 15th Floor
Brussels | Belgium
Tel: +32 (0)2 533 2020 | Fax: +32 (0)2 538 8486
Email: conferences@esf.org | www.esf.org/conferences

**www.esf.org**

## POSITIONS OPEN

### TWO AUXILIARY POSITIONS
**Department of Bioscience and Biotechnology**
**Drexel University, Philadelphia, Pennsylvania**

The Department of Bioscience and Biotechnology, Drexel University in Philadelphia, is seeking two **AUXILIARY TEACHING INSTRUCTORS** to teach undergraduate/graduate courses in biological sciences for the 2007-2008 academic year.

The successful candidate must have a Ph.D. in the biological sciences or related field and will teach at the main campus in University City Philadelphia. One of these positions will also be required to teach at the Burlington County Community College campus.

We are seeking Instructors with expertise in teaching in one of the following disciplines: general biology, biochemistry, molecular/cell biology, physiology, and statistical analysis. Demonstrated teaching experience preferred. One-year contracts with possibility of renewal.

The review of the applications will begin August 27, 2007, and continue until the positions are filled. Details on the Department can be found at **website: http://www.drexel.edu/academics/coas/bioscience/.**

Applicants are requested to submit full curriculum vitae, statement of educational interests, and the contact information for three or more references to the: **Department of Bioscience and Biotechnology, Attention: Bioscience Auxiliary Search Committee, Drexel University, 3141 Chestnut Street, Philadelphia, PA 19104,** or **fax: 215-895-1273.** *Drexel University is an Equal Opportunity Employer.*

---

### PROJECT COORDINATOR (SCIENTIFIC WRITER)

The Department of Pharmacology in the College of Medicine at the University of Illinois at Chicago is seeking a Project Coordinator who can assist in writing and coordinating NIH grants and scientific documents. Scientific/technical writing experience is required. Primary responsibilities include the preparation and editing of scientific progress reports, proposals, manuscripts, grant applications, slides, presentations, and other documents. Applicant will also review the stipulations of grant and program announcements and assure compliance. Applicant will work directly with the Department Head to assist with writing up scientific plans and reports and will be responsible for the organization and development of documents, with a specific eye toward clarity, coherence, persuasiveness, and the scientific integrity of the material. A Bachelor's degree (Master's preferred) in natural science and two to five years of experience is required. Previous experience in a university-based setting is helpful. For fullest consideration, applications must be submitted by September 15, 2007. Please respond to: **Aileen Baker (PC001), Department of Pharmacology M/C 868, College of Medicine, University of Illinois at Chicago, 835 S. Wolcott Avenue, E403 MSB, Chicago, IL 60612.** *UIC is an Affirmative Action/Equal Opportunity Employer.*

---

### MICROBIOLOGIST

Ripon College seeks a tenure-track **ASSISTANT PROFESSOR** starting August 2008 to teach microbiology, an upper-division molecular biology course, and participate in introductory courses for majors and nonmajors. The candidate must have a Ph.D. and be able to lead undergraduate research. Send letter of application, curriculum vitae, statements of instructional philosophy and research interests, three letters of reference, and arrange to have sent official undergraduate and graduate transcripts to: **Dr. George H. Wittler, Chair, Department of Biology, Ripon College, P.O. Box 248, Ripon, WI 54971.** Applicant review begins October 12, 2007, until position is filled. For more information visit **website: http://www.ripon.edu. E-mail: wittlerg@ripon.edu.** *Affirmative Action/Equal Opportunity Employer.*

## POSITIONS OPEN

### FACULTY POSITION
**in Gastrointestinal Research**

The Digestive Disease and Nutrition Center, Women and Children's Hospital of Buffalo, State University of New York, is seeking a basic **RESEARCH SCIENTIST** with a doctoral degree and at least three years of experience or a **PHYSICIAN SCIENTIST** for a tenure-track position. The successful candidate will run a laboratory studying the molecular basis for inflammation in the gastrointestinal tract and nonalcoholic steatosis and supervise the research of fellows during their second and third years of fellowship. Supervisory skills as well as firsthand knowledge of molecular biology and cell culture techniques are necessary. This is a chance to establish an independent research area with solid support.

Send curriculum vitae with references to: **Robert D. Baker, M.D., Ph.D.** or to: **Susan S. Baker, M.D., Ph.D., Digestive Disease and Nutrition Center, Women and Children's Hospital of Buffalo, 219 Bryant Street, Buffalo, NY 14222.** Or **e-mail: rbaker@upa.chob.edu** or **sbaker@upa.chob.edu,** or **telephone: 1-716-878-7198.**

*State University of New York at Buffalo is an Equal Opportunity, Affirmative Action Employer/Recruiter. Women and minorities are encouraged to apply.*

---

### FACULTY POSITIONS
**(ASSISTANT/ASSOCIATE/FULL PROFESSOR)**
**Molecular Medicine/**
**Neuropharmacology/Molecular Genetics**

Dr. Panjwani Center for Molecular Medicine and Drug Research, University of Karachi, Pakistan, announces faculty positions with an initial appointment of three years (extendable), involving research, teaching, and supervision of postgraduate research. Open to candidates of any nationality. Ph.D. in the relevant fields along with proven track record of original research is required. Salary: up to US$5,000 per month, along with on-campus accommodation, laboratory space, and an annual leave of one month. Generous startup grant and project-based financial support (up to US$0.2 million). Contact: **Professor Dr. M. Iqbal Choudhary, Co-Director, telephone: 92-21-4824824-25; fax: 92-21-4819018-19; e-mail: pcmd@cyber.net.pk; website: http://www.ices.edu.**

---

**FACULTY POSITIONS** in population genetics **(ASSISTANT PROFESSOR)** and fungal genomics **(ASSISTANT/ASSOCIATE PROFESSOR)** in a broadly based Plant Pathology Department. Expectations include an independent, extramurally funded research program and teaching in the area of expertise. Details at **website: http://www.plantpath.ksu.edu/.** Send curriculum vitae, statements of research and teaching interests, reprints of up to five relevant publications and three letters of reference to: **Bikram S. Gill (Population Genetics) or Barbara Valent (Fungal Genomics), Department of Plant Pathology, 4024 Throckmorton Plant Sciences Center, Kansas State University, Manhattan, KS 66506-5502.** *Kansas State University is an Equal Opportunity Employer.*

---

The Department of Biological Sciences at Dartmouth seeks applicants for a **LABORATORY INSTRUCTOR** for cell biology, physiology, genetics, and molecular biology undergraduate courses. Organizational ability, strong interpersonal skills, and a sincere interest in undergraduate teaching are required. Applicants that have a M.S. (or higher) degree in molecular/cell biology are preferred, though applicants without an advanced degree but with equivalent laboratory and/or teaching experience will also be considered. Please apply for position #0596500 at **website: http://www.dartmouth.edu/~hrs/employment/index.html.**

*Dartmouth is committed to diversity and encourages applications from women and minorities. Dartmouth College is an Equal Opportunity and Affirmative Action Employer.*

## POSITIONS OPEN

### ASSISTANT PROFESSOR of BIOCHEMISTRY
**The University of Akron**

The Chemistry Department at the University of Akron seeks applications and nominations for a tenure-track Assistant Professor of biochemistry. The Department currently has 18 full-time faculty and more than 65 graduate students pursuing the Ph.D. and M.S. degrees. We have modern instrumentation centers in the areas of nuclear magnetic resonance, mass spectrometry, X-ray crystallography, and laser spectroscopy. The Department also has a strong emphasis on organic and inorganic synthesis as well as opportunities for collaboration with the Ph.D. Program in Integrative Biosciences. More specific information about the Department can be obtained at the **website: http://www.uakron.edu/colleges/artsci/depts/chemistry/.** Applicants must possess a Ph. D. in any area of chemistry or biochemistry, have postdoctoral research experience, and have a strong publication record. The successful candidate will be expected to teach biochemistry at both the graduate and undergraduate levels and to establish an externally funded research program. To apply, submit a cover letter, current curriculum vitae, a description of proposed research, a teaching statement, and arrange to have three letters of recommendation sent to: **Biochemistry Search Chair, Department of Chemistry, The University of Akron, Akron, OH 44325-3601.** Applications will be reviewed from October 15, 2007, until the position is filled. *The University of Akron is committed to a policy of Equal Employment Opportunity and to the principles of Affirmative Action in accordance with state and federal laws.*

---

### POSTDOCTORAL ASSOCIATE POSITIONS
**in Human Cancer Immunology**

Two Postdoctoral Associate positions are available immediately at the University of Minnesota Cancer Center. The candidates should have a Ph.D. in immunology and/or molecular biology; or M.D. with research experience in immunology, hematology, and/or molecular biology. One position will investigate genetic modification of human hematopoietic stem cells with nonviral vectors using skills in cell culture, fluorescence activated cell sorter analysis, stem cells, cloning, integration analysis, and animal model. The second position will investigate transcriptional regulation of human T cell development, differentiation and function using skills in cell culture, DNA and RNA isolation, real-time PCR, Southern and Northern blot, microarray, and bioinformatics. Applicants should have peer-reviewed publications. Apply online to requisition number 148967 at **website: https://employment.umn.edu.** Submit curriculum vitae, letter of interest, and contact information for three references to the attention of **Dr. Xianzheng Zhou.** *University of Minnesota is an Equal Opportunity Educator and Employer.*

---

### ASSISTANT PROFESSOR
### WETLAND ECOLOGIST/SCIENTIST
**Utah State University**

The Department of Watershed Sciences **(website: http://www.cnr.usu.edu/departments/wats)** and the Ecology Center **(website:http://www.usu.edu/ecology)** at Utah State University **(website: http://www.usu.edu)** seek applications for a nine-month, tenure-track position in wetland ecology. We seek a broadly trained Wetland Ecologist/Scientist with areas of specialization that complement those of other faculty at Utah State University. Areas of specific expertise include, but are not limited to, biogeochemistry, hydrologic processes, ecosystem services, food web ecology, restoration, and toxicology. The complete position description (#050942) and instructions for applying are available at **website: https://jobs.usu.edu.** Review of applications starts 1 October 2007.

*Utah State University is an Affirmative Action/Equal Opportunity Employer and encourages applications from women and minorities.*

## POSITIONS OPEN

UNIVERSITY of ROCHESTER

### UNIVERSITY of ROCHESTER

The Department of Chemistry invites applications for one or more positions in organic and inorganic chemistry, broadly defined, at the **ASSISTANT, ASSOCIATE, and FULL PROFESSOR** levels. Candidates are expected to establish an outstanding program of original research and be effective teachers at the graduate and undergraduate levels. Applicants should send curriculum vitae, a statement of research plans, teaching interests, and arrange for three letters of recommendation to be sent, preferably in electronic form, to **Ms. Karen Dean, e-mail: dean@chem.rochester.edu,** or by mail to: **Chemistry Faculty Search Committee, c/o Ms. Karen Dean, Department of Chemistry, University of Rochester, RC Box 270216, Rochester, NY 14627-0216.** Review of applications will begin on October 15, 2007. *The University of Rochester is an Equal Opportunity Employer. Women and minority candidates are strongly encouraged to apply.*

---

**POSTDOCTORAL POSITION** is available immediately to study molecular mechanisms of Alzheimer's disease using transgenic/knockout mice and cell lines. The specific project, funded by National Institute on Aging grants, involves the investigation of the role of ABCA1 and other cholesterol transporters, LXR receptors, and lipid metabolism in Alzheimer's disease. Candidates should have Ph.D. or M.D. with a strong background in molecular and cell biology. Experience with molecular biology techniques, cell culture, fluorescent microscopy, and transgenic mice are desirable. Interested applicants should send curriculum vitae and names of three references to: **Dr. Radosveta Koldamova (telephone: 412-383-7197)** or **Dr. Iliya Lefterov (telephone: 412-383-6906), Department of Environmental and Occupational Health, University of Pittsburgh, 100 Technology Drive, Pittsburgh, PA 15219; e-mail: radak@pitt.edu** or **iliyal@pitt.edu.** *The University of Pittsburgh is an Equal Opportunity Employer.*

---

### POSTDOCTORAL POSITION

A Postdoctoral position is available immediately for a highly motivated individual interested in molecular mechanisms controlling immune system activation, autoimmunity, and tumor immunity **(website: http://www.columbia.edu).** We are looking for an individual (Ph.D. and/or M.D.) with a strong background in biochemistry, immunology, and molecular biology, and ability to work independently and cooperatively with other investigators in the Laboratory.

Send a brief statement of your interest, curriculum vitae, and names of three references to: **Dr. Hua Gu, Department of Microbiology, Columbia University, College of Physicians and Surgeons, 701 West 168th Street, HHSC, Room 6-611, New York, NY 10032 U.S.A. E-mail: hg2065@columbia.edu.**

*Columbia University is an Affirmative Action/Equal Opportunity Employer.*

---

NIH-funded **POSTDOCTORAL POSITION** available in the Molecular Pharmacology Research Center at Tufts-New England Medical Center in Boston, Massachusetts. *Drosophila* mutant lines are being utilized to identify novel genes regulating feeding and fat deposition. Follow-up characterization of corresponding mammalian homologs as candidate modulators of metabolic function includes biochemical and molecular pharmacological approaches in vitro and in vivo. Experience with *Drosophila* required. Please send curriculum vitae and names of three references to **Alan Kopin, M.D., e-mail: akopin@tufts-nemc.org.** *Tufts NEMC is an Equal Opportunity Employer.*

## ANNOUNCEMENTS

### INDO-U.S. SCIENCE AND TECHNOLOGY FORUM
**Fulbright House, 12 Hailey Road**
**New Delhi-110 001, India**
**Website: http://www.indousstf.org**
**THIRD CALL FOR PROPOSAL 2007**

The Indo-U.S. Science and Technology Forum (IUSSTF), established under an agreement between the Governments of India and the United States of America, is an autonomous, not-for-profit society that promotes and catalyzes the Indo-U.S. bilateral collaborations in science, technology, engineering, and biomedical research through substantive interaction among government, academia, and industry.

The IUSSTF seeks to support innovative programs aimed to stimulate interactions that have a strong potential for generating follow-on activities and building long-term Indo-U.S. S&T relationships.

The IUSSTF solicits proposals thrice a year (submission deadline-February, June, and October) jointly submitted by the U.S. and Indian Principal Investigators from academia, government funded institutions/laboratories and private R&D entities for: (1.) Knowledge R&D networked and public-private networked Indo-U.S. centers, (2.) Indo-U.S. workshop, conference, symposium, (3.) Training schools, and (4.) Travel grants (i.) to avail already awarded fellowship and sabbatical positions in U.S./India (ii.) For selected U.S. participants to attend international conferences/events in India (3.) For specific exploratory/planning visits aimed at large-scale collaborations.

Detailed format available at **website: http://www.indousstf.org.**

For further details and electronic submission: **Arabinda Mitra, e-mail: amitra@indousstf.org** and **Michael Cheetham, e-mail: mcheetham@si.edu.**

Submission deadline: 15 October 2007. Award announcement: mid January 2008.

---



## MARKETPLACE

# Powerful, Multi-modal Imaging

## Now so easy everyone is lining up to do it!

**Novel**
**KODAK X-SIGHT Imaging Agents & Antibody Conjugates**
**NOW AVAILABLE**

Ventral position imaging shows two optical signals generating metastatic lesions located in the cranial region of the mouse.

Subsequent lateral position imaging clearly separates the two lesions to specific jaw and skull locations.

*Images Courtesy Dr. Bohumil, Bednar, Merck Co., Inc.*

## Kodak Molecular Imaging Systems

The KODAK In-Vivo Imaging System FX Pro combines high-sensitivity Optical Molecular Imaging and high resolution digital X-ray to deliver precise anatomical localization of molecular and cellular biomarkers.

New full precision automation makes complex multi-modal imaging protocols easy and repeatable.

- Automated excitation and emission filters for outstanding fluorescent imaging sensitivity and flexibility from 390nm to 830nm
- 10x optical zoom and auto-focus lens for precise and repeatable results
- Automated imaging chamber enables remote switching between optical, X-ray or radioisotopic imaging without moving the subject

Whether you're performing multi-wavelength fluorescence, luminescence, X-ray, radioisotopic or a combination of these imaging modalities, the In-Vivo FX Pro fully automates the process for an entirely new level of sensitivity, throughput, repeatability, and ease-of-use.

**Find out more**
1-877-747-4357, exp. code 7
www.carestreamhealth.com/go/invivo4
www.carestreamhealth.com/go/X-Sight

Carestream HEALTH